Microbubbles in Vascular Imaging

Thesis submitted to Imperial College London for the degree of Doctor of Philosophy

Student: Brahman Dharmarajah MBBS MRCS MA

PhD Candidate Imperial College

Division of Experimental Medicine &

Section of Vascular Surgery

Faculty of Medicine

Imperial College, London

Supervisors

Professor Edward Leen

Professor of Radiology

Division of Experimental Medicine

Department of Medicine

Faculty of Medicine

Imperial College London

Professor Alun Davies

Professor of Vascular Surgery

Section of Vascular Surgery

Department of Surgery and Cancer

Faculty of Medicine

Imperial College London

This thesis is dedicated to my wife, Kate, whose love never lets me forget that the best is yet to be.

DECLARATION

I hereby declare that the material presented in this thesis is my original work. However, it would not have been possible without the help of collaborators and supervisors. Where results, previous work or figures have been reproduced from other authors the source is clearly acknowledged with permission.

ACKNOWLEDGEMENTS

I would first and foremost like to thank my supervisors Professor Edward Leen and Professor Alun Davies for the opportunity, support and guidance during the course of this thesis. This work would not have been possible without their steadfast commitment to develop my research and academic skills. I would also like to thank the members of the Section of Vascular Surgery and have no doubt that the friendship and community created within this group will remain its foundation for academic success for many years to come.

I would like to thank Dr. Tom McKinnon and Professor Michael Laffan from the Department of Haematology, Imperial College London for their guidance and supervision during the in-vitro sonothrombolysis study. I would like to thank Mr Ankur Thapar for collaborative work on both the carotid studies and sonothrombolysis literature review. I would like to thank Mr Viknesh Sounderajah for his collaborative work on the review of DVT ageing. I would like to thank all the Vascular Scientists who helped identify patients with carotid atherosclerosis. I would like to thank Dr. Damianos Christofides, Miss Christina Kali and Professor Mike Averkiou of the University of Cyprus who provided biomedical engineering support, guidance and analysis of contrast imaging in both carotid and DVT aspects of this work. I would like to thank Professor Thomas Wakefield, Dr. Daniel Myers, Dr. Jose Diaz and Shirley Wrobleski of the Conrad Jobst Vascular Research Laboratory, University of Michigan for their expertise and teaching during my Travelling Fellowship to the University of Michigan Medical School. I give my sincere thanks to all the patients who participated in this research. Finally, I would like to thank the Stroke Association, the European Venous Forum, the Royal Society of Medicine Venous Forum, the Association of Surgeons in Training and the Graham-Dixon Charitable Trust for their funding.

ABSTRACT

Introduction

Ultrasound is integral in diagnostic imaging of vascular disease. It is a common first line imaging modality in the detection of deep vein thrombosis (DVT) and carotid atherosclerosis. The therapeutic use of ultrasound in vascular disease is also clinically established through ultrasound thrombolysis for acute DVT. Contrast agents are widely used in other imaging modalities, however, contrast enhanced ultrasound (CEUS) using microbubbles remains a largely specialist clinical investigation with truly established roles in hepatic imaging only.

Aim

The aim of this thesis was to investigate diagnostic and therapeutic roles of CEUS in vascular disease. Diagnostically, carotid plaque characteristics were evaluated for stroke risk stratification in patients with carotid atherosclerosis. Therapeutically, microbubble augmented ultrasound thrombolysis was investigated in-vitro as a novel technique for acute thrombus removal in the prevention of post thrombotic syndrome.

Methods

A validated in-vitro flow model of DVT was adapted and developed for a formal feasibility study of microbubble augmented ultrasound thrombolysis.

Two cross sectional studies of patients with 50-99% carotid stenosis were performed assessing firstly, plaque ulceration and secondly plaque perfusion using CEUS.

Results

Using commercially available microbubbles and ultrasound platform, significantly improved thrombus dissolution was demonstrated using CEUS over ultrasound alone in the in-vitro flow model of acute DVT. In particular, increased destruction of the thrombus fibrin mesh network was observed.

CEUS demonstrated greater sensitivity than carotid duplex in the detection of carotid plaque ulceration with a trend toward symptomatic carotid plaques. A reduced plaque perfusion detected by both semi-qualitative and quantitative analysis was associated with a symptomatic status in patients with a 50-99% stenosis.

Conclusion

CEUS is a viable adjunct to vascular imaging with ultrasound. Microbubble augmented ultrasound thrombolysis is a feasible, non-invasive, non-irradiating intervention which warrants further investigation in-vivo. Carotid plaque CEUS may contribute to future scoring systems in stroke risk stratification but requires prospective validation.

ABBREVIATIONS

AAA – abdominal aortic aneurysm

ACCP – American College of Chest Physicians

ACST - Asymptomatic Carotid Surgery Trial

ACST-2 - Asymptomatic Carotid Surgery Trial 2

AHA – American Heart Association

ATTRACT - Acute Venous Thrombosis: Thrombus Removal with Adjunctive Catheter-directed Thrombolysis

A-V – arterio-venous

AVI – audio video interleaved

BMT –best medical therapy

CAR – carotid artery risk

CAS – carotid artery stenting

CaVenT- Additional Catheter-Directed Thrombolysis versus Standard Treatment for Acute Iliofemoral Deep Vein Thrombosis

CCA – common carotid artery

CEA – carotid endarterectomy

CECT – contrast enhanced computed tomography

CEMRI – contrast enhanced magnetic resonance imaging

CEUS – contrast enhanced ultrasound

CI – confidence interval

CDT – catheter directed thrombolysis

CREST – Carotid Revascularisation Endarterectomy versus Stenting Trial

CT – computed tomography

CVA - cerebrovascular accident

DCE-US - dynamic contrast enhanced ultrasound

DDFP – dodecafluoropentane

DICOM – Digital Imaging and Communications in Medicine

$DIOC_6$ - dihexyloxacarbocyanine iodide

DVT – deep vein thrombosis

DW-MRI – diffusion weighted magnetic resonance imaging

ECA – external carotid artery

ECST – European Carotid Surgery Trial

ECST-2 – European Carotid Surgery Trial 2

EDTA - ethylenediaminetetraacetic acid

EFSUMB - European Federation of Societies for Ultrasound in Medicine and Biology

EVAR – endovascular aneurysm repair

FDA - Food and Drug Administration

FLAIR - fluid attenuation inversion recovery

FITC - fluorescein isothiocyanate

GSM – grey scale median

HUVEC - human umbilical vein endothelial cells

IQR – interquartile range

IVC – inferior vena cava

MB – microbubbles

MHz – megahertz

MI – mechanical index

MRDTI - magnetic resonance direct thrombus imaging

MRI – magnetic resonance imaging

NASCET - North American Symptomatic Carotid Endarterectomy Trial

NHS – National Health Service

NICE – National Institute for Health and Clinical Excellence

NYHA - New York Heart Association

PE – pulmonary embolism

PESDA - perfluorocarbon-exposed sonicated dextrose albumin

PET – positron emission tomography

PMT – pharmacomechanical thrombolysis

PTS – post thrombotic syndrome

RCP – Royal College of Physicians

RCT – randomized controlled trial

ROI – region of interest

RR – risk reduction

rT-PA - recombinant tissue plasminogen activator

SD – standard deviation

TCD – transcranial Doppler

TIA – transient ischaemic attack

TIC – time intensity curve

TMP – tissue mimicking phantom

US – ultrasound

VTE – venous thromboembolism

vWF – von Willebrand Factor

TABLE OF CONTENTS

LIST OF FIGURES

List Of Tables

1. MICROBUBBLES IN VASCULAR IMAGING

1.1. Ultrasound Imaging

Ultrasound is one of the core modalities within medical imaging along with plain film radiography, computed tomography (CT), magnetic resonance imaging (MRI) and nuclear medicine. It describes a mechanical wave composed of compressions and rarefactions that are approximately 100 times more rapid than the oscillations of an audible wave and usually concentrate within a range of 1MHz – 20MHz in clinical radiology. The wave is produced by conversion of electrical energy into mechanical energy by piezoelectric crystals within an ultrasound transducer probe. The resultant wave is applied to a medium enabling its propagation through that structure through displacement of molecules. It is the behaviour of the wave within a particular medium (e.g. soft tissue, bone, fat, blood) which defines its acoustic properties, in particular, the wave propagation speed, acoustic impedance and attenuation coefficient. Additionally, the interface between mediums with differing characteristics produces acoustic reflections or echoes which are detected by the piezoelectric crystals within a transducer and converted back to electrical energy to provide spatial and contrast information which create the images acquired during an ultrasound examination.

Ultrasound is widely used in medical imaging as it is non-ionizing and therefore does not carry a risk of future malignancy. Coupled with its relatively cheap cost and accessibility in most centres, it provides a competitive alternative to plain film radiography, CT and MRI. Further advantages over these modalities are the ability to perform dynamic real-time examinations including Doppler evaluation which can provide simultaneous structural and pathophysiological information which is paramount in vascular ultrasound.

No single imaging modality is perfect and ultrasound carries inherent disadvantages. In particular, specific training is required to perform ultrasound to a competent level to ensure relative uniformity in examination quality and reduce operator dependence. Despite this it remains a subjective and qualitative assessment in current clinical practice which can sometimes limit its reproducibility and therefore reliability. Additionally, media such as bone and air with particularly poor acoustic characteristics cannot be evaluated, and therefore structures encased or adjacent to these media along the direction of the acoustic wave also cannot be accurately assessed, for example, brain parenchyma through the skull vault or mediastinal structures through the lung.

Throughout medical imaging improved resolution between tissue media has been sought after to improve the quality of imaging acquired. One strategy for this has been through the use of contrast agents which are well established for use in plain film radiography including fluoroscopy, CT and MRI. In particular, vascular imaging utilises contrast agents providing not only qualitative but quantitative diagnostic imaging as well as helping to guide real-time vascular intervention. Relative to these other modalities, the role of contrast agents in ultrasound is less well defined in clinical practice and the premise of this thesis is to explore potential roles for contrast enhanced ultrasound in vascular diagnostics and therapeutics.

1.2. Microbubbles

Microbubbles are gas filled microspheres typically 1-10μm in size that have unique acoustic properties enabling them to be visualized using specific modes of ultrasound imaging. The use of contrast agents was first described in 1968 by Gramiak using intracardiac injection of agitated saline to improve imaging of the aortic root using echocardiography (1). However, microspheres containing air are variable in size and are unstable as they are highly soluble in blood and are filtered by the pulmonary circulation making them inappropriate for imaging the left side of the heart and

structures beyond in the systemic circulation by intravenous injection. However, the unstable properties of agitated saline still forms the basis of the bubble echocardiogram investigation used to delineate the presence cardiac chamber abnormalities such as a patent foramen ovale (2). Identification of a patent foramen ovale through the presence of bubbles in the left side of the heart has a greater sensitivity than conventional transthoracic Doppler assessment for this common condition that affects 25-30% of the general population and is implicated where paradoxical embolus is suspected (3).

The first generation of microbubbles that were engineered contained room air but were stabilized with a thin shell acting as a surfactant to reduce the effect of surface tension (4). Examples of these first generation microbubble shells include albumin (Albunex) or galactose palmtic acid (Levovist). These microbubbles were able to pass through the pulmonary capillary bed to the left side of the heart, however, they failed to resist arterial pressure gradients. The second generation microbubbles currently used in clinical practice and research contain heavy molecular weight gases to reduce solubility and withstand greater pressures. Additionally, stabilization of the shell is further improved through the use of sonicated albumin and phospholipids whilst consistency for imaging is achieved through manufacturing of smaller, more consistent sized microbubbles of 2.5-5μM to improve both the passage through the pulmonary capillary bed and reduced distortion of microbubble oscillation (5) . The improved consistency in size also eliminates the potential risk of a gas embolus affecting either the pulmonary or cerebral circulations. In fact, the similarity in microbubble size to red blood cells leads to them being purely intravascular agents as they do not diffuse out of the circulation unless there is active bleeding. In contrast, iodinated CT agents and gadolinium based MRI agents tend to diffuse into the interstitial space after intravenous administration in the delayed phase. Therefore, microbubble imaging enables focused imaging of both the macrovasculature and microvasculature circulation (6). SonoVue is a second generation contrast agent containing the heavy gas, sulphur hexafluoride with a phospholipid shell and is currently licensed for use as an ultrasound contrast agent in Europe (7). Other

second generation microbubble contrast agents currently licensed for use across the world are shown in Table 1.

Microbubble	Shell	Gas	Mean Size (μM)	Manufacturer	Licensed countries
Optison	Albumin	Octafluoropentane	2-4.5	GE	Europe, Far East Asia
Definity	Lipid bilayer	Octafluropentane	1.1-3.3	Lantheus	North America, Australia
SonoVue	Phospholipid / surfactant	Sulphur hexafluoride	2-3	Bracco	Europe, Far East Asia, India, Brazil
Sonazoid	Phospholipid	Perfluorocarbon	3-4	GE	Japan, South Korea

GE – General Electric Healthcare

Table 1 Common second generation ultrasound contrast agents.

1.3. SonoVue Ultrasound Contrast Agent

SonoVue was originally reported as a novel ultrasound contrast agent in 1995 by Schneider et al. and was known as BR1(8). These microbubbles were prepared by the addition of normal saline (0.9% concentration) to a lyophilized powder of stabilized sulphur hexafluoride and lipid. The resulting suspension contained 2 x10^8 microbubbles per ml and importantly to enable capillary passage the mean diameter was 2.5 μM with greater than 90% of microbubbles being less than 8μM. As with the first generation microbubbles containing air, BR1 retained echogenicity over the

medical ultrasound frequency range (1-10MHz), however, improved stability of the shell against systemic pressure was demonstrated by imaging of the left side of the heart during systole in an animal model.

A subsequent Phase I study assessed both the safety and pharmacokinetic profiles of SonoVue in 12 healthy subjects (9). Sulphur hexafluoride diffused out of the phospholipid shell and was expired via the lungs with 80-90% removed after 11 minutes administration whilst the phospholipid shell was metabolised by the liver. This elimination was neither gender nor dose dependent within a range of 0.03 to 0.3ml/kg. No adverse events were reported either immediately or in a 24 hour follow-up period. Throughout Phase I-III clinical trials, no fatal adverse events were observed with SonoVue enabling the European Medicines Agency to grant marketing authorisation in 2001 (10). However, post marketing surveillance revealed three serious events with fatal outcomes in patients with coronary artery disease (11) which led to the addition of a contraindication for SonoVue in patients with acute coronary syndrome or other unstable cardiac conditions such as New York Heart Association (NYHA) Class III/IV heart failure (12).

New concerns regarding the use of SonoVue temporarily limited its use as an ultrasound contrast agent until a large retrospective analysis by the Italian Society for Ultrasound in Medicine and Biology (SIUMB) study group was published in 2006 (13). This study analysed the safety of 23,188 abdominal contrast enhanced ultrasound investigations using SonoVue across 28 Italian centres. All dosing remained within the manufacturer's guidance of a full dose of 4.8ml with repeat injections performed in approximately 15% of patients. There were no deaths and in total there were 29 adverse events reported; 2 were serious and 27 non-serious corresponding to a 0.125% rate for all adverse events and 0.0086% rate for serious adverse events. Of note, no adverse reactions occurred in patients who underwent multiple injections of SonoVue once again reinforcing the Phase I findings of there not being a dose dependent response. The two serious adverse events were classified

as anaphylaxis type reactions with symptoms of dyspnoea, bronchospasm, cutaneous rash and hypotension with a positive clinical response to steroid and antihistamine therapy. The non-serious adverse events did not require medical therapy and included symptoms such as itching, nausea, headache, dizziness and moderate, spontaneously resolving hypotension.

A retrospective analysis may incur greater reporting bias than a randomised controlled trial, however, when compared to another retrospective study assessing the safety of CT and MRI contrast media in 118,813 investigations at a single centre, all adverse events rates of 0.65% and 0.07% respectively indicates that an all adverse event rate of 0.125% for contrast enhanced ultrasound is acceptable.

At present, SonoVue has European marketing authorisation for use in echocardiography, Doppler imaging of macrovasculature (e,g. cerebral arteries) and of microvascularture (e.g. breast and liver lesions) (10, 14). However, it is stipulated only for diagnostic use and where unenhanced ultrasound imaging has been inconclusive. Contraindications to SonoVue administration include previous adverse reaction to sulphur hexafluoride, recent acute coronary syndrome or factors suggesting clinically unstable ischaemic cardiac disease (e.g. recent coronary artery intervention, severe cardiac failure (NYHA Class III/IV), patients with known right to left cardiac shunts, severe pulmonary hypertension, uncontrolled systemic hypertension, adult respiratory distress syndrome, pregnancy and lactation.

1.4. Contrast Enhanced Ultrasound Imaging

Exposure of microbubbles to an ultrasound wave can create a resonance at a frequency that coincidentally falls within the frequencies used in diagnostic medical ultrasound (2-10MHz) thus, microbubbles produce a detectable echo signal. However, in order for the microbubble signal to be useful in ultrasound imaging, it

requires separation from the echogenic signal of the surrounding tissue. The gas within the microbubble is readily compressible, therefore, as an ultrasound wave is applied there is microbubble contraction followed by immediate expansion in the rarefraction phase. In comparison, surrounding tissue is relatively incompressible. Additionally, the oscillation between contraction and expansion is asymmetrical or non-linear as a bubble is easier to contract than to expand. Therefore, an echo pattern containing frequencies that were not present in the originally transmitted fundamental ultrasound wave is returned which are known as harmonics (6).

Ultrasound modalities have been developed for imaging of harmonics which filter out tissue fundamental signals thus enabling microbubble specific ultrasound imaging. This is achieved by the fundamental wave being sent out with a paired mirrored or reversed phase pulse. If on receipt of the echo reflections at the transducer the two phases cancel each other out then the signal must be linear and therefore from tissue whilst if the two echoes do not cancel each other out then the signal must be from a non-linear reflector and thus a microbubble is detected. To increase sensitivity, modern ultrasound transducers will emit a range of paired phase frequencies to detect the range harmonics produced by the small variations in microbubble size as discussed earlier (5, 6).

Mechanical index (MI) is defined as the peak negative acoustic pressure (MPa) divided by the square root of the US frequency (MHz) at the location of the maximum pulse intensity integral (15). Early contrast ultrasound employed Doppler for microbubble detection as microbubbles were viewed as a useful adjunct to detect perfusion in conditions where conventional Doppler was not successful e.g. cerebral artery flow through the high attenuation of the skull. Despite returning a highly sensitive and strong signal, the image would immediately be lost. This was due to the use of very high MIs of Doppler imaging causing microbubble destruction. At these increased amplitudes (MI>0.07) microbubbles oscillate violently producing a rapid, concentrated, strong harmonic signal. However, this violent oscillation

destroys the microbubble shell leading to the release of the encapsulated gas into the surrounding media i.e. blood, therefore, the echo signal from the gas becomes scattered making it virtually undetectable by harmonic imaging (4, 7). To counteract this phenomenon, imaging of structures such as the liver was performed using a sweep of the transducer across the structure enabling continuously new areas of focus to imaged whilst allowing previous areas to replenish with microbubbles. Subsequently, manufacturers have developed non-destructive MI imaging which still allows creation and subsequent detection of harmonic signals (MI 0.05-0.07).

1.5. Diagnostic Use of Contrast Enhanced Ultrasound

1.5.1. Hepatic Applications

The primary clinical diagnostic use of contrast enhanced ultrasound (CEUS) is for the detection and characterisation of focal liver lesions. It carries an advantage over conventional B-mode and Doppler ultrasound as it able to display the microvasculature of the liver parenchyma as well as the larger hepatic artery and portal vein (16). Additionally, it carries similar enhancement patterns to contrast enhanced computer tomography (CECT) and contrast enhanced magnetic resonance imaging (CEMRI) through arterial, portal venous and late phases. It is in the late phase that differences arise between CEUS and CECT/CEMRI as ultrasound contrast microbubbles remain in the microvasculature of the parenchyma whilst CT and MRI contrast media clear to the extravascular space. CEUS has a number of other advantages such as higher temporal resolution from higher frame rates enabling dynamic assessment of lesions in the arterial phase, no requirement for specifically timed bolus tracking and the ability to give repeat microbubble administrations due to a more favourable safety profile especially with regard to nephrotoxicity (6). Limitations of CEUS also exist and include limited resolution to lesions of >3mm diameter, inability to visualise sub diaphragmatic lesions due to the costal margin of

the ribs, deeply placed lesions due to body habitus and lack of volume acquisition which particularly affects the arterial phase.

In 2012, a joint venture between the World Federation for Ultrasound in Medicine and Biology (WFUMB) and European Federation of Societies for Ultrasound in Medicine and Biology (EFSUMB) produced a third set of guidelines and recommendations for CEUS of the liver (17). Specific enhancement patterns for the three phases of CEUS of the liver enable clinicians to first detect benign from malignant and then go on to characterise specific lesions from both healthy liver parenchyma and cirrhotic liver echotexture. In the context of a healthy liver, lesions that do not enhance in the late phase are suspected of being malignant and it is the features in the arterial and portal venous phases that provide the exact nature of the lesion e.g. a hepatocellular carcinoma will not enhance in the late phase but hyper-enhance in the arterial phase due to preferential arterialisation of hepatic malignancy with areas of non-enhancement interspersed within the lesion secondary to necrotic areas within the malignant lesion.

Detection and characterisation of focal liver lesions is commonly performed subjectively by the clinician, however, recently there has been a shift toward objective quantification of liver lesions. In particular, CEUS of the liver has expanded to include the evaluation of a given intervention such as ablation or anti-angiogenic chemotherapy. Conventionally, response to treatment is performed using Response Evaluation Criteria in Solid Tumours (RECIST 1.1) criteria using CT (18), however, this is based on morphological lesion change which may not reflect internal pathological changes within a lesion such as necrosis from ablation or devascularisation from anti-angiogenic treatment. Application of a region of interest over a lesion can provide a time intensity curve (TIC) from the microbubble signal intensity from which a number of parameters can be derived that can be quantitatively compared and analysed (19). Examples of these parameters include area under the curve, rise time, peak intensity and wash in slope coefficient all of which are calculated offline by post processing. This quantification which can be

performed by an independent, blinded reader has been employed in research studies using CEUS as an early imaging biomarker of response to treatment (20-22).

Figure 1 Contrast enhanced liver ultrasound image acquisition in the arterial phase demonstrating peripheral enhancement with subsequent central filling of a liver metastasis indicative of tumour arterialisation. Contrast is also seen in the hepatic arteries and portal veins but the background liver parenchyma does not exhibit enhancement in this phase

In the United Kingdom, the National Institute for Health and Clinical Excellence (NICE) recommends the use of CEUS for the assessment of liver lesions where conventional ultrasound proves inconclusive (14). In this guidance a number of economic analyses were performed to assess the cost effectiveness of CEUS compared to both CECT and CEMRI. In a model of surveillance for cirrhosis, CEUS

dominated both CECT and CEMRI despite CEMRI yielding 0.022 more quality life adjusted years (QALYs) but at a greater cost of £48,454 per QALY compared to £20,000 per QALY for CEUS. Additionally, in a model of incidental focal liver lesion characterisation using pooled meta-analysis data from 4 studies, CEUS dominated both CECT and CEMRI costing £52 and £131 less respectively whilst also yielding additional QALYs due to a marginally higher sensitivity and specificity over both modalities.

1.5.2. Non-hepatic Applications

Since the introduction of CEUS, a number of non-hepatic applications have been investigated, the majority of which remain off-label for ultrasound contrast agents such as SonoVue. However, guidance from the EFSUMB was provided in 2011 summarising the indications and levels of evidence (23). Visceral organ imaging using CEUS features heavily with indications listed for the pancreas, spleen and kidneys. Pancreatic CEUS focusses on identification of pancreatic tumours from pancreatic pathology such as pseudocysts as well as characterisation of lesions through vascularity, margins and relationship to adjacent structures. This can also be performed via endoscopic CEUS. CEUS of the spleen also enables characterisation of tissue as benign or malignant as well as assessment for splenic infarction. Renal CEUS also enables identification of vascular disorders of the kidney as well providing differentiation between renal tumours and cystic lesions. Vesico-ureteric reflux provides the only use of ultrasound contrast that is not intravascular as microbubbles are administered intravesically with a voiding ultrasonography then performed for reflux into either of the ureters. This technique avoids the need for ionizing radiation used in a voiding cystourethrography and is therefore recommended in females and children. The EFSUMB guidance recognises the difficulty of implementing CEUS in paediatrics, however, it also recognises that CEUS may be an ideal imaging modality in this group of patients in whom exposure to harmful contrast agents and ionising radiation is to be avoided. In trauma, CEUS may provide an alternative to CT in stable, isolated blunt trauma particularly in

children. It can also be used as a follow up imaging modality for conservative management of injuries where repeated CT can be reduced.

1.6. Vascular Imaging using CEUS

Vascular disease is an attractive target for CEUS. As previously discussed, microbubbles are purely intravascular agents with the ability to uniquely reflect both the state of the macrovasculature and microvasculature due to a comparable size with red blood cells coupled with surrounding tissue suppression (6). Duplex imaging, utilising a combination of B-mode and Doppler ultrasound, is commonly used in vascular imaging providing both anatomical and flow information from peripheral vessels (24). CEUS can act as a valuable adjunct to Duplex augmenting further both structural and dynamic information. In addition, without exposure to ionising radiation or nephrotoxic contrast media, CEUS can provide an improved safety profile compared to angiography, CT and MRI. Particular areas of focus have included imaging disorders of the aorta and carotid arteries with only limited evidence in the literature for the use of CEUS in deep vein disease.

1.7. Aortic CEUS

1.7.1. Aneurysm Diagnosis

Duplex ultrasound is currently utilized as the imaging modality for the National Health Service abdominal aortic aneurysm screening programme (NAAASP) in the United Kingdom. Whilst some variation in reproducibility of aortic diameter measurements has been reported (25), screening has reduced the number of ruptured abdominal aortic aneurysms (AAAs) and has been cost effective in doing so (26, 27). Therefore, at present there is unlikely to be a role for CEUS within screening due to the extra expertise and cost required to perform this investigation. CEUS has previously been described in the diagnosis of ruptured AAAs. In a small case series

of 8 patients from 2005, aneurysm diameter, location, presence of a haemoperitoneum, active contrast extravasation and aneurysm thrombus were features that could be identified (28). Whilst the time required for the CEUS examination was shorter than that required for a CT, it was suggested that no further clinically relevant details was gained in the five patients who went on to have a CT. However, with the option of endovascular aneurysm repair (EVAR) in current clinical practice (29), a two dimensional CEUS acquisition will not provide the necessary information required to plan an endovascular procedure.

1.7.2. Endoleak Detection

The most studied use of CEUS in the aorta is for the detection of endoleaks after EVAR. EVAR was introduced into routine clinical practice after the EVAR-1 randomised controlled trial demonstrated an improvement in 30-day mortality by two thirds after EVAR compared to open surgery (30). Long term follow up displayed no advantage in all-cause mortality (31) whilst the EVAR-2 trial showed no difference in survival between patients unfit for open repair treated either conservatively or by EVAR (32). In the United Kingdom, NICE recommends EVAR over open repair in elective aneurysm repair (33) despite an increased rate of graft-related complications and costly reinterventions (34). One of the principal reasons for complications and re-intervention post EVAR is due to endoleaks which are defined as any form of persistent blood flow outside of the graft but within the aneurysm sac. They are classified between I-IV with re-intervention often determined by continued expansion of the aneurysm sac. Due to the frequency of endoleaks post EVAR, patients are required to undergo imaging surveillance, however, there is no consensus regarding modality or frequency of surveillance with angiography, CT and Duplex ultrasound all advocated (35).

CEUS has the potential to image an endovascular aortic graft in a dynamic fashion with the ability to adjust position to demonstrate flow direction and velocity (36). A recent meta-analysis compared the detection of endoleak after EVAR with

unenhanced ultrasound and CEUS using CECT as the gold standard (37). Twenty-one studies including 2601 patients were analysed in the meta-analysis of unenhanced ultrasound yielding a pooled sensitivity of 0.77 (95% CI 0.64-0.86; I^2 = 0.82) and a pooled specificity of 0.94 (95% CI 0.88-0.97; I^2 = 0.90). Seven studies including 285 patients were analysed in the meta-analysis of CEUS yielding a pooled sensitivity of 0.98 (95% CI 0.90-0.99; I^2 =0.32) and a pooled specificity of 0.88 (95% CI 0.78-0.94; I^2 =0.67). The greater sensitivity of CEUS compared to unenhanced ultrasound suggests that CEUS is the superior modality for the detection of endoleak after EVAR although it is noted that there was significant heterogeneity in the design of all studies included. Interestingly, the specificity of CEUS was less than that of unenhanced ultrasound which may suggest that CEUS is in fact more sensitive for endoleak than the gold standard of CECT. This has previously been suggested as a result of greater sensitivity of CEUS to detect low flow endoleaks (38). Whilst replacement of nephrotoxic contrast media of CT is attractive for improved long term survival after AAA repair (39), a robust prospective trial with stratification via type of endoleak is now required to assess whether CEUS can be used as a sole imaging modality for detection of endoleaks after EVAR.

1.8. Deep Vein Thrombosis CEUS

Conventional ultrasound is the current first line investigation for the detection of DVT (40). This is based upon a combination of vein non-compressibility and lack of colour flow Doppler imaging within the imaged deep vein (Figures 2 &3). This carries a sensitivity of 94.2% and specificity of 93.8% compared to the original reference standard of contrast venography (41). However, when imaging is performed below the knee this sensitivity falls to 63.5% resulting in high risk patients receiving anticoagulation therapy and repeat scanning after one week.

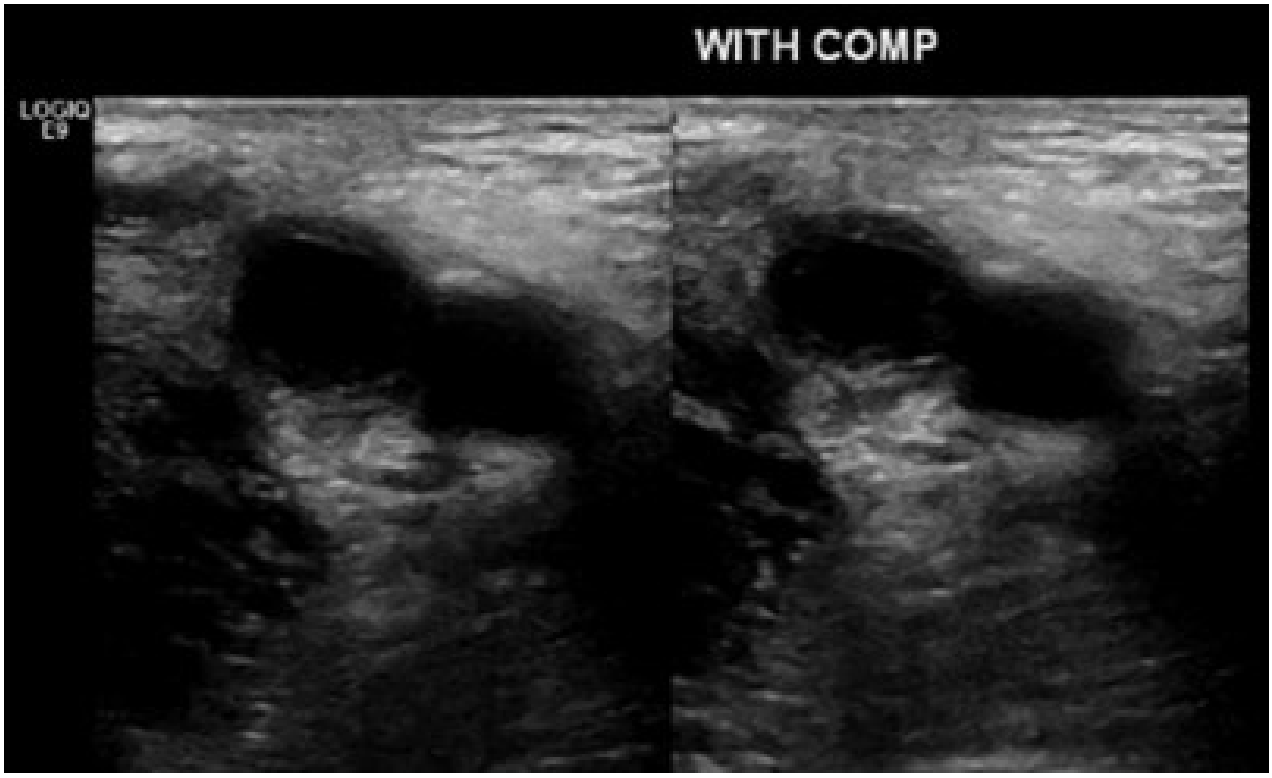

Figure 2 Side by side transverse section ultrasound images through the superficial femoral artery (left) and vein (right) with compression image on the right demonstrating non-compressibility of the superficial femoral vein indicating presence of thrombus

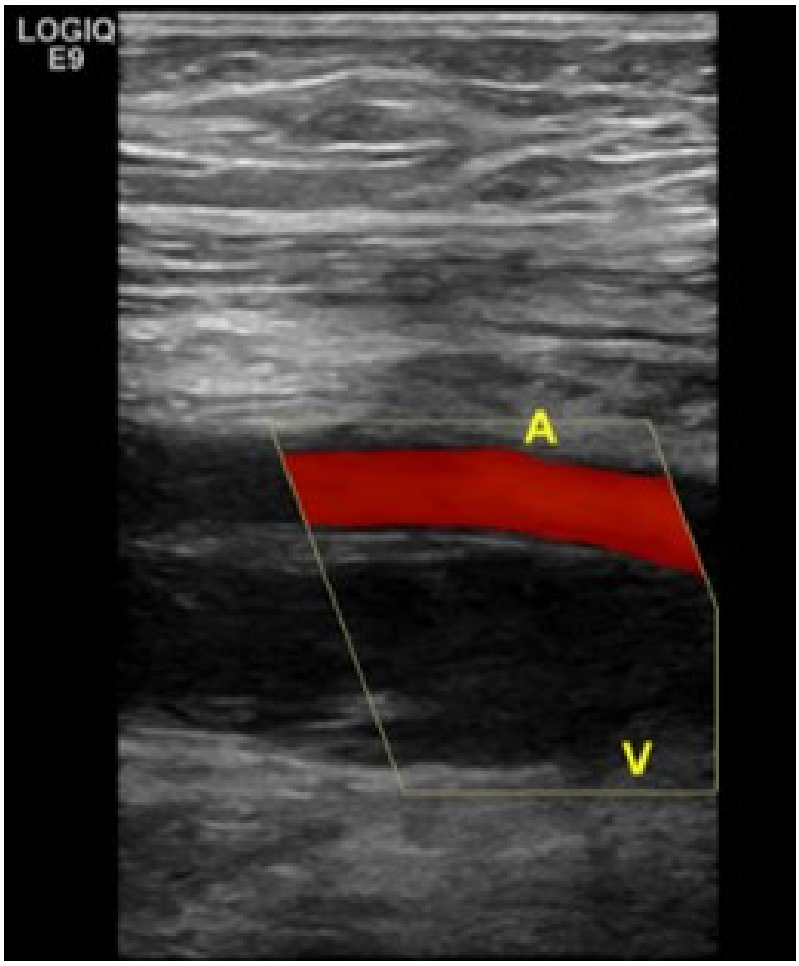

Figure 3 Longitudinal section Doppler ultrasound image through the superficial femoral vein (V) and superficial femoral artery (A) demonstrating lack of Doppler flow within the vein due to thrombus

CEUS has been shown in a small case series to significantly improve the detection of the popliteal, posterior tibial and peroneal veins over conventional ultrasound in a group of patients being assessed for DVT (42). Therefore, this may prevent patient morbidity from unnecessary interim treatment, reduce clinician time and reduce costs of repeat scanning. Quantitative assessment of DVT has also been preliminarily assessed with CEUS. In a rodent inferior vena cava model of DVT, thrombus quantified in-vivo by CEUS correlated well with the subsequent thrombus weight measured ex-vivo providing further evidence of accurate assessment of DVT using

CEUS (43). However, at present there is no widely accepted role in the literature for CEUS in the assessment of either acute or chronic deep venous disease (23).

1.9. Carotid Artery CEUS

1.9.1. Carotid Stenosis

In the United Kingdom, Duplex ultrasound is the first line investigation for identification and quantification of carotid artery plaque burden which is measured by luminal stenosis (44). Randomised controlled trial data recommends that carotid revascularization is undertaken in patients who have suffered neurological symptoms such as stroke, transient ischaemic attack or amaurosis fugax as a result of a carotid plaque measuring 70-99% NASCET stenosis (45, 46). The number needed to treat (NNT) to prevent one stroke in this group of patients is 6, however, the NNT increases to 13 in those patients with a symptomatic carotid plaque measured between 50-69% NASCET stenosis (47). Additionally, in patients who are asymptomatic but are found to have a 70-99% NASCET stenosis, the NNT for carotid revascularization to prevent one stroke is even further marginal at 20 (48).

In the assessment of luminal stenosis, Duplex ultrasound has a 97% accuracy compared to the gold standard of carotid angiography (49). Additionally, for the assessment of complete carotid artery occlusion it has a positive predictive value of 92.5% (50). Incremental improvement in the detection of complete occlusion from trickle flow can be provided by CEUS (51). This occurs as high and low velocity flows can be imaged simultaneously with CEUS unlike Doppler US where artifactual blooming is commonly inadvertently captured. This is important clinically as total carotid occlusion will not require revascularization as the risk of carotid thromboembolism has been abolished. CEUS has also demonstrated greater sensitivity than Duplex ultrasound in the detection of subclinical carotid atherosclerosis (52). In a study of 100 asymptomatic patients with cardiovascular

disease risk factors, subclinical atherosclerotic plaques were observed in 88% of patients using CEUS and 77% of patients using Duplex ultrasound. This was attributed to the greater sensitivity of CEUS to purely echolucent plaques as the microbubble dense lumen fills around these small plaques. However, it may be argued that such incremental improvement in sensitivity is not required as the clinical management of such plaques remains purely conservative.

1.9.2. In-stent Carotid Restenosis

Carotid revascularization can be performed surgically through carotid endarterectomy (CEA) or by endovascular approach using carotid artery stenting (CAS). The merits and disadvantages of these two techniques will be discussed later, however, in brief the Carotid Revascularisation Endarterectomy versus Stenting Trial (CREST) failed to show any significant difference in the primary outcomes of 30-day stroke or death between the two techniques (53). Surveillance post CAS for in-stent restenosis using Duplex ultrasound is limited by an alteration in the haemodynamic property of the vessel as well as increased artifactual signal both arising due to stent deployment. In a small study of 30 patients post CAS assessing Duplex ultrasound and CEUS as imaging modalities, 5 patients were found to have in-stent restenosis of which 2 cases could be seen only by CEUS. The presence of restenosis was only qualitatively graded visually as; detectable, partially detectable and readily detectable with no reproducibility reported in this small study. However, much like the assessment of complete carotid occlusion described earlier, the sensitivity of CEUS to detect both high and low velocities without artefact enables microbubble detection within the stent.

1.9.3. Carotid Plaque Neovascularisation

Histological analysis of carotid plaques from symptomatic individuals has revealed a number of pathological features identifying the vulnerable carotid plaque (54-56). Plaque rupture, haemorrhage and ulceration are implicated during symptomatic

episodes but it is believed to be uncoordinated angiogenesis that enables atherosclerotic lesions to first develop from the vasa vasorum. Development of these new vessels allows delivery of inflammatory cell mediators which cause porosity of the vessel walls enabling first oxygen and metabolic nutrient delivery followed by lipid deposition via macrophage foam cells (57). A biomarker that can reflect development or presence of these vulnerable features would enable improved risk stratification for treatment in both the symptomatic, moderate 50-69% stenosis and asymptomatic 70-99% stenosis carotid plaque patient groups.

The ability of second generation microbubbles to pass through capillary beds suggests that microbubbles can be detected in areas of neovascularization within carotid plaques. This has been demonstrated by a number of studies, however, many of the preliminary studies involved sub-clinically significant degrees of carotid stenosis and either asymptomatic patients or patients in whom time from an index event was not reported (58-61). Interestingly, across all of these groups microbubble signals were still observed within the plaques imaged. Additionally, the quantification of plaque neovascularization in these studies was based on a visual qualitative scoring system.

Further studies have attempted to validate CEUS findings with histological plaque analysis. Two studies assessing the dynamic phase of microbubble administration in the carotid plaque have been able to show statistically significant correlation between histological microvessel density and histological staining of vascular and angiogenic markers (CD31 & CD68) respectively with CEUS signal (62, 63). Additionally, both of these studies utilize a quantitative quantification method based on the microbubble signal intensity.

In the same manner that liver CEUS assesses different phases of a microbubble bolus injection, a similar assessment of the carotid plaque in the late phase has also been developed. In an initial study of 37 patients comprising of 16 symptomatic and 21

asymptomatic carotid plaques, flash imaging using an MI of 0.34 captured the microbubble plaque signal intensity at 6 minutes after bolus injection (64). After offline blinded image quantification, the late phase (LP) plaque signal was 0.39 (95% CI; -0.11-0.89) in the symptomatic group and -0.69 (95% CI; -1.04 – (-0.34)) in the asymptomatic group yielding a statistically significant difference between the groups ($p=0.0008$). A further histological validation study using quantitative immunohistochemical analysis of CD31 and CD68 correlated to the normalised LP-CEUS plaque signal was performed in 31 patients (65). Percentage area immunopositivity was significantly higher in patients with a LP signal intensity ≥ 0 versus < 0 for both CD68 (mean 11.8 versus 6.68, $p=0.004$) and CD31 (mean 9.45 versus 4.82, $p=0.025$. As CD31 and CD68 correspond to inflammation and angiogenesis respectively it was suggested that SonoVue was either adherent to the plaque endothelium or phagocytosed by macrophages enabling their retention for detection at 6 minutes after bolus administration.

Detection of carotid plaque neovascularization is not without its pitfalls. Visual grading systems for plaque signal have been employed due to both the naivety of available quantification software and the presence of artifactual signals e.g. calcium within or overlying the plaque which may produce spurious results if automated quantification is used. One particular phenomenon is observed in the far wall of carotid plaques during the dynamic phase of a microbubble bolus known as pseudoenhancement. This has been elegantly demonstrated in a study that revealed that this pseudoenhancement was dose dependent (66). Thirty-one patients with 50-99% NASCET carotid stenosis underwent a 2ml bolus of SonoVue with the final 10 patients also receiving 1ml SonoVue bolus after 15 minutes. Regions of interest using Philips QLab software were placed over the near wall, the far and the centre of the carotid lumen with TICs produced for each of these locations. The far wall was found to be significantly more echogenic than the near wall with a 2ml bolus ($p<0.001$). The signal intensity in the far wall was also significantly higher with a 2ml bolus compared to a 1ml bolus ($p=0.012$). This finding suggests that the concentration of microbubbles within the lumen has a proportional effect on the far

wall signal and this was confirmed by visual inspection of the far wall TIC with the TIC of the lumen revealing a synchronous rise which was not observed in the TIC of the near wall. This was believed to be due to non-linear propagation of microbubble signal through a contrast dense lumen. Therefore, this study suggests that if quantitative analysis of a carotid plaque is attempted, it should ideally be performed using the near wall plaque until methods of negating this pseudoenhancement are developed in quantification.

Ultrasound has been identified as the first line imaging modality in both DVT and carotid atherosclerosis. However, as well as the generic limitations of ultrasound imaging previously discussed, there are disease specific limitations for these two conditions specifically related to the sensitivity of these investigations. CEUS represents an incremental adjunct to the current imaging strategies for these conditions with potential for incremental improvement in diagnosis as well as moving toward aiding subsequent treatment decisions.

2. VENOUS THROMBOEMBOLISM AND POST THROMBOTIC SYNDROME

2.1. Definition

Deep vein thrombosis (DVT) occurs when a thrombus forms in a deep vein, commonly in the leg and has an estimated first episode incidence in Western populations of 50.4 per 100 000 person years (67). Pulmonary embolism (PE) occurs when a part of a DVT dislodges and travels to the lungs leading to a blockage in pulmonary blood flow. Venous thromboembolism (VTE) encompasses both conditions of DVT and PE and causes 25,000 deaths per year in the United Kingdom (68). This is normally as a result of PE and those that do survive life threatening episodes commonly have a protracted hospital stay, require lifelong warfarin and some develop post thrombotic syndrome (PTS) (68).

PTS is caused by chronic venous hypertension secondary to venous reflux and venous obstruction leading to valvular dysfunction(69). It is characterised by pain, swelling, a sensation of heaviness, oedema, pigmentation, and deterioration of the skin leading to possible venous ulceration (70). PTS develops in 25-50% of cases of DVT and leg ulceration is observed in 6-10% of cases (71, 72). This can lead to significant morbidity with reduced quality of life as well as a significant socioeconomic cost as the mean age of patients is 56 (71).

2.2. Current Management of VTE

The goals of therapy in VTE are undertaken to address the following sequelae of VTE:

1. Lower limb symptomatic disease
2. Development of pulmonary embolus
3. Recurrent venous thrombosis
4. Development of post thrombotic syndrome

Currently, the management of VTE focusses on anticoagulation, mobilisation and compression. The Antithrombotic and Thrombolytic Therapy Evidence Based Clinical Practice Guidelines from the American College of Chest Physicians 2012 recommend anticoagulation in the acute phase achieved using either low molecular weight heparin or unfractionated heparin both of which are inhibitors of clotting factor Xa. Treatment is then continued unless contraindicated with Vitamin K antagonists such as warfarin for 3-6 months for first episodes of VTE and lifelong for recurrent episodes of VTE. Compression using elastic compression stockings (class II, 30mmHg) should be started immediately and should be continued for a minimum of two years. Early ambulation is recommended as soon as is feasible in acute VTE (73).

Anticoagulation is effective in preventing thrombus propagation, PE, death and recurrence ,however, it does not achieve complete thrombus dissolution leaving residual venous obstruction and subsequent valvular dysfunction which as discussed can lead to PTS (69). Compression therapy has been shown to reduce the risk of PTS by 50% (74, 75). The exact mechanism by which this occurs is not well understood, however, it is hypothesized that compression assists the muscle pump and counteracts the effects of venous hypertension (76).

2.3. Thrombolysis for VTE

Thrombolysis is a treatment used to dissolve thrombus and subsequent emboli to restore blood flow in a vessel. Thrombolytic agents are enzymes which indirectly act to increase fibrinolysis and include urokinase, streptokinase and tissue plasminogen activator (tPA). Thrombolysis is used in conditions such as acute myocardial infarction, ischaemic stroke, acute peripheral artery thrombosis and PE.

A 2004 Cochrane review by Watson et al showed a significant risk reduction of developing PTS with thrombolysis compared to anticoagulation (RR 0.66; CI 0.47-0.94). Additionally, there was a non-significant trend toward less venous ulceration in the thrombolysis group and there was a significant improvement of vein patency on venography with thrombolysis. It was suggested that acute removal of thrombus in DVT by thrombolysis prevents valvular destruction and thus reduces the incidence of PTS in this population. However, it concluded that bleeding complications ranging from stroke to bleeding access sites was a major barrier to widespread clinical use of thrombolysis in the treatment of DVT with further work required to identify the optimum regimen, route of administration and suitable patient population (72).

2.4. Surgical Thrombectomy for VTE

Open surgical thrombectomy was historically the treatment of choice for extensive lower limb DVT. Thrombectomy was performed to restore venous circulation and this was commonly combined with ligation of the femoral vein to prevent PE. For extensive ileofemoral DVT, the procedure is performed via a groin incision and a thrombectomy catheter such as a Fogarty catheter is used to retrieve the thrombus (Figure 4). Distal embolisation is prevented by balloon occlusion or caval filter inserted via the contralateral groin or through use of positive pressure ventilation (77).

A meta-analysis performed by Casey et al identified 10 studies comprising 1186 patients comparing surgical thrombectomy to anticoagulation (78). When compared to anticoagulation, surgical thrombectomy was associated with a significant reduction in the risk of developing PTS (RR 0.67; 95% CI 0.52-0.87), however, the overall quality of the evidence was low. Additionally, no significant difference was observed between surgical thrombectomy and anticoagulation on the outcomes of death (RR 0.80; 95% CI 0.10-6.22), PE (RR 0.56; 95% CI 0.08-4.18) or recurrence of DVT (RR 0.69; 95% CI 0.24-2.01). Adverse events of surgical thrombectomy included wound seroma and below-the-knee amputations although overall reporting of adverse events across the studies included was poor.

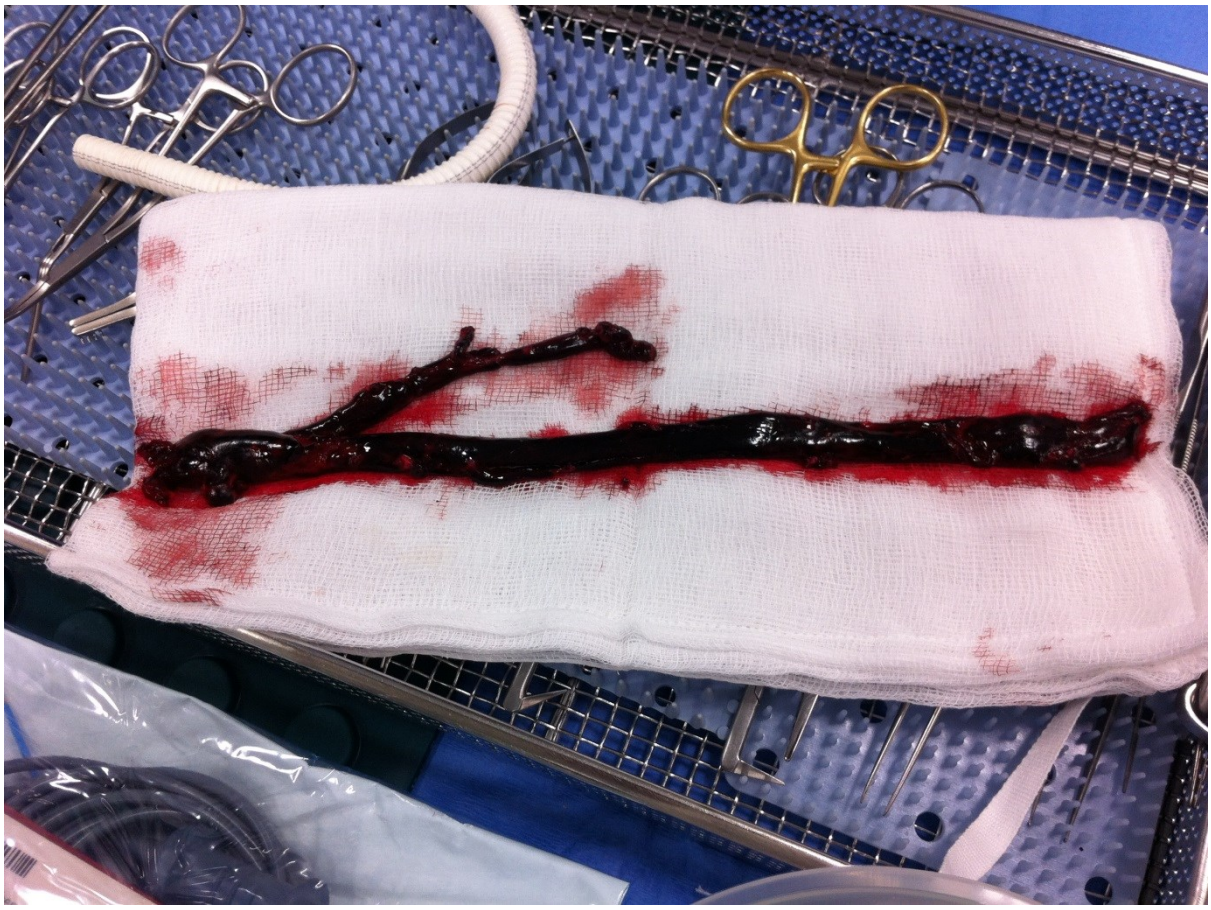

Figure 4 Surgical thrombectomy specimen of an extensive thrombus involving the common, superficial and profunda femoral veins. Picture reproduced with permission from I.J. Franklin.

Open surgical thrombectomy is only reserved for those who have contraindications to pharmacological thrombolysis, in whom other modalities have failed and in phlegmasia cerulea dolens (73, 79). However, currently surgical thrombectomy is now rarely performed due to the introduction of new percutaneous thrombolytic techniques which are less invasive and demonstrate a trend toward better outcomes (78, 80).

2.5. Catheter Directed Thrombolysis for VTE

Catheter Directed Thrombolysis (CDT) is a novel percutaneous technique used to treat acute DVT. A catheter is passed into the affected vein and advanced to the thrombosed segment. Thrombolytic agents are directly infused into the thrombus via multiple side holes at the end of the catheter allowing greater local concentration of thrombolytic agent whilst avoiding high and lengthy concentrations of systemic thrombolytic agent (15, 16).

Casey et al performed a meta-analyses comparing outcomes in CDT versus anticoagulation which identified five studies comprising both randomized clinical trials and cohort studies (12). When compared to anticoagulation, CDT was associated with a significant reduction in risk of developing PTS (RR 0.19; 95% CI 0.07-0.48). The overall quality of data was low and no conclusions could be drawn regarding outcomes of death, PE and recurrent DVT. In the same study an indirect comparison was made between CDT and surgical thrombectomy, however, again due to poor quality data only a non-significant trend toward reduction in risk of developing PTS with CDT (RR 0.33; 95% CI 0.00-2.28) could be demonstrated. Recently, Enden et al published results of the CaVenT trial which was an open label, multi-centre, randomized trial of 209 patients comparing conventional therapy of anticoagulation and elastic compression to conventional therapy plus CDT for ileofemoral DVT (81). At 24 month follow up, in 189 patients there was an absolute risk reduction for the endpoint of PTS assessed by Villalta scoring of

14.4% (95% CI 0.2–27.9) in those allocated to CDT compared to control with a number needed to treat of 7. Ileofemoral patency at 6 months was also significantly improved with CDT with 65.9% versus 47.4% in the control group. However, in 101 patients randomized to CDT there were 20 bleeding complications recorded although the authors suggest that only 8 were clinically relevant of which 3 were classified as major and 5 minor. The three major bleeding complications were related to the puncture site including one abdominal wall haematoma, one compartment syndrome of the calf and one inguinal haematoma although no impaired outcome was recorded. Although, this study showed a significant improvement in the clinically relevant long term outcome endpoint of PTS, bleeding complications still require improved technique and careful patient selection for CDT.

2.6. Pharmaco-Mechanical Thrombectomy for VTE

To improve the efficacy of CDT, combination with percutaneous mechanical thrombectomy devices has been developed known as pharmaco-mechanical thrombectomy (PMT). The PMT devices provide mechanical agitation and breakdown of the clot surface to increase the surface area that thrombolytic agents can act upon (Figure 5). Eligibility criteria for PMT follow the same as those for CDT which include: extensive proximal (ileofemoral) DVT less than 14 days from symptom onset or acute findings on duplex, life expectancy >1 year and low risk of bleeding (73).

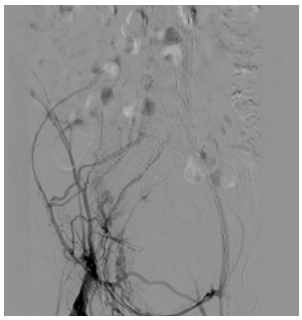

(A)

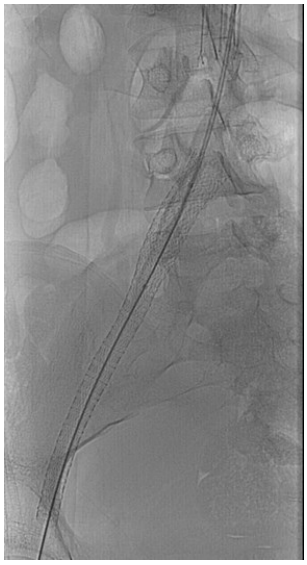

(B)

(C)

Figure 5 PMT and left common and external iliac vein stenting with IVC filter. A – prone venography demonstrating extensive thrombus within the left common and external iliac vein. B - Placement of 14 x 120 mm and 14 x 60 mm Veneti bare metal self-expanding stents. C – Completion venography with satisfactory flow with no residual stenosis and stents in situ

Thrombus removal of >50% was reported between 59-92% of cases in studies assessing both Angiojet and Trellis (82-84). When compared to CDT, PMT using Angiojet showed a significantly reduced mean intensive care unit admission and significantly reduced overall hospital length of stay with a correspondingly reduced lower total hospital cost (85). Whilst initial and midterm results of PMT using Angiojet and Trellis are encouraging, studies consist mainly of case series and retrospective cohort studies with poor reporting of long term clinical outcomes such as PTS.

The two PMT devices currently approved for use for the treatment of DVT by the US Food and Drug Administration (FDA) are: the Angiojet® Thrombectomy system (Medrad/Possis Inc., Minneapolis, MN, USA) and the Trellis™-8 Peripheral Infusion System (Covidien, Mansfield, MA, USA). The Angiojet system utilizes alternating water jets with low pressure to create a vacuum at the tip of the catheter to produce breakdown at the thrombus surface. Pulse spray infusion of thrombolytic therapy can then be applied to penetrate the thrombus and an efferent port can aspirate small particles produced (82). The Trellis system utilizes a rotating guidewire within a segment of thrombus isolated between distal and proximal balloons to breakdown the thrombus surface with thrombolytic agents infused and an aspiration port for residual particles once treatment is complete (86).

A further PMT device that is currently being investigated is ultrasound (US) accelerated CDT. The use of high frequency, low power microsonic energy increases lysis of a thrombus which enables enhanced penetration of the thrombus by thrombolytic agents (87). The EKOS Endowave® system (EKOS Corporation, Bothell, WA, USA) uses a multi-lumen drug delivery catheter with matching US coaxial core wires with transducer elements positioned approximately 1cm apart along the tip. In one case series of thirteen patients using EKOS Endowave, 85% complete clot lysis (defined as >90% restored patency) was achieved with no further occlusion identified after the initial hospital stay at 6 month follow up, however, no

further clinical outcome follow up was reported (88). Additionally, an 8% bleeding complication rate was reported due to bleeding at the catheter insertion site and in the calf muscle.

Randomized controlled trial data needed to fully evaluate the role of PMT in the treatment and long term clinical outcome in DVT should be provided by the ATTRACT trial which will enroll 692 participants to either PMT and anticoagulation versus anticoagulation alone with incidence of PTS assessed at two year follow up (89). Despite this forthcoming data, PMT remains limited by patient selection as up to 75% are excluded from intervention due to exclusion criteria such as age, renal impairment, prolonged symptom duration, short life expectancy and active malignancy (90). Therefore, novel strategies for acute thrombus removal in DVT should continue to be investigated and developed.

3. DEEP VEIN THROMBOSIS AGEING

3.1. Current Clinical Assessment of DVT Ageing

Risk stratification, such as the Wells score, helps guide pre-test probability for the diagnosis of DVT as clinical assessment alone is proven to be unreliable, however, these assessment tools do not determine the age of the thrombus (91-93). The current gold standard first line investigation for diagnosing DVT is venous duplex ultrasound, combining colour flow Doppler imaging with compression ultrasonography (40, 94). This modality is unable to accurately differentiate between acute and chronic thrombi (95, 96). Therefore, patient reporting of symptoms which is a known poor predictor of thrombus volume and characteristics remains the only clinically employed method of determining thrombus age (97).

Accurate staging of DVT has gained clinical relevance with the recent introduction of novel oral anticoagulants, such as Rivaroxaban, for the treatment of symptomatic DVT as well as refinement of techniques of acute thrombus removal for extensive proximal DVT to prevent the development of PTS (98-100). The majority of bleeding complications observed with Rivaroxaban occur in the first three weeks during twice daily dosing regimens, therefore, with accurate aging techniques, patients with proven older thrombi may be spared exposure to higher dosing (100). Catheter directed thrombolysis (CDT) and pharmacomechanical thrombolysis achieve local lysis of thrombus, preserving the vessel lumen and valvular function which is not achieved by anticoagulation therapy. Current recommendations for CDT in the USA and UK are within the first 14 days of symptoms to minimise the risk of complications from attempting to treat an older, organized thrombus (98, 99). However, evidence for this has been graded as 2C by the Society of Vascular Surgery (SVS) with recognition that a 14 day threshold period may be arbitrary and that benefit may still be gained by treating patients with symptoms greater than 14

days (101). Conversely, significantly poorer outcomes for vein and valve competence have been reported for patients with symptoms greater than 14 days compared to those with symptoms less than 14 days (50% vs. 84%, p=0.0004) (102). This demonstrates the potential weakness of relying on patient reporting of symptoms and highlights the need for improved accuracy of patient selection for acute thrombus removal to provide both improved prognostic markers for intervention and reduction of unnecessary exposure to procedural risk.

The aim of this review is to assess both experimental and clinical studies of imaging modalities that can objectively and accurately determine thrombus age for potential use in clinical practice.

3.2. Systematic Review Methodology

Preferred Reporting Items for Systematic reviews and Meta-Analyses (PRISMA) guidelines were followed to perform a systematic review of the literature (103). PubMed and EMBASE databases were searched from 1948 up until March 1st 2015 independently by two reviewers (BD, VS). The following, mutually agreed search terms were used: 'deep vein thrombosis ageing', 'deep vein thrombosis age', 'deep vein thrombosis stage', 'deep vein thrombosis staging', 'deep vein thrombosis imaging', 'deep vein thrombosis staging imaging', 'deep vein thrombosis aging imaging'. Studies were eligible for inclusion if endpoint measurements included assessment of venous thrombi age using imaging techniques. Experimental animal in-vivo studies and human clinical studies including randomised controlled trials (RCT) to case series were eligible for inclusion. All review articles, case studies, editorials, letters, articles not in English and duplicates were excluded. Manual searching of reference lists from articles included in the full-text stage of the review was performed as well as use of the "related citations" function on PubMed during the abstract stage of the search onwards. On completion of title and abstract

screening, full text articles were independently assessed by the two reviewers for methodological quality for inclusion and where discrepancies occurred a joint analysis was conducted to reach a consensus. Systematically extracted data was collected using the following sections: thrombosis aging modality, experimental or clinical setting, study design, thrombus ages assessed and thrombus aging outcomes.

Initial literature searches revealed a lack of RCTs assessing thrombus aging by any modality. Therefore, included clinical studies were assessed for bias using the QUADAS-2 tool (104). Experimental animal in-vivo studies were included in this review due to the lack of clinical RCT evidence and as no gold standard exists for the onset of thrombus formation in clinical studies in lieu of relying on patient reported symptoms which are known to be unreliable for such assessment (97). These experimental studies provide thrombi whose age can be precisely recorded and reliably correlated to the findings of the imaging modality being investigated as well as ex-vivo thrombus assessment which is also not always possible in clinical studies. Whilst humans are unique in their ability to develop spontaneous DVT, the application of animal models particularly in rodents and primates has been well validated for the investigation of thrombogenesis , resolution and treatment (105, 106). However, in the context of this review it is acknowledged that findings from experimental studies will require clinical translation and validation.

3.3. DVT Ageing Imaging Assessment

3.3.1. Search Results

The search terms returned 13,724 articles. After exclusion of duplicates, screening process and identification of further articles using a manual reference search or the "related citation" function, 20 studies were included for the review. The PRISMA diagram representing the search results of the systematic review is shown in Figure 6.

Previous analysis of techniques for aging DVT identified ultrasound (US) and magnetic resonance imaging (MRI) as key imaging modalities (107). This contemporary systematic search identified further studies in both US and MRI with 10 and 6 studies being included for each modality respectively. Photoacoustic and nuclear imaging modalities were also studied. Quantitative data synthesis could not be performed due to significant heterogeneity in study design and endpoint measurement across included articles most notably highlighted by the inclusion of animal in-vivo and human clinical studies. Quality assessment of human clinical studies using the QUADAS-2 tool demonstrated a high risk of bias across all domains of: patient selection, index test, reference standard and flow and timing. Methods and outcomes for US related studies are summarised in Table 2 whilst MRI studies are summarised in Table 3.

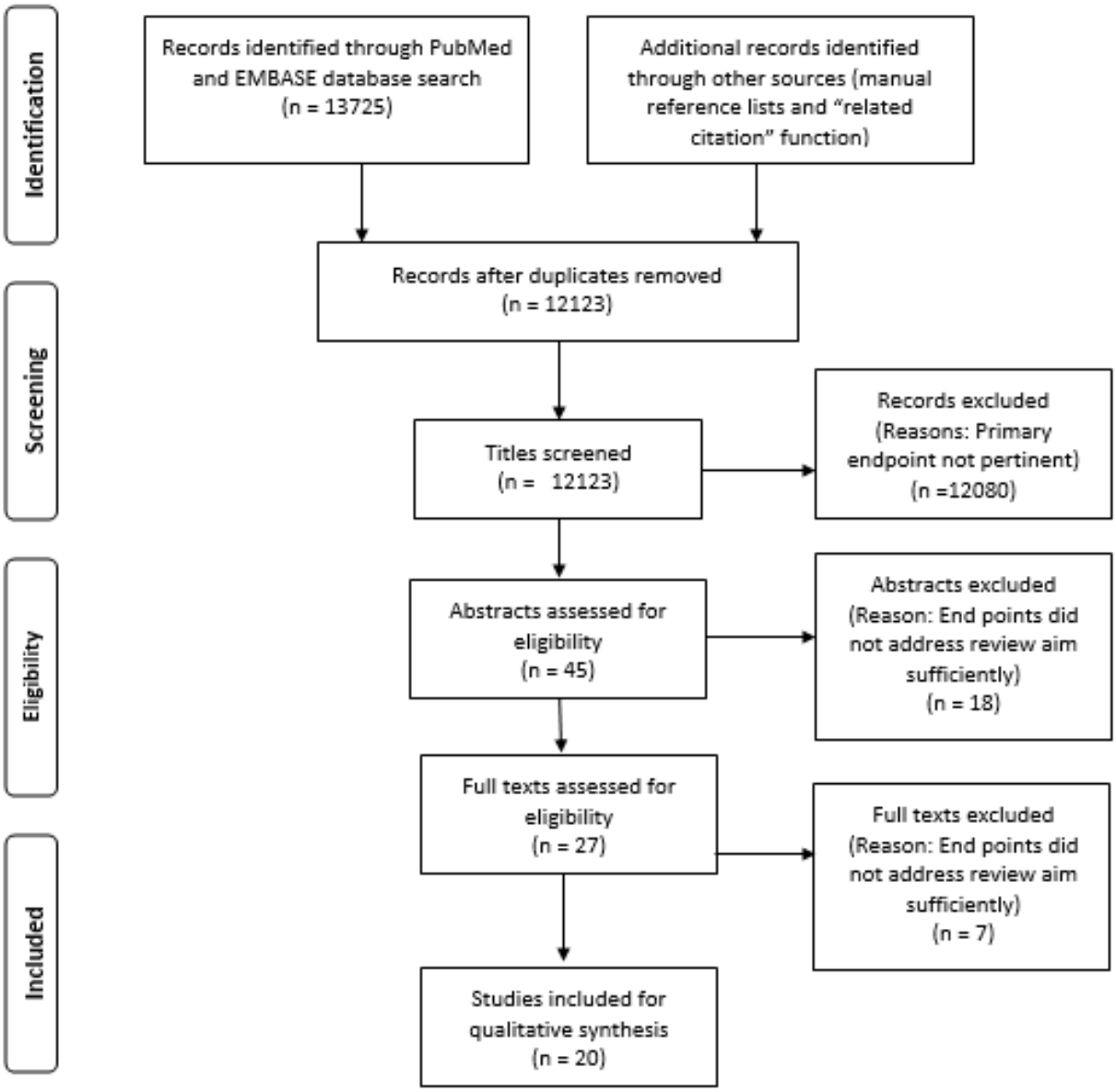

Figure 6 Preferred Reporting Items for Systematic Reviews and Meta-Analyses (PRISMA) diagram for DVT ageing review.

3.3.2. Ultrasound techniques

Ultrasound and ultrasound related techniques have been the most studied modality for the determination of age of DVT. Early studies investigated the use of conventional US, however, in order to remove the subjectivity and qualitative criteria traditionally employed in US assessment, quantitative measures were investigated. Spectrum analysis of radiofrequency ultrasound signals reflected from the ultrasound-tissue interface has been shown to enable tissue characterisation (108). In surgically induced thrombi within the jugular veins of pigs, thrombi of 7 and 14 days old were differentiated to acute thrombi at day 1 as they were shown to demonstrate a significantly different spectrum analysis using parameters of slope and intercept values. The difference in tissue characterisation over this time was explained by red cell mesh density reduction, which occurs due to partial spontaneous thrombolysis. Quantitative assessment of echogenicity has also been studied within in-vivo IVC ligation models of rats and primates (109). After calibration of gain for the intended field of view, B-mode images were transferred for offline image quantification using pixel values within a region of interest placed over the thrombus to provide a quantitative measurement of echogenicity. Echogenicity was found to significantly increase over 6 hours, 2 days and 6 days after thrombus induction in both the rat and primate models. In addition, this was significantly correlated with fibrin content analysis of the ex-vivo thrombi at these time points.

Clinical assessment of DVT echogenicity measurement has been investigated using Grayscale Median Analysis (GSM) which has been previously described in the analysis of atherosclerotic plaques (110, 111). In a study of 128 venous segments, GSM analysis of DVT age was compared to both time of symptom onset reported by patients and qualitative thrombi age assessment by 2 blinded expert sonographers (112). Mean GSM was significantly lower in thrombi with a symptom onset of less than 2 weeks whilst mean GSM was higher in thrombi aged between 2 weeks and 3 months. GSM agreement with the expert sonographers was 70% overall, however,

the agreement was only 58% for thrombi aged between 2 weeks and 3 months. Whilst measurements of echogenicity appear to depict the structural characteristics of the aging thrombi, it remains limited by initial subjective image calibration, in particular, the gain used at the time of image acquisition which can have a significant impact on offline GSM analysis.

Further insight into thrombus organisation with age led to the hypothesis that strain analysis by elastography can detect, diagnose and stage DVT. Elastography is a non-invasive, US adjunct that differentiates between tissues of different elasticity. This is based on an estimation of strain during tissue compression and expansion, which in its earliest form was delivered in a freehand fashion by the operator. In an initial study, thrombi were surgically induced in 15 rats and allowed to age for 2 days, 6 days or 9 days before imaging with US elastography prior to being euthanized and visual inspection of the clot and vessel being performed (113). As expected due to increased fibrin organisation, older clots were significantly firmer and more regular than younger ones, which was subsequently confirmed on further studies also assessing this method of freehand push elastography (114, 115).

Elastography accuracy to within an average of 0.8 days in thrombi aged up to 10 days of age was demonstrated in a similar rat model of thrombosis to early studies (116). This was subsequently validated using direct mechanical measurement of ex vivo thrombi compared to imaged thrombus elasticity measurements in vivo (117). Beyond 10 days, as organisation into a chronic thrombus occurs, discrepancies arose in accuracy between the ex vivo mechanical measurement and the in vivo imaging prediction.

US elastography has been assessed in preliminary clinical studies. A pilot study assessed two patients with thrombi at relatively different ends of the thrombus age spectrum; a 48 year old male with a chronic thrombus (at least 3 years in age) and a 42 year old male with a sub-acute thrombus (25 days in age) (118). Elastography

was used to provide a quantitative assessment of strain magnitude as an inverse surrogate measure of clot firmness normalised against the strain magnitude of the surrounding vessel wall. The chronic clot was homogeneous and had a strain magnitude less than 10 fold that of the vessel wall indicating a harder clot whereas the acute clot was more heterogeneous and had a strain magnitude which was 4 times greater than the surrounding vessel wall. The same group subsequently performed a prospective clinical study of 54 patients; 26 with acute DVT (mean age 5.7 days) and 28 with chronic DVT (mean age > 8 months)(119). The median normalised strain magnitude for acute cases was 2.78 (Interquartile Range (IQR): 2.4-3.71) suggestive of softer thrombi, compared to 0.94 (IQR: 0.48-1.36) in chronic cases with a median relative echogenicity of 1.4 (IQR: 1.17-1.54) for acute thrombi and 4.5 for chronic thrombi (IQR 2.5-7.5). Differences in both measures between acute and chronic thrombi were statistically significant.

Strain analysis using US elastography may be performed as a simple adjunct to the current gold standard for imaging acute DVT of venous duplex US (98, 99). Most mid to high end US platforms already incorporate the necessary software to perform elastography making it a cheap and easy to perform adjunct to conventional US as evidenced by its established role in liver, breast, pancreas and thyroid imaging (120-124). Whilst the techniques of freehand push elastography used in the described studies introduce potential variation in accuracy, US platforms that use an automated standardised propagation of mechanical waves delivered by the US probe such as shear wave elastography may provide improved quantification and reproducibility (124-126). Currently, the diagnosis of DVT includes compression ultrasonography, however, US Elastography could be implemented as an adjunct to aid detection of thrombus and provide subsequent assessment of acute versus chronic thrombus thereby reducing the pain that some patients experience from compressional US techniques (127).

Conventional US analysis at present appears unreliable for accurate assessment of thrombus age to guide contemporary intervention. However, adjunctive US Elastography may provide more detailed information regarding thrombus characteristics to provide an estimate of thrombus age. Ultrasound based techniques remain limited by variations in operator technique and subjective assessment of the imaged field of view. Despite objective offline image quantification, the analysis performed is dependent on the initial image acquisition. Therefore, further validation of these techniques will require rigorous assessment of imaging reproducibility. Additionally, quantification issues, such as accurately distinguishing thrombi corresponding to the sub-acute phase in humans, (117),(105) need to be resolved before suitability for CDT can be reliably performed in clinical practice using US based techniques.

Study, year	Ultrasound technique	Study setting	Thrombus model	Thrombus ages	Outcomes
Parsons et al [19], 1993	Colour Doppler Ultrasound	In vivo	Porcine jugular vein	30 minutes, 1, 7 & 14 days	Differences in spectrum analysis of radiofrequency ultrasound signal characterisation of thrombi statistically significant for thrombi at day 7 and day 14, P<0.01
Fowlkes et al[20], 1998	B mode ultrasound echogenicity	In vivo	Rat & Primate IVC	6 hours, 2, 6 & 13 days	Quantitative thrombus echogenicity measurements significantly increase between 6 hours, 2 and 6 days, P<0.05. Increased echogenicity correlates with histological thrombus fibrin content
Emelianov et al [24], 2002	Elastography	In vivo	Rat IVC	2, 6 & 9 days	Normalised strain measurements show increased clot Young's modulus demonstrated over days 2, 6 & 9 as it hardens, matures and organizes
Rubin et al [29], 2003	Elastography	Clinical	Lower limb DVT	25 days & 3 years	Chronic clot homogenous with strain x10 smaller than vessel wall. Subacute clot heterogeneous with strain x3-4 greater than vessel wall (n=2)
Xie et al [27], 2004	Elastography	In-vivo	Rat IVC	3, 4, 5, 6, 7 & 10 days	Strain magnitude progressively decreases as clot ages. Using normalisation from vessel wall, clot age could be estimated to within 0.8 days
Aglyamov et al [26], 2004	Elastography	In-vitro & in-vivo	Gelatin phantom & rat IVC	2 & 9 days	Circular simulation model developed for mechanical measurement in-vitro for improved elasticity reconstruction is feasible to provide accurate measurements of aging for real world elliptical vessel and clot as found in-vivo and clinically
Xie et al [28], 2005	Elastography	In-vivo & ex-vivo	Rat IVC	3, 6, 10, 12 & 14 days	Direct mechanical measurement of Young's modulus shows good temporal agreement up to 10 days in both ex-vivo and in-vivo conditions
Geier et al [25], 2005	Elastography	Ex-vivo	Explanted porcine iliac vein	1, 3, 6, 9, 12 & 15 days	Significant decline in mean thrombus strain between days 6 & 12, P<0.01. Three-fold increase in hardness correlated to increase in fibroblast and collagen histologically
Rubin et al 30, 2006	Elastography	Clinical	Lower limb DVT	Acute (<14 days) & Chronic (>8 months)	Median normalized strain value in acute group was 2.78 (n=26) and in the chronic group was 0.94 (n=28) which was highly significant, $P<10^{-7}$
Cassou-Birckholz et al [23], 2011	Gray Scale Median analysis	Clinical	Lower limb DVT	Acute (<14 days) & Sub-acute (0.5 – 3 months)	Thrombus mean GSM 23 ± 12 for acute thrombus (n=78) versus thrombus mean GSM 31 ± 14 for sub-acute thrombus (n=50), P=0.004

Table 2 Characteristics of included studies for DVT ageing using ultrasound techniques.

3.3.3. Magnetic Resonance Imaging Techniques

In modern clinical practice MRI is increasingly accessible; in particular, it is advocated as an imaging modality for diagnosis and extent of DVT, however, it remains a more expensive option compared to conventional US (127). In cases of suspected ileofemoral DVT that may considered for early thrombus removal, the

SVS recommends adjunctive imaging such as MRI to characterize the most proximal extent of the thrombus (101). This may be employed in cases where conventional US cannot determine the most proximal extent of a thrombus or where there is a high clinical suspicion of isolated ileofemoral DVT but where the US is negative.

Initial studies investigating staging DVT used Gadolinium enhanced magnetic resonance venography (MRV) in 14 patients (8 men, 6 female) in whom ileofemoral DVT had been diagnosed using Duplex US (128). Acutely thrombosed veins had a significantly larger diameter than normal veins (16.3 ± 0.84 mm vs 13.5 ± 0.55 mm, respectively; $p = 0.01$) whilst displaying a peripheral rim enhancement referred to as a "bull's-eye sign." Additionally, the rim-centre ratio, comparing signal intensity at the vessel rim compared to that of the lumen decreased significantly over time from a mean of 2.38 ± 0.17 over the first 14 days to 1.29 ± 0.44 from imaging performed over the following 14 days.

In an attempt to make the assessment of thrombus age more accessible for clinical reporting, the qualitative presence or absence of age dependent Gadolinium-enhanced MRI observations were assessed to characterize thrombi into acute, sub-acute, chronic and acute on chronic thrombi (129). As described, acute thrombi were dilated with thin walled rim enhancement, sub-acute thrombi displayed increased wall thickness and enhancement with minimal recanalization of the lumen, chronic thrombi had normal vessel and wall calibre but contained partial residual luminal thrombus and areas of fibrotic strands and acute on chronic thrombi displayed fibrotic strands within an acutely dilated vein containing homogenous low signal from a new thrombus. In this retrospective study of 53 cases, there was good reproducibility of age characterisation between both expert and novice MRI readers. However, in the absence of a true gold standard measurement of DVT age, comparison between the expert reader and patient reported symptom duration revealed a broad overlap in symptom duration between acute, sub-acute and chronic MRI characterised thrombi.

Magnetic Resonance Direct Thrombus Imaging uses methemoglobin as a surrogate for haemoglobin age. This eliminates the requirement for intravenous blood pool contrast agents, such as gadolinium, which carry the potential for adverse effects (130),(131) and has already been extensively studied clinically for the detection of haematomas and intracoronary arterial and venous thrombi (132-135). In a prospective study of 43 consecutive patients, there was normalisation of the hyper-intensive T1 signal in Magnetic Resonance Direct Thrombus Imaging in 90% of patients within 3 months and 100% of patients over a 6 month period (136). This result contradicted findings of compression ultrasonography performed on the same cohort which revealed that US images did not normalise in one third of the cohort over the same period.

With the development of novel MRI sequences for DVT aging, in-vivo studies have been required for validation. Thrombus protein content, acting as a surrogate for thrombus aging, can be detected using magnetic transfer (MT) and diffusion weighted imaging (DWI) MRI. In-vivo imaging of these two parameters was compared to thrombus histology using an inferior vena cava thrombosis mouse model (137). There was positive correlation between the MT rate and the histologically confirmed protein content of the thrombus which increased significantly at days 14, 21 and 28. The MT rate was also able to differentiate between erythrocyte and protein rich thrombi. Combined analysis of both MT and DWI MRI imaging was therefore able to identify intermediate, sub-acute aged thrombi in this model with good sensitivity and specificity.

Two recent MRI studies have moved away from determination of thrombus age specifically and instead used imaged thrombus properties to determine suitability for thrombolysis. In a mouse model of inferior vena cava thrombosis, the T_1 relaxation times of thrombi of different ages (Day 1, 4, 7, 10, 14 ,21 and 28) were quantified and compared with successful thrombolysis defined as restoration of greater than 50% of vessel flow 24 hours after treatment (138). Thrombi with the shortest T_1

relaxation time, which tended to occur at day 7, had the best result from thrombolysis therapy. T_1 shortening was caused by production of paramagnetic Fe^{3+} from the oxidized iron content of the erythrocyte rich acute clot. As thrombus organisation occurs after day 7, macrophages remove accumulated Fe^{3+}, and therefore, the T_1 lengthens until it equalises with that of the surrounding tissue. In a second study using the same in-vivo DVT model, the thrombus relaxation time using a gadolinium based fibrin specific contrast agent was assessed (139). The change in thrombus relaxation time pre and post fibrin specific contrast administration was greatest between days 7 and 10 indicating a fibrin rich clot which was also correlated with thrombus histology. Therefore, fibrin content identification using MRI was able to select those thrombi that would be susceptible to fibrin specific thrombolytic agents such as tissue-type plasminogen activator.

MRI presents a viable option for imaging DVT with evidence of accurate thrombus aging of acute, sub-acute and chronic thrombi as well as potential susceptibility to thrombolysis. Coupled with this accuracy of DVT staging, the use of MRI would also allow for complete assessment of the lower limb, pelvic and abdominal venous vessels to be undertaken, thus providing a comprehensive temporal, structural and anatomical guide for acute interventions such as CDT. Furthermore, whilst more expensive in comparison to US, MRI provides objective standardisation and simplification of the diagnostic process, with less operator dependency in comparison to free hand probe techniques although robust clinical validation of these novel techniques is required. Additionally, practical issues such as accessibility, in particular, of specific contrast agents and MRI sequences coupled with the cost effectiveness of implementation in comparison to US currently limit widespread clinical use.

Study, year	Imaging Modality	Study setting	Thrombus model	Thrombus ages	Outcomes
Froehlich et al [40], 1997	Gadolinium enhanced MRI	Clinical	Ileofemoral DVT	1, 3, 5, 7, 14, 21, 30 & 90 days	Ratio of gadolinium enhancement at rim and centre of thrombus derived, Rim-centre ratio was 2.38±0.17 (n=31) for thrombi <14 days and 1.29±0.44 (n=8) for thrombi >14 days, P<0.001
Westerbeek et al [48], 2008	MRDTI	Clinical	Lower limb DVT	2 days, 3 & 6 months	MRDTI signal normalised in all patients at 6 months (n=39) compared to 30.8% (12/39) who still had abnormal findings on compression ultrasound
Phinikaridou et al [49], 2013	MRI	In vivo	Mouse IVC	1, 7, 14, 21 & 28 days	%MTR of thrombus shows positive correlation with protein content of clot histologically with significant temporal increase in %MTR from day1 to day 28 thrombus, P<0.05. DW-MRI able to identify intermediate thrombus (days 7-14)
Saha et al [50]. 2013	MRDTI	In vivo	Mouse IVC	1, 4, 7, 10, 14, 21 & 28 days	Shortest T1 relaxation time observed at day 7 which correlated with the best result from thrombolysis therapy and highest Fe^{3+} content from erythrocyte rich thrombus
Arnoldussen et al [41], 2014	Gadolinium enhanced MRI	Clinical	Common Femoral DVT	2 – 32 days (n = 53)	Qualitative assessment for pre-determined imaging findings for acute, sub-acute and chronic thrombi showed good reproducibility between expert (κ=0.97) and novice readers (κ=0.82)
Andia et al [51], 2014	Fibrin specific gadolinium enhanced MRI	In vivo	Mouse IVC	2, 4, 7, 10, 14 & 21 days	Shortest thrombus relaxation time on contrast enhanced imaging correlated with greatest fibrin content histologically (R=0.0889) and prediction for susceptibility to thrombolysis by tissue-type plasminogen activator

Table 3 Characteristics of included studies for DVT aging using MRI techniques.

3.3.4. Other imaging modalities

Nuclear medicine imaging has been investigated with Technetium 99m-apticide used to radiolabel glycoprotein IIb/IIIa expressed in activated platelets, which are particularly plentiful in acute DVT (140). In a study of 78 patients with acute and chronic DVT there was a 92% sensitivity and 82-90% specificity between two expert readers in characterising acute from chronic DVT. In a further study, thrombus uptake of Technetium 99m labelled tissue plasminogen activator (rt-PA) was not present in all 29 patients imaged on day 30 compared to 72% with positive uptake on day 7 of an acute DVT (141). This was attributed to fewer fibrin sites available for rt-PA binding as thrombi progress from acute to chronic state. The use of functional imaging in a condition as common as DVT may not be feasible clinically, however, these techniques provide insight into the mechanisms of DVT propagation and resolution.

Photoacoustic imaging, a modality which utilises non-invasive measurements of optical absorption in tissue, has also been hypothesised for staging DVT due to thrombus changes at a cellular and molecular level. Experimental studies have demonstrated that a decrease in the fraction of blood cells over time may be represented by the magnitude of the photoacoustic signal being inversely proportional to the age of the clot (142, 143). Photoacoustic imaging may be implemented as a potential adjunct to US, however, at present, data is limited to tissue mimicking phantoms of DVT and ex-vivo animal model thrombi samples only.

3.4. Limitations

Several limitations of this study must be acknowledged. The quality of the included human clinical studies ranged from cohort studies to case series with a high risk of bias with no RCT evidence available for analysis. Additionally, the current lack of reference gold standard for DVT age in clinical practice makes robust assessment of imaging modalities especially compared to patient reported symptom duration difficult. Future studies may focus on the prognostic value of imaging modalities in predicting treatment success of acute thrombus removal or freedom from complications of treatment in acute thrombus removal and novel oral anticoagulant therapy. With respect to the experimental studies included, publication bias must also be considered and as discussed whilst animal models of DVT have limitations, these models are well validated for the investigation of thrombus biology.

3.5. Conclusion

There is significant heterogeneity and presence of bias in the data for the determination of DVT age using imaging techniques; however, the advent of many novel techniques is encouraging. A reliable imaging tool is required to help guide

safe therapy such as acute thrombus removal for ileofemoral DVT or novel oral anticoagulant treatment in lieu of relying upon a patient's history. US Elastography and MRI have demonstrated preliminary clinical translation to broadly distinguish between acute and chronic DVT with MRI also identifying sub-acute thrombi in an in-vivo setting. As both imaging modalities are clinically utilised in deep venous imaging, they warrant further investigation. Large cohort human studies, ideally with side by side comparison of modalities, will demonstrate accuracy and reproducibility as well as establish cost effectiveness for clinical implementation of these novel techniques.

4. SONOTHROMBOLYSIS

4.1. Ultrasound thrombolysis

4.1.1. Experimental Evidence

Ultrasound has been shown to accelerate thrombolytic agent fibrinolysis of clot in vitro (87, 144, 145). In early studies, application of ultrasound alone did not produce clot thrombolysis indicating that ultrasound was augmenting the effect of thrombolytic agents (144, 145). Use of radiolabelled rT-PA showed both a significantly greater rate of uptake and significantly deeper spatial penetration of rT-PA with ultrasound and rT-PA compared to rT-PA alone (87). The mechanism of ultrasound augmented thrombolysis is not well understood. Whilst the heating effect of ultrasound may increase enzymatic action, the degree of heating is insufficient to account for the significant increase in fibrinolysis (145). Ultrasound promotes oscillation of naturally occurring gas bubbles within a fluid medium. Oscillation of these gas bubbles creates an increase in local fluid motion known as microstreaming. At an interface between fluid and solid, such as an occlusive thrombus within a blood vessel, the increased fluid velocity may be able to mechanically shear the thrombus at its surface. Additionally, application of a higher intensity of ultrasound creates significant pressure changes which collapse the gas bubbles creating a local cavitation effect. The oscillation and collapse of gas bubbles by ultrasound is collectively known as acoustic cavitation which when occurs at a fluid-solid interface can cause jets in the solid enabling penetration of the solid and thus increased delivery of the thrombolytic agent into a clot (87).

In vivo animal studies have also demonstrated the use of ultrasound to dissolve thrombus. An animal study by Kawata et al. designed to model acute myocardial infarction used thrombus induced in rabbit femoral arteries by percutaneous balloon

injury (146). US combined with both high and low dose rT-PA produced significantly better angiographic grades of Thrombolysis in Myocardial Infarction (TIMI) flow than rT-PA alone again highlighting the augmentation of thrombolysis produced by ultrasound. Additionally, there was no significant difference between the grades of vessel recanalization found between high and low dose rT-PA with US. This finding may provide a role for low dose thrombolytic dosing and thus reduce unwanted side effects of thrombolytic agents. In a porcine model of DVT by Maxwell et al., thrombus was formed in the femoral vein by balloon occlusion and thrombin infusion and then exposed to pulses of therapeutic US guided by a second US imager used to align the therapeutic beam (147). In 7 out of 12 models, improved flow was seen on Doppler assessment after US treatment. In this study no thrombolytic therapy was used, instead the authors suggest that bubble cavitation represented by a cloud observed over the area of treatment on ultrasound caused mechanical breakdown of the thrombus. This contradicts earlier findings of Kawata et al. (146) despite both studies using 1MHz ultrasound and similar ranges of negative peak intensity of 0.5-1W/cm^2. The difference observed may be due to different models of thrombosis as Kawata et al. used an arterial model of thrombosis suggested to be platelet rich whilst Maxwell et al. (147) used a venous model of thrombosis which has a greater concentration of red blood cells. Additionally, the ultrasound application techniques used between the studies was different with Kawata et al. using continuous US whilst Maxwell et al. used pulsed therapeutic ultrasound guided by diagnostic ultrasound.

Studies of ultrasound thrombolysis have also demonstrated the efficacy of varying both the ultrasound frequency and power output. Nilsson et al. reported that the fibrinolytic effect of streptokinase was equally affected within a relatively low frequency range of 0.5-2.3 MHz whilst the optimal power output for clot lysis was between intensities of 0.5-1.5 W/cm^2 (148). Paradoxically, greater intensities of ultrasound resulted in reduced clot lysis with streptokinase alone displaying significantly better clot lysis than streptokinase and ultrasound at an intensity of 4 W/cm^2. Histological analysis of both in-vitro and in-vivo clot after high intensity

ultrasound application has revealed possible explanations for this phenomenon. Using an in-vitro model of endothelial cell culture, greater intercellular separation of endothelial cells with increased adhesion of leukocytes after exposure to 1MHz ultrasound at an intensity of 1.6 W/cm^2 has been observed (149). Subsequently, thrombi within a rabbit femoral artery model exposed to 1 MHz ultrasound at 2 W/cm^2 in the presence of streptokinase displayed endothelial cell vacuolation and increased platelet accumulation (150). Both studies suggest that at these higher intensities, an inflammatory process is activated by ultrasound which may create a pro-thrombotic environment leading to failure of clot lysis or rapid reocclusion.

4.1.2. Clinical Ultrasound Thrombolysis

One of the key therapeutic targets for ultrasound thrombolysis has been in the treatment of patients with acute ischaemic stroke. Systemic administration of thrombolytic agents, in particular recombinant tPA, has been shown to improve neurological outcome after ischaemic stroke through recanalisation of occluded vessels enabling restoration of flow to the threatened ischaemic penumbra of neuronal tissue within the brain (151). However, systemic thrombolysis carries a bleeding risk with symptomatic intracerebral haemorrhage observed in 6-7% of patients (152). Therefore, novel strategies to improve recanalisation rates whilst not increasing bleeding complications have been investigated. To hasten clinical translation, commercially available ultrasound platforms used clinically for transcranial Doppler (TCD) monitoring were assessed for the augmentation of clot lysis with recombinant t-PA. These TCD platforms used a frequency of 2MHz which as discussed earlier may not be in the optimal frequency range for clot lysis. Additionally, application of TCD leads to a highly variable 86-100% attenuation in ultrasound energy due to variations between patients in the temporal bone window with a subsequent variation in the intensity of ultrasound received by the target intracranial vessel to be treated (153).

The largest study assessing the 2 MHz TCD platform was the multi-centre randomized control trial Combined Lysis of Thrombus in Brain Ischaemia Using Transcranial Ultrasound and Systemic tPA (CLOTBUST) (154). One hundred and twenty-six patients with middle cerebral artery occlusion were randomized to either continuous 2 MHz TCD or placebo for 3 hours during their intravenous t-PA infusion. Whilst there was a significant difference in immediate recanalization or dramatic clinical recovery between the TCD and placebo groups (49% vs. 30%; $p=0.03$), this difference was not extended to clinical end point assessments at 24 hours and 3 months.

The Transcranial low-frequency Ultrasound Mediated Thrombolysis in Brain Ischemia (TRUMBI) trial assessed the safety and efficacy of a dedicated low frequency ultrasound probe using 300 KHz (155). As discussed, low frequency ultrasound had already been shown to have better efficacy in pre-clinical studies compared to commercially available 2MHz probes. Additionally, specific to stroke therapy, use of low frequency did not require specific temporal bone window positioning as well as having a greater area of insonation. Twenty-six patients entered the trial and were non-randomly assigned in alternating order to tPA alone or tPA plus ultrasound if they presented with a stroke within 6 hours and had no evidence of cerebral haemorrhage on MRI. The trial was stopped prematurely as 5 out of 12 patients assigned to tPA and ultrasound had symptomatic intracranial haemorrhages within 3 days ($p<0.01$). Also, as observed in the CLOTBUST study there was no significant difference in recanalization or clinical morbidity at 3 months. Whilst it is surprising that efficacy was not improved by the use of a dedicated low frequency probe, the true concern from this trial was the safety outcomes which were poorly understood. One explanation is an increased permeability of the blood brain barrier included in the larger area of ultrasound insonation. A further explanation suggests that the low frequency pulse length reflecting multiple times within the "closed box" of the skull led to a summation of ultrasound waves increasing the amplitude and thus energy intensity well above the mechanical index predicted for this therapy (156). Both of these explanations

present complications specific to ultrasound thrombolysis within the brain, however, since this study untargeted, very low frequency insonation has been avoided both for ultrasound treatment of stroke and thrombolysis in other areas of the body.

In an attempt to improve targeting of ultrasound insonation, endovascular ultrasound catheters were developed. The EKOS MicroLysUS (EKOS Corporation, Bothell, WA, USA) infusion catheter enabled direct infusion of thrombolytic therapy through a distal port whilst also containing ultrasound transducers in a ring configuration proximally on the catheter to create a microenvironment of insonation. This catheter used a 2.1 MHz transducer with an average power of 0.21-0.45 W/cm^2. The Interventional Management of Stroke (IMS) II Study assessed the use of adjunctive intra-arterial thrombolysis with ultrasound insonation to intravenous thrombolysis alone (157). In this study of 81 patients, there was a trend toward improved mortality at 3 months of 16% in the combined intravenous and intra-arterial treatment group compared to 21% in the intravenous only treated group. However, there was also a trend toward symptomatic intracranial haemorrhage in the endovascular group (9.9%) versus the intravenous only group (6.6%). Despite this a Phase III open label, randomized control trial, IMS III, was carried out to assess the benefit of adjunctive endovascular therapy in thrombolysis for stroke (158). This study was stopped early after 656 patients had been recruited as no clinical functional improvement was observed at 3 months between the groups although it was noted that there was also no difference in safety outcomes with regard to mortality (19.1% vs. 21.6%, p=0.52) and symptomatic intracranial haemorrhage (6.2% vs. 5.9%, p=0.83) between the groups either.

With an apparent futility of endovascular ultrasound thrombolysis for stroke, other peripheral vessel targets have been investigated, in particular, the treatment of peripheral arterial, pulmonary and venous thrombosis (159-161). The most studied target has been in the treatment of DVT. A study by Grommes et al. assessed the safety and feasibility of the EKOS Endowave system (EKOS Corporation, Bothell,

WA, USA) which utilized a core of ultrasound transducers separated 1cm apart at the distal tip of the catheter each delivering a 2MHz frequency at 0.45W/cm^2 energy combined with urokinase (88). In this study, thrombolysis, defined as >50% patency restored, was successful in 11 out of 13 patients although early re-occlusion was observed in 4 of these patients who required further adjunctive procedures. Additionally, bleeding complications occurred in 8% due to catheter insertion site haemorrhage, however, no bleeding at the site or related area of ultrasound insonation was observed. The efficacy of the EKOS Endowave system still remains under investigation through the Phase III, multi-centre, open label, randomized control ATTRACT trial (89). This study which will assess a variety of pharmacomechanical catheter directed thrombolysis modalities, will determine whether adjunctive use of these devices can improve the occurrence of post thrombotic syndrome at 2 years over conventional anticoagulation therapy alone in symptomatic proximal DVT.

4.2. Microbubble Augmented Thrombolysis

4.2.1. In-vitro Evidence

The proposed mechanism of acoustic cavitation by expansion and collapse of gas bubbles led Tachibana et al. to test the ability of albumin microbubbles used in contrast ultrasound imaging to augment ultrasound thrombolysis (162). Using a static in-vitro experimental setup, clot exposed to ultrasound in the presence of both Urokinase and albumin microbubbles (Albunex) showed 51.3±7.7% clot mass reduction, ultrasound and urokinase showed 33.3±5.8% clot mass reduction and urokinase alone was 26.6±4.8%. The clot mass reduction through addition of microbubbles to ultrasound thrombolysis was statistically significant, however, in this study neither ultrasound and microbubbles or microbubbles alone showed any significant difference in clot mass reduction to control clot suggesting that the mechanism of action was an augmentation of fibrinolysis by thrombolytic agents

from microbubble action only. It was suggested by the authors that clearing of the microbubbles on US imaging from the experimental setup was believed to have happened by microbubble destruction which enabled the cavitational thrombus dissolution.

The role of microbubbles in thrombus dissolution, was further investigated through assessment of different types of microbubble structures on t-PA mediated ultrasound thrombolysis (163). The three types of microbubble used were as follows: room air filled sonicated albumin shell bubbles, room air filled galactose shell bubbles and 2% dodecafluoropentane (DDFP) gaseous bubbles. After insonation of a thrombus for ten minutes with each of these bubbles, the thrombus weight reduction was significantly greater in the DDFP group (49±8%) compared to the galactose shell group (22±7%), the albumin shell group (8±5%) and US only control group (-5±1%). In this study, the ultrasound used was 10 MHz frequency and 1.02 W/cm^2 intensity. This frequency was particularly high compared to the frequencies used in the studies previously discussed investigating ultrasound thrombolysis, however, this was the author's intention so as to highlight the thrombus dissolution produced by the microbubbles rather than ultrasound. The microbubbles used in this study represented the evolution of stability of bubbles discussed earlier with the albumin shell bubbles being the least stable whist the DDFP group were the most stable. It was suggested that the presence of a stable bubble provided a lower energy threshold for both microstreaming and acoustic cavitation to occur thereby reducing the ultrasound energy required to perform thrombus dissolution. This phenomenon occurs as energy is not required to create air bubbles from the native solution as is the case in ultrasound thrombolysis. Instead, energy is only required to oscillate and resonate existing bubbles to achieve microstreaming and acoustic cavitation. Additionally, it was suggested that a reduced threshold due to this improved efficiency would also enable the dose of thrombolytic agent to be reduced.

A number of studies have gone on to investigate the effectiveness of microbubble augmented ultrasound thrombolysis known as sonothrombolysis (164-173) as described in Table 4. In-vitro studies measuring clot mass reduction as an endpoint have demonstrated significant clot mass reduction with the combination of US, microbubbles and thrombolytic agents (166, 170). However, the same studies demonstrate that clot mass reduction could be achieved with US and microbubbles alone. Wu et al showed a clot mass reduction of 30% with US and microbubbles compared to 50-65% with US, microbubbles and thrombolytic agent (166). A microscopic analysis performed of clot treated revealed a smooth surface with intact red cells in the control group. In clot exposed to US and microbubbles a rough, porous surface with damaged red cells was observed whilst clot exposed to thrombolytic agent had an irregular surface and overall global shrinkage. US, microbubbles and thrombolytic agent showed large cavities of approximately 200μm both on the surface and throughout the clot (170). The authors suggest that the porous surface seen was as a result of microstreaming created by US and microbubbles whilst the further addition of thrombolytic agents enables a combined inertial cavitational effect throughout the clot.

Reference	Microbubble	Clot Mass Reduction, %		
		US	US + MB	US + MB + Thrombolytic
Porter et al, 1996	PESDA	24 ± 13	43 ± 17	60 ± 14
Nishioka et al, 1997	DDFP	72 ± 18	98 ± 4	n/a
Wu et al, 1998	MRX-408	n/a	30	65
Cintas et al, 2004	Levovist	6.1 ± 1.9	10.9 ± 3.6	30.7 ± 9.5
Prokop et al, 2007	Optison	n/a	0.95 ± 1.33	0.95 ± 1.33
Datta et al, 2008	Definity	n/a	6.3	26.2
Holscher et al, 2009	Definity	19.1 ± 4.5	20.5 ± 4.8	26.9 ± 2.9
Kutty et al, 2010	Definity	31 ± 10	55 ± 19	n/a

Table 4 Summary of in-vitro sonothrombolysis studies assessing percentage clot mass reduction as an endpoint.

A further in-vitro study showed a clot mass reduction of 55±19% with US and microbubbles (174) which was higher than the previously discussed in-vitro studies. In the previous studies, US was applied continuously, however, in this study, pulses of high MI US were guided by low MI US to allow replenishment of microbubbles over the clot. The technique of disruption-replenishment is well established in the diagnostic use of microbubbles for the quantification of tumour vascularity using dynamic contrast enhanced ultrasound (22). Using this technique, microbubbles are initially imaged using a low MI which keeps microbubble disruption to a minimum, followed by a short burst of high MI which leads to microbubble destruction. In diagnostic imaging, the replenishment of microbubbles after a high burst is then quantified to assess vascularity of a lesion, however, in therapeutic sonothrombolysis re-accumulation of microbubbles is allowed to occur at the thrombus surface before high MI application is repeated enabling a targeted cavitational effect.

4.2.2. In-Vivo Sonothrombolysis

Studies investigating sonothrombolysis have been performed in-vivo, however, the focus of research in this field has focused on animal models of stroke and acute myocardial infarction as demonstrated in Table 5. A number of these animal models have used peripheral vessel occlusions providing preliminary evidence for feasibility and further investigation of sonothrombolysis in the recanalization of DVT.

Two studies have used the model of thrombi within surgically occluded ileofemoral arteries in rabbits to investigate sonothrombolysis (164, 165). Birnbaum et al. used perflurocarbon-exposed sonicated dextrose albumin (PESDA) microbubbles infused intravenously in bilateral thrombotically occluded femoral arteries (165). US was applied unilaterally allowing the contralateral limb to serve as a control exposed to PESDA only. All ten ileofemoral occlusions treated with US and PESDA recanalized angiographically within one hour of treatment whilst none of the contralateral limbs exposed only to PESDA recanalized ($p=0.00006$). Additionally, on histological analysis nine out of ten of the ileofemoral arteries exposed to US and PESDA revealed <25% cross sectional area obstructed by thrombus. Nishioka et al. used intra-arterial injection of dodecafluoropentane (DDFP) microbubbles with angiographic TIMI grading as an endpoint of ileofemoral artery recanalization (164). In those occlusions treated with US and DDFP, 13 out of 17 (76%) vessels showed TIMI grade II or III recanalization after 45 minutes treatment which was significantly greater than those vessels treated with US alone (9%, $p=0.0075$) or DDFP alone (0%, $p=0.0152$). In both studies, the thrombotic occlusions were acute with subsequent treatment conditions applied within an hour of occlusion to model the situation of acute myocardial infarction or acute limb ischaemia with no experiments conducted on older occlusions as found in DVT.

A limitation of the study by Nishioka et al. was the finding of damage to both the skin and vessel walls of the rabbits treated. Tissue temperatures around the vessel rose to 42.6±0.9°C after 10 min of US exposure whilst skin temperatures rose to 73.3±4.7°C after 10 minutes of US exposure. Histologically, mild focal necrosis of the vessel was found in 4 out of 17 (24%) vessels treated whilst 25-50% vessel wall necrosis was observed in vessels in which mural thrombus was still present; attributed to longer exposure to ultrasound (164). Additionally, rabbit dermis and subcutaneous soft tissue at the site of transducer application revealed necrosis and focal hemorrhage secondary to thermal damage. These complications of treatment may be explained by the use of very low frequency ultrasound (24.8kHz) outside the range of commercially available clinical ultrasound probe frequencies and continuous application of high energy ultrasound.

Xie et al. investigated the use of a commercially available and FDA approved diagnostic ultrasound platform to achieve thrombus dissolution in a canine model of thrombosis (169). The canine model was produced by the creation of an arteriovenous fistula through placement of a graft between the femoral artery and femoral vein in three mongrel dogs. Acute thrombosis was created by double suture ligation and manual pressure of the graft for 30 minutes. Intravenous microbubbles, MRX-801 (ImaRx Therapeutics, Tucson, Arizona), were then infused and the thrombosed grafts were then randomized to either continuous low MI (MI <0.5) ultrasound or intermittent high MI impulses (MI 1.9) guided by a low MI contrast specific pulse sequence. Successful recanalization was defined as a TIMI score of 3 on angiography. The intermittent high MI group recanalization was 71% and 79% at 30 and 45 minutes respectively which was significantly different from the low MI group whose recanalization was 20% and 30% at the same respective time points. There was no significant difference between recanlization at 20 minutes and the authors suggest that at this early time point fewer channels exist within the thrombus leading to slower microbubble replenishment and therefore greater intervals between high MI impulses. This was shown by the interval between high MI impulses at 40 minutes being 8±8sec whilst at 10 minutes the interval was 21±19sec. This study is

further evidence supporting the technique of disruption-replenishment discussed earlier with microbubbles being allowed to fill channels within the thrombus enabling the greatest cavitational effect of a high MI impulse. Additionally, although not assessed in this study there may be a further advantage to the use of disruption-replenishment to minimise the thermal effects of sonothrombolysis to the skin, surrounding tissue and vessel wall being treated.

Reference	Thrombosis model and microbubble	Recanalisation Success	
		US	US + MB
Nishioka et al, 1997	Rabbit ileofemoral artery, Echogen	9%	82%
Birnbaum et el, 1998	Rabbit ileofemoral artery, PESDA	0%	100%
Culp et al, 2003	Canine prosthetic femoral A-V graft, Optison	13%	100%
Xie et al, 2005	Canine prosthetic femoral A-V graft, Definity	12.5%	100%
Tsutsui et al, 2006	Canine prosthetic femoral A-V graft, MRX-815	17.6%	91.6%
Xie et al, 2009	Canine prosthetic femoral A-V graft, MRX-801	n/a	79%
Kutty et al, 2012	Pig central venous catheter in superior vena cava, MRX-801	10%	60%

Table 5 Summary of in-vivo sonothrombolysis studies assessing percentage recanlisation success as an endpoint.

The sonothrombolysis studies highlighted in Tables 4 & 5 of in-vitro and in-vivo experiments respectively utilize low frequency ultrasound within a range of 24.8kHz to 2MHz. Whilst this range is consistent with that observed in ultrasound thrombolysis discussed earlier, only three studies use diagnostic ultrasound platforms to achieve microbubble cavitation with a frequency range of 1.5MHz to 1.7MHz (168, 174, 175). As discussed earlier, not only does use of a commercially available ultrasound platform aid clinical translation but it also has the ability to guide treatment through alternating between therapeutic ultrasound and diagnostic ultrasound. This combination of low frequency diagnostic contrast enhanced ultrasound combined with targeted therapy raises the potential of sonothrombolysis being used transcutaneously to treat thrombosed vessels. Low frequency ultrasound can be applied to structures at depth without significant attenuation (176), therefore, with better targeting and less energy intensity required to achieve cavitation the risk of unwanted side effects like those observed with ultrasound thrombolysis should be reduced.

4.2.3. Thrombosis models

Significant heterogeneity in study design exists across both the in-vitro and in-vivo studies of sonothrombolysis. In particular, a large variation in clot and thrombus models in-vitro and in-vivo respectively do not allow quantitative comparison between studies.

In-vitro clot models varied from simply allowing human venous blood to clot within a glass tube for 2-3 hours to use of recalcified blood combined with thrombin within a 37ºC water bath (164, 177). In an attempt to standardize the in-vitro clot models used to refine sonothrombolysis techniques, Roessler et al. developed a novel, reproducible model that showed closer resemblance to thrombi seen in-vivo (171). In this study, the novel clot model was compared to both recalcified human venous blood and spontaneously clotted human venous blood as used in previous studies.

Briefly, this model involved a platelet rich clot achieved by separation by centrifugation of the platelet rich supernatant plasma layer which was then mixed with the erythrocytes of the boundary layer. This mixture was then recalcified and incubated at 37ºC for 2 hours. It was observed that this platelet rich clot was the most stable to thrombolytic therapy and pulsatile flow conditions whilst also displaying the lowest variability in clot mass measurements which as discussed has been the most popular endpoint measurement for the in-vitro experiments. Additionally, histological comparison of the three in-vitro clot models to embolic thrombi samples retrieved from cerebral arteries of stroke patients revealed that the platelet rich clot was the most similar with a layered assembly of erythrocytes and leucocytes over a fibrin mesh. Whilst this model is undoubtedly superior to the two other clot formations used in this study, it should be highlighted that this model is very specific to an arterial thrombosis. Platelets require conditions of high shear stress, as found in the arterial circulation, to adhere to sites of endothelial cell wall injury and subsequently activate coagulation (178). The resulting clot is therefore platelet rich or a "white clot" in comparison to venous thrombi which are known as "red clots" due to their higher erythrocyte content which form under conditions of low shear stress as found in the venous circulation (179). Thus far, there have been no in-vitro sonothrombolysis studies replicating the characteristics of a venous thrombus although future studies could adopt those models used in haematological assessment of venous thrombi (180).

Similarly, variation exists within the in-vivo models of thrombus used in sonothrombolysis studies. Akin to the situation in-vitro, much of the work in this field has focused on arterial sonothrombolysis to model clinical situations of stroke and acute myocardial infarction. The most favoured model is creation of a femoral arterial thrombosis by balloon injury, electrical endothelial activation or intra-arterial thrombin injection within rabbits (146, 164, 165). A separate group have developed an artificial femoral arterio-venous fistula model using a PTFE graft with thrombosis induced through double suture ligation of the graft in an attempt to recreate the conditions of an occluded dialysis access graft (167-169, 181). Whilst the nature of

thrombi between the models will be different, the proximal surface of the clot remains part of the arterial circulation, therefore, delivery of microbubbles to the site of thrombosis remains high flow and shear stress. Only one model has been investigated in the venous circulation but this involved a thrombosed central venous catheter within the internal jugular vein of a pig (174). This model cannot be considered a representative model of venous thrombosis for sonothrombolysis as the thrombus was formed within the catheter rather than the vein wall and microbubbles were delivered directly to the thrombus via the proximal catheter lumen rather than via the systemic circulation. Future studies of sonothrombolysis in-vivo should utilize validated models of venous thrombosis already in use to investigate mechanisms of formation, resolution and therapy (105, 106).

4.2.4. Clinical Sonothrombolysis

The current clinical application of sonothrombolysis is far less than that of ultrasound thrombolysis. A Cochrane Review from 2012 assessing the augmentation of thrombolysis using ultrasound in the treatment of acute ischaemic stroke was only able to include 2 microbubble studies from an initial search of 52 studies comprising 22.3% of the total number of patients included for analysis (182). It was demonstrated in a subgroup analysis that the risk of haemorrhagic transformation following sonothrombolysis for acute stroke was significantly increased (OR 7.30, 95% CI 1.37 to 38.90), however, it was conceded that this was based on only 55 patients. Examining the two included studies closely, both used 2MHz ultrasound using either TCD or TCCD, however, one study revealed a microbubble dose dependent increase in haemorrhagic transformation. In this study, patients were randomized to receive either 1.4ml or 2.8 ml of MRX-801 microbubbles over 90 minutes in addition to their t-PA with a further control group receiving t-PA only (183). There were no haemmorhagic complications in the control group, whilst the low dose 1.4ml group had 17% bleeding complications and the high dose 2.8ml group had a significantly greater 36% incidence of bleeding complications ($p<0.05$).

The authors of this study suggest that this increased rate of bleeding complications may have been as a result of imbalance between groups, in particular, poorer hypertensive control in the 2.8ml group. However, it cannot be excluded that the same ultrasound amplitude potentiation effects observed with ultrasound thrombolysis within the cranial vault may have occurred in this study leading to an uncontrolled excess of ultrasound energy which in the presence of both thrombolytic therapy and microbubbles increases the bleeding risk significantly. Additionally, it should be noted that MRX-801 is not a licensed microbubble for use in either Europe or the USA where this study took place. As observed from many of the in-vivo studies of sonothrombolysis, ultrasound and microbubbles alone may be sufficient to achieve thrombus dissolution and whilst there may be an incremental benefit in recanalization with the addition of thrombolytic therapy the risk of bleeding complications may outweigh this benefit.

At present, there is an ongoing multicenter clinical trial assessing the benefit of adjunctive sonothrombolysis in acute myocardial ischaemia. The Microvascular Reperfusion Utilizing Sonothrombolysis in Acute Myocardial Infarction (MRUSMI) trial will randomize patients with acute myocardial infarction to either conventional therapy of acute cardiac percutaneous intervention and revascularization or conventional therapy as described plus two sessions of sonothrombolysis pre and post cardiac catheterization (184). Ultrasound will be applied using a modified commercially available ultrasound platform and the microbubbles used will be either Definity® or Optison™ based on the licensing regulations of the recruiting centre. This study will assess the ability of sonothrombolysis to not only achieve thrombus dissolution in the coronary vessels but also in the surrounding capillaries of cardiac muscle, therefore, outcomes will be based on event free survival and myocardial muscle assessment by MRI and diagnostic CEUS. Although this study is yet to report results, the assessment of ultrasound and microbubbles alone in a clinical setting without thrombolytic therapy will be of interest to evaluate both safety and the translation of pre-clinical in-vitro and in-vivo sonothrombolysis studies also utilizing ultrasound and microbubbles only.

The use of ultrasound thrombolysis has evolved from the initial target of acute ischaemic stroke to peripheral vessels including thrombus removal in DVT. However, despite similar pathways of research and study design this has not been extended to sonothrombolysis. With safety concerns regarding systemic thrombolysis for DVT (72) and the use of microbubbles and thrombolytic therapy in acute stroke, sonothrombolysis for DVT must focus on the combination of ultrasound and microbubbles only to achieve thrombus dissolution. Therefore, models of venous thrombosis incorporating specific thrombus composition and venous flow conditions are required both in-vitro and in-vivo to formally assess feasibility and safety of sonothrombolysis for the treatment of DVT.

5. DEVELOPMENT OF AN IN-VITRO FLOW MODEL FOR SONOTHROMBOLYSIS

5.1. Parallel Plate Flow Chambers

Over the past 10 years there has been considerable development and use of both custom made and commercial flow devices to investigate the process of thrombus formation in an in-vitro setting (185, 186). In particular, the parallel plate flow chamber is capable of providing real time assessment of functions of thrombus formation including platelet adhesion and activation, thrombus buildup and fibrin formation (180). Whilst other devices such as the Impact cone and plate(let) analyzer (DiaMed, Cressier, Switzerland) and Platelet Function Analyzer-100 (Siemens Healthcare Diagnostics, Inc., Deerfield, IL) are able to measure platelet aggregate formation they are only able to do so under high shear flow which is analogous to the conditions of arterial vasculature, however, parallel plate flow chambers can provide thrombus for investigation at both arterial, high shear and venous, low shear flow conditions (187). In addition to providing conditions of accurate venous shear flow that have previously not been investigated for sonothrombolysis, the parallel plate flow chamber uses perfusion of whole blood throughout its circuit which again provides a novel experimental condition for sonothrombolysis.

The Ibidi (Martinsried, Germany) μ-slide 1 parallel plate flow chamber is a commercially available chamber that is in routine use at a number of institutions according to a recent survey assessing standardization of flow chamber based assays for thrombus formation (180, 188). The flow chamber providing the largest thrombus volume is shown in Figure 7, with dimensions of 50mm x 5mm containing a total volume of 200μl within the chamber. This flow chamber requires connection to the dedicated Ibidi flow circuit to provide the pre-defined shear flow for thrombus formation.

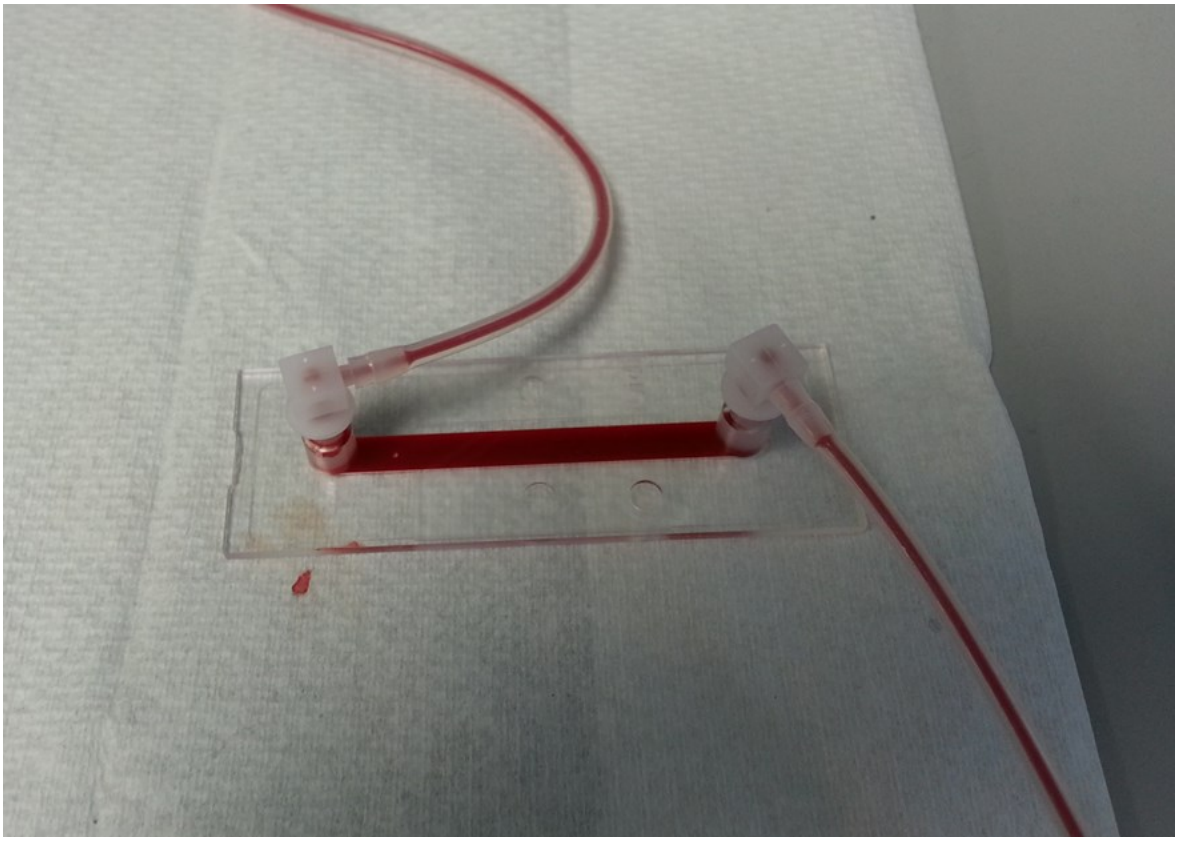

Figure 7 An Ibidi (Martinsried, Germany) µ-Slide 1 parallel plate flow chamber (50mm x 5mm)

In order to promote thrombus formation in flow conditions, the flow chambers require coating with thrombogenic substrate. A number of coating materials are commercially available and represent thrombogenic substrate either found within blood serum or on vessel walls. An example of a blood serum substance is von Willebrand Factor (vWF) which tethers with platelets via glycoprotein (GP) Ib-V-IX to form platelet aggregates (189). Vessel wall type substrates are broadly divided into collagen and non-collagen surface complexes. In particular, Collagen types I and III are highly platelet adhesive and have been validated previously within whole blood assays (190-192). They bind to vWF present in blood plasma which itself binds to two platelet collagen receptors; glycoprotein (GP) VI, and integrin $\alpha_2\beta_1$ (193). The subsequent secretin, integrin activation and procoagulant activity of this

platelet-collagen complex induces thrombus formation within a time period of only several minutes (194). Non-collagen substrates include fibrinogen, fibronectin and fibrin. These substrates enable single platelet adhesion via integrins $\alpha_{IIb}\beta_3/\alpha_v\beta_3$ and $\alpha_5\beta_1$ which subsequently trap vWF to propagate mass platelet adhesion as previously described, however, in these models this occurs within a fibrin meshwork structure (195, 196).

5.2. Blood Preparation for Flow Circuit

Blood can be prepared with or without coagulation activation which in-vitro is largely dependent on calcium and magnesium concentrations. Commonly, prevention of coagulation activity has been used for sole assessment of platelet function (197). However, in developing an in-vitro model representative of DVT, platelet activation as well as coagulation cascade activation is more appropriate (198). Human blood can be sampled and immediately anticoagulated using an appropriate medium such as sodium citrate or Ethylenediaminetetraacetic acid (EDTA). The blood is then incubated at 37 degrees Celsius for 10-15 minutes to allow the platelets to resensitize (180). At this time, a sample of blood is checked using microscopy for a normal platelet count as a reduced count can represent platelet activation which can occur during blood collection and preparation. Just prior to entering the parallel plate flow chamber, the blood is re-calcified using calcium chloride which if using a collagen substrate stimulates coagulation via the intrinsic pathway and if using a fibrin based substrate in combination with tissue factor stimulates coagulation via the extrinsic pathway.

In this model, blood from healthy subjects is used in combination with a thrombogenic substrate on the microslide to promote thrombus formation. The type of thrombogenic substrate and flow conditions used determine the production of a venous specific thrombus. There are a wide range of aetiologies that create the pro-thrombotic state leading to clinical DVT including; malignancy, thrombophilia,

dehydration, trauma, sepsis and immobilization (100). Each of these aetiologies results in differing blood constituents which lead to DVT and whilst it would be ideal to assess sonothrombolysis in thrombi formed under each of these constituents, this falls outside the remit of this feasibility study and could never truly be exhaustive given the extensive number of aetiologies that exist. Additionally, as discussed in the earlier review chapter of ultrasound augmented thrombus dissolution as well as in the randomized controlled trials assessing catheter directed thrombolysis for acute DVT, there have been no assessments or sub groups analyses of efficacy for the different aetiologies of thrombus (199).

Blood for the in-vitro model is also prepared for endpoint measurement. As parallel plate flow chambers allow real time assessment of clot formation, different parameters within a clot can be assessed. Blood can be loaded with the appropriate fluorescent or Brightfield probe to enable end-point measurement. In order to quantify platelets only whilst on a background of plasma, a label with a high affinity for platelet binding is required. The most widely used is the membrane probe 3,3-dihexyloxacarbocyanine iodide ($DiOC_6$) which enables platelet surface area coverage as real time and end stage endpoint measurements (188, 200). For overall thrombus burden, fluorescein isothiocyanate (FITC) labels fibrinogen which forms part of the overall clot complex structure and thus provides a surrogate for overall thrombus volume (201).

5.3. Parallel Plate Flow Chamber Circuit

Figure 8 shows an example experimental set up of the Ibidi parallel plate flow chamber circuit with prepared blood contained within Ibidi fluidic units. Depending on the volume of blood required for a single experiment, one or two blood pool reservoirs can be utilized. Prior to the addition of blood to the reservoirs of the Ibidi fluidic unit which perfuses the blood to the flow chamber, the fluidic unit and corresponding tubing are flushed with isotonic buffer to ensure that all air bubbles are

purged through the circuit. The fluidic unit is connected to a computer controlled air pump which using custom software defines flow rate and thus shear stress of the whole circuit based on the dimensions of the parallel plate flow chamber being used. Distal to the fluidic unit, a fluidic rectifier ensures that reservoirs do not run dry and that unidirectional flow over the flow slide is maintained (Figure 9). The flow chamber is initially connected to the fluidic unit via tubing proximally in the circuit then connected distally to complete the circuit only once blood fills the chamber to prevent air in the circuit which can produce artifact on image acquisition (180).

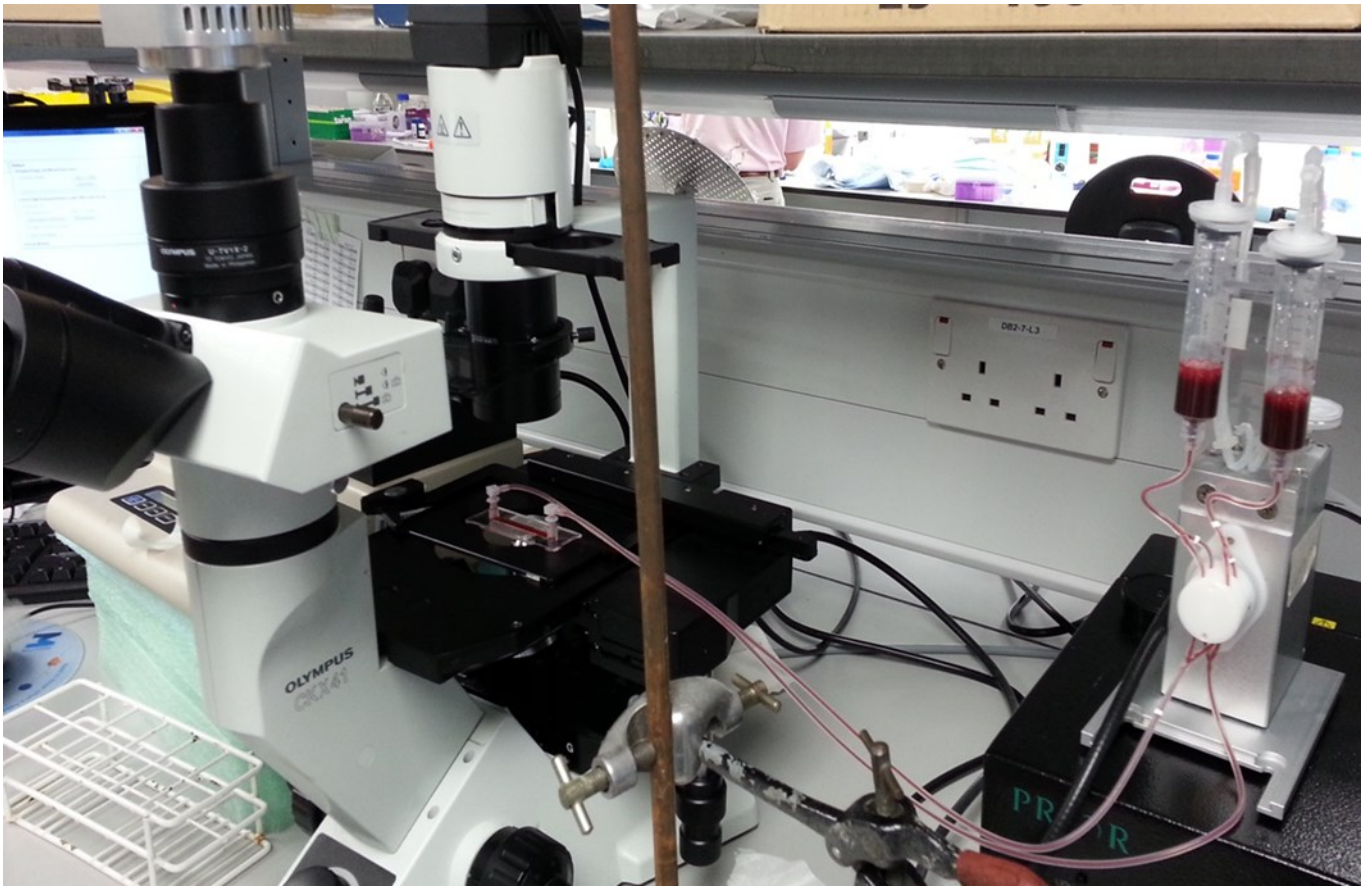

Figure 8 Experimental set up for the Ibidi parallel plate flow chamber. The flow chamber is placed on the microscope stage for acquisition of images for quantification of platelet surface area coverage. An Ibidi fluidic unit with two resevoirs is shown on the right. The corresponding air pressure pump and computer for control of flow rate and shear stress are not shown.

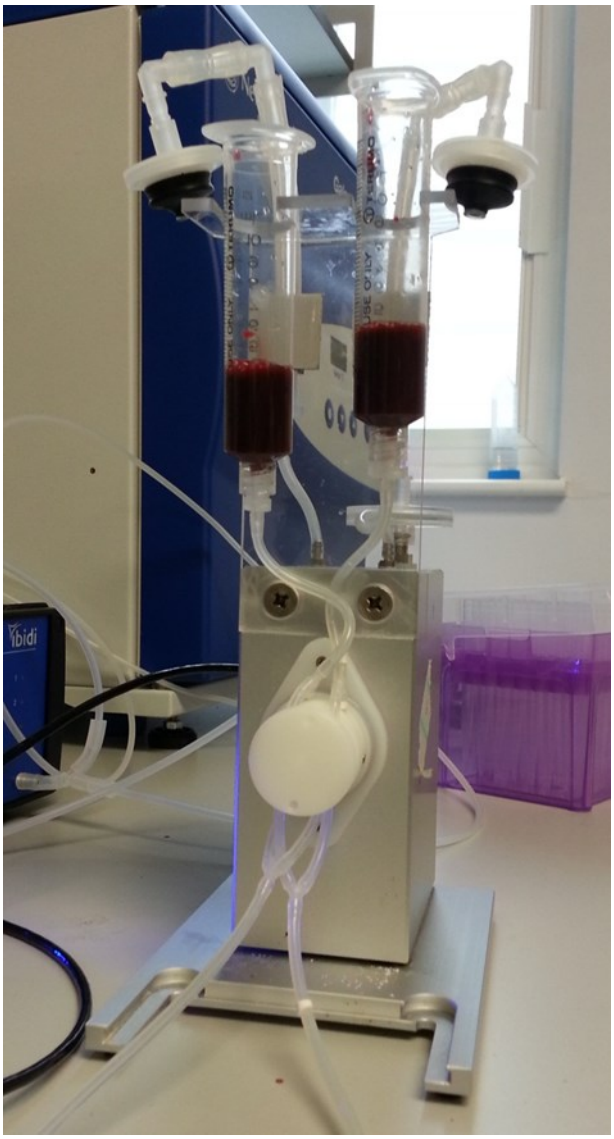

Figure 9 The Ibidi fluidic unit with two reservoirs containing blood. The fluidic rectifier housed in the circular plastic casing below the reservoirs provides continuous unidirectional flow to the flow chamber.

5.4. Image Acquisition and Analysis

During flow within the parallel plate chamber flow circuit, fluorescence microscopy video capture can be acquired at predefined time points usually at a x10 magnification (Figure 10). Thrombus volume is measured by the surrogate of $DiOC_6$-labelled platelets or FITC labelled fibrin surface area coverage (180, 202, 203). In-focus video at 25 frames per second of a representative area of thrombus is acquired with photobleaching of fluoroscopically tagged elements avoided by capture of a two second clip only. The video files are transferred in the AVI format for offline image quantification.

Using VirtualDub software (Version 1.9.11, Open source), the AVI file is segmented into 6 frames (representing 0.24 seconds) and checked to ensure that the in plane region of interest does not move across the flow slide over that time (Figure 11). This segmented file is then saved and transferred to ImageJ software (Version 1.47, National Institute for Health, USA). Using the Z-stack function all six frames are stacked to create one image with only consistent image features across all 6 frames represented. This method enables only the fluoroscopically tagged elements within fixed, stable thrombus within the flow chamber to be captured and removes artifactual signal from passing plasma and non-fixed fluoroscopic elements moving across the field during flow (204, 205). The stacked image is converted to grey scale providing fluoroscopically tagged elements to appear white. The image can then be quantified using the Analyze tool for percentage surface area coverage of white regions thus providing the surrogate clot surface area coverage measurement (Figure 12).

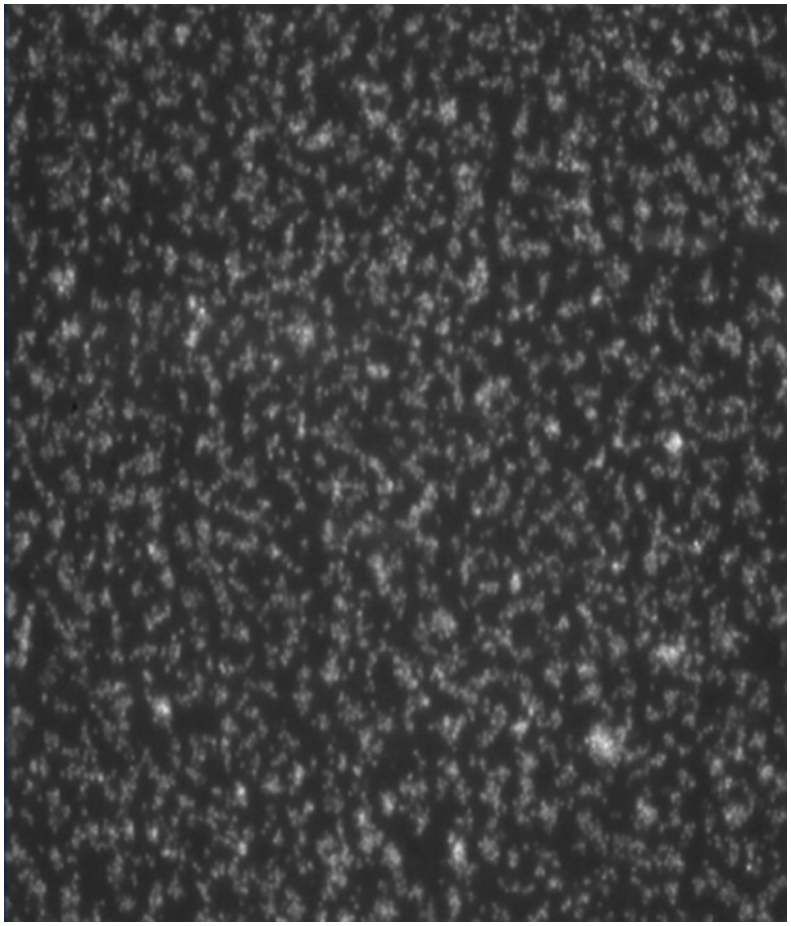

Figure 10 Fluorescence microscopy image of DiOC6-labelled platelet aggregates shown as discrete bright white areas which can be used to determine platelet surface area coverage. Microscopy performed using the Olympus CKX41 epifluorescent microscope and video captured via the ROllera XR Camera and StreamPix6 software (QImaging).

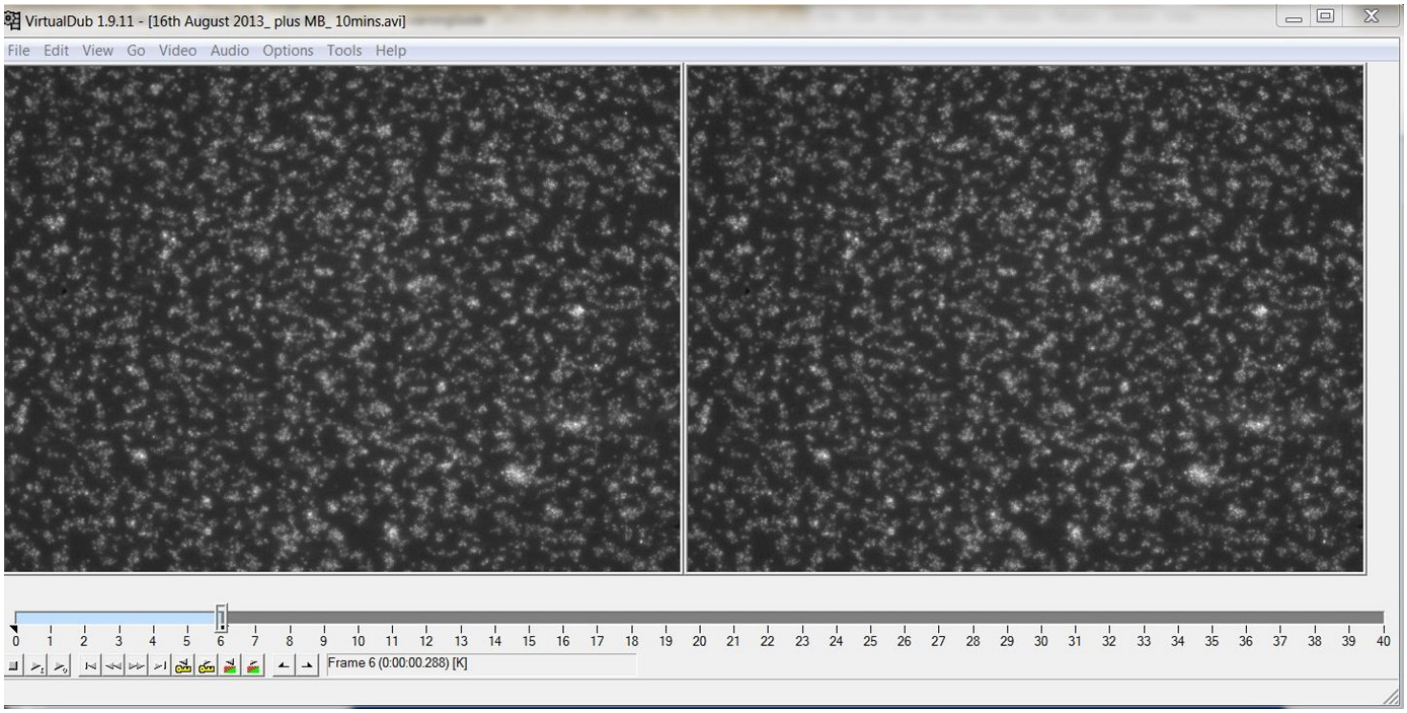

Figure 11 Image capture of the VirtualDub program (Version 1.9.11, Open source). Two frames are pictured from within the 6 segmented frames used for transfer for image quantification.

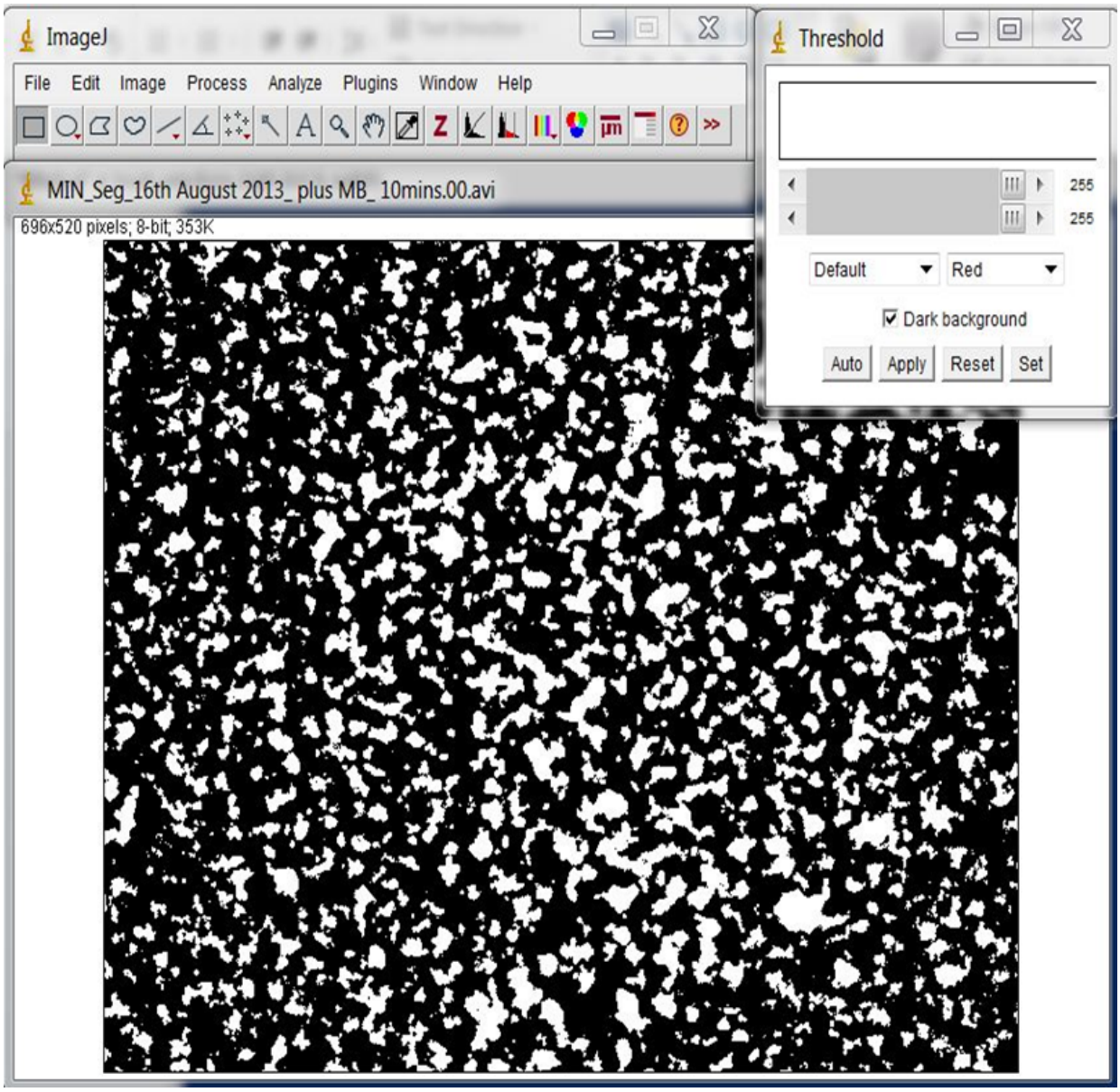

Figure 12 Image capture from ImageJ (version 1.47, National Institute for Health, USA). This image has been converted to grey scale leaving only fixed DiOC6-labelled platelets within platelets visible as white from which surface area coverage can be quantified.

5.5. Adaptation of Flow Circuit for Sonothrombolysis

5.5.1. Compatibility with Microbubbles

The image quantification methodology discussed earlier is validated for the removal of passing plasma and non-fixed fluoroscopically tagged elements moving across the field during flow to enable quantification of fixed fluoroscopically tagged elements for surface area coverage (204, 205). However, the presence of microbubbles within such a circuit has never previously been investigated. Therefore, for adaptation of parallel plate flow chambers for sonothrombolysis, the potential artifactual effect of the presence of microbubbles on thrombus formation and subsequent endpoint measurement was assessed. For this investigation, $DiOC_6$-labelled platelets were used as these were the smallest possible element that could be fluoroscopically tagged for a potential in-vitro DVT model and thus the most likely to suffer from artefact from microbubble presence.

Ibidi parallel plate flow circuits were utilised as previously described using a 50mm x 5mm flow chamber lined with Type III Collagen as a thrombogenic substrate. A total blood volume of 7ml was perfused in the circuit with a shear rate of 300 s^{-1}. SonoVue (Bracco, Italy) microbubbles were added at a concentration corresponding to physiological human concentrations of microbubbles previously described of 0.2% (14μL) (206). Experiments were divided into two groups; the first group SonoVue and whole blood within the circuit and the second group whole blood only within the circuit to serve as a control. Endpoint measurement was recorded as $DiOC_6$-labelled surface area percentage coverage at 5 minutes of flow quantified as described earlier using VirtualDub and ImageJ software packages. To enable true comparison and examine potential artifactual microbubble effect, samples from the first and second aforementioned groups were paired from the same blood source for endpoint measurement as thrombus formation can vary between different blood sources. As a result a paired t-test was used for statistical analysis using Prism Version 6.01

(GraphPad Software Inc., La Jolla, CA, USA) software. Statistical significance was taken as $P<0.05$.

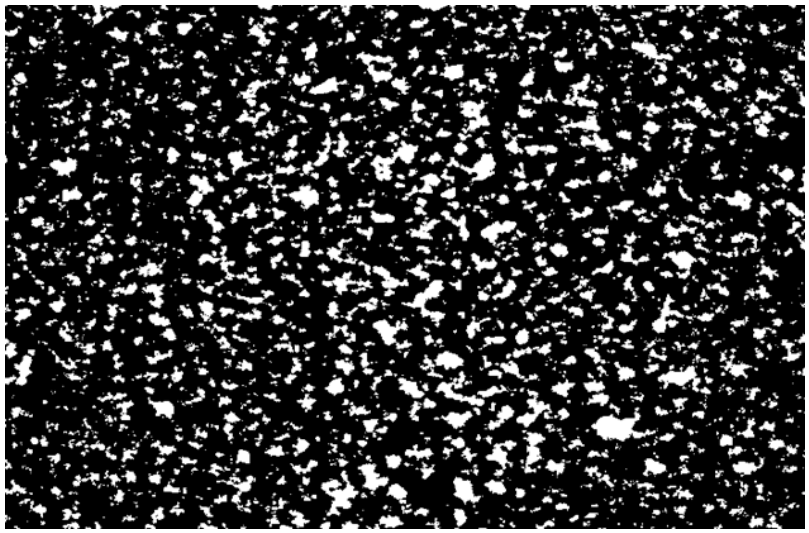

(a)

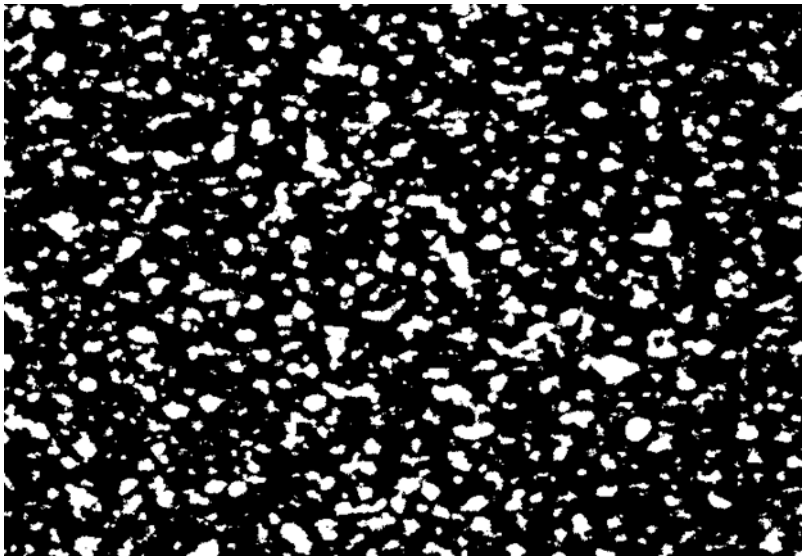

(b)

Figure 13 Representative paired samples from ImageJ which have been stacked and converted to grey scale for surface area percentage coverage quantification. In (a) the microbubble with whole blood surface area percentage shown is 19.4% and in (b) the whole blood only surface area percentage shown is 19.8%.

A total of 10 experiments were analysed; 5 in the microbubble and whole blood group and 5 in the whole blood only group. The mean percentage surface area coverage in the microbubble and whole blood group was 34.17 ± 3.820 % whilst the mean percentage surface area coverage in the whole blood only group was 34.10 ± 3.796 %. There was no statistical difference between the two groups (P=0.8245).

This methodology experiment demonstrates that microbubbles can be added to the Ibidi parallel plate flow chamber circuit without any significant effect on thrombus formation and previously validated endpoint quantification of surrogate surface area percentage coverage using VirtualDub and ImageJ software. It is also highlights the requirement of paired control samples from a given blood source to truly quantify differences in percentage surface area coverage if a given treatment is being studied.

5.5.2. Compatibility with Ultrasound

The ability to apply ultrasound to the parallel plate flow chamber is imperative to studying sonothrombolysis using this in-vitro flow model of venous thrombus. Development of suitable experimental set up was designed and tested. Simultaneous imaging using fluorescence microscopy and ultrasound was not possible on the microscope stage due to conflicting imaging planes required for the microscope and ultrasound. During ultrasound application, the flow chamber was suspended using clamps at either end to enable ultrasound to be applied from below. This was required as the inlet wells on the top of the flow chamber would not allow suitable contact between the ultrasound transducer and flow slide surface. Using this method, the flow slide can easily be transferred to the microscope stage for fluorescence microscopy at dedicated time points throughout experiments.

Pilot experiments testing this set up were performed using the Sonoscape SSI (Shenzhen, China) ultrasound machine with a 3.5MHz SC6-1 curvilinear probe in standard contrast with B-mode side-by-side setting using MI 0.07 for imaging and

manually increasing the MI to 1.5 for microbubble destruction. A parallel plate flow circuit was used as previously described using 7ml blood perfused at a shear rate of 300 s^{-1}. Additionally, as before, a 50mm x 5mm flow chamber lined with Type III Collagen as a thrombogenic substrate was used. Conditions tested in this experiment were as follows: ultrasound applied to the flow chamber with Sonovue microbubbles at a concentration of 0.2% (14µL) within the flow circuit, ultrasound only applied to the flow chamber and a control with the flow circuit alone. To ensure a true control, the blood for these experiments came from the same source. Ultrasound application involved direct contact with the flow slide from below using standard ultrasound acoustic gel to maintain contact between the flow slide and curvilinear ultrasound transducer. High MI 1.5 ultrasound was manually applied using a 1 second manual flash setting every 10 seconds. Each experiment was conducted for 5 minutes after an initial period of 5 minutes to ensure thrombus formation within each of the flow chambers.

The results are shown in Figure 14. After 10 minutes, the control experiment with blood flow had 58.9% platelet surface area coverage. After 5 minutes thrombus formation and 5 minutes treatment, the ultrasound and blood flow experiment had 54.5% platelet surface area coverage corresponding to 7.5% thrombus reduction. After 5 minutes thrombus formation and 5 minutes treatment, the ultrasound, microbubbles and blood flow experiment had 35.1% platelet surface area coverage corresponding to a 40.5% thrombus reduction compared to the control group.

Whilst the results of this initial development experiment are encouraging and are in keeping with previous sonothrombolysis studies discussed earlier, there were some limitations to this experimental set up that halted further repeat experiments. Figure 15 shows the ultrasound image acquisition which demonstrates significant reverberation artifact. Additionally, as the ultrasound probe is in direct contact with the underside of the flow slide, it was difficult to accurately image the microbubbles within the flow chamber as the ultrasound focus could not be adjusted to this depth

using this transducer. Subsequently it was therefore not possible to image microbubble destruction within the flow chamber to prove the mechanism by which thrombus dissolution was occurring as well as any potential microbubble destruction not being as efficient as possible due to this disparity in depth of flow chamber and depth of focus.

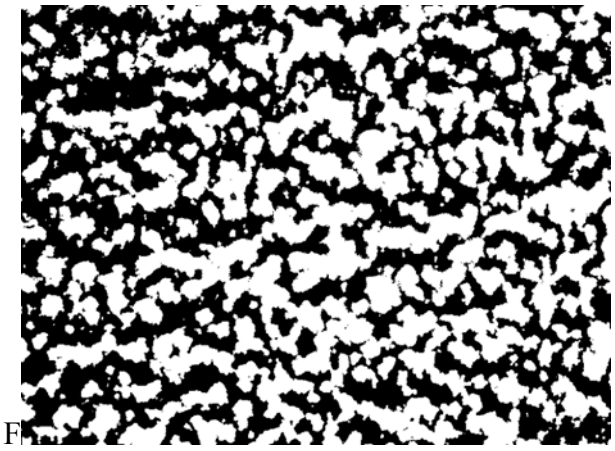

F (a)

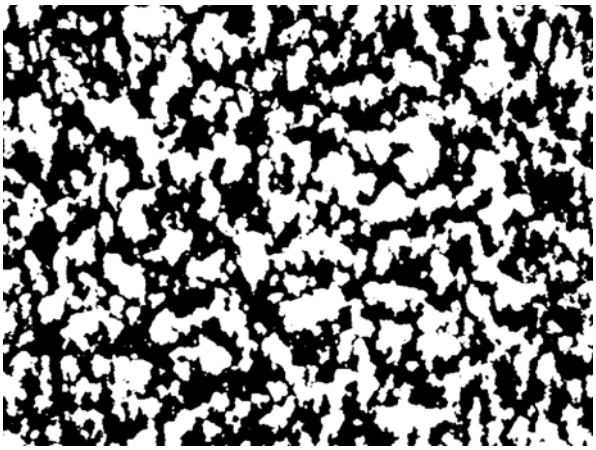

(b)

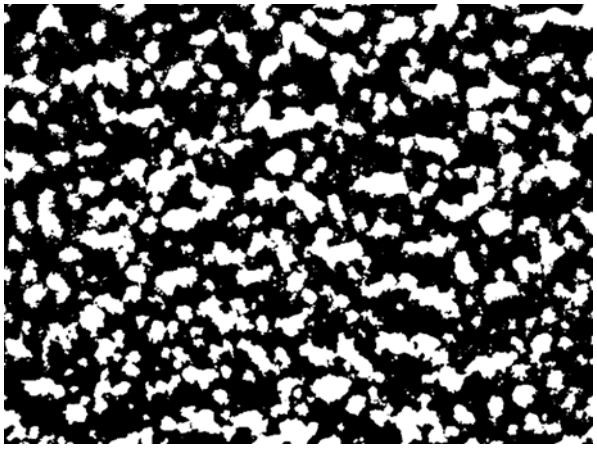

(c)

Figure 14 Stacked grey scale images of platelet surface area coverage for quantification. In (a) the control experiment with flow only shows a 58.9% surface area coverage, in (b) with ultrasound and flow only there is a 7.5% surface area reduction compared to (a), and in (c) with ultrasound, microbubbles and flow there is a 40.5% surface area reduction.

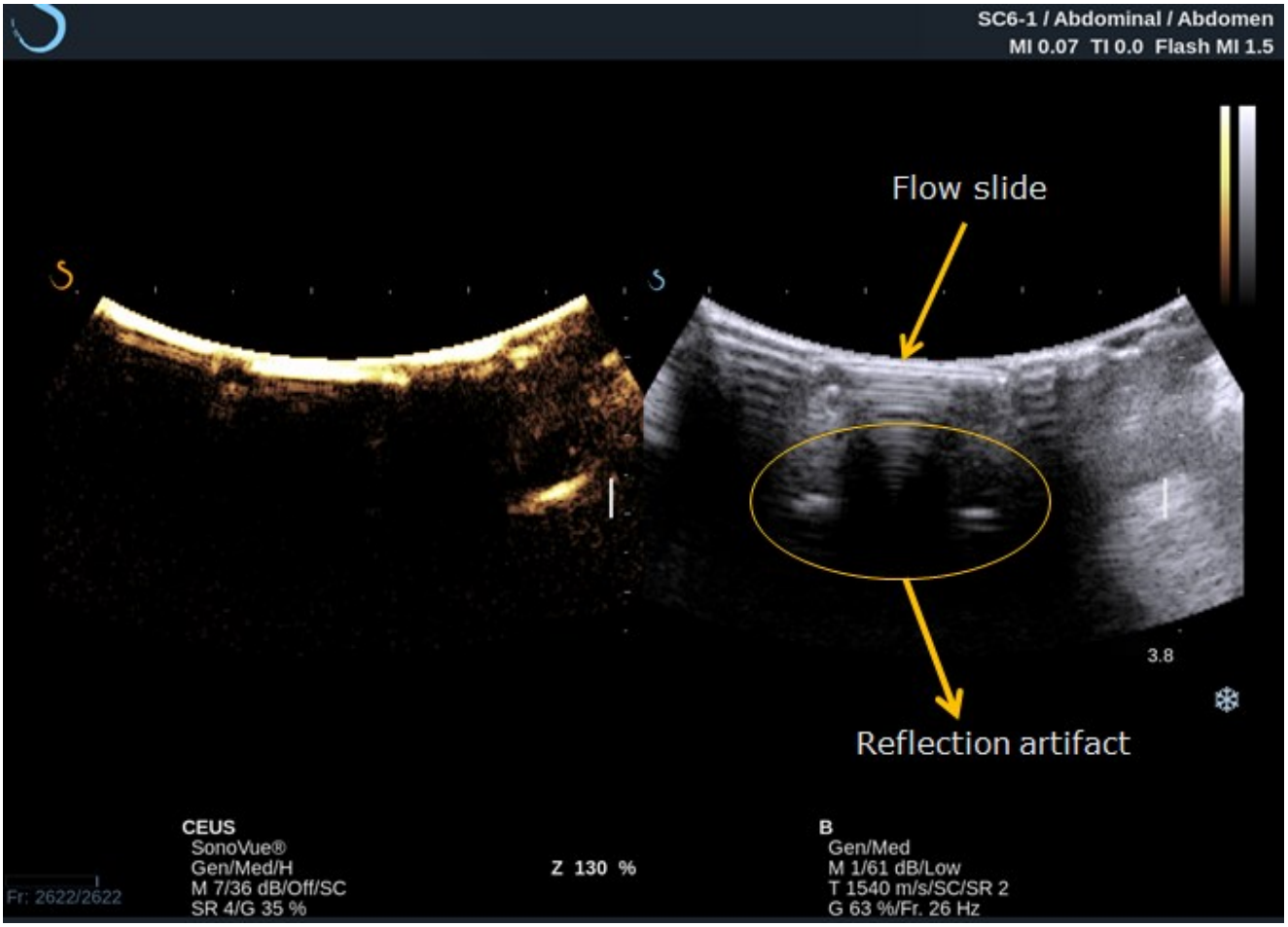

Figure 15 Contrast and B-mode side-by-side image acquisition from the Sonoscape SSI ultrasound machine using a 3.5MHz SC6-1 abdominal probe. Microbubbles cannot be visualized within the flow chamber and significant reflection artifact from the flow chamber and flow chamber wells is noted.

In an attempt to improve both the reverberation artifact and microbubble imaging within the flow chamber, an offset was introduced into the experimental set up. This offset using degassed ultrasound gel within a latex casing at a depth of 3cm. Once again a 7ml parallel plate flow circuit was used at a shear flow of 300 s^{-1} using a 50mm x 5mm flow chamber coated with Type III collagen substrate. As the aim of this experiment was to optimize imaging and destruction of microbubbles and reduce the reflection artifact, only ultrasound applied to the flow chamber with SonoVue microbubbles at a concentration of 0.2% (14μL) within the flow circuit was compared to the control with blood flow only through the circuit. Ultrasound was applied using the same imaging protocol of manual flash high MI 1.5 every 10 seconds with attempted diagnostic low MI 0.07 at all other times. As before, thrombus was allowed to develop initially over a period of 5 minutes before a subsequent 5 minute treatment period before endpoint measurement using video microscope fluoroscopy.

The results are shown in Figure 16. After 10 minutes, the control experiment with flow only had total platelet surface area coverage of 47.2%. After ten minutes treatment of ultrasound, microbubbles and flow combined, a platelet surface area coverage of 28.6% corresponding to a 39.4% thrombus reduction compared to the control was demonstrated.

Once again, in this development experiment there appears to be thrombus dissolution with the combination of microbubbles and ultrasound. Additionally, from an imaging perspective Figure 17 reveals a reduction in the reverberation artifact, however, it is still present. Nonetheless, using the 3cm depth offset, microbubbles were now visible within the flow slide. Furthermore on application of a manual high 1.5 MI flash microbubbles were seen to disappear from the flow slide immediately afterwards and then re-accumulate as flow continued.

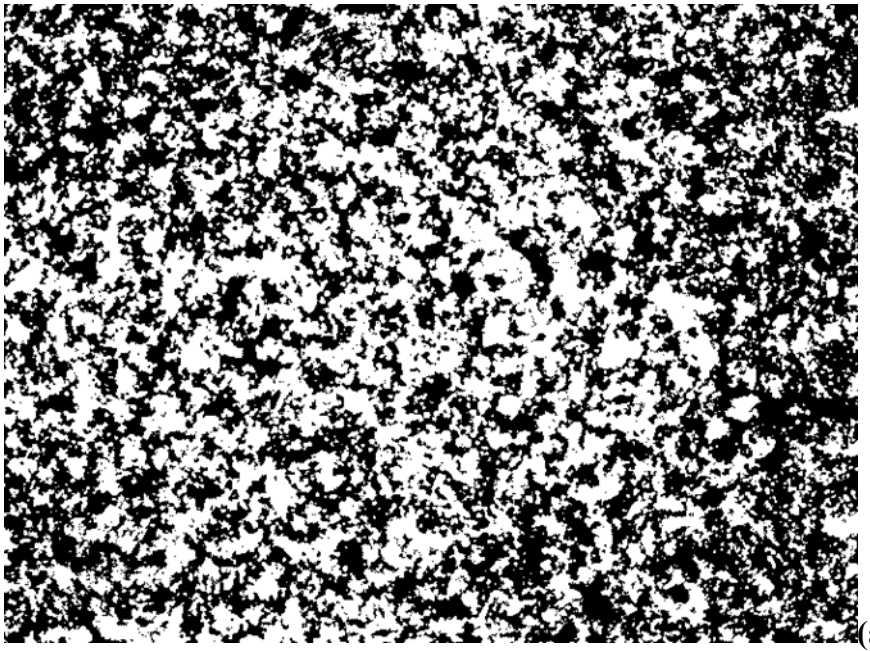

(a)

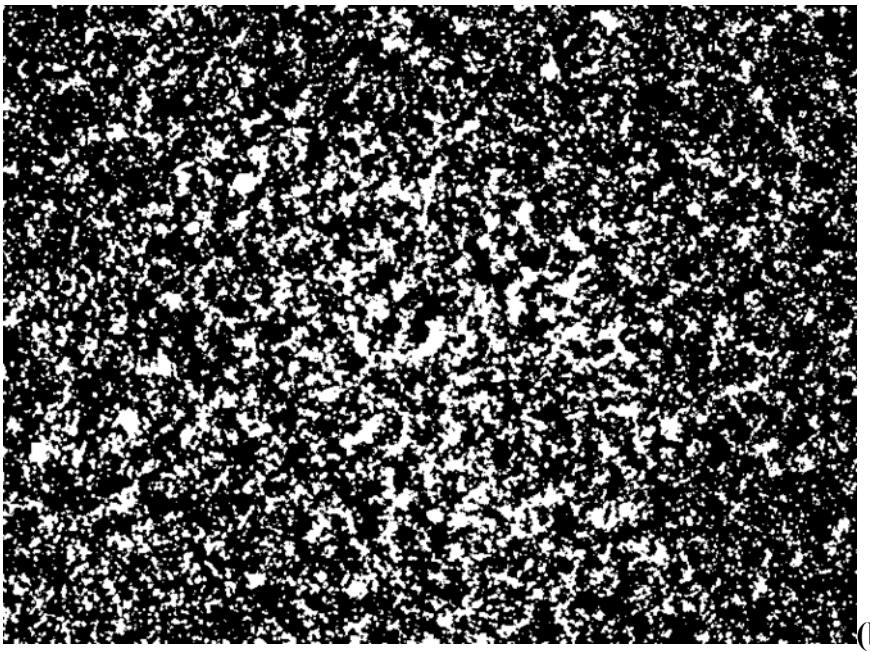

(b)

Figure 16 Stacked grey scale images of platelet surface area coverage for quantification. In (a) the control experiment with flow only shows a platelet surface area coverage of 47.2%. In (b) the ultrasound, microbubble and flow experiment shows a 39.4% platelet surface area reduction

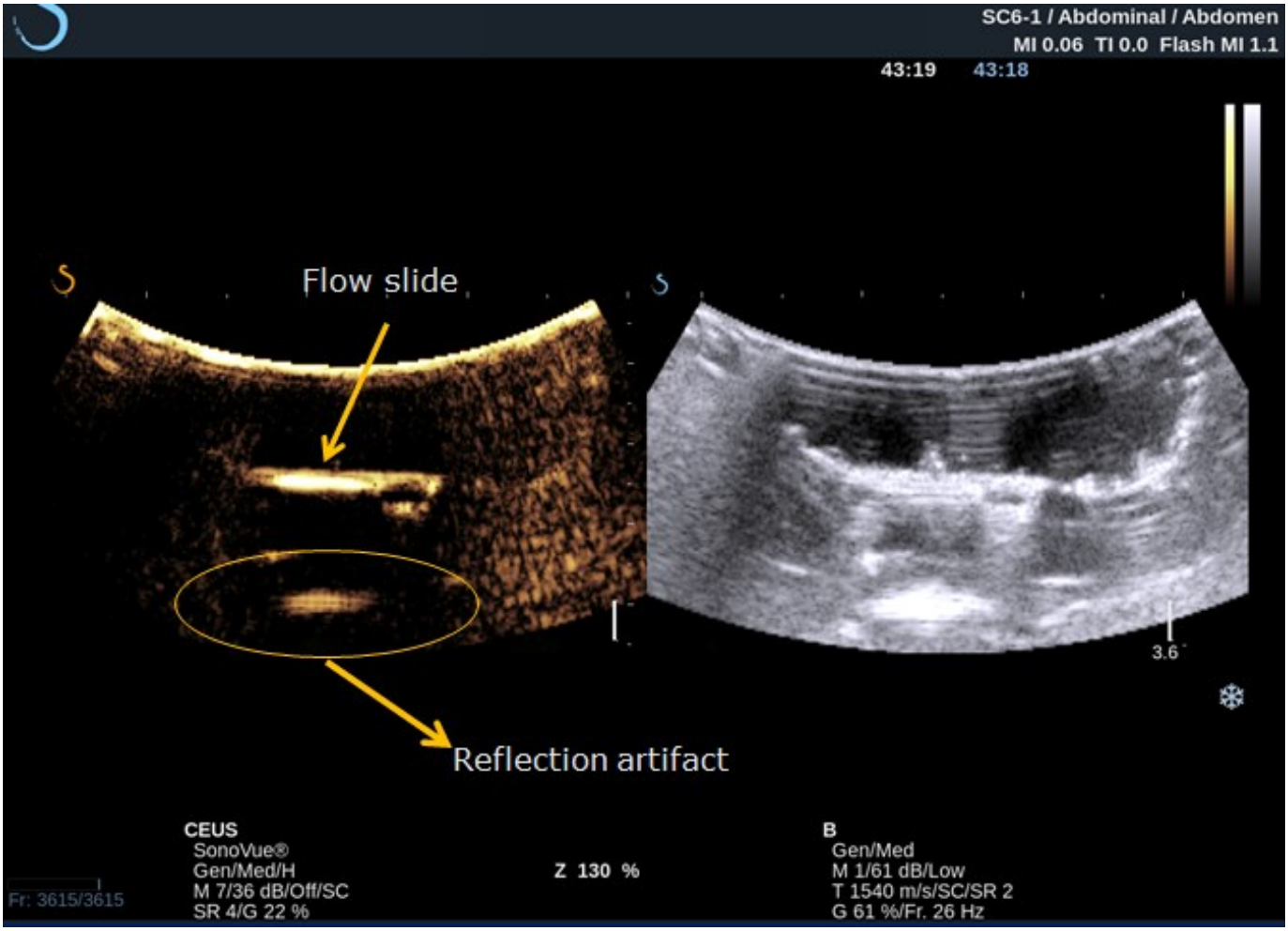

Figure 17 Contrast and B-mode side-by-side image acquisition from the Sonoscape SSI ultrasound machine using a 3.5MHz SC6-1 abdominal probe. Using a 3cm depth degassed gel offset microbubbles can be imaged within the flow slide. A reflection artifact whilst improved is still present.

These further development experiments demonstrate initial feasibility that the parallel plate flow chamber model can be adapted for insonation by externally applied ultrasound. Imaging of microbubbles within the flow chamber and the subsequent destruction after the high MI pulse, in particular, highlights that changes in thrombus burden after ultrasound treatment are due to microbubble augmented ultrasound thrombolysis.

Further refinement of ultrasound imaging may be performed for the parallel plate flow chamber circuit to be used in sonothrombolysis experiments. The degassed ultrasound gel offset can be replaced with a formal tissue mimicking phantom with an attenuation of approximately 0.3 dB/cm/MHz, which is equivalent to that of human tissue (23) to not only improve the reflection artifact but also enhance the reproduction of the intended transcutaneous application of ultrasound for sonothrombolysis. Additionally, to improve the reflection artifact, a piece of acoustic material should be placed over the parallel plate flow chamber during ultrasound application to absorb the ultrasound, thus reducing the reflection artifact produced from the insonation applied from below. Finally, the pulse sequence for ultrasound application can be improved from a single manual high MI flash using standard ultrasound contrast settings on the Sonoscape SSI ultrasound platform to custom settings specific for both low MI microbubble imaging and automated pulsed high MI bubble destruction modes which are achievable using diagnostic, commercially available ultrasound platforms such as the Philips iU-22 (Bothell, WA)with a curvilinear low frequency C5-1 probe. In addition, the frequency can be optimized for bubble destruction rather than bubble imaging. The Sonoscape SSI used in these experiments used a frequency of 3.5 MHz which as discussed in earlier chapters is relatively high for microbubble augmented ultrasound thrombolysis with many previous studies using frequencies closer to 1 MHz albeit with custom transducers rather than commercially available transducers (148-150).

5.5.3. Safety of contrast enhanced ultrasound

Given these desirable ultrasound qualities of a contrast enhanced ultrasound sequence for sonothrombolysis, an adaptation of the generic “contrast abdomen” settings of the Philips iU-22 (Bothell, WA) ultrasound platform with curvilinear C5-1 probe provided a custom pulse sequence. This included the following imaging parameters: frequency 1.7MHz, contrast (therapy) ultrasound and diagnostic side by side imaging, contrast (therapy) ultrasound MI 1.31 pulsed every 1500 ms, diagnostic imaging MI

0.06, frame rate 15 Hz, Time Gain Control centered, 2D gain ~25-60% based on lowest level of noise on diagnostic imaging and focus depth 4.5cm.

Whilst this was only an adaptation of a commercially available, clinically utilized ultrasound sequence, a preliminary assessment of its safety was performed. This was performed using Human Umbilical Vein Endothelial Cells (HUVEC) as previously described (149). In brief, commercially available pre-cultured HUVEC cells were placed on the 50 x 5 mm Ibidi parallel plate flow chamber microslide and coated and subsequently dried with fibronectin culture. This was then incubated at 37 ºC for one hour to allow absorption. The microslide was then washed with phosphate buffer solution and the slide assessed with x10 microscopy to ensure development of a monolayer with normal cobblestone cellular adhesion pattern (207).

The parallel plate flow chamber was then connected to a flow circuit using 7ml PBS perfused at a shear rate of 300 s^{-1}. PBS was used in this instance as the use of blood in the flow circuit would inhibit microscopy analysis due to the lack of florescence tagging of HUVEC in this experimental setup. Ultrasound as above with a 3.5 cm degassed ultrasound gel offset was applied to the flow chamber with SonoVue microbubbles at a concentration of 0.2% (14µL) within the flow circuit for 5 minutes whilst the HUVEC cells exposed to flow only for 5 minutes was used as a control. Video acquisition of the x10 microscopy was then transferred offline for blinded, qualitative assessment.

In the control experiments with flow only there was a satisfactory monolayer of HUVEC cells with a normal cobblestone cellular adhesion pattern observed indicating that flow alone did not affect the integrity of the HUVEC cell culture as expected given the origins of this cell line. In the experiments with HUVEC exposed to flow with ultrasound and microbubbles, the appearance of the cells themselves was preserved but there was a qualitative mild increase in the cellular separation between cells (Figure 18).

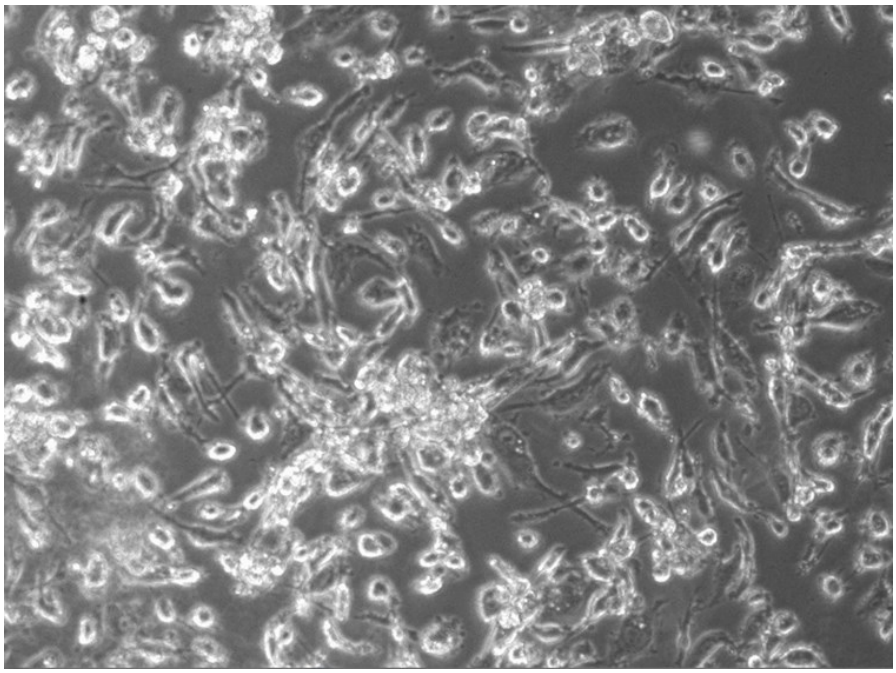

(a)

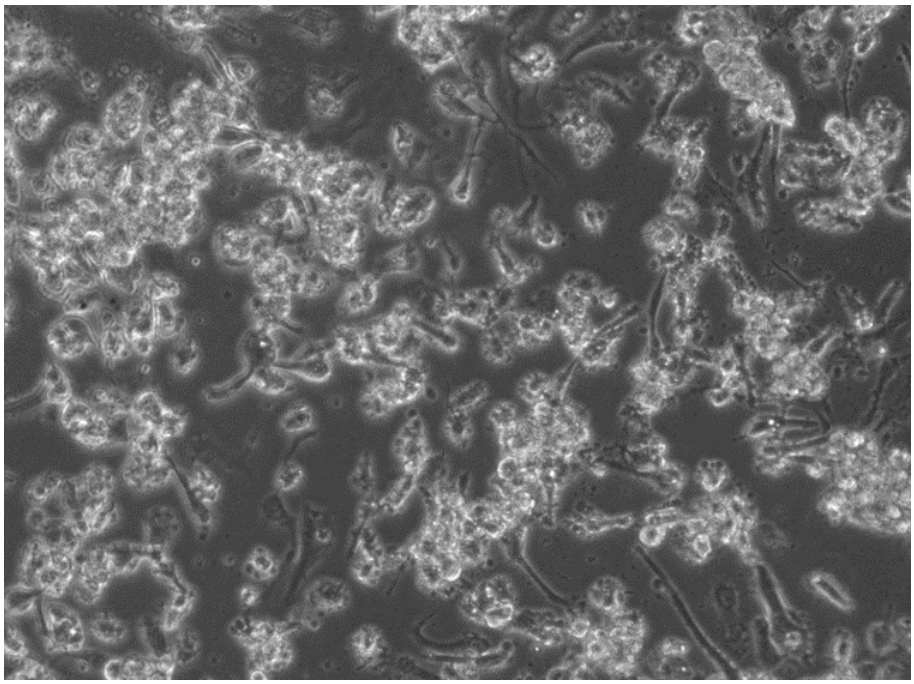

(b)

Figure 18 Microscopy x10 parallel plate flow chamber still images of A – Control HUVEC cells under flow conditions and B – HUVEC cells under flow conditions with ultrasound and microbubbles demonstrating intact cellular structure but increased cellular separation

This increase in cellular separation is in keeping with previous literature using continuous application of therapeutic 1.6 W/cm^2 1MHz ultrasound only (149). This separation was described as likely being secondary to the microstreaming effect of ultrasound. The significance of this cellular separation was the possibility of potentiating further inflammatory reaction. However, in this study and the current experiment there was no reduction in cellular viability. This is in contrast to a previous study using 2 W/cm^2 1 MHz continuous ultrasound which demonstrated not only separation but vacuolation of the endothelial cells.

Therefore, this current custom ultrasound sequence with microbubbles using a higher frequency and lower overall power due to pulsing of 1.31 MI does not preliminarily appear to cause any further damage to vascular endothelial cells compared to previous studies of ultrasound only which is currently in clinical use for acute thrombus removal. However, there remains a potential risk of vascular endothelial structural disruption which in itself may potentiate a pro-inflammatory or even pro-thrombotic state and this should continue to be formally assessed in future studies in-vivo.

5.5.4. Parallel plate flow chamber venous thrombosis models

For the purposes of developing an in-vitro clot model of DVT to illustrate the translational feasibility of sonothrombolysis, the clot model should have characteristics that resemble those of a venous thrombus and subsequently flow delivery of microbubbles to the thrombus must also represent venous flow. Additionally, within the constraints of the 200µl parallel plate flow chamber, the largest possible thrombus volume should be produced.

The Type III collagen model with endpoint measurement through fluoroscopically tagged platelets discussed thus far requires a minimum shear flow of 300 s^{-1} but can be investigated at shear flow of up to 1700 s^{-1} (191). Categories of shear flow have

been described which represent conditions of different types of thrombus formation; low shear venous flow (50-1000 s^{-1}), arterial flow (1000-4000 s^{-1}), and high pathological flow representative of a stenosis within the arterial circulation (>4000 s^{-1}) (208). The Type III collagen model spans both venous and arterial shear flow through its platelet interaction with GPIb and GPVI at the venous and arterial ends of the shear flow spectrum respectively (191) . The fibrin and tissue factor model, which uses platelet interaction through GPIb receptors with endpoint measurement of fluroscopically tagged fibrinogen, produces thrombus formation at low shear flow of 50-700 s^{-1} only (195, 196, 209). Within a parallel plate flow chamber in conditions of parabolic flow, the shear rate is defined by the following equation (186):

$$\text{Shear rate } (s^{-1}) = \frac{100 \times \text{Volumetric flow rate (ml/min)}}{\text{Chamber height (mm)}^2 \times \text{Chamber width (mm)}}$$

Therefore, using the 50 x 5 mm Ibidi parallel plate flow μ-slide 1 chamber, the chamber width is 5 mm and the chamber height is 0.2 mm. The volumetric flow rate can then be derived from this equation using the desired shear rate for a given thrombus model. Subsequently, for a 10 minute experiment as previously described with 5 mintutes for thrombus formation and 5 minutes for treatment, the required volume of blood can be calculated with an extra 1ml added to that volume to allow for 700 μL of dead space tubing within the circuit. The Type III collagen model and the fibrin with tissue factor model were compared for optimal measurable thrombus formation under venous shear flow in the presence of microbubbles.

For both models anticoagulated human blood using EDTA was used. As previously described, the blood was incubated at 37 degrees Celsius for 10-15 minutes to allow the platelets to resensitize (3). Just prior to use, the blood was re-calcified with calcium chloride and depending on the thrombus model being investigated, the appropriate fluorescent marker was added for endpoint measurement. In the Type III Collagen model, the platelet membrane probe 3,3-dihexyloxacarbocyanine iodide ($DiOC_6$) enabling platelet surface area coverage was used (188, 200). For the fibrin

with tissue factor model, fluorescein isothiocyanate (FITC) which labels fibrinogen was added to provide fibrin surface area coverage assessment (201). SonoVue microbubbles were also added just prior to the experiments at a physiological concentration of 0.2%.

The Collagen Type III and fibrin with tissue factor models were prepared as follows. A glass slide was degreased using 2M HCl in 50% ethanol. For the Collagen Type III model, a micropipette was then used to apply a 0.3µL spot of Collagen Type III at a concentration of 50µg/ml to the slide. For the fibrin with tissue factor model, a 0.3µL spot of lipidated tissue factor (Innovin) diluted to 5þM/µL was placed on to the glass slide. Both were then allowed to adhere at room temperature within a humidified box for 60 minutes. The non-adhered coating was then washed off after this time using 0.9% saline solution and the Ibidi 50 x 5 µ-slide 1 placed over the top of the slide to complete the flow chamber. The flow chamber was then flushed with phosphate buffer solution (PBS) three times then allowed to incubate at room temperature for 15 minutes (180).

For the Collagen Type III model, the intended shear rate for this model was $300s^{-1}$ Therefore, given a chamber height of 0.2 mm and a chamber width of 5 mm, the volumetric flow rate was 0.6 ml/min requiring a total circuit volume of 7 ml for a 10 minute experiment allowing for 700µL of dead space tubing. The shear rate of the fibrin with tissue factor clot model was 50 s^{-1}, therefore, given the same dimensions of the flow chamber and tubing, the volumetric flow rate was 0.1 ml/min thus requiring a total circuit volume of 2 ml for a ten minute experiment. In order to provide a microbubble concentration of 0.2%, 14µL of SonoVue was added to the 7 ml blood volume for the Collagen Type III model and 4µL added to the 2 ml blood volume for the fibrin with tissue factor model.

Endpoint measurement was recorded as either $DiOC_6$-labelled platelet surface area percentage or FITC labelled fibrin surface area percentage for the respective models

using quantification as described earlier using VirtualDub and ImageJ software packages. To enable true comparison, samples from the first and second aforementioned groups were paired from the same blood source for endpoint measurement as thrombus formation can vary between different blood sources. As a result a paired t-test was used for statistical analysis using Prism Version 6.01 (GraphPad Software Inc., La Jolla, CA, USA) software. Statistical significance was taken as $P<0.05$.

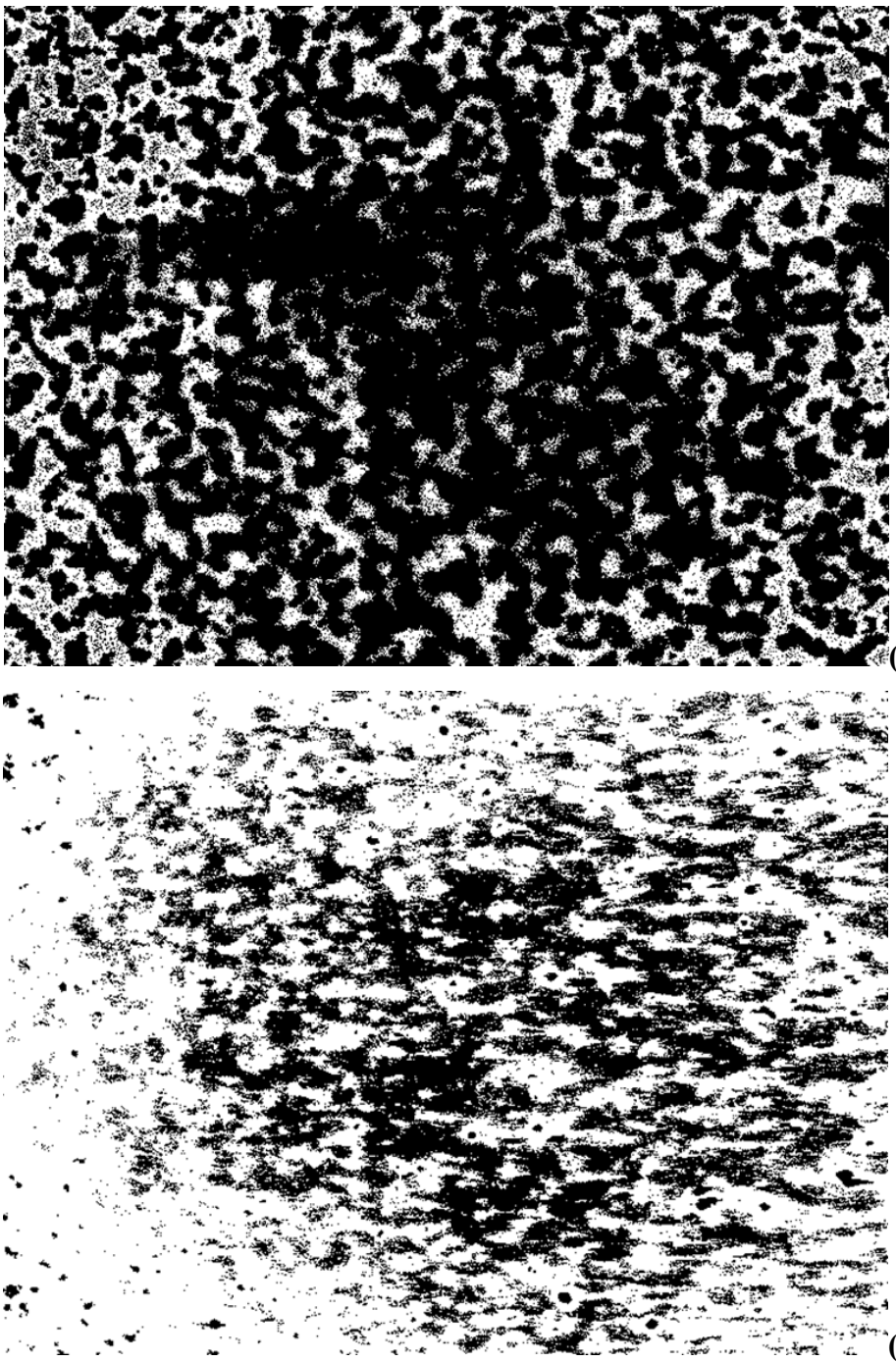

Figure 19 Example stacked grey scale images of thrombus model surface area coverage in the presence of SonoVue microbubble. In (a) the Collagen Type III model demonstrating 35.6% surface area coverage of $DiOC_6$-labelled platelets. In (b) the fibrin with tissue factor model demonstrating 84.2% FITC tagged fibrin surface area coverage.

A total of 10 experiments were performed; 5 in the Collagen Type III model and 5 in the fibrin with tissue factor model. The mean percentage surface area coverage of $DiOC_6$ tagged platelets in the Collagen Type III model was 34.18 ± 3.17 %. The mean percentage surface area coverage of FITC tagged fibrin in the fibrin with tissue factor model was 86.43 ± 2.52 % (Figure 19). Using a paired t-test there was a statistically greater measured thrombus formation in the fibrin with tissue factor model compared to the Collagen Type III model ($p=0.0002$).

As previously demonstrated the addition of microbubbles does not appear to effect thrombus formation within the parallel plate flow chamber using either model. However, there was greater thrombus volume measured using the fibrin with tissue factor model compared to the Type III Collagen model. One reason for this finding may be that the shear rates used in this experiment may not be suited for optimal thrombus formation using the Collagen Type III model. It has been previously described that large platelet aggregates do not form on the surface of vWF in collagen models unless there is a very high shear rate of 800 - >10,000s^{-1} (210, 211), therefore, at a shear rate of 300 s^{-1} a lower degree of thrombogenic activity can be expected. This finding fits with the traditional perception that arterial thrombi which are formed under these high shear rates in stenosed vessels are platelet rich as has been demonstrated in both previous work investigating sonothrombolysis for arterial thrombi in stroke and acute myocardial infarction as well as parallel plate flow chamber studies demonstrating the efficacy of anti-platelet therapies under different shear conditions (171, 208).

Conversely, parallel plate flow chamber models using tissue factor with fibrin coverage endpoint measurement have been utilized at low shear rates (<600 s^{-1}) in studies assessing factor Xa inhibition for novel oral anticoagulants in the treatment of venous thromboembolism (209). An additional benefit of using the fibrin with tissue factor model is also the reduced volume of blood at this lower shear rate required for each experiment which enables more efficient use of resources and reduced volumes

for laboratory handling. Whilst the fibrin with tissue factor clot model appears to be the suitable model for progression in the assessment of sonothrombolysis for DVT, the use of a platelet rich clot model in the earlier described experiments demonstrates a degree of reproducibility with previous in-vitro sonothrombolysis studies further demonstrating feasibility of the use of parallel plate flow chambers for the assessment of sonothrombolysis (166, 172, 177).

A limitation of this comparative assessment was the different endpoints used for each type of model with $DiOC_6$ tagged platelets in the Collagen Type III model and FITC tagged fibrin for the tissue factor model. Whilst repeat experiments with crossover of endpoint measurements could have been performed, the intention of this experiment was to assess previously validated parallel plate flow chamber models for use in the novel setting of sonothrombolysis rather than develop a novel parallel plate flow chamber model to subsequently be used in sonothrombolysis experiments (180, 190, 195).

The results of these preliminary development experiments have demonstrated that the use of parallel plate flow chambers using whole blood and in particular, the tissue factor and fibrin DVT specific model, can be combined successfully with the presence of ultrasound microbubbles. In addition, using the appropriate surrounding acoustic environment, ultrasound can be applied to these parallel plate flow chambers to both image and destroy microbubbles within the chambers. The combination of these conditions demonstrates the feasibility for the in-vitro assessment of sonothrombolysis for DVT using parallel plate flow chambers.

6. CONTRAST ENHANCED ULTRASOUND FOR THROMBUS DISSOLUTION IN AN IN-VITRO MODEL OF ACUTE DEEP VEIN THROMBSOSIS

6.1. Introduction

Acute thrombus removal in patients with ileofemoral DVT is recommended as part of clinical practice to prevent the long term development of PTS (98, 99). Current strategies to achieve this include the use of catheter directed thrombolysis (CDT) and pharmaco-mechanical thrombolysis (PMT) which includes devices such as the EKOS intravascular ultrasound catheter (EKOS Corporation, Bothell, WA, USA) (81, 88). The removal of thrombus is believed to preserve deep venous valvular function and prevent venous hypertension with an absolute risk reduction in the development of PTS of 28% after 5 years described with CDT (199). However, these devices require endovascular access and use of thrombolytic therapy resulting in an all cause bleeding risk of up to 20%.

Transcutaneous ultrasound accelerated thrombolysis without thrombolytic therapy has been described in an in-vivo model of DVT achieving thrombus dissolution through destruction of bubbles created through fluid insonation at the fluid-thrombus interface (147). However, this required the use of a non-commercially available ultrasound platform to achieve this mechanism of acoustic cavitation. Thrombus dissolution using ultrasound and microbubbles, commonly known as sonothrombolysis, has been successfully described in arterial models of thrombosis in-vitro and in-vivo in an attempt to target acute ischaemic stroke and acute myocardial infarction (164-168, 170, 172, 173, 181, 212). Using pre-formed microbubbles at the fluid-thrombus interface reduces the energy threshold and thus increases the efficiency required to achieve acoustic cavitation. To our knowledge, the assessment of thrombus removal using ultrasound and microbubbles in DVT

specific models has not been performed despite the potential advantages over current techniques which require thrombolytic therapy, endovascular access and irradiation.

In this study, the feasibility of thrombus dissolution by sonothrombolysis compared to ultrasound insonation only and control conditions was performed using a commercially available ultrasound platform in combination with a licensed microbubble preparation using a previously described validated in-vitro flow model of DVT (180).

6.2. Methods

6.2.1. Thrombus and whole blood preparation

The in-vitro model of DVT for this study was created using a parallel plate flow chamber set up which has previously been used to assess functions of thrombus formation in real time under venous flow conditions using whole blood (180). The commercially available Ibidi (Martinsried, Germany) µ-slide 1 parallel plate flow chamber with dimensions of 50mm x 5mm x 0.2mm with a volume of 200µl was used to create the thrombus model. A tissue factor thrombogenic substrate model which provides platelet interaction through GPIb receptors at low venous shear stress of 50-700 s^{-1} was used as previously described (195, 196, 209). Briefly, a glass slide was degassed using 2M HCl in 50% ethanol. A 0.3µL spot of lipidated tissue factor (Innovin) diluted to 5þM/µL was placed on to the glass slide and then allowed to adhere at room temperature within a humidified box for 60 minutes. The non-adhered coating was then washed off using 0.9% saline solution and the Ibidi µ-slide 1 placed over the top of the slide to complete the flow chamber. The flow chamber was then flushed with phosphate buffer solution (PBS) three times and then allowed to incubate at room temperature for 15 minutes (180).

The whole blood used within the flow circuit was prepared using anticoagulated human blood placed in Ethylenediaminetetraacetic acid (EDTA) and incubated at 37 degrees Celsius for 10-15 minutes to allow platelets to resensitise. Prior to use, blood was drawn onto 10% (v/v) citric acid/citrate dextrose (ACD) and re-calcified with calcium chloride. It was then loaded with fluorescein isothiocyanate (FITC) at a concentration of 75µg/ml which labels fibrinogen to provide fibrin surface area coverage assessment (201). Additionally, a sample blood was checked using microscopy for satisfactory platelet count to ensure that platelet activation had not occurred during preparation.

6.2.2. In-vitro flow circuit

The Ibidi µ-slide 1 parallel plate flow chamber was connected proximally via tubing to a single reservoir Ibidi fluidic unit containing the whole blood preparation. The fluidic unit was controlled by a computer controlled pump using custom software to provide the desired flow rate and thus shear stress required within the flow chamber to model venous flow conditions. Distally, the parallel plate flow chamber was connected to a closed waste reservoir. Prior to the addition of the whole blood preparation for each experiment, the fluidic unit, tubing and parallel plate flow chamber were flushed with PBS to purge any air bubbles within the circuit to prevent variations in shear stress within the circuit.

The flow within a parallel plate flow chamber mimics parabolic flow observed within blood vessels, therefore, the shear rate can be defined using the following equation (186):

$$\text{Shear rate } (s^{-1}) = \frac{100 \times \text{Volumetric flow rate (ml/min)}}{\text{Chamber height (mm)}^2 \times \text{Chamber width (mm)}}$$

The shear rate used to represent venous conditions was 50 s^{-1} (195). Therefore, given the aforementioned dimensions of the Ibidi µ-slide 1 parallel plate flow chamber, the flow rate used for all experiments was 0.1 ml/min. Allowing for ten minute experiments consisting of 5 minutes of thrombus formation and 5 minutes of treatment time as well as approximately 700µL of dead space tubing within the circuit, a total of 2 mL of whole blood preparation was required for each experiment.

6.2.3. US and microbubble treatment

Ultrasound application was designed to mimic transcutaneous insonation of the common femoral vein in an average adult patient. During insonation, the parallel plate flow chamber containing the thrombus was suspended using clamps at either end enabling ultrasound application from below in a transverse plane to the direction of flow. A commercially available Philips (Bothell, WA) iU-22 platform with C5-1 curvilinear probe was used for experiments. A custom designed sequence based on the standardly available abdominal contrast enhanced setting was developed with the following imaging and therapy settings: frequency 1.7MHz, contrast (therapy) ultrasound and diagnostic side by side imaging, contrast (therapy) ultrasound MI 1.31 pulsed every 1500 ms, diagnostic imaging MI 0.06, frame rate 15 Hz, Time Gain Control centered, 2D gain ~25-60% based on lowest level of noise on diagnostic imaging and focus depth 4.5cm. The side-by-side imaging enabled direct visualization of microbubbles within the parallel plate flow as well as confirmation of bubble destruction. The interval pulse application of high MI was based on previous in-vitro and in-vivo data suggesting improved efficacy of therapy (147, 174). A focal depth of 4.5 cm was used to represent the depth of the common femoral vein in an average adult. Additionally, to mimic the potential attenuation of ultrasound insonation, a tissue mimicking phantom with an attenuation of approximately 0.3 dB/cm/MHz equivalent to that of human soft tissue was used (150). Finally to reduce reverberation artefact on diagnostic imaging and prevent reflection echoes amplifying the acoustic energy of treatment as previously described

(156), a piece of custom shaped acoustic material, Aptflex F28 (Precision Acoustics, Dorchester, UK) measuring 10 mm in depth with an attenuation of approximately 30dB/cm/MHz was placed on top of the parallel plate flow chamber during insonation.

The commercially available and European licensed microbubble ultrasound contrast agent, SonoVue (Bracco, Italy) was used for sonothrombolysis experiments. As described earlier, SonoVue did not have significant effect on either thrombus formation in the parallel plate flow chamber or endpoint quantification of thrombus. SonoVue was prepared as per the manufacturer's guidance which briefly involves the addition of 4.8 ml of 0.9% normal saline to a single vial of 25mg of lyophilized sulphur hexafluoride powder just prior to use. The average physiological concentration of SonoVue during infusion of 2 vials which is the maximum recommended single dose has been previously described as 0.2% (206). Therefore, given an average adult intravascular blood volume of 5 L and the 2 ml volume of blood in experimental flow circuit, 4 μL of SonoVue was added to the whole blood preparation within the fluidic unit proximal to the parallel plate flow chamber immediately prior to each experiment.

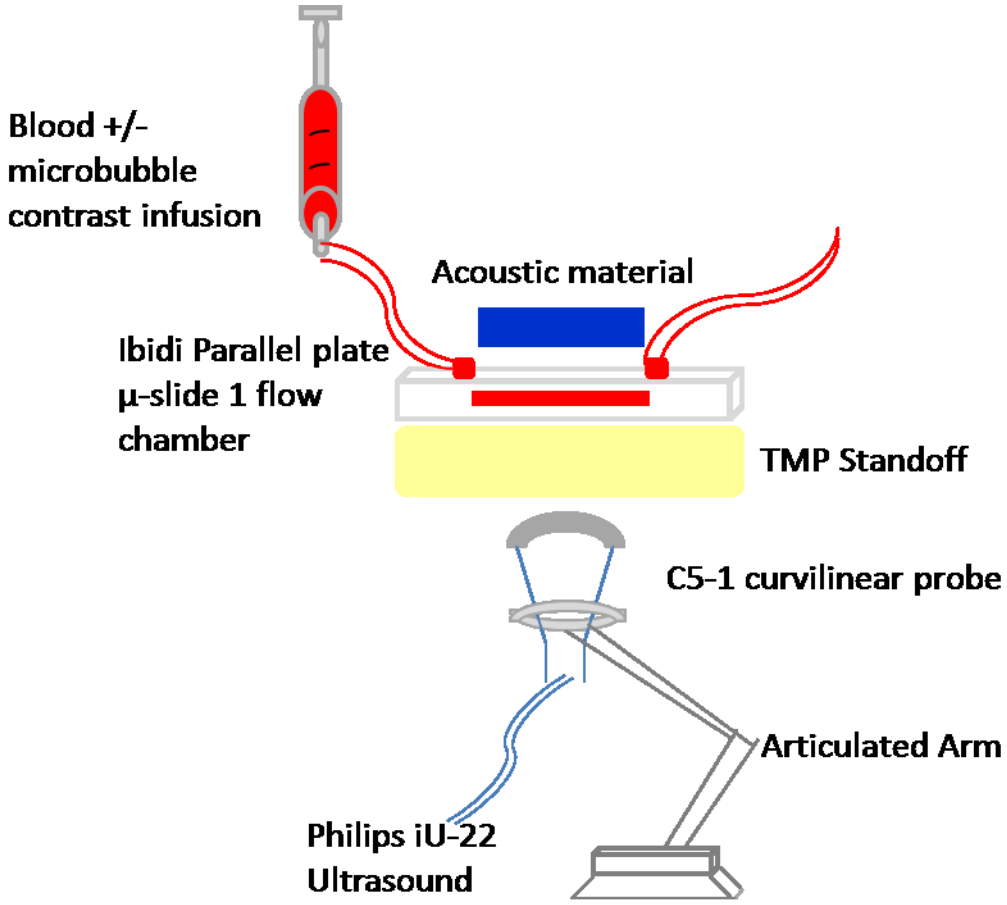

Figure 20 Schematic of in-vitro parallel plate flow circuit sonothrombolysis experimental setup (not to scale).

6.2.4. Endpoint quantification and image analysis

Endpoint quantification was performed using the surface area coverage of fibrin fluoroscopically tagged by FITC which provides a well validated surrogate assessment of thrombus volume (180, 202, 203). A microscopic qualitative assessment of overall thrombus structure was also performed x10 and x40 magnification. As described, FITC was loaded onto the whole blood preparation and during flow thrombus forms on the lipidated tissue factor thrombogenic substrate on

the parallel plate flow chamber. The FITC was then imaged using an epifluorescence CKX41 microscope (Olympus, Japan) with real time video acquisition using a magnification of x10 at a capture rate of 25 frames per second via a Rollera XR Camera (QImaging, Surrey, Canada) and StreamPix6 V.4 software (NorPix, Montreal, Canada). To avoid photo bleaching only 2 second video clips were acquired of representative areas of the thrombus. The thrombi were imaged at 2 time points during experiments; at 5 minutes to ensure thrombus formation and at 10 minutes after therapy.

Video files were transferred in the AVI format for blinded offline image quantification. Using VirtualDub software (Version 1.9.11, Open source), the AVI file was segmented into 6 frames (representing 0.24 seconds) and checked to ensure that the in plane region of interest did not move across the flow slide over that time. This segmented file was then saved and transferred to ImageJ software (Version 1.47, National Institute for Health, USA). Using the Z-stack function all six frames were stacked to create one image with only consistent image features across all 6 frames represented. This method enabled only the fluoroscopically tagged fibrin within fixed, stable thrombus within the flow chamber to be captured and removes artifactual signal from passing plasma and non-fixed FITC moving across the field during flow (204, 205). The stacked image was then converted to grey scale providing fluoroscopically tagged elements to appear white. The image was then quantified using the Analyze tool for percentage surface area coverage of "white regions" thus providing the surrogate clot surface area coverage measurement.

6.2.5. Experimental parameters and Statistical Analysis

The groups assessed in this in-vitro feasibility study included: control using whole blood preparation flow only, ultrasound insonation only during flow and ultrasound with SonoVue microbubbles during flow. Each group contained 8 individual experiments.

Mean surface area coverage for each group was presented as mean ± SD with differences between the experimental groups assessed using the one-way analysis of variance (ANOVA). A p value of <0.05 was considered statistically significant.

Offline image analysis was performed blindly by two imaging research fellows with at least 3 years of medical image quantification experience. Intra- and inter-reader reproducibility for quantification of percentage surface area coverage was assessed using Pearson's correlation coefficient. Statistical analysis was performed using Prism V.6 (GraphPad, La Jolla, USA) and SPSS V.22 (IBM, New York, USA).

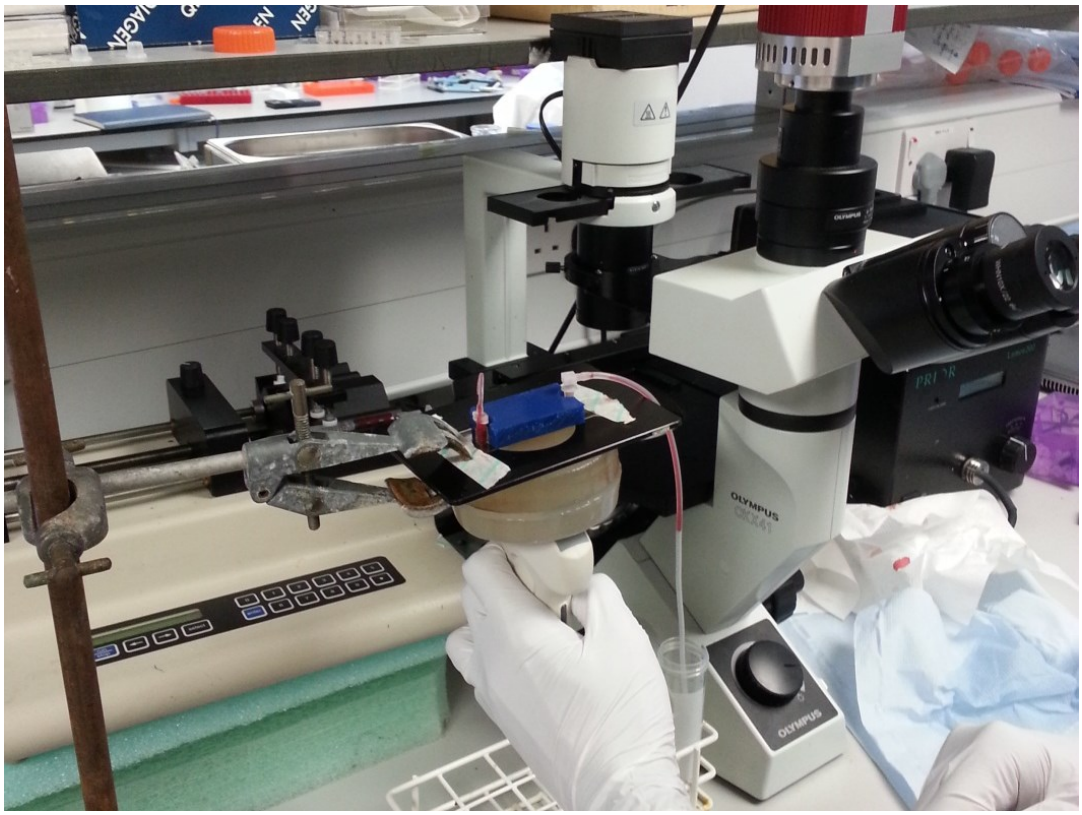

Figure 21 In-vitro flow experimental set up demonstrating ultrasound insonation with a curvilinear probe in a transverse plane to the parallel plate flow chamber with tissue mimicking phantom between the probe and thrombus and acoustic material placed above the parallel plate flow chamber.

6.3. Results

6.3.1. Qualitative assessment

Control experiments with flow of whole blood preparation into the parallel plate flow chamber containing the tissue factor thrombogenic substrate demonstrated cessation of flow secondary to thrombus formation in 7 out of 8 experiments with 8 out of 8 experiments demonstrating complete flow cessation at 10 minutes. At x10 magnification, cessation of flow was seen in association with almost complete surface area coverage with FITC. At x40 magnification, a large number of red bloods cells (RBCs) were observed caught within an organized fibrin mesh network in keeping with that expected of a venous thrombus (179).

Experiments examining ultrasound insonation only with flow of whole blood preparation demonstrated cessation of flow and almost complete surface area coverage with FITC in 8 out 8 experiments at 5 minutes during thrombus formation. After 5 minutes of ultrasound insonation, at x10 magnification thrombus was still present but 5 out of 8 experiments showed changes in morphology characterised by interrupted edges and internal porosity. This was associated with some partial restoration of flow. At x40 magnification, the interrupted edges and porosity were identified as ulcers and perforations in the thrombus through RBCs, however, the fibrin mesh network still appeared intact.

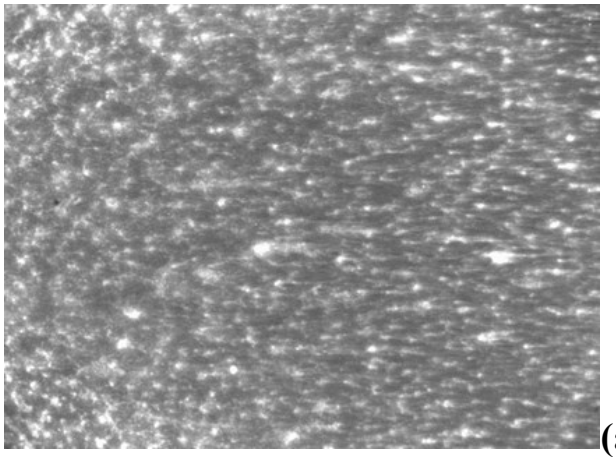

(a)

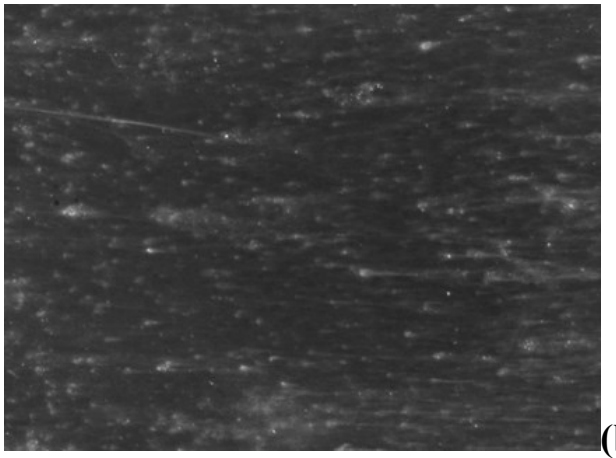

(b)

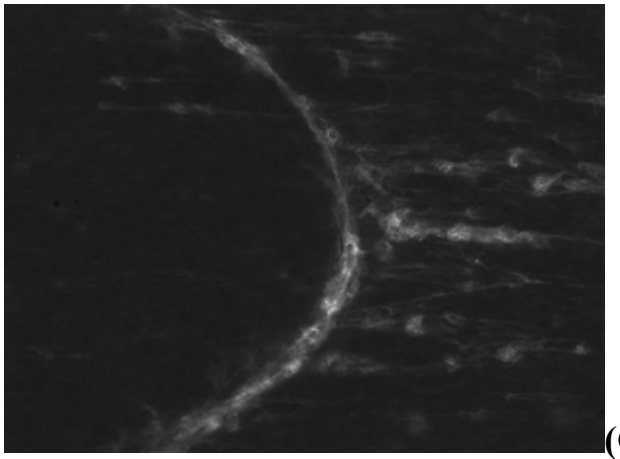

(C)

Figure 22 Epifluorescent microscope images at x10 magnification. A – Control with flow only with almost complete surface area coverage with FITC. B – Ultrasound only demonstrating thrombus porosity. C – Ultrasound and microbubble therapy shows almost complete thrombus dissolution with only sparse fibrin mesh networks remaining

In the ultrasound and SonoVue group with flow of whole blood preparation, cessation of flow with almost complete surface area coverage with FITC was visualized in 8 out 8 experiments at 5 minutes. After 5 minutes of ultrasound insonation in the presence of SonoVue, 6 out 8 experiments demonstrated almost complete thrombus dissolution with only scattered fibrin strands observed at x40 magnification. This was associated with complete restoration of normal flow. In the remaining 2 experiments, there was internal porosity and ulceration noted as seen in the ultrasound only group as well as an overall reduction in the surface area coverage of the fibrin mesh network. Representative examples from each of the three groups are shown in Figure 22.

6.3.2. Quantitative assessment

The quantitative FITC surface area coverage for each group is illustrated in Figure 23 & Figure 24. Reported values correspond to the mean ± one SD. Control experiments with flow of whole blood preparation demonstrated 85.8 ± 5.6% (n=8) surface area coverage with FITC after ten minutes. Addition of ultrasound only in the presence of whole blood preparation flow demonstrated a surface area coverage of 52.7 ± 7.6% (n=8). The group with both ultrasound and SonoVue therapy demonstrated only 10.7 ± 12.4% (n=8) surface area coverage with FITC. There was statistically significant difference between the three groups ($p<0.0001$, one-way ANOVA).

Intra-reader reproducibility for surface area percentage coverage image quantification was good (r=0.939). Inter-reader reproducibility was also good (r=0.873).

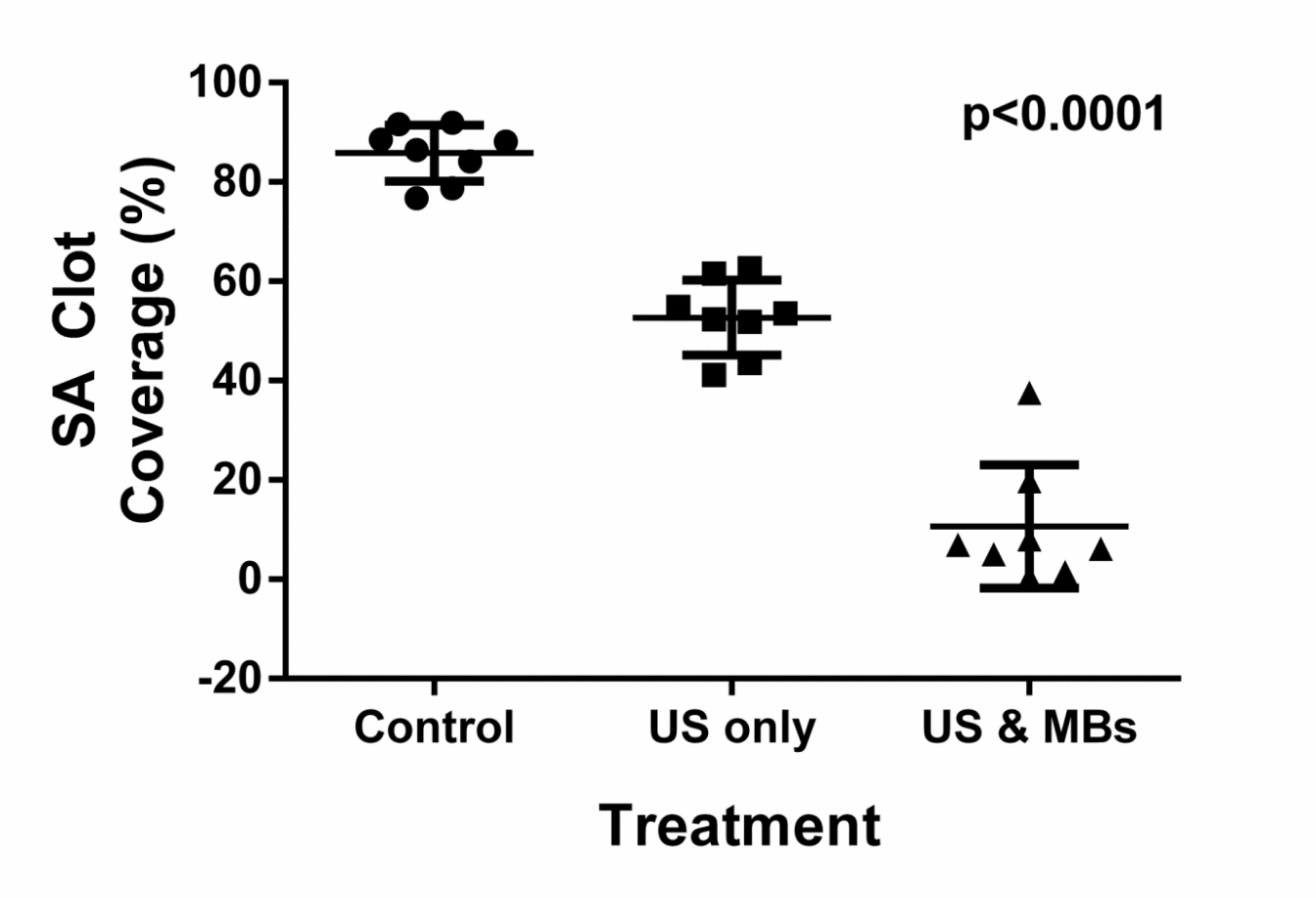

Figure 23 Scatter plot of surface area percentage coverage with mean ± SD in the three groups (control, ultrasound only and ultrasound & SonoVue) demonstrating statistical difference using a one-way ANOVA.

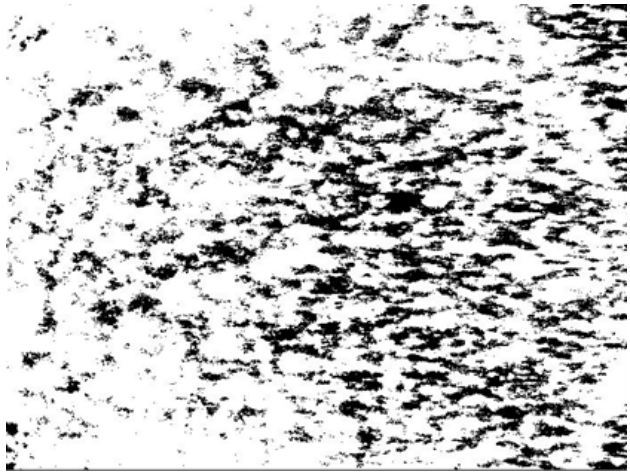
(a)

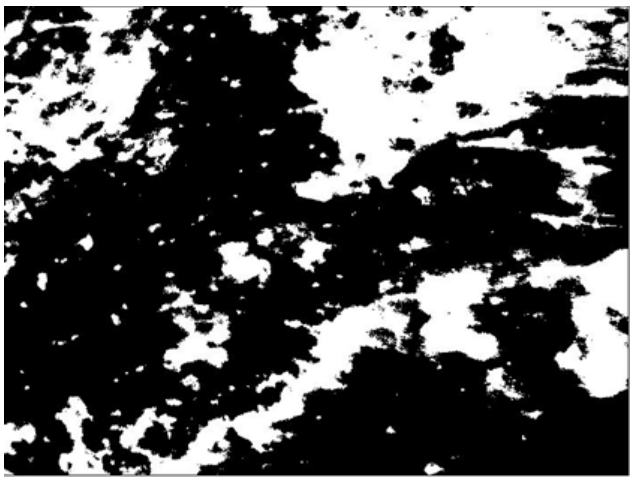
(b)


(c)

Figure 24 Image J grayscale converted Z-stacked images. A – Control with flow only demonstrating 86.4% surface area thrombus coverage. B – Ultrasound and flow demonstrating 54.8% surface area coverage. C- Ultrasound and SonoVue demonstrating 6.9% surface area coverage.

6.4. Discussion

This in-vitro study demonstrates the feasibility of ultrasound and microbubble contrast agent to achieve thrombus dissolution in the context of DVT specific conditions. In particular, it highlights a possible non-invasive, non-irradiating technique which does not require thrombolytic therapy and is significantly better at achieving thrombus removal than ultrasound alone using a commercially available ultrasound platform.

In this study the commercially available ultrasound platform and transducer was used at a frequency of 1.7 MHz. This is comparable to previous studies using commercially available ultrasound platforms for sonothrombolysis with a range of 1.5 – 1.7 MHz reported and as found in this study, statistical incremental benefit was also observed in these studies between ultrasound alone and ultrasound with microbubbles for therapy (168, 174). Whilst these studies were conducted in-vivo, the reported recanalization success of 60–91.6% is relatively comparable to the improvement in thrombus surface area coverage over control conditions of 75.1% observed in the current study.

The use of side-by-side diagnostic and therapeutic imaging in this study also provides further validation of the use of pulsed high MI imaging over continuous ultrasound insonation. Previous in-vitro studies using continuous ultrasound insonation with microbubbles demonstrated variable arterial model clot mass reduction of 1-43% (166, 172, 177). However, when pulses of high MI were used guided by low MI diagnostic imaging achievable on diagnostic ultrasound platforms, clot mass reduction was reported as 55% (175). During the current study, microbubble accumulation within the parallel plate flow chamber was observed on diagnostic low MI imaging in between the pulses of high MI as shown in Figure 25. Microbubbles in the imaging field were then destroyed with the high MI pulse and it is likely that destruction by acoustic cavitation at the fluid-solid interface contributed

to thrombus dissolution as evidenced by the thrombus porosity visualized. This fluid-solid accumulation of microbubbles may be prevented in continuous insonation as microbubbles may be destroyed proximally within the fluid medium as soon as they enter the field of insonation. This interval between high MI pulses may be of particular importance in the venous circulation compared to the arterial circulation as lower flow rates may predispose to a longer time to microbubble replenishment.

The main strengths of this study lie within the in-vitro flow model used to mimic conditions of DVT. This is the only in-vitro study to our knowledge investigating sonothrombolysis to use a whole blood preparation with previous studies using PBS buffers or other similar agents to deliver microbubbles to a pre-formed clot (166, 170, 174). This may account for the higher level of thrombus dissolution observed in the current study with results being more comparable to those seen in-vivo as described earlier as the use of a whole blood medium may provide naturally occurring thrombolytic enzymes such as t-PA and urokinase within the circuit to aid thrombus dissolution. This combination of enhanced acoustic cavitation using microbubbles and resultant delivery of naturally occurring thrombolytics to within the thrombus may negate the need for adjunctive thrombolytic therapy which would reduce the significant bleeding risk associated with acute thrombus removal currently within clinical practice. Additionally in this study, microbubbles were delivered to the thrombus in an analogous manner to an intravenous infusion of microbubbles under low flow venous conditions at physiological concentrations observed with the currently licensed maximum single dose of SonoVue. Therefore if translational, this technique would not require endovascular access which again would minimise bleeding risk.

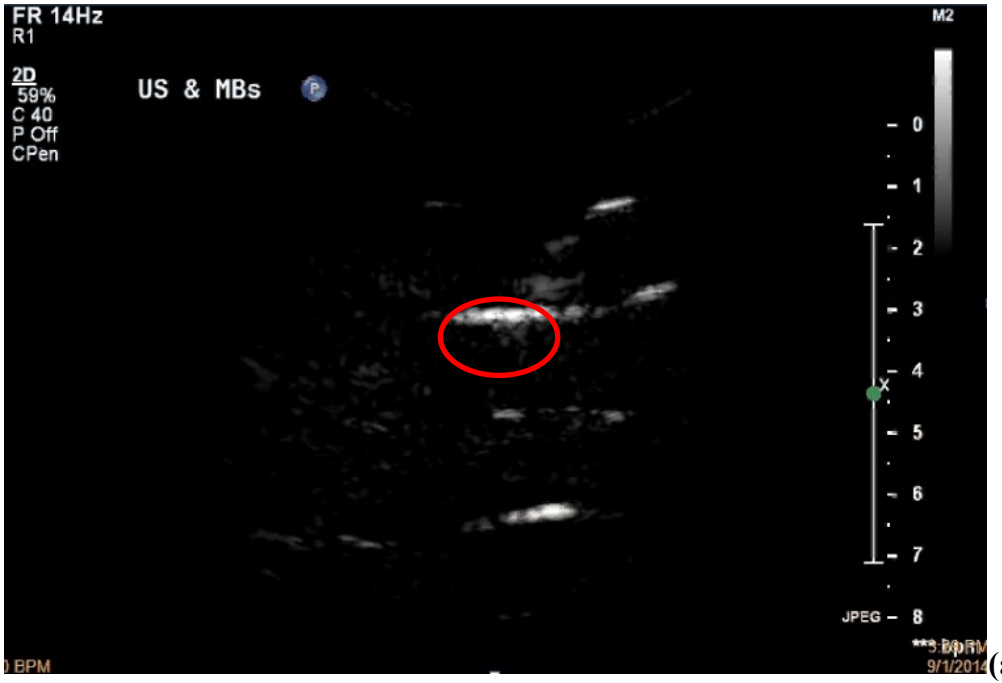

(a)

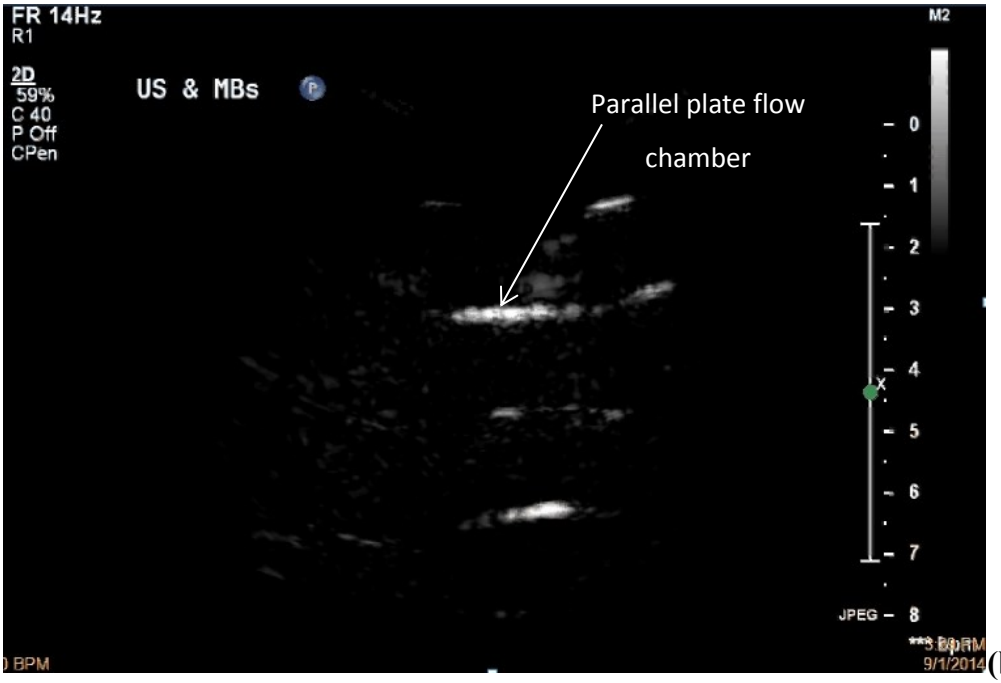

(b)

Figure 25 Ultrasound image acquisition with low MI (0.06) during treatment demonstrating (a) accumulation of microbubbles (red circle) within the parallel plate flow chamber and (b) subsequent destruction of accumulated microbubbles immediately after a high MI pulse (1.31)

A further strength of this model is the use of an existing validated in-vitro thrombus model of DVT. Previous in-vitro and in-vivo sonothrombolysis studies have demonstrated significant heterogeneity in thrombus formation (150, 162-164, 166, 170, 173) with many thrombus models being designed de-novo for sonothrombolysis experiments. Attempts have been made to standardize the thrombi used to assess sonothrombolysis using histological correlation, however, this correlation has been performed with arterial clots seen in acute ischaemic strokes rather than DVT and as yet has not been widely reproduced (212). The use of parallel plate flow chambers and in particular use of the tissue factor model used in this study has already been validated in the haematological assessment of thrombus formation and fibrin formation under venous shear stress conditions (180, 195). Therefore, after confirming that thrombus formation and endpoint assessment were not altered by the presence of microbubbles within the circuit, this established model of DVT formation could be used reliably to assess this novel therapy.

Limitations of this in-vitro model should however be acknowledged. No vein wall interactions were present in this DVT model which is not only important for clot formation but also for the assessment of vein wall damage secondary to ultrasound insonation which has previously been described using endothelial cell damage and activation (149, 150). However, both of studies used continuous ultrasound insonation compared to the current study that used pulses of high MI. Additionally, through the use of whole blood within the flow circuit and a venous shear stress, two out of three of Virchow's triad were represented in this model.

Physical constraints of the model did not enable simultaneous application of ultrasound and imaging with epifluorescence microscopy which would have provided assessment and insight into the mechanisms of thrombus dissolution. However, incremental changes in qualitative assessment between the experimental groups suggested a likely increase in acoustic cavitation activity with ultrasound and microbubbles as previously discussed.

The thrombus was relatively acute, however, formation of older thrombi using this model would require a significantly larger volume of whole blood to create the necessary flow circuit which would not have been appropriate in this feasibility study. Further translational assessment of sonothrombolysis should assess efficacy in sub-acute and chronic venous thrombi which represent different stages of thrombus organization (105) although it is noted that currently within clinical practice only acute and sub-acute thrombi are considered for acute thrombus removal (98, 99). Additionally, the overall thrombus volume produced in this study was relatively small compared to clinical ileofemoral DVT, however, the microbubble volume in the flow circuit was maintained to physiological concentrations. Additionally, the therapy time was also appropriately scaled down to 5 minutes with comparisons drawn to mean PMT treatment times of 76 minutes and mean CDT treatment time of 22 hours (213).

This study has demonstrated the feasibility of thrombus dissolution using a combination of ultrasound and microbubbles over ultrasound alone in a validated in-vitro flow model of acute DVT. Additionally, this technique did not require adjunctive thrombolytic therapy and is non-invasive and non-irradiating potentially conferring an advantage over current clinical methods of acute thrombus removal in DVT. Future translational studies must focus on continued efficacy in the presence of vein wall and in older, organized thrombi as well as assessment of safety outcomes secondary to thrombus dissolution and application of ultrasound energy.

7. STROKE & CAROTID ATHEROSCLEROSIS

7.1. The Burden of Stroke

Stroke is defined by the World Health Organisation as a clinical syndrome of a focal neurological deficit lasting greater than 24 hours of vascular origin comprising either thrombotic or embolic occlusion or haemorrhage of a vessel (214). In contrast, the same clinical syndrome which resolves within 24 hours is termed a transient ischaemic attack (TIA) also resulting from the same vascular causes as well as low blood flow (215).

Stroke is the leading cause of death and disability in the world with 1 in 6 people suffering from a stroke in their lifetime with a subsequent 25% risk of death one year after an index event (216). The United Kingdom reflects these statistics with an estimated 120 000 strokes per year and it is also the leading cause of disability resulting in annual costs of approximately £4 billion to the National Health Service (NHS) which represents 5.5% of the total NHS annual budget (217).

Recognition of the symptoms of stroke or TIA is required to provide early and efficient access to the appropriate emergency care. The FAST acronym which comprises Facial drooping, Arm weakness, Speech difficulties and Time is the recommended tool for pre-hospital clinicians and has been used in a number of public health awareness national campaigns although it is noted that stroke syndromes exist outside of these symptoms (218). More detailed assessment of the severity of stroke is quantified through scoring systems such as the modified Rankin Scale (mRS) and the National Institutes of Health Stroke Scale (NIHSS) (219, 220). The mRS is a simplified scale from 0-6, which represents the spectrum of functional disability in normal activities secondary to stroke. The NIHSS is a detailed

neurological assessment comprising of assessments of consciousness, gaze, vision, facial palsy, motor arm deficit, motor leg deficit, limb ataxia, sensation, language, speech and inattention using a scale of 0-42 providing an objective, reproducible assessment for the severity of stroke. Patients presenting with a TIA undergo assessment using the $ABCD^2$ score which incorporates age, blood pressure, clinical syndrome, duration of symptoms and the presence of diabetes (221). The resultant score provides an estimated risk for subsequent stroke in the following 2 and 7 days enabling resources to be efficiently distributed whilst providing early intervention in those with the highest risk.

The National Clinical Guideline for Stroke from the Royal College of Physicians recommends the commissioning and organisation of specialised hyperacute stroke units (HASU) for patients presenting with symptoms suggestive of acute stroke (218). Early presentation to a HASU is associated with a reduction in long term brain damage and disability through the provision of a number of services including: specialist Stroke healthcare professionals, access to acute imaging, thrombolysis therapy, access and completion of all necessary investigations (e.g. echocardiogram, carotid duplex), an acute vascular surgery service, a neurosciences unit often comprising neurosurgical and interventional radiology service and subsequent access to a specialist rehabilitation centre.

One of the first assessments in the acute presentation of stroke is defining whether a stroke is ischaemic or haemorrhagic which is often initially assessed using CT imaging within 1 or 12 hours depending on the nature of presentation (Figure 26). Approximately 78-85% of all strokes are ischaemic and 15-22% are haemorrhagic (222). Haemorrhagic stroke consists of intraparenchymal and subarachnoid haemorrhage. Ischaemic stroke consists of: small artery occlusion, cardio-embolic source, carotid atherosclerosis, vertebro-basilar disease or multiple combinations of all of these as well as unknown causes.


(A)


(B)


(C)

Figure 26 Initial assessment of stroke with CT. (A) - an acute left middle cerebral artery territory ischaemic stroke characterised by sulcal effacement and loss of grey-white matter differentiation in the left fronto-parietal region. (B) – bilateral high density material between the sulci along the falx cerebri representing subarachnoid haemorrhage. (C) –focus of high density material centered over the left basal ganglia from a hypertensive intraparenchymal haemmorhagic stroke

Identifying the cause of ischaemic stroke and TIA is necessary to efficiently guide secondary prevention therefore as discussed, access to basic stroke "work up" investigations are recommended including assessment for: arrhythmias including atrial fibrillation, structural and functional cardiac disease and carotid artery stenosis (218). Carotid atherosclerosis is reported to account for 10-20% of ischaemic stroke (223, 224), therefore, efficient identification and accurate assessment is required as part of high quality stroke and TIA clinical care provision.

7.2. Identification of Carotid Atherosclerosis

Atherosclerosis is the result of pathological thickening and proliferation of the intimal layer of the arteries. These intimal thickenings can organise into focal entities termed plaques or atheromata and are often seen at sites of turbulence such as the carotid bifurcation resulting in carotid atherosclerosis of the common and internal carotid arteries (225). Within Europe, asymptomatic moderate to severe carotid atherosclerosis is reported in 2-5% of women and 2-8% of men aged over 60 years (226).

Carotid atherosclerosis is a recognised and common cause of ischaemic stroke and TIA. Carotid stroke is caused by emboli from surface thrombosis of a ruptured atherosclerotic carotid plaque. It can present clinically with ipsilateral anterior and middle cerebral artery territory neurological symptoms such as amaurosis fugax, retinal infarction, contralateral body neurology and visuospatial neglect. In left sided disease, language centres may also be affected resulting in symptoms such as dysphasia. Additionally, silent infarcts without clinical neurology may be detected with CT whilst acute infarcts confirmed with magnetic resonance imaging techniques (Figure 27) (227).

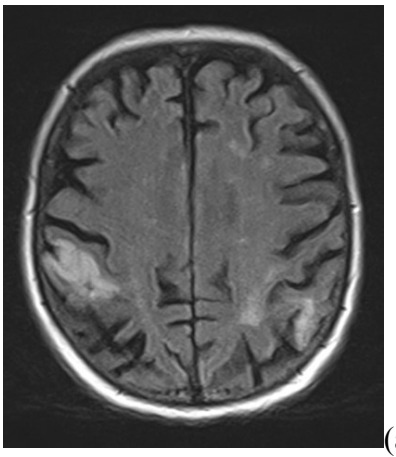
(a)

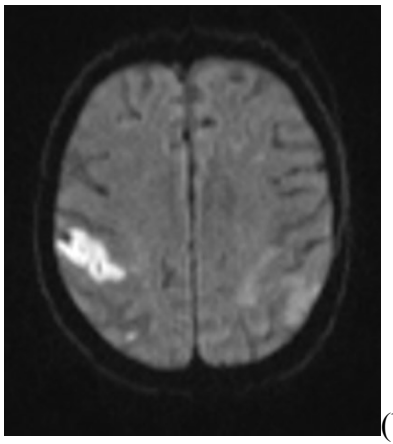
(b)

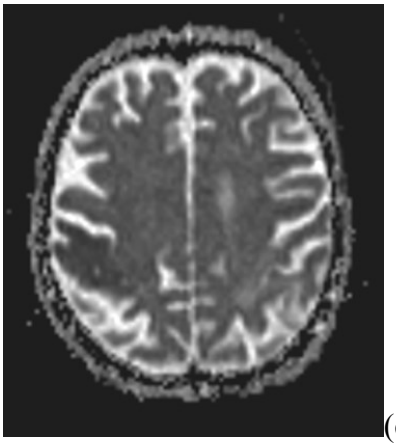
(c)

Figure 27 MRI assessment of acute ischaemic stroke. High signal abnormality in the right post central gyrus on axial T2 FLAIR imaging (A) corresponds to high signal on DWI imaging (B) and restriction on the corresponding ADC map (C) in keeping with acute right MCA territory stroke. FLAIR and DWI high signal but facilitated diffusion in the left posterior parietal region represents a chronic left MCA territory infarct.

Figure 28 Axial non-contrast CT image of patient with symptomatic carotid stroke. Focal hypodensity in the anterior limb of the right internal capsule is in keeping with sub-acute ischaemia whilst more subtle hypodensity in the genu of the right internal capsule represents acute ischaemia representing typical findings secondary to anterior circulation emboli.

Original assessment of carotid atherosclerosis was performed by conventional angiography and early randomised controlled trials used angiographic assessment as their gold standard tool to measure luminal stenosis (45, 46). However, the procedure itself carries a contemporary stroke and TIA risk of 0.3% as well as a 0.4% risk of significant groin haematoma and is therefore no longer considered first line for imaging (228).

Instead, carotid duplex ultrasound is recommended as first line and has been demonstrated as such in 93.8% of symptomatic patients in the United Kingdom (44). Carotid duplex ultrasound is non-invasive, non-irradiating, cheap and can be performed by the bedside. Carotid plaque location can be identified using ultrasound and Doppler is then used to measure the peak systolic velocity which occurs at the point of greatest stenosis (229). This peak systolic velocity can then be converted to the equivalent angiographic luminal stenosis as reported by the North American Symptomatic Carotid Endarterectomy Trial (NASCET) (45). However, carotid duplex ultrasound has a variable reliability with a reported sensitivity of 83-90% and specificity of 54-94% (230, 231). Therefore, a second temporal imaging investigation is recommended for corroboration and whilst this may include CT or MRI modalities, approximately half of patients underwent a further carotid duplex ultrasound in the United Kingdom (Figure 29) (44).

As discussed, the pathway for carotid imaging is well defined in patients presenting with anterior and middle cerebral artery territory stroke or TIA. The assessment for carotid atherosclerosis in asymptomatic patients is less well defined due to controversy in the subsequent definitive management in this group of patients which is discussed later in this chapter. However, it has been described that even if screening was performed in patients with peripheral vascular disease who represent a high risk subset with a 15% prevalence of >70% NASCET stenosis, compared to 2-8% in the comparable general population, it would still cost approximately £76,000 to prevent one stroke and require 133 patients to be screened (232).

Figure 29 Contrast enhanced CT with coronal mean intensity projection reconstruction demonstrating mixed calcified and soft 70% NASCET stenosis of the proximal left internal carotid artery and 50% NASCET stenosis of the right proximal internal carotid artery.

7.3. The Management of Carotid Atherosclerosis

7.3.1. Medical Management

Risk factors for carotid atherosclerosis include; age, smoking history, hypertension and hypercholesterolemia as reported by a Framingham study sub-group analysis (233). Additionally, diabetes is also considered as demonstrated by its addition to the original ABCD score to create the currently utilised $ABCD^2$ risk stratification tool (221). Therefore, medical management has an important role in acute stroke and TIA as well as subsequent secondary prevention. Additionally, randomised control trial long term data suggests that patients with carotid atherosclerosis are in fact more likely to die from cardiovascular disease than stroke, therefore, require exemplary risk factor modification (45, 234).

In the acute phase, antiplatelet therapy is recommended with aspirin which requires an initial loading dose (218). Additionally, if surgical carotid revascularisation is being considered, the addition of clopidogrel to aspirin therapy prior to surgery has been proposed as a means of reducing peri-operative micro-infarcts but is not common practice (235). Anti-platelet therapy benefit continues into secondary prevention with a 22% reduction in all vascular events including cardiovascular, stroke or peripheral vascular aetiology (236). The National Clinical Guideline for Stroke recommends clopidogrel as first line whilst aspirin in combination with dypyridamole is reserved for those cannot tolerate clopidogrel in secondary prevention (218).

Lipid lowering statin therapy is also recommended in both the acute phase and as part of secondary prevention in carotid stroke and TIA. In particular, high dose statin therapy is associated with a reduction in cerebral microemboli detected by transcranial Doppler (237). Additionally, plaque stabilisation has been reported with

statin therapy, characterised by a reduction in cardiovascular serum biomarkers and increased carotid plaque echogenicity which is correlated with greater plaque stability (238).

Hypertensive control is also recommended in carotid atherosclerosis with a target blood pressure of less than 130/80 mmHg apart from in patients with bilateral carotid stenosis in whom a systolic range of 130-150 mmHg is acceptable. Additionally, a number of modifiable lifestyle modifications is recommended; the most pertinent being the cessation of smoking which should be performed using pharmacological and psychological methods as required (218). This is supported by early evidence suggesting that patients who smoke demonstrate echolucent, potentially more vulnerable plaques whilst plaques of ex-smokers are more echogenic and therefore comparably more stable (239).

Best medical therapy (BMT) continues to improve as evidenced by falling stroke and TIA rates in patients with carotid atherosclerosis (48, 234). Regardless of whether carotid revascularisation takes place, BMT forms the foundation of treatment as it is observed in combination with revascularisation as well as on its own in a trial setting. Additionally, as previously discussed, these patients carry a significant cardiovascular risk which carotid revascularisation cannot address further underpinning the role of BMT in secondary prevention for carotid atherosclerosis.

7.3.2. Carotid Endarterectomy

The first reported surgical intervention for carotid atherosclerosis was performed by Debakey in 1953 who performed a thromboendarterectomy in the USA. whilst in the United Kingdom, Eastcott resected the diseased carotid artery and performed an end to end anastomosis in 1954 (240). Contemporary registry data estimates suggest that approximately 3,300 carotid endarterectomy (CEA) operations are performed per

year in the United Kingdom with the majority performed using a standard endarterectomy technique while only 7.3% used an eversion technique (44). A carotid patch which reduces the incidence of peri-operative stroke and re-stenosis was used in 68.6% of patients (241).

CEA may be performed under local or general anaesthetic with no significant difference in stroke, myocardial infarction or death reported at 30 days between the two techniques (242). This is reflected in registry data with 49% of CEA operations performed under local anaesthetic, however, fewer shunts were required in this group compared to those who had general anaesthetic (10.3% vs 72.8%).

Complications from CEA exist but the most severe and therefore benchmark used for reporting is the 30 day stroke and death rate. Early trial data from NASCET reports this rate as 5.8% (45). However, safety of carotid surgery appears to have improved with an average of 2.4% reported in the National Vascular Registry Report on Surgical Outcomes in the United Kingdom albeit this figure includes both symptomatic and asymptomatic CEA operations (243).

Appropriate surgical selection remains an important factor in outcomes. In particular, patients with previous neck dissection have been considered at higher risk of complications due to distorted tissue planes and possible increased risk of nerve damage making them more suitable candidates for carotid artery stenting (CAS) (244). Contrary to previous opinion, patients with previous neck irradiation do not present an increased risk, with similar complication rates between CEA and CAS in this group which are also comparable to those without prior neck irradiation (245).

However, the greatest challenge in surgical selection arises from identifying those at greatest risk of future stroke who would therefore gain the most benefit from carotid revascularisation. This will discussed in further detail later in this chapter but a brief

cross sectional snapshot of contemporary surgical practice demonstrates that only 16.4% of CEA operations are performed for asymptomatic carotid atherosclerosis in the United Kingdom (44) whilst 92% of CEA operations were performed for asymptomatic carotid atherosclerosis in the USA (246) demonstrating a substantial disparity in approach to management.

7.3.3. Carotid Stenting

The first reported endovascular carotid intervention was by Kerber and colleagues who in 1980 performed a retrograde balloon angioplasty of a proximal common carotid artery stenosis concomitantly at the time of a surgical left CEA for bifurcation carotid atherosclerosis (247).

The endovascular practice of carotid intervention has evolved and now largely focuses on carotid bifurcation atherosclerosis with carotid artery stenting (CAS) of the diseased segment now the interventional treatment of choice (Figure 30). In the USA where the practice has had the greatest uptake, an estimated 6,600 CAS procedures are performed annually (248).

A number of well documented randomised control trials have been performed comparing CAS with CEA and a Cochrane review of the data encompassing 16 trials with a total of 7572 patients demonstrated an increased risk of stroke or death in the first 30 days after symptomatic treatment with CAS; a finding which is further accentuated in patients greater than 70 years old (249). However, CAS was associated with a lower 30 day rate of myocardial infarction, cranial nerve palsy and access site haematoma.


(a)

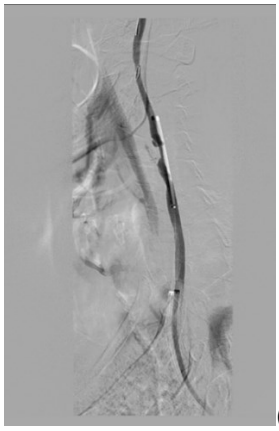
(b)

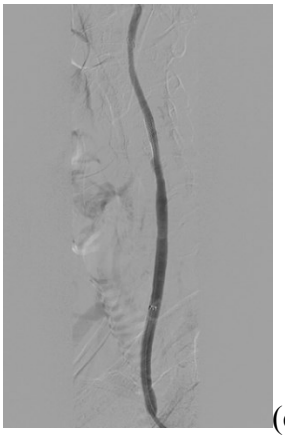
(c)

Figure 30 Left internal carotid artery stenting (A) - Intra-arterial DSA of the left common and internal carotid artery demonstrating a 90% focal stenosis with tiny penetrating ulcers. (B) Carotid wall stent positioning crossing the carotid stenosis. (C) – Completion DSA with restoration of angiographic satisfactory flow across the deployed carotid stent

Ten year follow up data from the Carotid Revascularization Endarterectomy versus Stenting Trial (CREST) has demonstrated that of 2502 patients, no significant difference exists between CAS and CEA for the composite end point of stroke, death or myocardial infarction at ten years (250). For the endpoint of ipsilateral stroke, it was reported at 6.9% (95% CI, 4.4 to 9.7) in the CAS group and 5.6% (95% CI, 3.7 to 7.6) in the CEA group although this was not statistically significant. However, it is the perceived short and long term stroke risk coupled with the equalisation of risk of the remaining end points in the long term which limits uptake of CAS. In the United Kingdom, CAS is only recommended by the Vascular Society of Great Britain and Ireland within high volume centres with low audited procedural outcomes only (251).

Sub-group analysis of CAS versus CEA data for asymptomatic carotid atherosclerosis also demonstrates no significant difference for the aforementioned end points at 30 days or ten years with reported differences between the groups much smaller than in the symptomatic groups (250, 252). It is this relative equipoise that has led to the development of the specifically designed ongoing ACST-2 trial comparing CAS with CEA in asymptomatic patients (253). However, this trial does not have a medical arm and is recommended for patients in whom carotid revascularisation has already been clinically decided prior to recruitment. Whilst the contemporary safety and efficacy of the two interventions is necessary, its subsequent clinical application will be limited without interpretation of their relationship to BMT which as previously described has potentially transformed since previous randomised controlled trials.

A more established role for CAS in symptomatic carotid atherosclerosis may be developing. Randomised controlled trial evidence now exists for endovascular therapy for large artery anterior circulation intracranial occlusion over the currently recommended practice of intravenous thrombolysis which has limited recanlisation success (254, 255). As discussed, 10-20% of these patients will have carotid strokes

and a retrospective multicentre study of 170 patients has described concomitant emergency stenting of the extracranial carotid artery in combination with anterior circulation thrombectomy with a symptomatic intracranial haemorrhage rate of 9% (256). Whilst the haemorrhage rate described is comparable to that seen with mechanical thrombectomy only, further robust randomised controlled trial evidence is still required with reporting of short and long term neurological outcomes in addition to technical success and haemorrhage.

7.4. Symptomatic Carotid Atherosclerosis

The National Clinical Guideline for Stroke from the Royal College of Physicians recommends that all patients with a 50-99% NASCET symptomatic carotid stenosis be considered for carotid revascularisation with CEA being the primary procedure of choice (218). This is largely based on data from NASCET and the European Carotid Surgery Trial (ECST) and the subsequent pooled data of these two trials (45-47) and therefore only applies to those patients with non-disabling stroke or TIA. The pooled data suggests a 5 year absolute risk reduction of ipsilateral stroke of 16% for CEA in patients with 70-99% NASCET stenosis despite a perceived perioperative historical stroke risk of 7% in this analysis demonstrating the superiority of surgery in this high risk group.

No significant benefit was demonstrated in patients with a 30-49% NASCET stenosis and CEA increased the stroke risk in patients with <30% NASCET stenosis. It is the symptomatic group with moderate 50-69% NACET stenosis who present the greatest challenge to decision making. From the pooled NASCET and ECST data, sub-group analysis identified significant treatment effect modifiers including: age, gender, type of index event, time from index event and carotid plaque surface morphology (257). Using these treatment effect modifiers, the ECST risk prediction model was developed which demonstrates a highly variable 5 year risk of ipsilateral stroke in the 50-69% NASCET stenosis group of <10% to 40-45% thus demonstrating that a

generic treatment policy cannot be applied to this group. The ECST risk prediction model has been developed further taking into account the improvement in BMT to provide more contemporary 5 year stroke risk estimates termed the carotid artery risk (CAR) score. This forms the basis of the ongoing ECST-2 trial which aims to assess the role of CEA, CAS and BMT within subsets of CAR score risk stratification as a means for both randomisation and subsequent validation of this tool (258).

Symptomatic carotid intervention is recommended within 1 week of symptoms and it has been demonstrated that the stroke reduction benefit from CEA reduces as the time from the index event increases with no benefit demonstrated in ECST if CEA took place after 50 days (46, 218). This is because a significant proportion of secondary stroke risk occurs in the first 14 days with histological correlation of greater unstable plaque features demonstrated in patients who underwent surgery within 14 days compared surgical plaques resected between 7-28 days after their index event (259). The same phenomenon is observed with patients presenting with TIA as evidenced by the $ABCD^2$ score and retrospective analysis of stroke patients suggests that TIA precedes stroke within 48 hours in 26% of patients (221, 260). However, peri-procedural stroke risk does increase within this termed hyperacute period although conversely it is noted that a delayed operation also exposes the patient to potentially unnecessary risk (261). The timing of surgery in patients who have received intravenous thrombolysis for acute ischaemic stroke is poorly defined, however, recent systematic review suggests level 1C evidence that stroke or death outcomes in patients who had CEA within 14 days of thrombolysis are comparable to symptomatic CEA patients who did not undergo thrombolysis (262).

7.5. Asymptomatic Carotid Atherosclerosis

Randomised controlled trials in asymptomatic carotid atherosclerosis have shown a net benefit in patients with 70-99% NASCET stenosis with a 1% reduction (50% risk

reduction) in stroke per year over BMT with particular benefit conferred in those less than 75 years old (263, 264). However, the background stroke risk in the non-surgical group was approximately 2% per year, therefore, the gross number of overall events occurring at 5 years is relatively low compared to the overall incidence of all stroke reducing the impact of the significant risk reduction described for surgery. Therefore, the number needed to treat with CEA to prevent 1 stroke was approximately 20 which is very high compared to the number needed to treat symptomatic 70-99% NASCET stenosis patients which is estimated at 6.

Additionally, to truly confer this population benefit, all patients with asymptomatic disease must first be identified and then treated which would involve great cost and approximately 940 per 1000 patients having unnecessary operations (265). A United Kingdom cost effectiveness study model based on the 10 year data from ACST demonstrated that CEA was cost effective but only in those less than 75 years old with some additional benefit to women over men, however, it was noted that if the background stroke rates fell below 1% then no carotid intervention would be cost effective in asymptomatic patients (266). Additionally, patients entered this cost effectiveness model at the point of randomisation into the trial therefore the cost of identifying these patients is not included.

As discussed earlier, there has been significant improvement in best medical therapy since ACST and the Asymptomatic Carotid Atherosclerosis Study (ACAS), primarily driven by anti-platelets and statins but also consisting of diet, exercise, smoking cessation, blood pressure control and diabetic management (218). A meta-analysis of BMT in asymptomatic carotid disease has elegantly demonstrated a reduction in background stroke and TIA rates reported in published data over a 25 year period with the most contemporary data suggesting that stroke and TIA rates whilst on BMT are at least equivocal with those reported in the carotid revascularisation groups and unsurprisingly more cost effective (48). The benefit of BMT is also highlighted in the 10 year follow up data from ACST which described reduced long term stroke risk

in patients taking statins from both the immediate CEA and non-surgical groups (234).

However, as BMT improves, surgery has not stood still. Improvements in the outcomes of asymptomatic CEA have also been reported with systematic review evidence assessing trial and registry data encompassing approximately 209,000 procedures over 30 years (267). An annual reduction rate of 6% in stroke and death rates is described with contemporary stroke or death risk now predicted at 1.2% for asymptomatic CEA. Additionally, the benefits of BMT in secondary prevention are not always observed in patients outside of a trial setting. The EUROASPIRE IV cross sectional study performed by the European Society of Cardiology demonstrated 48.6% persistent smokers, little or no exercise in 59.9% and 80.5% with LDL cholesterol above accepted standards (268).

National recommendation within the United Kingdom is for asymptomatic CEA to only be performed in patients unable to tolerate BMT or within a trial setting (218). As previously discussed the ongoing ACST-2 and ECST-2 trials are recruiting patients with asymptomatic carotid atherosclerosis to either CEA or CAS in ACST-2 or CEA, CAS or BMT in ECST-2 in an attempt to clarify the safety and efficacy of contemporary practice (253, 258).

Quantifying the stroke or death risk to guide treatment for patients with carotid atherosclerosis continues to present a clinical challenge especially in patients with either asymptomatic 70-99% NASCET stenosis or symptomatic 50-69% NASCET stenosis. It is undeniable that some of these patients will go on to have a stroke or fatal event in current practice but as discussed blanket aggressive revascularisation in these patients will also result in unnecessary harm and at great cost; neither of which is acceptable or feasible within the utilitarian structure of the NHS. Luminal stenosis on its own is not a good enough predictor of future stroke risk in these subsets of patients (265). Therefore, further biomarkers for risk stratification are required to

provide patients with a personalised quantification of risk enabling informed decision making and provision of safe, efficacious treatment for their carotid disease.

8. DECISION MAKING IN SYMPTOMATIC MODERATE CAROTID ATHEROSCLEROSIS

8.1. Risk Scoring in Symptomatic Carotid Stenosis

Pooled data from both the North American Symptomatic Carotid Symptomatic Carotid Endarterectomy Trial (NASCET) and the European Carotid Surgery Trial (ECST) shows the benefit of carotid endarterectomy remains marginal in patients with moderate (50-69% NASCET) symptomatic carotid stenosis in whom 13 operations are required to prevent any stroke or operative death at 5 years (47).

In an attempt to identify the greatest beneficiaries of carotid endarterectomy, sub-group analysis of the pooled data from NASCET and ECST defined further clinical characteristics of: age, gender, type of index event, time from index event and carotid plaque surface morphology as significant treatment effect modifiers (257). Using these variables, the ECST stroke risk prediction model was derived and then validated against patients with 50-99% symptomatic carotid stenosis randomised to medical therapy in NASCET (269, 270). Use of prognostic risk prediction models is common in cardiovascular disease; providing individual risk in conditions such as myocardial infarction, atrial fibrillation and transient ischaemic attacks (221, 271, 272). Whilst scoring systems for carotid atherosclerosis have been developed their use is not common practice (273-275), however, the ECST risk prediction model is recommended for decision making in symptomatic carotid surgery in the 4th National Clinical Guideline for Stroke produced by the Royal College of Physicians in the UK (218).

Opinions regarding intervention have previously been investigated in asymptomatic carotid disease, however, there is little literature exploring decision making in

symptomatic moderate carotid stenosis (276, 277). This study aims to explore current decision making of stroke physicians and vascular surgeons within the UK regarding management of patients with symptomatic moderate stenosis and assess the impact of the recommended ECST risk model.

8.2. United Kingdom Stroke Physician and Vascular Surgeon Survey Methodology

Institutional ethical review categorised this survey as service evaluation therefore formal ethical approval was not required. Using the ECST model risk score tables, three hypothetical scenarios of recently symptomatic moderate carotid stenosis patients with low (<10%), moderate (20-25%) and high (40-45%) 5-year absolute risk of ipsilateral stroke on medical treatment were devised (269, 270). The low risk (<10%) case presented was a 63 year old male with left amaurosis fugax three days ago with a smooth 65% left internal carotid artery stenosis plaque on duplex ultrasound. The moderate risk (20-25%) case presented was a 76 year old female with a transient ischaemic attack affecting her right arm one week ago with an ulcerated 60% left internal carotid artery stenosis plaque on duplex ultrasound. The high risk (40-45%) case presented was a 79 year old male with persistent left arm weakness for two days with an ulcerated 55% right internal carotid stenosis plaque on duplex ultrasound. Management options available for the scenarios included: best medical therapy (BMT), carotid endarterectomy (CEA) or unsure. Carotid artery stenting was not included as it is not widely practised across UK centres and whilst randomised controlled trial evidence suggests no significant difference exists between carotid artery stenting and carotid endarterectomy for composite outcomes of stroke or death in carotid intervention, current guidance limits its practice to high volume centres with low audited procedural complications only (251, 278).

In order to assess current decision making, all three scenarios were first presented to the respondents with only clinical information regarding age, gender, degree of stenosis, carotid plaque morphology, type of neurological event and time from index event. Subsequently, a description of the ECST model was provided followed by the same three scenarios with the addition of the risk score from the ECST model. Respondents were asked to assume equal baseline co-morbidities, a life expectancy of >5 years, no alternative source of stroke e.g. atrial fibrillation, appropriate fitness for surgery, a contralateral internal carotid artery stenosis of <20% and no strong patient preference across all scenarios.

The complete survey was tested and validated by stroke physicians and vascular surgeons with internal and external assessors for both content and construct validity as previously described (279). Test-retest stability for reliability was not possible as the survey led to acquisition of new knowledge that would affect responses at a second retest time point. Invitations to complete the survey were sent via email to 503 members of the British Association of Stroke Physicians (BASP) and 432 members of the Vascular Society of Great Britain and Ireland (VSGBI) (http://freeonlinesurveys.com/s.asp?sid=icropocgwl6hjp190262).

Data was collated by a survey server (FreeOnlineSurveys.com, St. Austell, United Kingdom) over a 4 month time period between February and May 2013. All data was anonymised and analysed using Microsoft Excel 2010 (Microsoft Corporation, Redmond, WA, USA) and Prism Version 6.01 (GraphPad Software Inc., La Jolla, CA, USA) software. The Chi-square test was used and statistical significance taken as $P<0.05$.

8.3. Survey Results

Two-hundred and one completed survey responses were received with all data sets analysed and none excluded. One hundred seven (53%) surveys were received from stroke physicians representing a 21% response rate and 94 (47%) surveys were from vascular surgeons representing a 22% response rate. Overall, 76% (153/201) of all respondents, comprised of 82% (88/107) of stroke physicians and 68% (64/94) of vascular surgeons, found the ECST model risk score useful.

8.3.1. Scenario 1 – Predicted 5 year stroke risk 40-45%

Figure 31 demonstrates combined and specialty specific responses for Scenario 1. Presented with clinical information only, 21% (42/201) of respondents chose BMT, 67% (134/201) chose CEA and 12% (25/201) of respondents were unsure. Addition of the predicted 5 year stroke risk of 40-45% from the ECST model yielded 13% (27/201) of responses for BMT, 80% (161/201) of responses for CEA and 7% (13/201) of respondents were unsure revealing a significant trend toward surgery compared to responses without the risk score (P=0.009).

Stroke physician response pre- and post-introduction of the ECST model risk score also showed a preference toward surgery with 21% vs 15% for BMT, 62% vs 79% for CEA and 17% vs 15% being unsure respectively (P=0.008). However, vascular surgeon response only showed a trend toward surgery with 20% vs 12% for BMT, 72% vs 81% for CEA and 8% vs 7% unsure (P=0.276). There was no significant difference in response choices between stroke physicians and vascular surgeons either pre- (P=0.109) or post-introduction (P=0.716) of the ECST model risk score for this high risk case.

8.3.2. Scenario 2 – Predicted 5 year stroke risk <10%

Figure 32 illustrates the combined and specialty specific responses for Scenario 2. Responses for this case with clinical information only were 23% (47/201) for BMT, 64% (129/201) for CEA and 13% (25/201) were unsure. After introduction of the ECST model 5 year stroke risk score of <10%, responses showed preference toward BMT with 57% (115/201) for BMT, 35% (71/201) for CEA and 8% (15/201) were unsure (P<0.001).

Stroke physicians pre- and post-introduction of the ECST model risk score also demonstrated a swing toward BMT with 25% vs 72% for BMT, 62% vs 20% for CEA and 13% vs 8% were unsure respectively (P<0.001). A swing toward BMT was also demonstrated by vascular surgeons with 21% vs 41% for BMT, 67% vs 53% for CEA and 12% vs 6% were unsure (P=0.014). There was no difference in response choices between stroke physicians and vascular surgeons with clinical information only (P=0.728), however, the introduction of the ECST model risk score resulted in a significant difference between groups with an overall preference toward BMT from stroke physicians whilst CEA was still preferred by vascular surgeons for this low risk case (P<0.001).

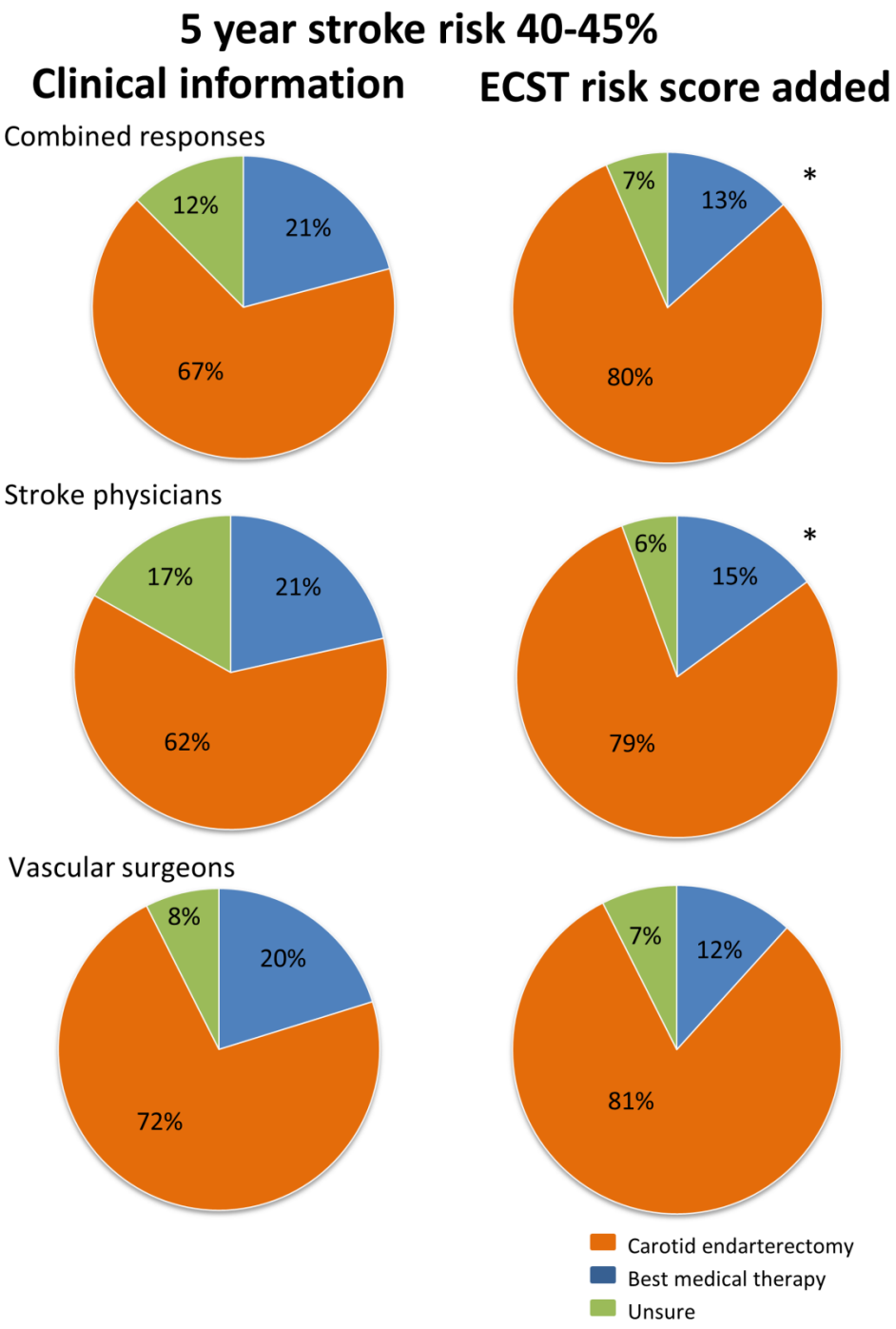

Figure 31 Preferences in management for high risk moderate carotid stenosis pre- and post-introduction of a 5 year stroke risk of 40-45%. A – Combined responses. B – Stroke physician responses. C – Vascular surgeon responses. (*denotes statistical significance)

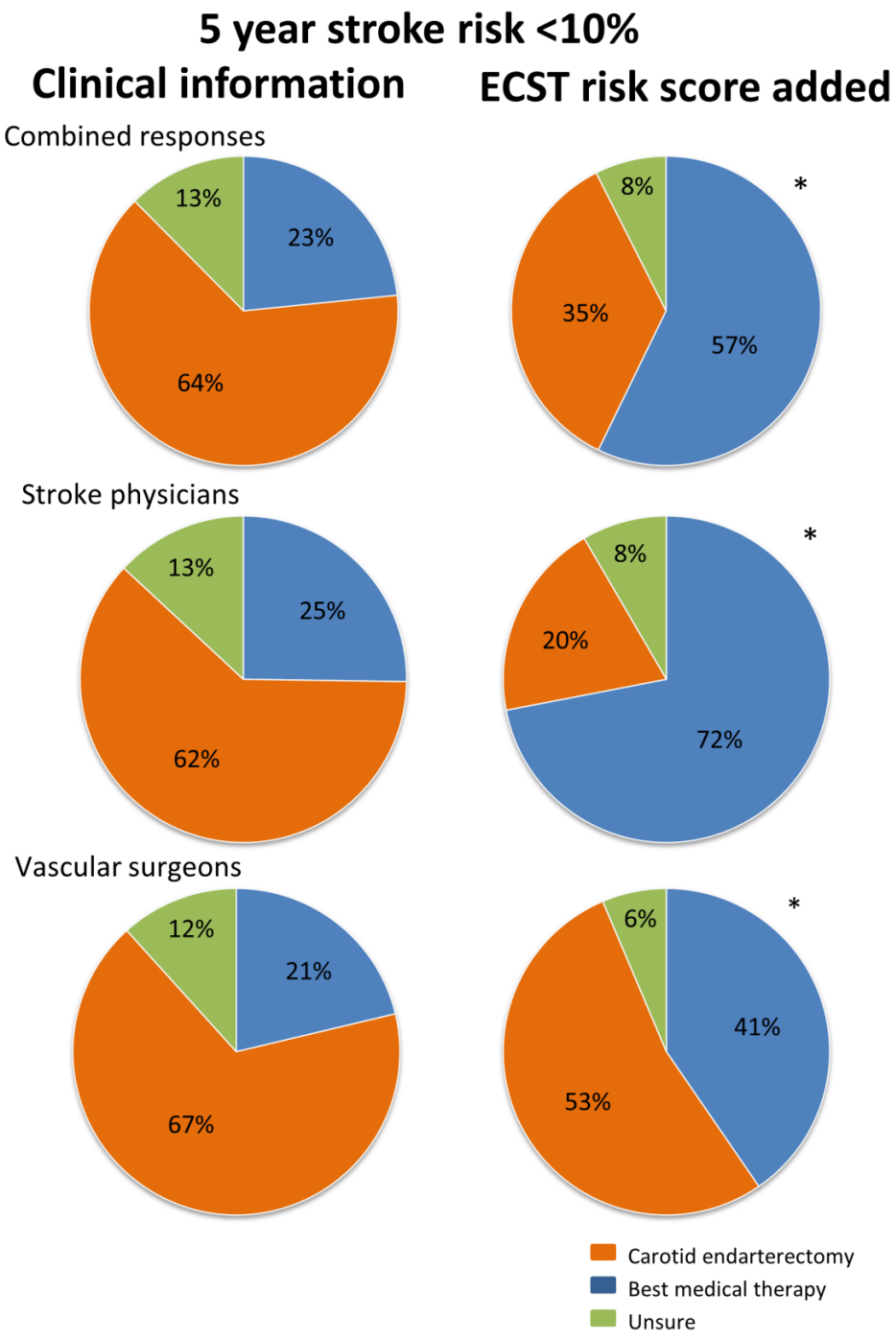

Figure 32 Preferences in management for low risk moderate carotid stenosis pre- and post-introduction of a 5 year stroke risk of <10%. A – Combined responses. B – Stroke physician responses. C – Vascular surgeon responses. (*denotes statistical significance)

8.3.3. Scenario 3 – Predicted 5 year stroke risk 20-25%

Figure 33 represents combined and specialty specific responses for Scenario 3. With clinical information only responses were 17% (35/201) for BMT, 72% (144/201) for CEA and 11% (22/201) were unsure. Despite the introduction of a 20-25% 5 year stroke risk from the ECST model, there was no significant change in management choices with 16% (32/201) for BMT, 76% (152/201) for CEA and 8% (17/201) were unsure (P=0.609).

Stroke physician management choices were not influenced with the introduction of the risk score with 21% vs 19% for BMT, 64% vs 67% for CEA and 15% vs 14% unsure (P=0.837). Vascular surgeons also showed no difference in management with 13% vs 13% for BMT, 81% vs 85% for CEA and 6% vs 2% were unsure (P=0.350). Overall, both groups preferred CEA, however, vascular surgeons displayed a significantly greater preference toward CEA compared to stroke physicians both before (P=0.022) and after (P=0.003) the introduction of the ECST model risk score for this moderate risk group.

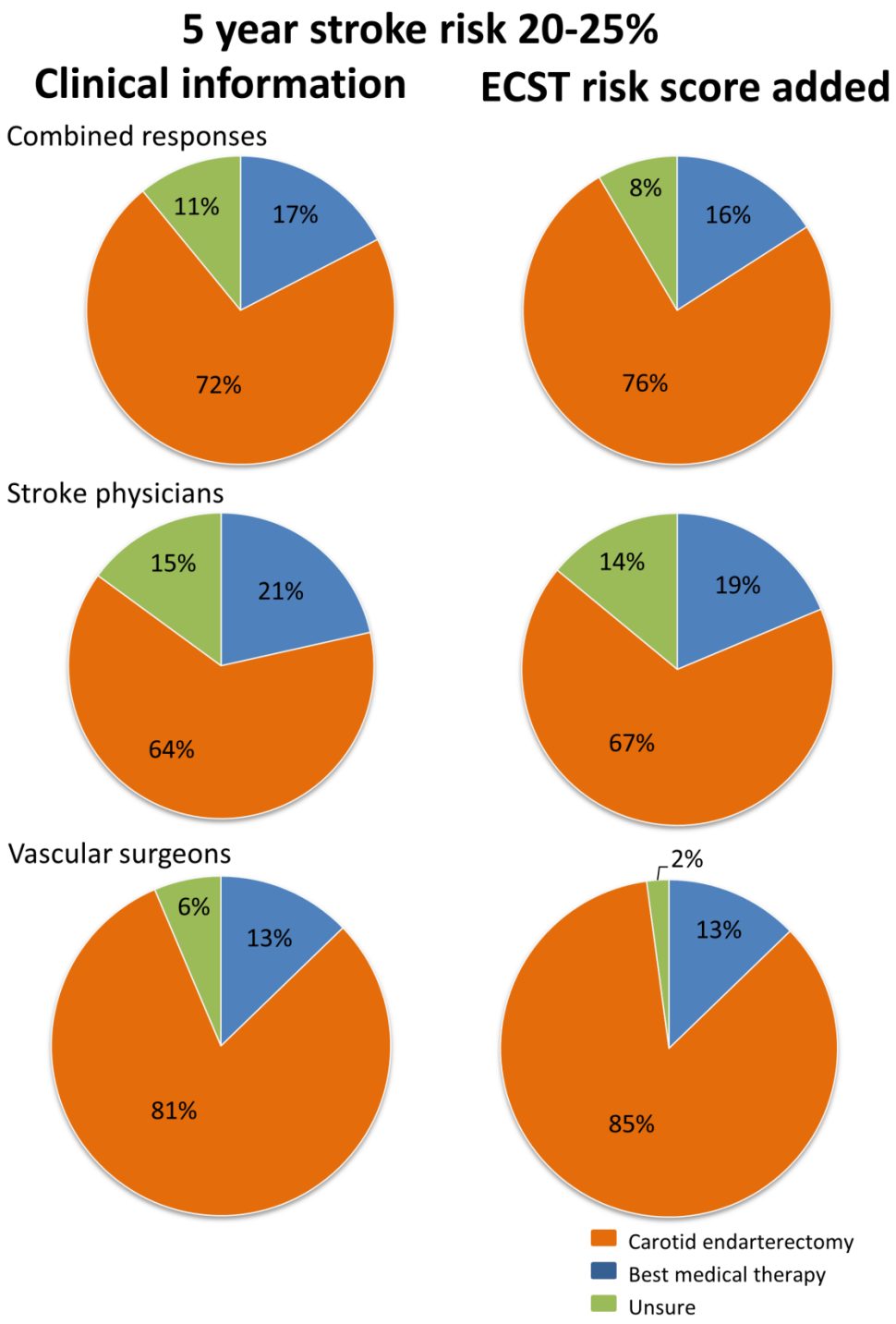

Figure 33 Preferences in management for moderate risk moderate carotid stenosis pre- and post-introduction of a 5 year stroke risk of 20-25%. A – Combined responses. B – Stroke physician responses. C – Vascular surgeon responses.

8.4. Discussion

This is the first study assessing decision making of clinicians for patients with symptomatic 50-69% stenosis and the impact of quantitative risk scores on those decisions. These results demonstrate that prior to the introduction of the ECST model risk score, the majority of clinicians would treat all of the scenarios presented with CEA. After introduction of the ECST model risk score, high and moderate risk patients would still be treated with CEA whilst low risk patients would be treated with BMT. Greater than two-thirds of clinicians involved in decision making for this group of patients found the ECST risk score useful.

In the high risk scenario, there was no significant difference in responses between stroke physicians and vascular surgeons, however, there was an overall increase in those choosing CEA on introduction of a 5 year stroke risk of 40-45%. Even assuming the generously high CEA procedural stroke or death rate of 5.8% from NASCET (45), there would have to be a substantial improvement in current BMT to justify withholding revascularisation in this scenario. This is supported by the on-going ECST-2 trial which uses the hypothesis that the risk of stroke has halved with improvements in BMT since the original ECST and NASCET trials (45, 46, 258). The original risk score from the ECST model is halved to produce a Carotid Artery Risk (CAR) score providing stratification for randomisation. Patients with a CAR score of >15% (equivalent to a >30% ECST risk score) are excluded from the trial and clinicians are recommended to consider these patients for immediate revascularisation outside of the trial which is in keeping with results observed for the high risk scenario in this survey.

In the low risk scenario, when presented with clinical information only there was no significant difference between stroke physicians and vascular surgeons with the majority initially opting for CEA. Interestingly, on introduction of a 5 year stroke risk of <10%, there was a significant swing toward BMT in both groups suggesting

that identification of low risk patients is poor. A 5 year stroke risk of <10% is comparable to patients with asymptomatic 60-99% carotid stenosis in whom there is a reported 5 year stroke or death risk of approximately 10% (263, 264). The debate regarding intervention for asymptomatic carotid stenosis is well documented with differing opinions amongst clinicians with the suggestion that only 1 in 20 of these patients benefit from revascularisation (280-282). Results of an online poll of 4669 healthcare professionals showed that 49% of respondents would treat a 67 year old male with a 70-80% asymptomatic carotid stenosis with BMT (276, 277) which is comparable to the 57% response for BMT observed in this survey with equivalent levels of future stroke risk.

In the moderate risk scenario, CEA was preferred with no significant difference in management after introduction of the ECST risk score in either stroke physicians or vascular surgeons, although there was a greater preference toward CEA overall from vascular surgeons. This consistent difference in opinion may represent divergent views between the specialities regarding current relative benefits of BMT and CEA in the moderate risk group and highlights the need for multidisciplinary neurovascular discussion of patients. Using asymptomatic carotid atherosclerosis as an example, a recent meta-analysis has suggested that BMT is now safer than carotid intervention in asymptomatic carotid disease; commonly attributed to the introduction of high dose statins (48). Indeed, a dose dependent effect of statins has been demonstrated to stabilise carotid plaques both in symptomatic and asymptomatic patients with moderate carotid stenosis (238), suggesting that improvements in BMT may be applicable to symptomatic carotid disease. Conversely, the safety of symptomatic carotid surgery has also improved with recent randomised control trial data reporting procedural stroke or death rates of 3.2% for CEA (53). Applicable to the respondents in this survey, the safety of carotid surgery has also improved with prospective cohort data from the UK reporting a 30 day operative mortality rate of 0.9% and stroke rate of 2.1%, however, it is noted that 16.4% of operations performed were for asymptomatic disease (44).

The main limitation of this study comes from use of the ECST model risk score itself. As highlighted, the model is based on data compiled and published 14 years ago which users may feel is now out of date with current practice. Information about the ECST model including its age and potential improvements in BMT was provided to respondents during the survey and it was also highlighted that the model is recommended as an adjunct to decision making in the 4th National Clinical Guidelines for Stroke published in 2012 (218). Additionally, respondents were not provided with a procedural risk of stroke or death from CEA which as previously discussed has changed over time and may differ between surgeons and centres. Subsequently, in this survey it was intended that responses gathered would reflect clinician's current assessment of the balance of stroke risk versus procedural risk of CEA. Since completion of online survey responses, the National Vascular Registry Report on Surgical Outcomes in the United Kingdom has been published and whilst it exhibits some variation in procedural risk between vascular surgeons, the report concludes that all surgeons submitting data had risk-adjusted outcomes within the expected range for their given level of activity (243).

The use of duplex ultrasound as the imaging modality in the scenarios may be questioned as it may fail to reliably identify carotid plaque ulceration which forms part of the ECST model risk score (283). However, at present in the United Kingdom duplex ultrasound is the predominant modality for both first line and confirmatory pre-operative imaging (44, 225). Furthermore, it is interesting that the absolute degree of stenosis did not influence the participants with the lowest risk scenario having the highest percentage stenosis and the highest risk scenario having the lowest percentage stenosis. Instead, even before the introduction of the ECST risk score the lower absolute percentage stenosis plaques that were ulcerated were deemed of higher risk by the respondents in this survey. It is already known that stenosis alone is not a good enough predictor of stroke risk (265) and this survey further demonstrates the importance of evaluating plaque morphology through imaging to accurately guide decision making.

In this survey, not all clinical aspects contributing to decision making were included in the scenarios such as acute thrombolysis, neck anatomy or brain imaging (225, 245, 284). Whilst these and other factors are undoubtedly important in a clinical setting, the intention of the survey was to examine decision making based on the treatment effect modifiers identified in the ECST model (257). Finally, patient preference was not taken into account, however, results from previous clinician and patient surveys in asymptomatic carotid disease have yielded similar preferences for management (277, 285).

In this survey, it has been demonstrated that without risk stratification clinicians have a preference toward CEA for patients with 50-69% symptomatic carotid stenosis. However, the addition of a risk prediction model appears to influence their choices with CEA preferred in high and moderate risk patients whilst BMT is preferred in low risk patients. This highlights the need for risk scoring, such as the ECST model, to be utilised as part of multidisciplinary decision making in this particularly challenging group of patients. Trials currently recruiting moderate and low risk symptomatic carotid patients will provide informative data regarding contemporary outcomes for BMT and carotid intervention. However, for risk scoring to be implemented, adequate methods of identifying the components of a given model are required which in the case of ECST model requires robust clinical assessment of index symptoms and accurate imaging assessment of plaque morphology.

9. Assessment Of Carotid Plaque Ulceration With Dynamic Contrast Enhanced Ultrasound

9.1. Carotid plaque ulceration and the vulnerable carotid plaque

Carotid atherosclerosis contributes toward 15% of all strokes; occurring due to sudden thrombus formation following carotid plaque rupture and subsequent communication between luminal blood and the plaque's thrombogenic core (54). Histological studies of ruptured carotid plaques have demonstrated plaque surface defects, termed ulcers found in complicated AHA type VI lesions (286, 287). Additionally, previous randomized clinical trial data has revealed that in symptomatic patients, ulceration on angiography is associated with a greater risk of stroke (288).

At present, in the United Kingdom the first line investigation to assess carotid disease is color Doppler ultrasound to assess luminal stenosis (225). However, luminal stenosis alone is a weak predictor of future stroke especially in the groups of patients with moderate symptomatic 50-69% stenosis and asymptomatic 70-99% stenosis in whom carotid intervention remains controversial with a number needed to treat of 1 in 20 for carotid endarterectomy (257, 289). Furthermore, as discussed earlier the presence of ulceration over absolute percentage stenosis is a greater determinant of future stroke risk in contemporary decision making amongst Vascular Surgeons and Stroke Physicians. Contrast enhanced carotid ultrasound is a new clinic-based, structural and functional imaging modality which can act as a simple adjunct to current color Doppler ultrasound to assess carotid atherosclerosis (290). Color Doppler ultrasound may fail to reliably identify carotid ulceration (283); however

Dynamic Contrast Enhanced Ultrasound (DCE-US) may visualize plaque surface defects more readily.

The aim of this pilot study was to assess the potential benefits of DCE-US in the assessment of plaque ulceration. The hypothesis was that an increased prevalence of ulceration would be visible with DCE-US in comparison with color Doppler ultrasound thus providing a predictor for symptomatic status.

9.2. Study Methodology

Ethical approval was obtained prior to commencing the study (Ref 09/H0706/89). Patients gave written informed consent to participate in this prospectively recruited, cross-sectional study. Seventy-two consecutive patients with a discrete 50-99% internal carotid artery stenosis (NASCET equivalent (229)) were recruited from neurovascular clinics between January 2011 and January 2012 (Figure 34). Inclusion criteria were: male or female patients aged 18 years or over with a discrete 50-99% (NASCET equivalent(229)) internal carotid artery stenosis. Exclusion criteria were: atrial fibrillation, mechanical heart valve, cardiomyopathy, elevated troponin, contrast contraindication, NYHA III/IV cardiac failure, myocardial infarction within 3 months and ischemic symptoms >4 weeks previously. An independent stroke physician assigned the diagnosis of carotid territory ischemic symptoms after a workup including intracranial computed tomography, 24 hour electrocardiogram, troponin result, echocardiography and for cases of amaurosis fugax, an ophthalmic opinion. If no history of stroke, transient ischemic attack or amaurosis were present, an asymptomatic status was recorded.

9.2.1. Image Acquisition

The initial color Doppler ultrasound scan was performed by an independent vascular scientist (minimum 2 years' carotid ultrasound experience) where luminal stenosis and plaque ulceration (>1.5mm discrete surface indentation with pulsating color fill) were recorded as per standard clinical imaging protocol for our institution. Ulceration on color Doppler was recorded live at the time of examination and was therefore not assessed for reproducibility.

DCE-US was performed with a Philips iU22 system by (vascular clinical research fellow 2 years' carotid DCE-US experience). An L9-3 probe and the following standard settings were used: mechanical index 0.06, 2D gain 80%, focal depth 4cm, vertical centered time-gain curve, XRES on and persistence at medium. 2ml of intravenous SonoVue™ (Bracco, Milan, Italy) was injected into a 20 gauge cannula in the right antecubital fossa. A one minute digital video loop from the point of contrast injection was captured, centered on the plaque in longitudinal section. After 10 minutes this was repeated. Patients were observed for 30 minutes post injection for adverse events.

9.2.2. Image Analysis

DICOM video loops were exported for blinded, offline analysis by an independent vascular radiologist (10 years' vascular carotid ultrasound experience). This was repeated by a vascular clinical research fellow for inter-reader comparison. A training phase where ten pre-recorded image loops were graded in consensus was performed before the main study. Ulceration was recorded if a ≥1.5mm discrete surface indentation on the carotid plaque communicating with the vessel lumen was visible on DCE-US (Figure 36).

9.2.3. Statistical Analysis

Statistical analysis was performed using MedCalc v11 (MedCalc software, Mariakerke, Belgium). Continuous variables were checked for normality and differences between the groups assessed using the student's t-test or the Mann-Whitney test. Differences in proportions were assessed using Fisher's exact test. Intra and inter-observer reproducibility were assessed using Cohen's kappa. Sample size calculation was performed using PASSv11 (NCSS, Utah, USA) using a one degree of freedom chi-squared test, taking statistical significance as $p<0.05$.

9.3. Results

9.3.1. Patient Demographics

Seventy two (72) patients were assessed for eligibility. Sixteen (16) patients were excluded for the following reasons: 5 declined, 3 severe cardiorespiratory co-morbidity, 3 severe calcification, 2 alternate embolic source, 1 tandem carotid lesions, 1 contraindication to SonoVue, 1 recurrent stenosis following endarterectomy, leaving a total of 56 patients available for analysis. Of the symptomatic patients, 11/26 (42%) had an ipsilateral carotid territory stroke, 10/26 (38%) had an ipsilateral carotid territory transient ischemic attack and 5/26 (19%) had ipsilateral amaurosis fugax. Of the control patients who had been tested for asymptomatic carotid disease, 18/30 (47%) were referred from a neurologist, 10/30 (33%) were referred from a vascular surgeon because of arterial disease in another territory and 2/30 (7%) were referred because of risk factors. Demographic details of the 56 patients are shown in Table 6. Symptomatic patients had a higher degree of stenosis (79% IQR 68-90 versus 63% IQR 54-80, P=0.03) and were less likely to be on antiplatelet therapy (17/26 [65%] versus 28/30 [93%], P=0.02).

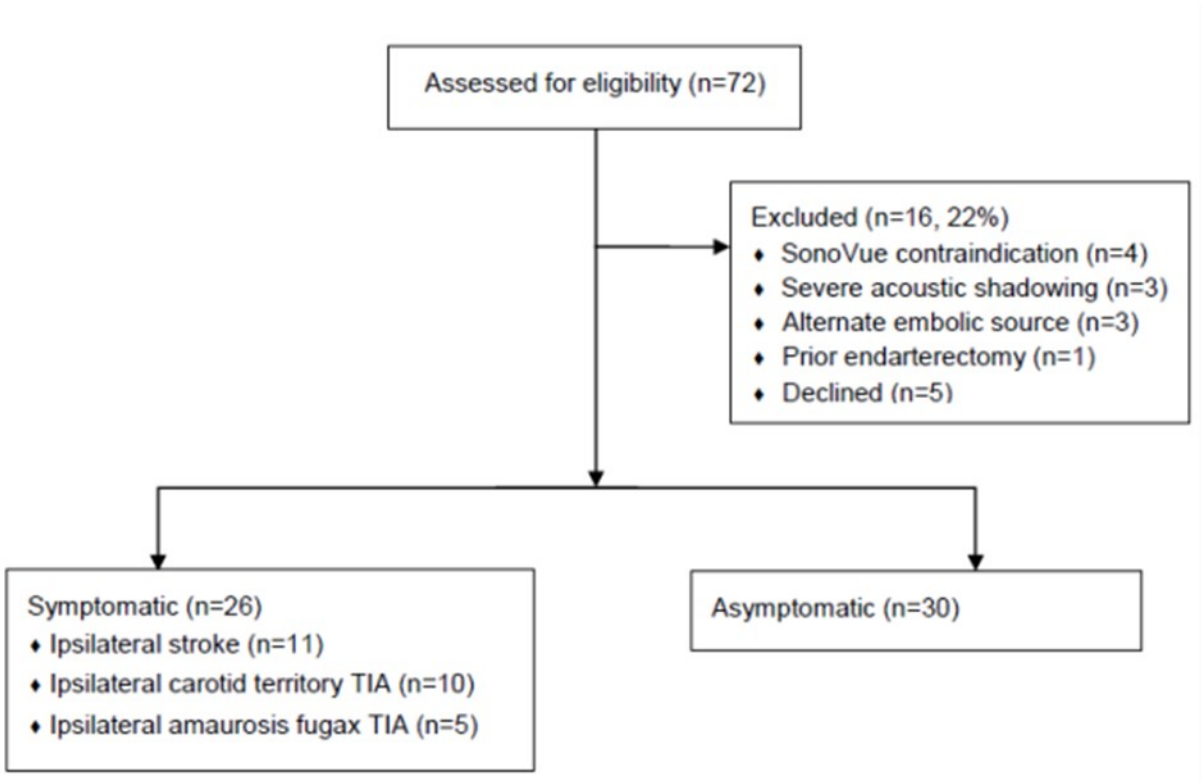

Figure 34 STARD diagram illustrating patient flow. n = number of patients.

Variable	Asymptomatic	Symptomatic	P-value
Number of patients	**30**	**26**	**-**
Age (years)	**68 (SD 9)**	**73 (SD 11)**	**0.06**
Male gender	**21 (70%)**	**15 (58%)**	**0.41**
Ipsilateral NASCET stenosis (%)	**63 (IQR 54-80)**	**79 (IQR 68–90)**	**0.03***
Prior ipsilateral CORI	**2 (7%)**	**4 (15%)**	**0.40**
Contralateral CORI	**8 (27%)**	**2 (8%)**	**0.09**
Diabetes	**6 (20%)**	**6 (23%)**	**1.00**
Antihypertensive therapy	**22 (73%)**	**20 (77%)**	**1.00**
Statin therapy	**24 (80%)**	**18 (69%)**	**0.38**
Antiplatelet therapy	**28 (93%)**	**17 (65%)**	**0.02***
History of smoking	**20 (67%)**	**12 (46%)**	**0.18**
Parental CVA	**8 (27%)**	**4 (15%)**	**0.35**
PAD	**11 (37%)**	**5 (19%)**	**0.24**
MI	**5 (17%)**	**1 (4%)**	**0.20**

Table 6 Demographic details of the included 56 patients. Of the 26 symptomatic patients, 11 (42%) had an ipsilateral carotid territory stroke, 10 (38%) had an ipsilateral carotid territory TIA and 5 (19%) had ipsilateral amaurosis fugax.

9.3.2. Carotid Plaque Ulceration

Ulceration was seen in 4/56 (7%) of patients with color Doppler and 9/56 (16%) with DCE-US (P=0.24). Using color Doppler there was no significant difference in ulceration between symptomatic or asymptomatic patients (1/26 v 3/30, P=0.62). With DCE-US there was a trend towards more ulceration in symptomatic patients (7/26 v 2/30, OR 5.16, 95% CI 0.96 – 27.58, P=0.07) (Figure 35). The sensitivity, specificity, positive predictive value and negative predictive value of ulceration with contrast for identifying patients with ipsilateral symptoms were 27%, 93%, 78% and 60% respectively. Median stenosis was higher in ulcerated plaques on DCE-US, although the sample size was small (88% IQR 73-94 versus 70% IQR 55-85, P=0.03).

When considering the North American clinical threshold of ≥60% stenosis and ulceration on DCE-US as a combined variable, versus all other plaques, the odds ratio for ipsilateral symptoms increased to 10.68 (95% CI 1.21 – 93.97, p=0.02), yielding a sensitivity, specificity, positive predictive value and negative predictive value of 27%, 97%, 88% and 60%.

For ulceration on DCE-US, intra-reader reproducibility was good (κ=0.87) and inter-reader reproducibility was also good (κ=0.64).

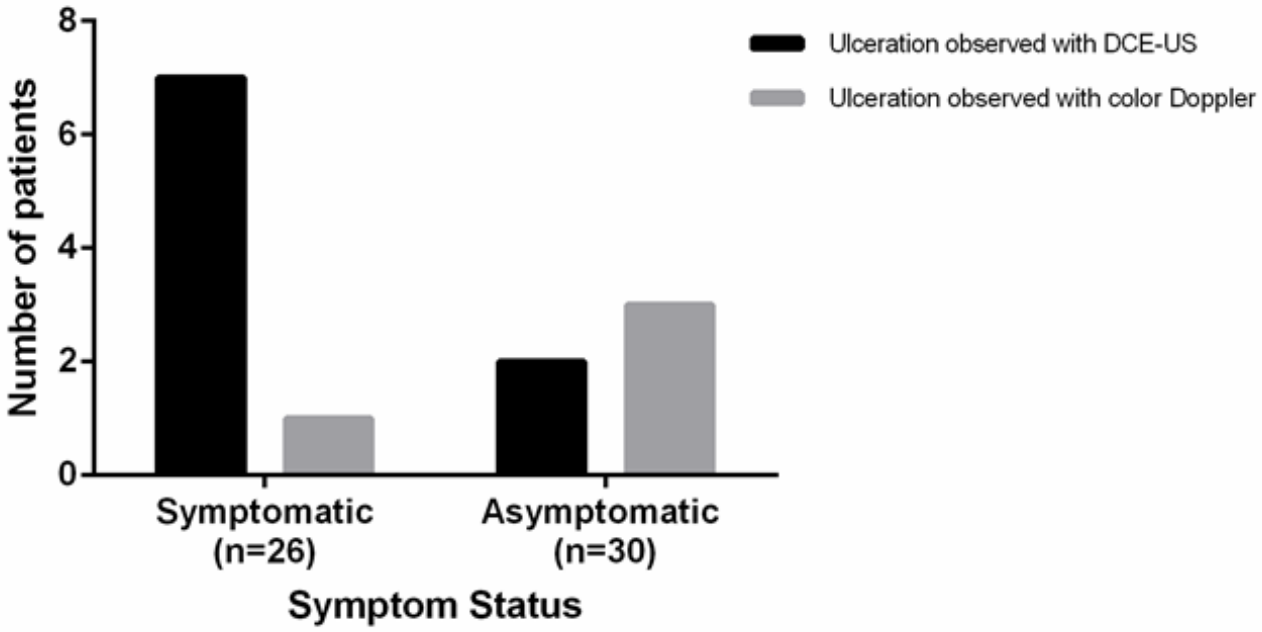

Figure 35 Graph demonstrating the comparison of detection of ulceration between DCE-US and color Doppler ultrasound. A trend toward greater detection of ulceration with DCE-US in symptomatic patients is observed (P=0.07).

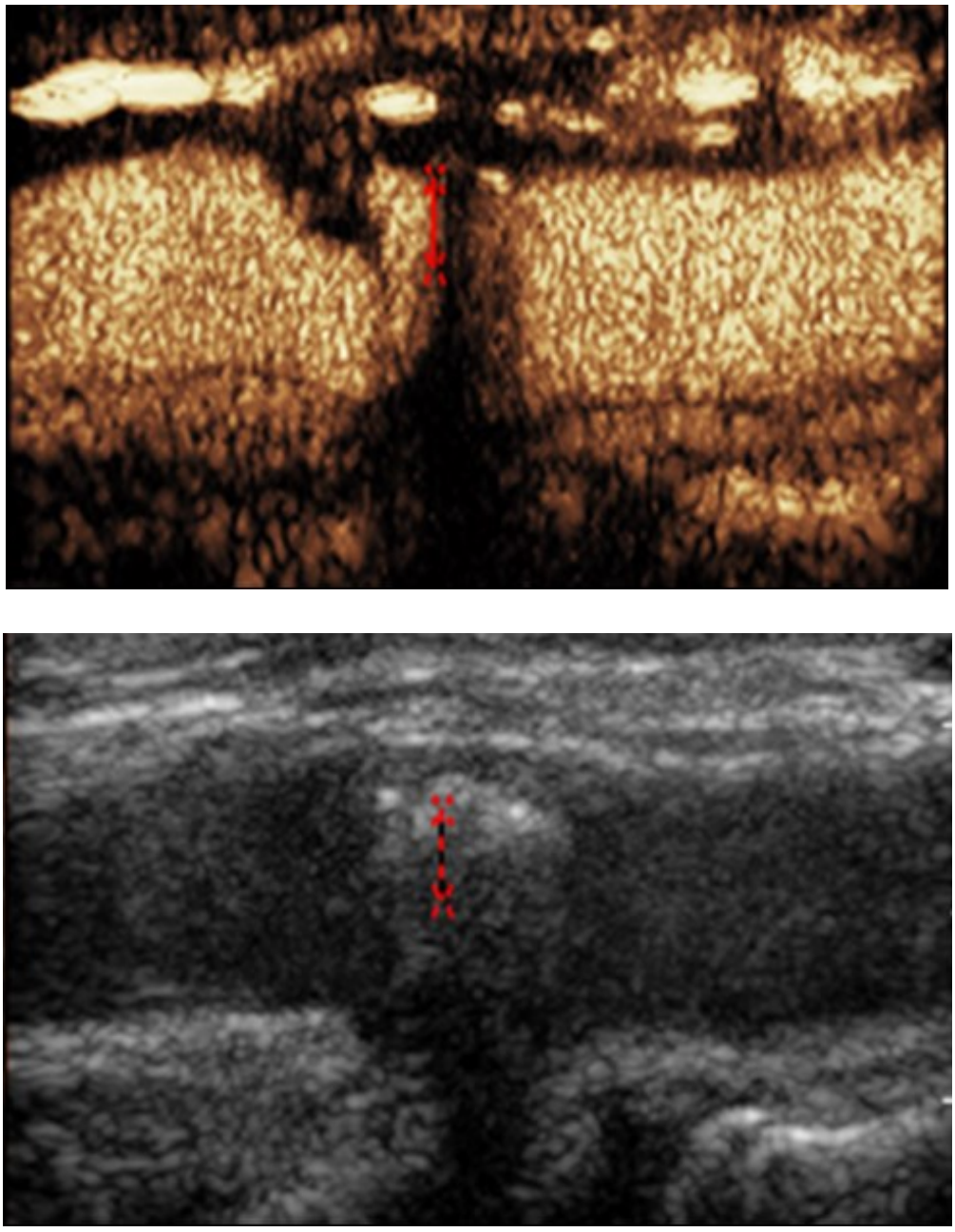

Figure 36 The superior image demonstrates the DCE-US of the carotid plaque with a discrete surface defect of >1.5mm which was classified as an ulcer with the inferior image showing the corresponding B-mode ultrasound image.

9.4. Discussion

The principal result of this study was that DCE-US imaging demonstrated a trend for more ulcers in symptomatic patients than color Doppler ultrasound, with good reproducibility.

Ulceration on DCE-US was very specific to patients with ipsilateral symptoms yet addition of ulceration to the North American clinical threshold of ≥60% stenosis(291), although improving the diagnostic odds ratio, reflecting increased confidence in identifying those with symptoms, still missed three quarters of patients with ipsilateral symptoms. However, from randomized controlled trials only 1 stroke per 6-13 symptomatic patients(47) and 1 stroke per 20 asymptomatic patients(234, 263) is saved with endarterectomy, a similar proportion to those patients with ulceration in this study. It would be interesting to observe follow up on best medical management for both the symptomatic moderate stenosis and asymptomatic patients with ulceration on DCE-US to determine if they are the groups who go on to experience future stroke.

One previous study has examined the use of contrast enhanced ultrasound for the detection of ulceration (292). In this study of symptomatic patients only, there was greater detection of ulceration using contrast enhanced ulceration over color Doppler ultrasound which is in keeping with the findings of this study. Additionally, the inter-reader reproducibility for contrast enhanced ultrasound ulceration detection was κ=0.65 in that study which compares favorably with our own inter-reader reproducibility (κ=0.64) providing further validity for this technique. Previous studies assessing ulceration using ultrasound have defined the presence of an ulcer as a ≥1mm surface defect at the plaque-lumen border (292, 293). In our study we defined the presence of an ulcer as a ≥1.5mm surface defect as we felt that this was most the accurate threshold within the 1 mm resolution of the acquisition and

analysis platforms used. Interestingly in the previous studies using the smaller threshold, 38% of the ulcers detected using contrast enhanced ultrasound by ten Kate et al. could not be corroborated by the reference standard whilst Madani et al. found that the presence of ≥2 ulcers on three-dimensional ultrasound was required to provide a significant risk prediction.

The strengths of this study are that it was a reader blinded study, with an independent stroke physician assessing presenting symptoms. This study is the first to assess DCE-US for the detection of ulceration in both symptomatic and asymptomatic patients. DCE-US is a simple, low-cost, practical adjunct to conventional color Doppler ultrasound for the assessment of ulceration which remains one of the vulnerable features of the carotid plaque previously established by histology (286, 287) and forms part of recognized clinical risk scoring tables recommended for use for symptomatic patients in the United Kingdom (218) .

The limitations of this study are that DCE-US is often unsuccessful in assessing calcified lesions, 3 of which had to be excluded in this study. For these lesions, other risk stratification techniques such as transcranial Doppler may be more appropriate, however, these examinations can be lengthy and uncomfortable for patients (294). Improvements in low mechanical index imaging such as the removal of static reflectors within areas of calcification or at tissue interfaces would be of benefit to future investigators (295). Angiography performed either by magnetic resonance or multidetector computed tomography was not performed in this study as this is not routine practice at our institution in keeping with accepted practice within the United Kingdom for carotid imaging (44, 225) and was therefore not ethical to be included. This study lacked a histological reference standard, however, histological examination did not appear justified for this pilot study which included both symptomatic and asymptomatic groups but should be investigated in future studies of patients undergoing carotid surgery.

The lower median stenosis in asymptomatic patients may simply reflect a selection bias, as patients with high grade asymptomatic stenosis are considered for endarterectomy at our institution. Additionally, this selection bias may account for the differences in anti-platelet therapy between the groups with a proportion of asymptomatic patients being referred from vascular surgeons due to arterial disease elsewhere and therefore already on best medical therapy including anti-platelet therapy.

Further research should focus on whether ulceration on DCE-US is corroborated by histological endarterectomy specimens with subsequent prospective studies examining the use of DCE-US as a risk prediction tool in moderate stenosis symptomatic and asymptomatic carotid atherosclerosis patients.

10. DYNAMIC CONTRAST ENHANCED ULTRASOUND FOR ASSESSMENT OF PLAQUE PERFUSION & ULCERATION

10.1. Identifying the Vulnerable Carotid Plaque

At present, color Doppler ultrasound assessing luminal stenosis is the recommended first line imaging modality to assess carotid disease in both the United States of America and United Kingdom (225, 296). However, luminal stenosis alone is a weak predictor of future stroke especially in the groups of patients with moderate symptomatic 50-69% stenosis and asymptomatic 70-99% stenosis in whom carotid intervention remains controversial with a number needed to treat of 1 in 13 and 1 in 20 respectively for carotid endarterectomy (257, 289).

Dynamic contrast enhanced carotid ultrasound (DCE-US) is a novel clinic-based, structural and functional imaging modality which can act as a simple adjunct to color Doppler ultrasound to assess carotid atherosclerosis (290). Histological studies of carotid plaques have demonstrated a number of characteristic features which may be imaged in real-time using DCE-US including ulceration as previously discussed and proliferation of abnormal, immature, intraplaque microvessels, termed neovascularization (55, 56, 63, 297-299). This neovascularization has been demonstrated with greater density in ruptured plaques compared to non-ruptured plaques and has also been more frequently observed in plaques from symptomatic patients compared to asymptomatic patients (56, 300). Therefore, these histological findings suggest that for a carotid plaque to become vulnerable increased plaque neovascularization must occur during its evolution.

Previous studies assessing DCE-US in carotid atherosclerosis have demonstrated significant associations between carotid plaque contrast signal and both histological

microvessel density and patient symptom status using both qualitative and quantitative image analysis techniques (62, 167, 299, 301). However, these studies were performed using quantification techniques that do not correct for the recently described pseudoenehancement that occurs in far-wall carotid plaques secondary to non-linear propagation that can result in perceived, artifactual microbubble signal being misinterpreted for carotid plaque neovascularisation (295).

The aim of this pilot study was to assess the potential benefits of DCE-US in the assessment of plaque perfusion using qualitative and quantitative analysis. A novel DCE-US quantification method was developed to measure the extent of low intensity microflow within carotid plaques whilst addressing potential artifactual ultrasound contrast agent signal from pseudoenhancement. The qualitative and quantitative techniques were used to detect the differences in neovascularization in carotid plaques of asymptomatic and symptomatic patients.

10.2. Study Methodology

10.2.1. Patient Selection

Ethical approval was obtained prior to commencing the study (Ref 09/H0706/89). Written informed consent was obtained from all patients. Patients with a discrete 50-99% internal carotid artery stenosis in relation to the normal distal internal carotid diameter (NASCET equivalent (229)) were recruited from neurovascular clinics between January 2011 and April 2012. Inclusion criteria were: male or female patients aged 18 years or over with a 50-99% (NASCET) internal carotid artery stenosis. An independent stroke physician assigned the diagnosis of carotid territory ischemic symptoms within the prior 4 weeks after a workup including intracranial computed tomography, 24 hour electrocardiogram, troponin result, echocardiography and for cases of amaurosis fugax, an ophthalmic opinion to exclude any other

aetiology for the index event. If no history of stroke, transient ischemic attack or amaurosis were present, an asymptomatic status was recorded. Exclusion criteria were: atrial fibrillation, mechanical heart valve, cardiomyopathy, elevated troponin, contrast contraindication, NYHA III/IV cardiac failure, myocardial infarction within 3 months and neurovascular ischemic symptoms >4 weeks previously.

10.2.2. DCE-US Image Acquisition

Prior to patient inclusion and to identify suitable patients, an initial color Doppler scan was performed by an independent vascular scientist (minimum 2 years' carotid ultrasound experience) where luminal stenosis were recorded as per standard clinical care at our institution.

DCE-US was performed with a Philips iU22 ultrasound platform (Philips, Bothell, WA, USA) using a L9-3 linear array probe and the following standard settings: mechanical index 0.06, frame rate between 13-16 Hz, vertical centered time-gain-compensation (TGC) curve, XRES on and persistence at medium. The 2D gain was adjusted just above the noise floor for maximum sensitivity. The focus was set below the depth of the plaque for a uniform pressure field (302). A 2ml intravenous bolus of SonoVue™ (Bracco, Milan, Italy) was injected via a 20 gauge cannula in the right antecubital fossa. A one minute digital video loop from the point of contrast injection was captured, centered on the plaque in longitudinal section at the point of greatest stenosis as previously described (60, 62, 63, 299). A constant imaging plane was maintained by monitoring the "tissue" side of the acquisition. After 10 minutes this was repeated. Patients were observed for 30 minutes post injection for adverse events. Acquired DCE-US loops were transferred for offline independent, blinded qualitative and quantitative analysis.

10.2.3. Qualitative Image Analysis

Anonymized DICOM video loops were exported for blinded, offline analysis using QLAB version 8.1 (Philips Medical Systems, Bothell, WA). Qualitative assessment of perfusion was performed by an independent vascular radiologist (10 years' vascular carotid ultrasound experience). This was repeated for inter-reader comparison. Moving microspheres within the carotid plaque region of interest were considered as qualitative plaque perfusion. Static microbubble signal as a result of either intraplaque calcification or non-linear propagation artefact were not considered as active plaque perfusion. The observer would visually compare the area that had moving microbubbles to the total area of the plaque. A simple binary grading system for perfusion was used: 0 representing 0-50% of plaque area containing moving microspheres and 1 representing >50% area of plaque area containing moving microspheres. Other groups have used a three point grading system for plaque perfusion to include; no perfusion, <50% area perfusion and >50% area perfusion (303). The difficulty with this is distinguishing absent from low grade perfusion (occasionally a single microsphere). Hence we simplified this to a binary grading system, as in fact this group has now also done (61). The observer changed zoom, contrast and brightness in low light ambient conditions to optimize viewing of the DCE-US loop images.

10.2.4. Quantitative Image Analysis

The quantitative analysis was divided into two stages. The first stage of the analysis was performed in QLAB version 8.1 (Philips Medical Systems, Bothell, WA). The data derived from the QLAB stage of the analysis were then accessed from MATLAB (2012b, The MathWorks Inc., Natick, MA) in order to quantify the extent of perfusion in the carotid plaques.

For the first stage of the analysis the anonymized DICOM files of the acquired DCEUS loops were transferred to QLAB. A region of interest (ROI) was drawn around the plaque using the ROI polygon tool of QLAB's quantification suite (Fig.1a-c). Caution was taken not to include any nearby tissue or arterial lumen in the ROI. Frames in which there was an excessive amount of out of plane motion were manually removed. In-plane motion was treated with the motion compensation tool of QLAB. Manual corrections in the position of the ROI were also performed as a final step in ensuring that the ROI encompassed only the plaque. The steps described enable accurate quantification of the loops since the low intensity microflow signal within the carotid plaque can be contaminated by high intensity signal from within the vessel lumen and the surrounding tissue, thus introducing error into the quantification results.

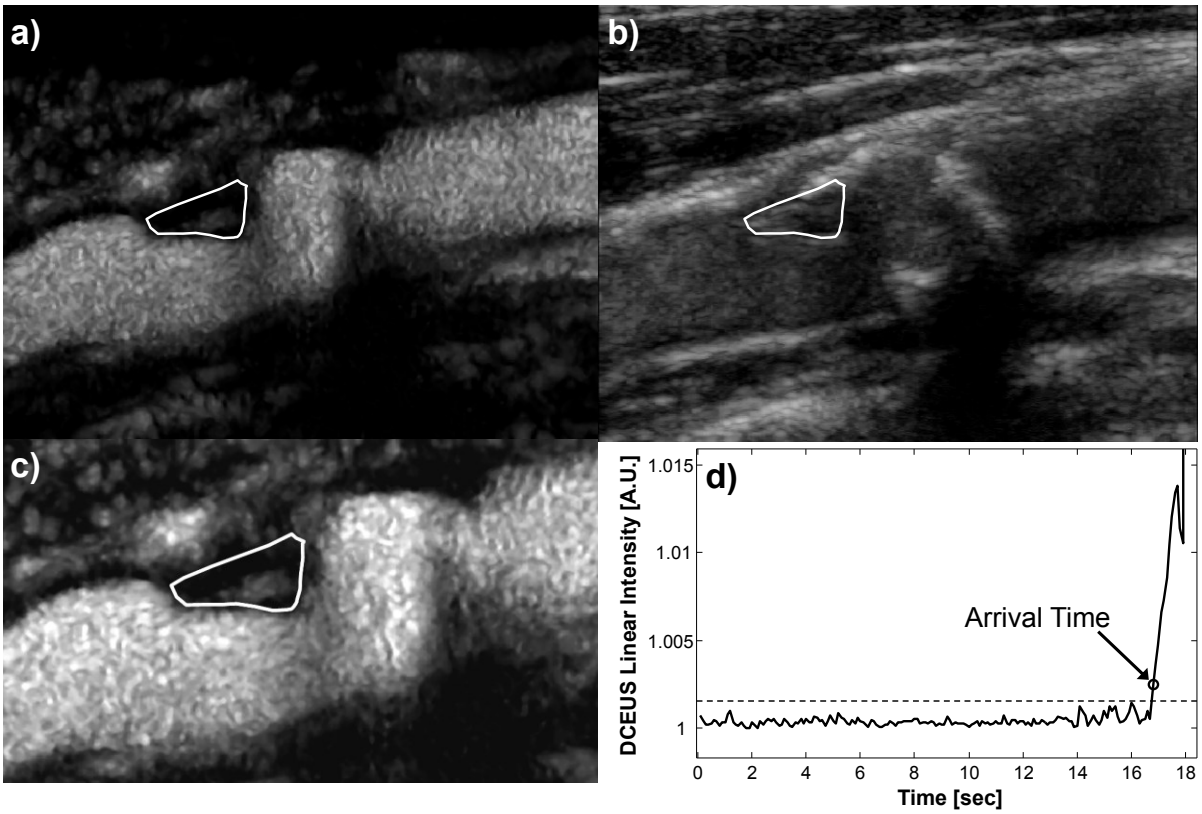

Figure 37 a) Contrast side of the dual-contrast imaging carotid plaque acquisition with the carotid plaque delineated using QLAB's polygon tool to draw the region of interest (ROI), b) tissue side of the dual-contrast imaging carotid plaque acquisition and c) zoom-in on the carotid plaque on the contrast image with the upper level of the contrast window decreased to enhance the low intensity signal within the plaque. d) Detection of microbubble arrival in carotid atherosclerotic plaques. The arrival time was defined as the first time instance at which the mean linear intensity value from within the ROI encompassing the plaque exceeds the maximum value present in the background noise (dashed line).

The second stage of the quantitative DCE-US analysis was performed in MATLAB. The DCE-US loop image data from QLAB were imported into MATLAB. For each loop, the ROI was reconstructed in MATLAB using the coordinates of the vertices of QLAB's polygon ROI. The coordinates of the polygon vertices were imported into MATLAB from the "parameters.xml" file, as well as the 2D translation values from the motion compensation, the rejected frame indices and the time intensity curve (TIC) of the ROI.

The first step in the MATLAB quantification analysis was to determine the arrival time of the contrast agent in the ROI. The arrival time was defined as the first time instance at which the TIC intensity value exceeds the maximum value of the background noise recorded (Fig.1d). The ROI was then applied as a binary mask on each valid frame of the DCEUS loop. At each pixel location within the ROI the distribution of image intensity values recorded before the arrival of the contrast agent in the ROI were considered to be a sample from the noise or artifact distribution. For each pixel the noise distribution sample was compared to the distribution of image intensity values after the arrival of the contrast agent. The comparison of the two samples was performed using the two sample Kolmogorov-Smirnoff test at a significance level of 0.1%. If the two samples differed significantly (i.e. p-value<0.001) then that pixel location was considered to be perfused, since the distribution of image intensity values after the arrival of the contrast agent differs significantly from that of noise. The number of pixels in the ROI that were perfused was divided by the total number of pixels in the ROI to evaluate the percent perfusion coverage of the plaque (Fig.2).

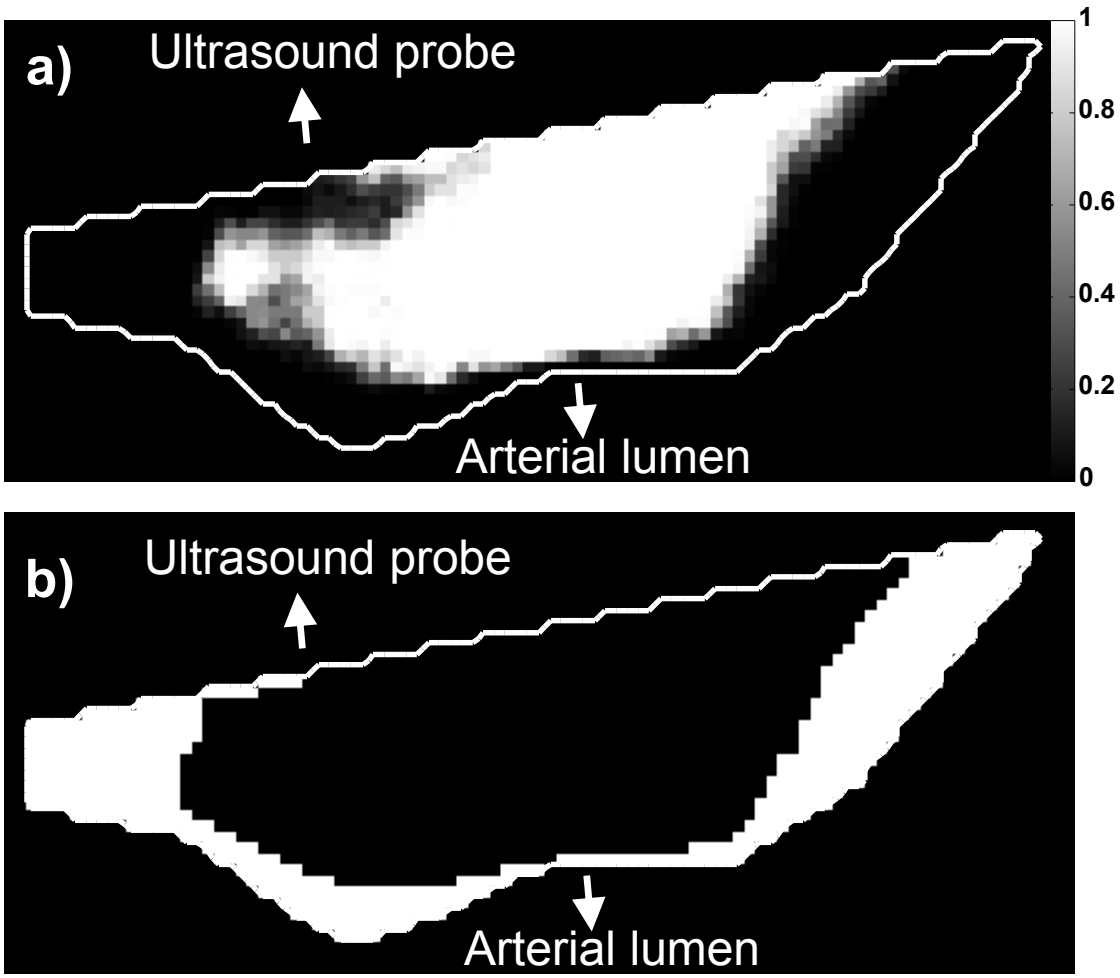

Figure 38 Results of dynamic contrast-enhanced ultrasound (DCE-US) quantification analysis of a near-wall carotid plaque (delineated with white line) from a symptomatic patient. a) Parametric map of p-values from the two sample Kolmogorov-Smirnoff test used to detect intraplaque perfusion is shown. b) A threshold of 0.001 is used on the p-value parametric map to differentiate between perfused (p-value<0.001) and non-perfused pixels (p-value≥0.001). In this symptomatic patient the plaque had 32% perfusion coverage.

10.2.5. Statistical Analysis

The qualitative and quantitative analysis was performed by a Vascular Surgery clinical research fellow and repeated by a Professor of Bioengineering with more than 20 years of experience in clinical ultrasound research. Inter-observer agreement was calculated using the intraclass correlation coefficient and Cohen's kappa for the quantitative and qualitative analysis respectively. The qualitative scores reported were mutually agreed upon following the inter-observer agreement analysis. From the quantitative analysis the mean of the percent perfusion coverage calculated by the two observers was reported.

Differences in the qualitative scores between asymptomatic and symptomatic patients were tested using Fisher's exact test. The Mann-Whitney U test was used to calculate differences in the percent perfusion coverage of the carotid atherosclerotic plaques between symptomatic and asymptomatic patients. Furthermore the results from the quantitative analysis were placed into two groups based on their qualitative score. The differences between the two groups were compared using the unpaired two sample t-test. The significance level for the statistical tests was set at a p-value of 0.05. The data were analyzed using the R programming language (R Foundation for Statistical Computing, Vienna, Austria).

10.3. Results

10.3.1. Patient Demographics

Twenty seven patients were included in this study. Fifteen were asymptomatic and 12 symptomatic. Of the 12 symptomatic patients, 6 (50%) had cerebrovascular accidents (CVA), 3 (25%) had transient ischaemic attacks (TIA) and 3 (25%) had amarousis fugax. Asymptomatic patients were referred for imaging from neurologists

and vascular surgeons due either the presence of risk factors or peripheral arterial disease in another territory. Further baseline demographic data is demonstrated in Table 7. All 27 data sets were included for image analysis.

Variable	Asymptomatic	Symptomatic	P-value
Number of patients	15	12	-
Age (years)	81 (SD 3)	75 (SD 3)	0.17
Male gender	13 (87%)	8 (67%)	0.23
Ipsilateral NASCET stenosis (%)	67 (IQR 55-80)	78 (IQR 70–90)	0.05
Diabetes	3 (20%)	5 (42%)	0.41
Antihypertensive therapy	8 (53%)	8 (67%)	0.50
Statin therapy	9 (60%)	9 (75%)	0.50
Antiplatelet therapy	12 (93%)	10 (65%)	0.83
History of smoking	10 (67%)	4 (33%)	0.09
Parental CVA	3 (20%)	2 (17%)	0.83

Table 7 Baseline demographic details of the 27 patients imaged in this study. Groups were compared with an unpaired T-test with significance taken at P<0.05.

10.3.2. Qualitative Perfusion

Qualitative plaque perfusion of >50% area of the plaque with moving microspheres was seen in 4/12 (33%) of symptomatic patients and 12/15 (77%) of asymptomatic patients (P<0.05) (Figure 39). There was a good agreement between the two observers with a Cohen's Kappa of 0.703.

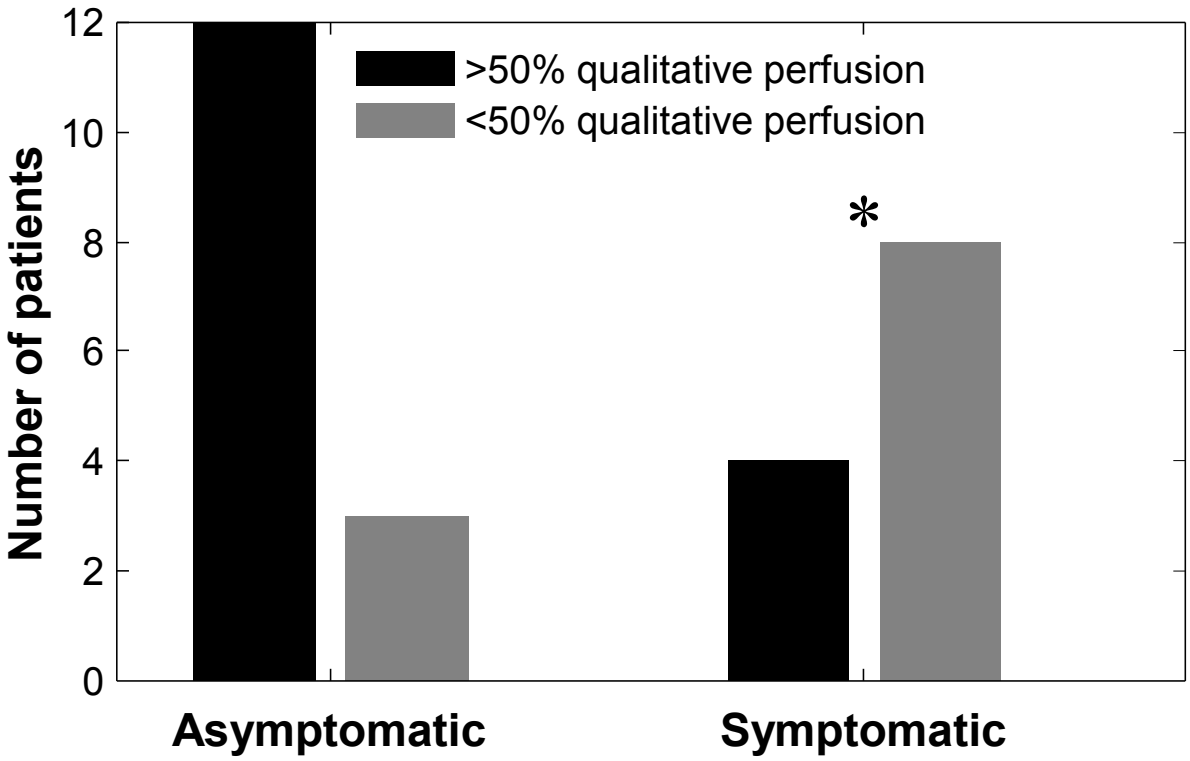

Figure 39 Bar plot of the results from the qualitative analysis of the carotid plaque DCEUS scans. Symptomatic patients showed significantly higher proportions of plaques graded as having moving microbubbles in less than 50% of their area. * = P≤0.05

10.3.3. Quantitative Perfusion

The percent perfusion coverage for symptomatic patients concentrated in their majority (8/12) below 50% with the further 4/12 of symptomatic patients exhibiting percent perfusion coverage of over 80%. The percent perfusion coverage of plaques in asymptomatic patients was evenly spread between 40-100%, with 14/15 demonstrating perfusion coverage of greater than 50% (Fig.4). Therefore, asymptomatic plaques demonstrated greater overall percentage plaque perfusion coverage compared to symptomatic plaques ($P<0.05$). The results of the quantitative analysis were compared with the qualitative visual scores (Fig.5) and a significant increase of the percent perfusion coverage was demonstrated for the plaques that received a qualitative score of higher than 50% perfusion coverage ($p<0.05$). Strong inter-observer agreement was demonstrated for the quantification analysis with a calculated intraclass correlation coefficient of 0.831 (95% confidence interval, 0.662-0.919).

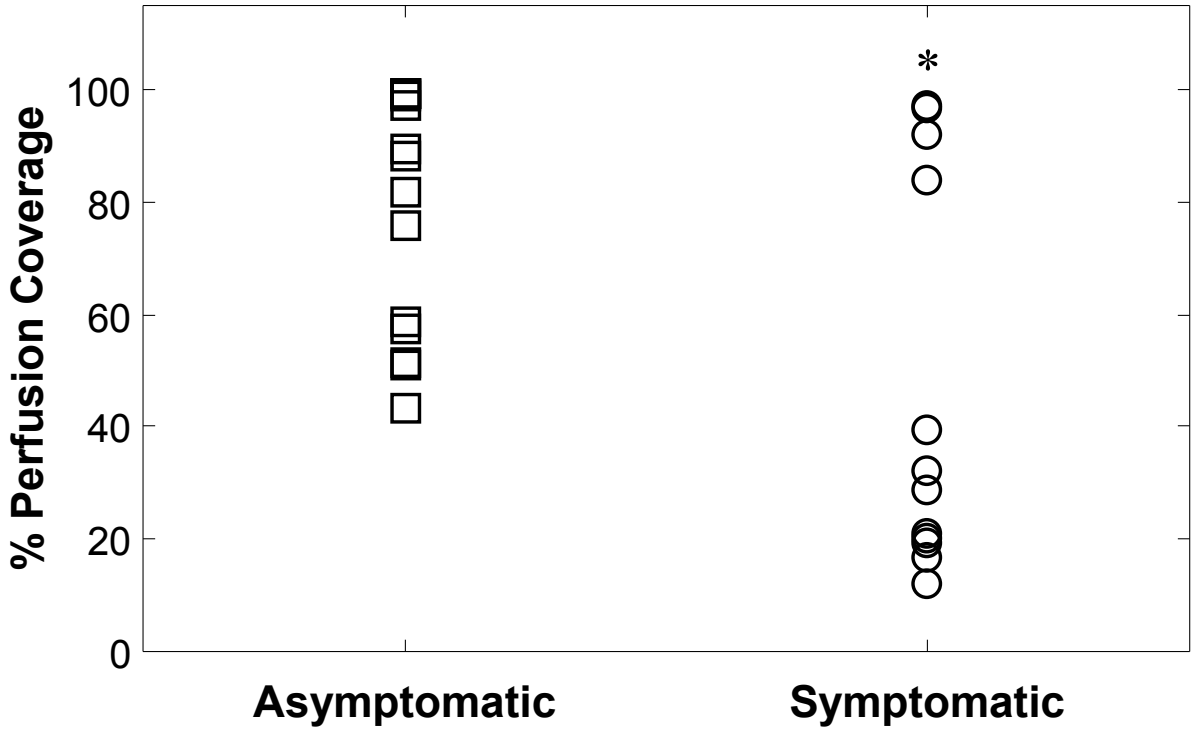

Figure 40 Scatter plot of percentage perfusion coverage of plaques between symptomatic and asymptomatic patients. Plaques in asymptomatic patients have percentage perfusion coverage values covering the range between 40 to 100% whereas the majority of plaques from symptomatic patients (8/12) have less than 50% perfusion coverage. * = P≤0.05.

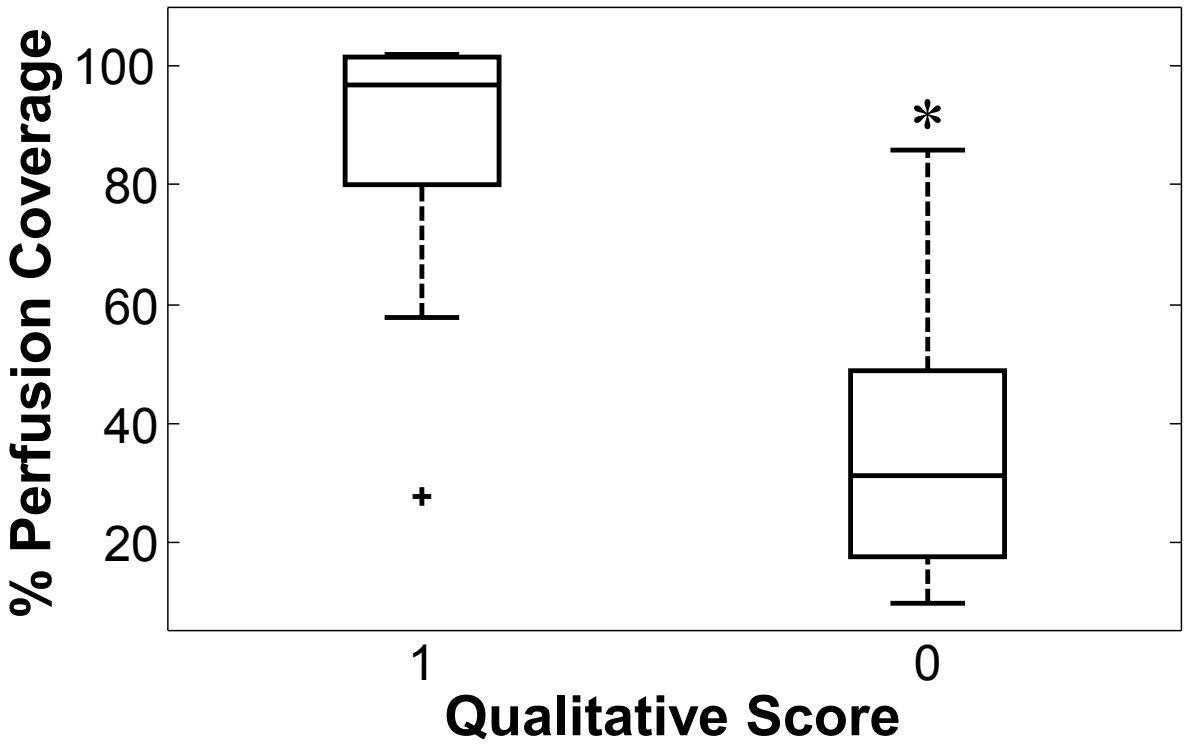

Figure 41 Boxplots of the quantitative percentage perfusion coverage of carotid plaques grouped according to results of the qualitative analysis. Carotid atherosclerotic plaques that received a qualitative score of 1 were considered to be perfused in more than 50% of their surface area and a score of 0 considered as less than 50% of their surface area. The quantitative percentage perfusion coverage values were significantly higher in the group with a qualitative score of 1 compared with the values that received a qualitative score of 0. * = P≤0.05, Power=1.0.

10.4. Discussion

Both the qualitative and quantitative analysis of this study found that carotid atherosclerotic plaques from symptomatic patients exhibit significantly less perfused area compared with asymptomatic patients. The results of the qualitative and quantitative analysis were examined for inter-observer variability with correlation

scores demonstrating good and strong agreement respectively. In addition the results of the quantitative analysis were validated against the qualitative scores.
Akkus et al performed a DCE-US quantitative study of 45 symptomatic carotid plaques using an adaptive image threshold technique to detect the perfusion within the plaques (301). The patients participating in the study presented with symptomatic stenosis exhibiting a mean percentage perfusion coverage of 32.7% ± 24.7% (mean ± standard deviation). In the current study, the mean percentage perfusion coverage for symptomatic patients was 47.4% ±34.9% (N=12) compared to 80.1% ±21.2% for asymptomatic patients (N=15). A similarity of the results for the symptomatic patients between this study and the one by Akkus further supports the finding that carotid plaques from symptomatic patients may have reduced perfusion coverage compared to asymptomatic patients.

In a quantitative DCE-US study by Hoogi et al active contouring image segmentation was used to detect the microflow within carotid plaques (62). Regions of contrast signal within a plaque were considered areas of neovascularization. Strong correlation was reported between the ratio of intraplaque area neovascularization calculated using DCE-US and plaque microvessel density on histology. However, no differences could be shown between the symptomatic and asymptomatic patients. Although this contradicts the findings of the current study there are differences in the methodology and carotid plaque characteristics to be considered. In particular, the current study uses statistics to differentiate perfusion from noise and artefact in each vector position within the carotid plaques whereas Hoogi et al utilize image segmentation with all contrast agent detected being registered as neovascularization making this later method more susceptible to inclusion of contrast pseudoenhancement.

Xiong et al used an indicator dilution model to calculate neovascularization in carotid plaques using the ratio of the contrast signal peak intensity (PI) in plaques to the PI in the lumen of arteries (299). The study found that plaques from symptomatic patients

exhibit more intense contrast agent enhancement than asymptomatic patients. Although indicator dilution models have been used in the quantification of liver lesion perfusion and myocardial blood flow, the relative low flow state observed in carotid plaques compared to that of the carotid lumen do not satisfy the assumptions made by indicator dilution models (304-306). Furthermore, previous investigators have demonstrated poor correlation between the indicator dilution technique and qualitative visual scores of carotid plaque neovascularization prompting them to disregard any further consideration of this quantification (301).

DCE-US qualitative analysis studies have also shown a strong correlation between visual scores of enhanced plaque perfusion and predictors of plaque vulnerability including histological microvessel density (60, 307). This study aimed to detect differences in the perfusion characteristics between plaques from symptomatic and asymptomatic patients. Within a group of asymptomatic patients there may be plaques with a mixed of degree of vulnerability. This may be evident from the 40-100% range of percentage perfusion coverage values for the asymptomatic patients in this study (Fig.4). Furthermore, as a carotid plaque becomes symptomatic there is a high probability that rupture, characterised by haemorrhage and thrombosis, has occurred which may disrupt the microvessel network and thus demonstrating reduced perfusion of the carotid plaque.

Although the statistical results of this study show that plaques from symptomatic patients have significantly less perfusion compared with asymptomatic patients, further examination of the quantitative data demonstrates two relatively distinct groups within the symptomatic cohort (Figure 40). Whereas the symptomatic perfusion data are mostly concentrated below 50% (8/12) the remaining four plaques have perfusion coverage of more than 80%. These four cases are not necessarily outliers but instead could be vulnerable plaques with extensive neovascularization that have caused symptoms without their microvessel network being disrupted as previously described. Similarly, examination of the perfusion of asymptomatic

patients, identifies a spectrum of plaque perfusion from 40-100%. This may suggest that asymptomatic patients with higher degree of perfusion are more likely to develop symptoms in the future thus suggesting that they may be the ones with the vulnerable plaques.

Several limitations can be identified in this pilot study. Although the results indicate statistical significance, further powered studies with a larger number of patients will provide further confirmation of the findings. Misclassification of a small proportion of patients as symptomatic or asymptomatic may have occurred. This was minimized in the symptomatic group by excluding all those with cardiac abnormalities. In asymptomatic patients, current UK data demonstrate that only 2.1% of patients annually experience an ipsilateral carotid territory stroke or TIA (308). Another limitation is that the findings of the current study have not been verified against histology. Even though some histological results were available for the symptomatic patients that did undergo carotid revascularization, asymptomatic patients with 50-99% NASCET stenosis do not routinely have intervention as is standard clinical care at our institution in accordance with the Royal College of Physicians National Clinical Guideline for Stroke in the United Kingdom (218). Therefore, there was no ethical justification for histological comparator data in this observational, pilot study and any comparison of the histological results with DCE-US analysis would be biased towards those patients deemed at higher risk clinically. Furthermore the current study aimed to identify differences in the extent of carotid plaque perfusion based on the appearance of symptoms rather than performing a direct comparison with histology.

The percent perfusion coverage calculated in the quantitative analysis of this study is representative of only a 2D sampled slice through the plaque. Future volumetric 3D studies can provide additional insight into the perfusion patterns of vulnerable plaques and also increase sensitivity but are as yet unproven for this level of quantification. In addition, in 2D DCE-US, the plaque might not be perfectly centered perpendicular to the longitudinal plane of the ultrasound image which may

introduce vessel lumen signal into the ROI or fail to capture optimum plaque perfusion in that plane. Differences in bolus kinetics between patients may have affected quantitative analysis, however, this technique used the baseline level of signal noise for normalization with subsequent production of a relative ratio of surface area coverage allowing comparison of different patients. This was further demonstrated through comparable results between the quantitative and qualitative analysis suggesting consistency. Finally, inherent limitations to carotid plaque DCE-US include the presence of acoustic shadowing from plaque calcification, insufficient resolution and limited sensitivity in detecting the perfusion on a microscopic scale of plaque vasculature. These sources of uncertainty do not just affect the current study but are intrinsically present in all of the DCE-US studies and will be greatly improved through refinement of low mechanical index ultrasound contrast imaging to improve resolution and tissue cancellation whilst removing artifactual image signals (309).

In conclusion, a new quantification tool for plaque neovascularization, percent plaque perfused area, was developed and independently, blindly assessed in a group of both symptomatic and asymptomatic patients. This quantification technique is currently more appropriate for plaque perfusion quantification than other metrics due to relative cancellation of noise and artifactual signal. The findings of this pilot study illustrate that symptomatic carotid plaques had reduced perfused area, possibly due to intraplaque hemorrhage, large necrotic cores and thrombus formation. The opposite was observed in asymptomatic patients and their plaques had increased perfused area. Increased perfusion in asymptomatic patients may represent a subset group of asymptomatic patients whose plaques are vulnerable. Thus, a more appropriate study in the future would be one in which plaques are identified in asymptomatic patients and prospectively evaluated through a period of time in order to elucidate plaque microvessel flow progression and its relationship with neurological symptom status.

11. FINAL DISSCUSSION

11.1. Sonothrombolysis for Deep Vein Thrombosis

The aim of this part of the thesis was to assess the feasibility of contrast enhanced ultrasound thrombus dissolution. In particular, having assessed the literature the novel target of DVT for this technique was identified with previous pre-clinical and clinical studies having already been completed in models of arterial thrombosis mimicking the acute management stroke and myocardial infarction.

The motivation to investigate DVT arose from clinical studies including randomised controlled trial evidence suggesting that the rate of post thrombotic syndrome after DVT can be reduced by acute thrombus removal which currently is performed by either catheter directed thrombolysis or pharmacomechanical thrombolysis (199). However, early data from the largest randomised controlled trial in this field to date, ATTRACT, has identified that acute thrombus removal may not be beneficial to all patients with regard to both the prevention of PTS long term and increased risk of short term bleeding complications compared to conventional anticoagulation therapy (310). It does appear that there is benefit in subgroups of patients including those less than 65 and with ileofemoral DVT but further subgroup analysis is awaited with further adequately powered studies likely required in the future to confirm these findings. Therefore, it could be argued that at present both the patient selection and intervention itself are flawed.

This thesis has explored one aspect of patient selection in acute thrombus removal through the review of DVT ageing imaging. At present, a DVT is viewed in a binary fashion but greater analysis of thrombus characteristics may help identify those patients in whom thrombus removal will be successful and likewise experience fewer bleeding complications. This is highlighted by a significant risk reduction in PTS in

the CaVenT trial which included patients with a symptom duration of 14 days compared to ATTRACT which included patients with a symptom duration of up to 21 days but was not able to demonstrate the same benefit over anticoagulation treatment. The emerging imaging modalities would appear to be ultrasound elastography and MRI with the primary imaging target of both being the differentiation between the acute and sub-acute DVT. Additionally, as acute thrombus removal gains traction histological correlation with novel imaging techniques may diverge away from absolute age and instead identify imaging thrombus characteristics that inform clinicians regarding the susceptibility of the thrombus to intervention.

Both CaVent and ATTRACT report significant bleeding complications and whilst patient selection has a role within this, the actual intervention itself may be unsatisfactory. This is highlighted in ATTRACT where a heterogeneous group of interventions were included from catheter directed thrombolysis to multiple types of pharmacomechanical devices suggesting that quorum is yet to be reached on the optimal type of intervention.

In this thesis, a non-invasive, non-irradiating technique without the use of thrombolytic agents has been investigated. The feasibility has been proven in an adaptation of a well validated in-vitro model of DVT. In particular, the in-vitro model developed is advantageous over previous in-vitro models assessing sonothrombolysis as whole blood was used, therefore, incorporating two parts of Virchow's original triad of thrombosis through blood constituents and flow. It has been shown that in this model, the addition of microbubbles to ultrasound thrombolysis leads to a significant improvement in thrombus dissolution over ultrasound alone which as discussed is already in clinical use in combination with thrombolytic therapy. In particular, contrast enhanced ultrasound thrombus dissolution resulted in dissolution of the fibrin mesh network of the thrombus which was not observed with ultrasound alone.

There were limitations in this feasibility study which relate largely to the in-vitro model including the fixed acute age of the thrombi investigated, a lack of vessel wall interaction, no assessment of differing constituents of the flowing blood and assessment of safety endpoints. Further development of contrast enhanced ultrasound thrombus dissolution should progress from feasibility to safety and efficacy. This should again employ a well validated model of DVT and in order to address the aforementioned limitations an animal model should be considered. There are a number of rodent models of DVT based around the creation of thrombus within the IVC. These include a suture ligation of the infra-renal IVC, a chemical ferric chloride model and electrolytic induced IVC thrombosis (105). As safety is an important endpoint moving forward, any model which inherently causes damage to the vessel wall should be discounted which excludes the ferric chloride and electrolytic models which require chemical and electrical vessel wall injury respectively to induce thrombosis. This leaves the IVC suture ligation model as the likely candidate for a suitable animal model.

This rodent model is the same as that used in the ultrasound elastography ageing studies identified in the DVT imaging ageing review earlier thus demonstrating that ultrasound can readily identify these IVC thrombi for investigation. The thrombi in this model will be of greater volume compared to those of the in-vitro model and additionally different thrombus ages can be assessed as there are well validated time intervals when the rodent thrombus matches the histological profile of acute, sub-acute and chronic human thrombi (105). The safety analysis can be conducted by assessment for tissue damage within the IVC vessel wall and subcutaneous tissue ex-vivo as well as assessment for distal embolisation within the lungs. Therefore, the rodent IVC suture ligation model of DVT is likely to represent a robust, incremental progression in the further assessment of feasibility, safety and efficacy of contrast enhanced ultrasound thrombus dissolution.

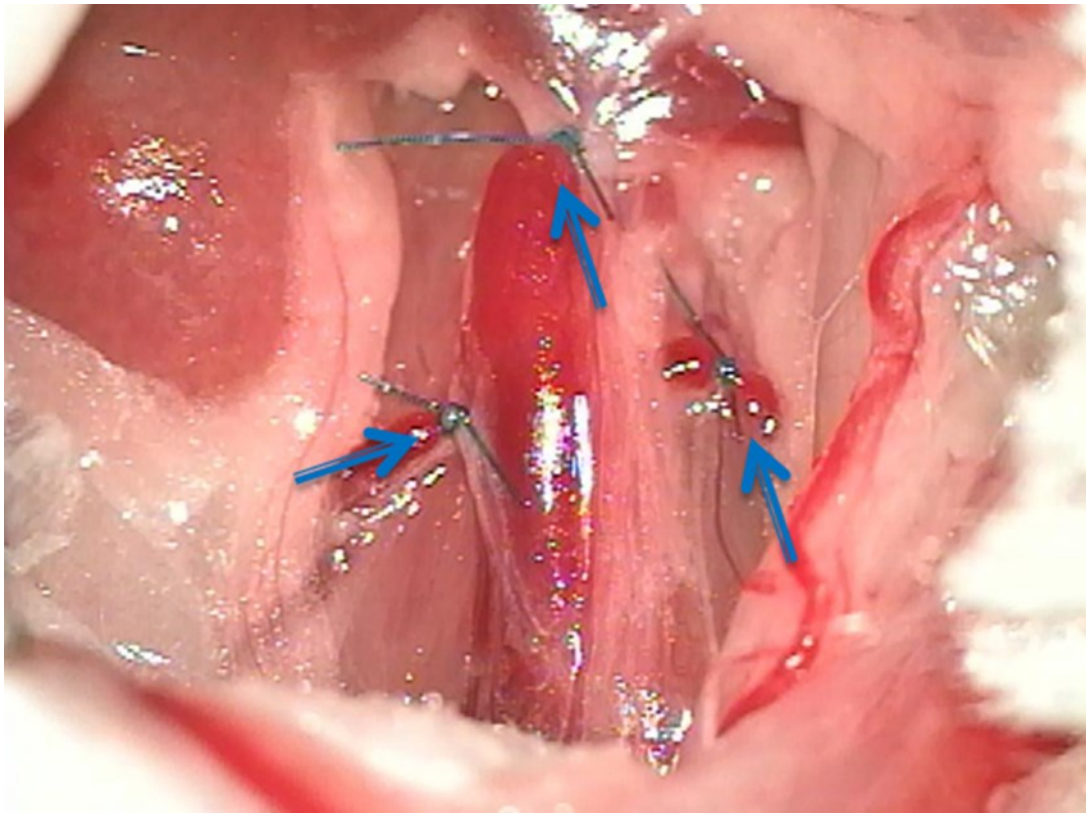

Figure 42 Intraoperative photo of a C57BL/6 mouse. Completed mouse IVC ligation model with side branches and infrarenal IVC ligated with 7-0 Prolene suture. Immediate dilatation of the IVC is observed upon ligation.

11.2. Contrast Enhanced Ultrasound for Carotid Atherosclerosis

It is well documented that the numbers needed to treat to prevent one stroke with carotid revascularisation are not favourable in both asymptomatic 70-99% and symptomatic 50-69% carotid atherosclerotic stenosis. Contrast enhanced ultrasound has been investigated in this thesis to identify imaging characteristics that can differentiate symptom status and thus begin to develop an imaging biomarker that

can aid in the identification of patients who would benefit from revascularisation in these subgroups.

The survey performed of vascular surgeons and stroke physicians in the UK regarding their current management of patients with symptomatic 50-69% carotid stenosis demonstrated the current difficulties faced in this subgroup of patients with similar outcomes observed compared to a previous global physician survey assessing the management of asymptomatic 70-99% carotid stenosis (277). In particular, there was divergence in opinion between vascular surgeons and stroke physicians across all presented scenarios highlighting the potential variation in patient care received for the same disease across the UK currently. The addition of the ECST 5 year stroke risk score in the survey also led to significant changes in decision making which identifies a role for such adjunctive scoring systems in this controversial subgroup.

One of the components that makes up the ECST 5 year stroke risk score is carotid plaque morphology; namely the presence of ulceration. An adaptation of this scoring system, CAR, is being used in the currently recruiting ECST-2 trial and whilst the results of this study as well as ACST-2 will hopefully better inform management in these subgroups, the use of plaque characteristics in a large randomised controlled trial opens up this area to assessment of carotid plaques beyond luminal stenosis only.

Whilst imaging modalities such as CT angiography, MRI and PET rise to prominence, carotid duplex ultrasound remains the first line imaging choice for carotid atherosclerosis in most centres in the UK (44). Therefore, contrast enhanced ultrasound represents a relatively simple adjunct that is non-irradiating with a favourable safety profile that can be performed by the bedside or in clinic in combination with the existing imaging practice of carotid duplex.

Contrast enhanced ultrasound was initially investigated to assess carotid plaque ulceration. There was a trend toward greater sensitivity of contrast enhanced ultrasound compared to carotid duplex in the detection of plaque ulceration. Additionally, this enhanced ulcer detection was also associated with a trend toward symptomatic patients with good reproducibility of the technique also noted. This is an important finding as accurate assessment of carotid plaque ulceration is required to reliably employ the ECST 5 year risk score. The original assessment of plaque ulceration in ECST and NASCET was based on carotid angiography which is no longer routinely performed, however, the addition of an intravascular contrast agent to ultrasound imaging appears to incrementally improve the sensitivity and specificity of ulcer detection. Despite it being a different imaging modality, this is likely due to contrast enhanced ultrasound being akin to contrast angiography through the use of luminal intravascular contrast to fill carotid plaque contour irregularities to identify ulceration.

Carotid plaque contrast enhanced ultrasound perfusion was also assessed. Using lessons learnt from previous studies, qualitative and quantitative assessment of plaques was developed and performed to avoid pitfalls such as inappropriate inclusion of plaque pseudoenhancement and luminal signal from vessel pulsation motion artefact (295). Using these refined techniques both methods of assessment demonstrated a reproducible, significantly reduced perfusion in symptomatic patients compared to asymptomatic patients. Whilst histological studies undoubtedly suggest that there is a greater microvessel density within symptomatic carotid plaques secondary to neovascularisation, the perfusion observed on dynamic in-vivo imaging may in fact be reduced as a symptomatic plaque will usually undergo rupture and thrombosis with possible subsequent occlusion of these intraplaque microvessels. Therefore, it may be tentatively suggested that a reduction in dynamic perfusion in vivo may be a heralding sign of plaque thrombosis and rupture.

Both of the studies assessing carotid plaque characteristics using contrast enhanced ultrasound had similar limitations. In particular, the sample sizes were limited and more importantly these studies were cross sectional rather than prospective evaluations. A prospective study would provide an accurate correlation of the imaging findings with the natural history of the disease, however, as discussed only 1 in 13 to 1 in 20 of patients recruited in the moderate symptomatic and asymptomatic carotid stenosis groups respectively will become symptomatic so recruitment would need to be extensive. Given the infancy of the techniques in these studies this was not ethically justified. Additionally, many of these patients are currently being recruited into ongoing large studies such as ECST-2 and ACST-2. With various other imaging, biochemical and metabonomic biomarkers also being simultaneously investigated currently, large scale randomised controlled trials should endeavour to include these biomarkers to capture and compensate for the relatively low but nevertheless important stroke rates in these controversial groups to avoid a plethora of promising but ultimately inconclusive studies to be performed.

Specific to contrast enhanced ultrasound, the technique is limited as it is currently two dimensional single planar dynamic image acquisition. This is in contrast to CT imaging which is volumetric allowing multiplanar reconstruction as well as 3-tesla MRI which also has the capability of multiplanar reconstruction although this remains in a research capacity at present. The use of 3D contrast enhanced ultrasound imaging for carotid atherosclerosis should reduce the sampling error and therefore as discussed increase the sensitivity of both ulceration and perfusion assessments.

11.3. Conclusion

Ultrasound is well established in the imaging of vascular disease, in particular, within DVT and carotid atherosclerosis. Contrast enhanced ultrasound represents a natural evolution of this imaging modality as other common modalities such as CT and MRI also employ contrast agents to identify pathology through improved soft tissue resolution. Contrast administration has led to the development of quantification methods progressing imaging from subjective to objective assessment which has long been a perceived disadvantage of ultrasound imaging. Additionally, the microstreaming and acoustic cavitation produced by ultrasound are now being employed in vascular intervention. As shown, the presence of contrast microbubbles augments these desired effects of ultrasound thrombolysis and thus again represents natural evolution of ultrasound intervention.

Correct patient selection for carotid revascularisation is clearly paramount and remains poorly defined in the asymptomatic and moderate carotid stenosis subgroups. This need for patient selection arises from the inherent risk of intervention by either endarterectomy or stenting in these patients over best medical therapy to prevent future stroke. Contrast enhanced ultrasound may yet have a role to play in that selection. Acute thrombus removal in DVT represents a similar paradigm which is only starting to be realised as the identification of patients in whom PTS can be prevented has comparatively only just begun. Once again imaging thrombus characteristics is likely to form part of that assessment, in particular, thrombus ageing may contribute to a future scoring system. Finally, to aid patient selection, an intervention with a more favourable risk-benefit balance itself may be employed. A non-invasive, non-irradiating technique such as contrast enhanced ultrasound thrombus dissolution may provide a more acceptable risk profile while still gleaning the future reduction in PTS.

12. APPENDIX

12.1. Supplementary Information for Symptomatic Moderate Carotid Atherosclerosis Survey

The following transcript is taken from the web pages of the online survey (http://freeonlinesurveys.com/s.asp?sid=icropocgwl6hjp190262) that UK Vascular Surgeons and Stroke physicians were invited to complete:

12.1.1. Web Page 1

Many thanks for taking the time to complete this survey. We are conducting this survey to assess current decision making and management in symptomatic 50-69% NASCET carotid artery stenosis across both stroke physicians and vascular surgeons within the United Kingdom.

The survey comprises of six short scenarios and should take approximately 10 minutes to complete. For the purposes of the following scenarios we ask you to assume identical baseline comorbidities, a life expectancy of > 5 years, patients are surgically fit and have a contralateral internal carotid stenosis of <20%. Additionally, we ask you to assume that the patients show no strong preference and that your institution does not perform other procedures such as carotid stenting.

12.1.2. Web Page 2

Please state your specialty

Stroke physician Vascular surgeon

12.1.3. Web Page 3

Scenario 1

A 79 year old male presents with persistent left arm weakness for two days with a 55% right internal carotid artery stenosis and an ulcerated plaque on Doppler ultrasound.

Best medical therapy Carotid endarterectomy Unsure

12.1.4. Web Page 4

Scenario Two

A 63 year old male presents with left amaurosis fugax three days ago with a 65% left internal carotid artery stenosis and a smooth plaque on Doppler ultrasound.

Best medical therapy Carotid endarterectomy Unsure

12.1.5. Web Page 5

Scenario Three

A 76 year old female presents with a transient ischaemic attack affecting her right arm one week ago. Doppler ultrasound reveals a 60% left internal carotid artery stenosis and an ulcerated plaque.

Best medical therapy Carotid endarterectomy Unsure

12.1.6. Web Page 6

Thank you, this completes the first three scenarios. We would now like to re-present the SAME three scenarios to you but with a predicted 5 year stroke risk using a risk assessment derived from the European Carotid Surgery Trial (ECST). The data which this 5 year stroke risk has been calculated is from 1999 and we anticipate that improvements in medical therapy mean that the stroke risk will be lower than this. However, the draft 2012 National clinical guideline for stroke from the Royal College of Physicians recommends the use of this risk table as an adjunct to decision making regarding carotid surgery.

As before, we ask you to assume an identical baseline medical co-morbid status, a life expectancy of > 5 years, that patients are surgically fit and have a contralateral internal carotid stenosis of <20%. Additionally, we ask you to assume that the patients show no strong preference and that your institution does not perform other procedures such as carotid stenting.

12.1.7. Web Page 7

Scenario One – predicted 5 year stroke risk 40-45%

A 79 year old male presents with persistent left arm weakness for two days with a 55% right internal carotid artery stenosis and an ulcerated plaque on Doppler ultrasound.

Best medical therapy Carotid endarterectomy Unsure

12.1.8. Web Page 8

Scenario Two – predicted 5 year stroke risk <10%

A 63 year old male presents with left amaurosis fugax three days ago with a 65% left internal carotid artery stenosis and a smooth plaque on Doppler ultrasound.

Best medical therapy Carotid endarterectomy Unsure

12.1.9. Web Page 9

Scenario Three – predicted 5 year stroke risk 20-25%

A 76 year old female presents with a transient ischaemic attack affecting her right arm one week ago. Doppler ultrasound reveals a 60% left internal carotid artery stenosis and an ulcerated plaque.

Best medical therapy Carotid endarterectomy Unsure

12.1.10. Web Page 10

Did you find the introduction of a five year predicted stroke risk useful?

Yes No

If not, why?

12.1.11. Web Page 11

Many thanks for your time and co-operation with this survey.

B Dharmarajah, A Thapar, A H Davies

Section of Vascular Surgery

Imperial College, London

Contact:

Brahman Dharmarajah

Clinical Research Fellow

4 North

Charing Cross Hospital

Fulham Palace Road

London W6 8RF

Email – b.dharmarajah@imperial.ac.uk

12.2. Scientific Publications

Scientific publications related to the thesis

Dharmarajah B, Thapar A, Salem J, Lane TRA, Leen ELS, Davies AH. Impact of risk scoring on decision making in symptomatic moderate carotid atherosclerosis: A UK survey of stroke physicians and vascular surgeons. British Journal of Surgery. 2014 April;101:475-480. DOI: 10·1002/bjs.9461

Dharmarajah B, Sounderajah V, Rowland SP, Leen ELS, Davies AH. Aging techniques for deep vein thrombosis; a systematic review. Phlebology. 2015 March;30:77-84. DOI: 10.1177/0268355514528691

Dharmarajah B, Thapar A, Kasivisvanathan V, Leen ELS, Davies AH. Sonothrombolysis – A non-invasive method of thrombus dissolution using microbubble augmented ultrasound. International Angiology; 2013 October; 32 (Suppl. 1 to issue No. 5): 108-109 (Abstract publication)

Dharmarajah B, Thapar A, Kasivisvanathan V, Leen ELS, Davies AH. Sonothrombolysis – A non-invasive method of thrombus dissolution using microbubble augmented ultrasound. Phlebology; 2013; 28: 332 (Abstract publication)

Dharmarajah B, McKinnon TA, Keravnou C, Averkiou MA, ELS Leen, Davies AH. Contrast-Enhanced Ultrasound for Thrombus Dissolution in an In Vitro Model of Acute Deep Venous Thrombosis. Journal of Vascular Surgery; Venous and Lymphatic Disorders. 2015 Jan;3(1):121. DOI: http://dx.doi.org/10.1016/j.jvsv.2014.10.017 (Abstract publication)

Thapar A, Zheng Y, **Dharmarajah B**, Averkiou M, Shalhoub J, Davies AH, Leen ELS. Assessment of carotid plaque perfusion and ulceration with dynamic contrast enhanced ultrasound. International Journal of Stroke; 2012 Dec; 7 (Suppl. s2): 60 (Abstract publication)

Further Carotid and Deep Venous publications unrelated to the thesis

Kasvisvanathan V, Thapar A, Shalhoub J, **Dharmarajah B**, Davies K, Davies A H. Outcomes following intervention for post-radiotherapy carotid stenosis. Journal of Vascular Surgery. 2012 Oct;56(4): 1143-52

Thapar A, Shalhoub J, **Dharmarajah B**, Davies AH. Should we stop testing for asymptomatic carotid atherosclerosis? Journal of Neurointerventional Surgery. 2013 Mar 1;5(2):94-6.

Dharmarajah B, Lane TRA, Moore HM, Neumann HM, Rabe E, Wittens CH, Davies AH. The Future of Phlebology in Europe. Phlebology. 2014 May;29(Suppl 1):180-185

Rowland SP, **Dharmarajah B**, Moore HM, Dharmarajah KL, Davies AH. Major venous injuries in paediatric trauma: Systematic review of injuries and management. Journal of Trauma and Acute Care Surgery, 2014 Aug; 72(2):356-63. doi: 10.1097/TA.0000000000000312.

Mandavia R, Qureshi M, **Dharmarajah B**, Davies AH. Safety of carotid intervention following thrombolysis in acute ischaemic stroke. European Journal of Vascular and Endovascular Surgery. 2014 Nov;48(5):505-512. doi: 10.1016/j.ejvs.2014.08.012. Epub 2014 Sep 10.

Seager MJ, **Dharmarajah B**, Davies EB, Davies AH, Franklin IJ. The use of functional imaging in the diagnosis of carotid patch infection. Vascular. 2015 Oct;23(5):542-4. doi: 10.1177/1708538114560605. Epub 2014 Nov 17.

Rowland SP, **Dharmarajah B**, Moore HM, Lane TRA, Cousins J, Ahmed AR, Davies AH. IVC filters for prevention of venous thromboembolism in obese patients undergoing bariatric surgery: A systematic review. Annals of Surgery. 2015 Jan;261(1):35-45. doi: 10.1097/SLA.0000000000000621

Mandavia R, **Dharmarajah B**, Qureshi M, Davies AH. The role of cost-effectiveness for vascular surgery service provision in the United Kingdom. Journal of Vascular Surgery. 2015 May;61(5):1331-1339. doi: 10.1016/j.jvs.2015.01.034.

Seager MJ, Bussutiil A, **Dharmarajah B**, Davies AH. Editor's Choice - A systematic review of endovenous stenting in chronic venous disease secondary to iliac vein obstruction. European Journal of Vascular and Endovascular Surgery, 2016 Jan; 51(1): 100-120. doi: 10.1016/j.ejvs.2015.09.002. Epub 2015 Oct 10.

Cheung WK, Williams KJ, Chritensen-Jefferies K, **Dharmarajah B**, Eckersley RJ, Davies AH, Tang MX. A temporal and spatial analysis approach for automated segmentation of microbubble signals in contrast enhanced ultrasound images – application to quantification of human lower limb perfusion. Ultrasound Med Biol. 2017 Jul 7. pii: S0301-5629(17)30244-2. doi: 10.1016/j.ultrasmedbio.2017.05.021. [Epub ahead of print]

Sung Y, Spagou K, Kafeza M, Kyriakides, **Dharmarajah B**, Diaz JA, Wakefield T, Holmes E, Davies AH. Deep vein thrombosis exhibits characteristic serum and vein wall metabolic phenotypes in the inferior vena cava ligation mouse model. Revisions submitted to Thrombosis and Haemostasis, May 2017

12.3. Scientific Presentations (Selected)

Sonothrombolysis – A non-invasive method of thrombus dissolution using microbubble augmented ultrasound. **Dharmarajah B**, Thapar A, Kasivisvanathan V, Leen ELS, Davies AH. XVII World Meeting of the International Union of Phlebology, Boston, USA, September 2013. *Top 3 Electronic Abstract Score – Selected for Oral Prize Session

Decision making in symptomatic moderate carotid atherosclerosis: A survey of UK Vascular Surgeons and Stroke Physicians. **Dharmarajah B**, Thapar A, Salem J, Lane TRA, Leen ELS, Davies AH. Annual Meeting of the Society of Academic & Research Surgery (SARS), Cambridge, UK, January 2014

Contrast Enhanced Ultrasound for Thrombus Dissolution In An In-vitro Model Of Acute Deep Vein Thrombosis. **Dharmarajah B**, McKinnon TA, Keravnou C, Averkiou M, Laffan MA, Leen ELS, Davies AH. 27th Annual Meeting of The American Venous Forum (AVF), Palm Springs, USA, February 2015 *Awarded AVF Annual Meeting Best Paper Prize

Identification of the Vulnerable Carotid Plaque using Dynamic Contrast Enhanced Ultrasound. **Dharmarajah B**, Averkiou M, Christofides D, Thapar A, Davies AH, Leen ELS. Radiological Society of North America (RSNA) 101st Scientific Assembly and Annual Meeting, Chicago, USA, November 2015

Microbubble augmented ultrasound thrombolysis of deep vein thrombosis in an in-vitro model. **Dharmarajah B**, McKinnon TA, Keravnou C, Averkiou M, Laffan MA, Leen ELS, Davies AH. Radiological Society of North America (RSNA) 101st Scientific Assembly and Annual Meeting, Chicago, USA, November 2015

Ageing deep vein thrombosis. Dharmarajah B, Davies AH. 38th Charing Cross International Vascular Symposium 2016, London, U.K., April 2016 *Invited oral presentation

12.4. Grants & Prizes awarded

Grants Awarded as Main Applicant

Graham-Dixon Charitable Trust. Ageing deep vein thrombosis – An in-vivo study of ultrasound shear wave Elastography for the evaluation of thrombus age. £5754 2014-2015

The Royal Society of Medicine Venous Forum Pump Priming Grant 2014. Ageing Deep Vein Thrombosis – An in-vivo study of Ultrasound Shearwave Elastography for the evaluation of thrombus age £5000 2014-2015Graham-Dixon Charitable Trust.

Sonothrombolysis – An in-vivo study of thrombus dissolution using contrast enhanced ultrasound. £6000 2013-2014

European Venous Forum Pump Priming Grant. Sonothrombolysis – A novel therapy for thrombus dissolution using contrast enhanced ultrasound. €15000 2012-2013

Graham-Dixon Charitable Trust. Sonothrombolysis – A novel therapy for thrombus dissolution using contrast enhanced ultrasound. £5030 2012-2013

The Royal Society of Medicine Venous Forum Travelling Fellowship Grant 2012-2013. Continuous Flow Models of Deep Vein Thrombosis. Conrad Jobst Vascular Research Laboratory, University of Michigan Medical School. £1000 2012-2013

Association of Surgeons in Training (ASiT) Covidien Travelling Fellowship Grant Runner-up prize 2012-2013. Continuous Flow Models of Deep Vein Thrombosis.

Conrad Jobst Vascular Research Laboratory, University of Michigan Medical School. £1000 2012-2013

European Society for Vascular Surgery Congress Travel Grant. European Society for Vascular Surgery XXVI Annual Meeting, Bologna, Italy. €200 2012

Prizes

Top 3 Electronic Abstract Presentation – Electronic Abstract Poster Session, XVII World Meeting of the International Union of Phlebology, Boston, USA, 2013

Graham-Dixon Prize for Surgery 2014 – The Graham-Dixon Charitable Trust, Surrey, United Kingdom, 2014 (£500 awarded)

3rd Place Royal Society of Medicine Young Trainee of the Year – Representing the RSM Venous Forum at the Royal Society of Medicine Wesleyan Young Trainee of the Year Final, London, November 2014 (£500 & One Year's membership to the RSM awarded)

Best Paper Award – American Venous Forum 27th Annual Meeting, Palm Springs, USA, 2015

13. REFERENCES

1. Gramiak R, Shah PM. Echocardiography of the aortic root. Invest Radiol. 1968;3(5):356-66. Epub 1968/09/01.
2. Stewart MJ. Contrast echocardiography. Heart. 2003;89(3):342-8. Epub 2003/02/20.
3. Kerut EK, Norfleet WT, Plotnick GD, Giles TD. Patent foramen ovale: a review of associated conditions and the impact of physiological size. J Am Coll Cardiol. 2001;38(3):613-23. Epub 2001/08/31.
4. Stride E, Saffari N. Microbubble ultrasound contrast agents: a review. Proceedings of the Institution of Mechanical Engineers Part H, Journal of engineering in medicine. 2003;217(6):429-47. Epub 2004/01/02.
5. Stride E. Physical principles of microbubbles for ultrasound imaging and therapy. Cerebrovasc Dis. 2009;27 Suppl 2:1-13. Epub 2009/04/25.
6. Cosgrove D. Ultrasound contrast agents: an overview. European journal of radiology. 2006;60(3):324-30. Epub 2006/08/30.
7. Dijkmans PA, Juffermans LJ, Musters RJ, van Wamel A, ten Cate FJ, van Gilst W, et al. Microbubbles and ultrasound: from diagnosis to therapy. European journal of echocardiography : the journal of the Working Group on Echocardiography of the European Society of Cardiology. 2004;5(4):245-56. Epub 2004/06/29.
8. Schneider M, Arditi M, Barrau MB, Brochot J, Broillet A, Ventrone R, et al. BR1: a new ultrasonographic contrast agent based on sulfur hexafluoride-filled microbubbles. Invest Radiol. 1995;30(8):451-7. Epub 1995/08/01.
9. Morel DR, Schwieger I, Hohn L, Terrettaz J, Llull JB, Cornioley YA, et al. Human pharmacokinetics and safety evaluation of SonoVue, a new contrast agent for ultrasound imaging. Invest Radiol. 2000;35(1):80-5. Epub 2000/01/19.
10. EMEA. European Medicines Agency. SonoVue. European public assessment report. . Available from www.emea.eu.int/humandocs/pdfs/EPAR/sonvue/005301en1.pdf; 2001.
11. EMEA. European Medicines Agency. Public statement on SonoVue. New contraindication in patients with heart disease. Restriction of use in non-cardiac imaging. . Available from wwwemeaeuint/pdfs/human/press/pus/021204enpdf. 2002.
12. EMEA. European Medicines Agency. Press release. EMEA committee for Medical Products for Human Use. July 27-29. Available from wwwemeaeuint/pdfs/human/press/pr/2155004enpdf. 2004.
13. Piscaglia F, Bolondi L. The safety of Sonovue in abdominal applications: retrospective analysis of 23188 investigations. Ultrasound Med Biol. 2006;32(9):1369-75. Epub 2006/09/13.
14. NICE. SonoVue (sulphur hexafluride microbubbles) - contrast agent for contrast-enhanced ultrasound imaing of the liver. National Institute for Health and Clincal Exellence. 2012;DG5.
15. Kobayashi N, Yasu T, Yamada S, Kudo N, Kuroki M, Kawakami M, et al. Endothelial cell injury in venule and capillary induced by contrast ultrasonography. Ultrasound Med Biol. 2002;28(7):949-56. Epub 2002/09/05.
16. Claudon M, Cosgrove D, Albrecht T, Bolondi L, Bosio M, Calliada F, et al. Guidelines and good clinical practice recommendations for contrast enhanced ultrasound (CEUS) - update 2008. Ultraschall Med. 2008;29(1):28-44. Epub 2008/02/14.
17. Claudon M, Dietrich CF, Choi BI, Cosgrove DO, Kudo M, Nolsoe CP, et al. Guidelines and good clinical practice recommendations for Contrast Enhanced Ultrasound (CEUS) in the liver - update 2012: A WFUMB-EFSUMB initiative in cooperation with representatives of AFSUMB, AIUM, ASUM, FLAUS and ICUS. Ultrasound Med Biol. 2013;39(2):187-210. Epub 2012/11/10.
18. Eisenhauer EA, Therasse P, Bogaerts J, Schwartz LH, Sargent D, Ford R, et al. New response evaluation criteria in solid tumours: revised RECIST guideline (version 1.1). Eur J Cancer. 2009;45(2):228-47. Epub 2008/12/23.

19. Lassau N, Chebil M, Chami L, Bidault S, Girard E, Roche A. Dynamic contrast-enhanced ultrasonography (DCE-US): a new tool for the early evaluation of antiangiogenic treatment. Target Oncol. 2010;5(1):53-8. Epub 2010/04/10.
20. Lassau N, Koscielny S, Albiges L, Chami L, Benatsou B, Chebil M, et al. Metastatic renal cell carcinoma treated with sunitinib: early evaluation of treatment response using dynamic contrast-enhanced ultrasonography. Clin Cancer Res. 2010;16(4):1216-25. Epub 2010/02/11.
21. Lassau N, Koscielny S, Chami L, Chebil M, Benatsou B, Roche A, et al. Advanced hepatocellular carcinoma: early evaluation of response to bevacizumab therapy at dynamic contrast-enhanced US with quantification--preliminary results. Radiology. 2011;258(1):291-300. Epub 2010/10/29.
22. Leen E, Averkiou M, Arditi M, Burns P, Bokor D, Gauthier T, et al. Dynamic contrast enhanced ultrasound assessment of the vascular effects of novel therapeutics in early stage trials. European radiology. 2012;22(7):1442-50. Epub 2012/02/04.
23. Piscaglia F, Nolsoe C, Dietrich CF, Cosgrove DO, Gilja OH, Bachmann Nielsen M, et al. The EFSUMB Guidelines and Recommendations on the Clinical Practice of Contrast Enhanced Ultrasound (CEUS): update 2011 on non-hepatic applications. Ultraschall Med. 2012;33(1):33-59. Epub 2011/08/30.
24. Olin JW, Kaufman JA, Bluemke DA, Bonow RO, Gerhard MD, Jaff MR, et al. Atherosclerotic Vascular Disease Conference: Writing Group IV: imaging. Circulation. 2004;109(21):2626-33. Epub 2004/06/03.
25. Hartshorne TC, McCollum CN, Earnshaw JJ, Morris J, Nasim A. Ultrasound measurement of aortic diameter in a national screening programme. European journal of vascular and endovascular surgery : the official journal of the European Society for Vascular Surgery. 2011;42(2):195-9. Epub 2011/03/29.
26. Darwood R, Earnshaw JJ, Turton G, Shaw E, Whyman M, Poskitt K, et al. Twenty-year review of abdominal aortic aneurysm screening in men in the county of Gloucestershire, United Kingdom. Journal of vascular surgery : official publication, the Society for Vascular Surgery [and] International Society for Cardiovascular Surgery, North American Chapter. 2012;56(1):8-13. Epub 2012/04/17.
27. Glover MJ, Kim LG, Sweeting MJ, Thompson SG, Buxton MJ. Cost-effectiveness of the National Health Service abdominal aortic aneurysm screening programme in England. The British journal of surgery. 2014;101(8):976-82. Epub 2014/05/28.
28. Catalano O, Lobianco R, Cusati B, Siani A. Contrast-enhanced sonography for diagnosis of ruptured abdominal aortic aneurysm. AJR American journal of roentgenology. 2005;184(2):423-7. Epub 2005/01/27.
29. Powell JT, Sweeting MJ, Thompson MM, Ashleigh R, Bell R, Gomes M, et al. Endovascular or open repair strategy for ruptured abdominal aortic aneurysm: 30 day outcomes from IMPROVE randomised trial. BMJ. 2014;348:f7661. Epub 2014/01/15.
30. Greenhalgh RM, Brown LC, Kwong GP, Powell JT, Thompson SG. Comparison of endovascular aneurysm repair with open repair in patients with abdominal aortic aneurysm (EVAR trial 1), 30-day operative mortality results: randomised controlled trial. Lancet. 2004;364(9437):843-8. Epub 2004/09/08.
31. Endovascular aneurysm repair versus open repair in patients with abdominal aortic aneurysm (EVAR trial 1): randomised controlled trial. Lancet. 2005;365(9478):2179-86. Epub 2005/06/28.
32. Endovascular aneurysm repair and outcome in patients unfit for open repair of abdominal aortic aneurysm (EVAR trial 2): randomised controlled trial. Lancet. 2005;365(9478):2187-92. Epub 2005/06/28.
33. NICE. TA 167 Endovascular stent-grafts for the treatment of abdominal aortic aneurysms. National Institute for Health and Clincal Excellence. 2009.
34. Greenhalgh RM, Brown LC, Powell JT, Thompson SG, Epstein D, Sculpher MJ. Endovascular versus open repair of abdominal aortic aneurysm. The New England journal of medicine. 2010;362(20):1863-71. Epub 2010/04/13.
35. Veith FJ, Baum RA, Ohki T, Amor M, Adiseshiah M, Blankensteijn JD, et al. Nature and significance of endoleaks and endotension: summary of opinions expressed at an international conference.

Journal of vascular surgery : official publication, the Society for Vascular Surgery [and] International Society for Cardiovascular Surgery, North American Chapter. 2002;35(5):1029-35. Epub 2002/05/22.
36. Staub D, Partovi S, Imfeld S, Uthoff H, Baldi T, Aschwanden M, et al. Novel applications of contrast-enhanced ultrasound imaging in vascular medicine. VASA Zeitschrift fur Gefasskrankheiten. 2013;42(1):17-31. Epub 2013/02/07.
37. Mirza TA, Karthikesalingam A, Jackson D, Walsh SR, Holt PJ, Hayes PD, et al. Duplex ultrasound and contrast-enhanced ultrasound versus computed tomography for the detection of endoleak after EVAR: systematic review and bivariate meta-analysis. European journal of vascular and endovascular surgery : the official journal of the European Society for Vascular Surgery. 2010;39(4):418-28. Epub 2010/02/04.
38. Napoli V, Bargellini I, Sardella SG, Petruzzi P, Cioni R, Vignali C, et al. Abdominal aortic aneurysm: contrast-enhanced US for missed endoleaks after endoluminal repair. Radiology. 2004;233(1):217-25. Epub 2004/09/30.
39. Walsh SR, Tang TY, Boyle JR. Renal consequences of endovascular abdominal aortic aneurysm repair. Journal of endovascular therapy : an official journal of the International Society of Endovascular Specialists. 2008;15(1):73-82. Epub 2008/02/08.
40. Bates SM, Jaeschke R, Stevens SM, Goodacre S, Wells PS, Stevenson MD, et al. Diagnosis of DVT: Antithrombotic Therapy and Prevention of Thrombosis, 9th ed: American College of Chest Physicians Evidence-Based Clinical Practice Guidelines. Chest. 2012;141(2 Suppl):e351S-418S. Epub 2012/02/15.
41. Goodacre S, Sampson F, Stevenson M, Wailoo A, Sutton A, Thomas S, et al. Measurement of the clinical and cost-effectiveness of non-invasive diagnostic testing strategies for deep vein thrombosis. Health Technol Assess. 2006;10(15):1-168, iii-iv. Epub 2006/05/19.
42. Smith A, Parker P, Byass O, Chiu K. Contrast sonovenography - Is this the answer to complex deep vein thrombosis imaging? Ultrasound. 2016;24(1):17-22. Epub 2016/07/20.
43. Guenther F, Herr N, Mauler M, Witsch T, Roming F, Hein L, et al. Contrast ultrasound for the quantification of deep vein thrombosis in living mice: effects of enoxaparin and P2Y12 receptor inhibition. Journal of thrombosis and haemostasis : JTH. 2013;11(6):1154-62. Epub 2013/04/05.
44. Rudarakanchana N, Halliday AW, Kamugasha D, Grant R, Waton S, Horrocks M, et al. Current practice of carotid endarterectomy in the UK. The British journal of surgery. 2012;99(2):209-16. Epub 2011/12/23.
45. Beneficial effect of carotid endarterectomy in symptomatic patients with high-grade carotid stenosis. North American Symptomatic Carotid Endarterectomy Trial Collaborators. The New England journal of medicine. 1991;325(7):445-53. Epub 1991/08/15.
46. MRC European Carotid Surgery Trial: interim results for symptomatic patients with severe (70-99%) or with mild (0-29%) carotid stenosis. European Carotid Surgery Trialists' Collaborative Group. Lancet. 1991;337(8752):1235-43. Epub 1991/05/25.
47. Rothwell PM, Eliasziw M, Gutnikov SA, Fox AJ, Taylor DW, Mayberg MR, et al. Analysis of pooled data from the randomised controlled trials of endarterectomy for symptomatic carotid stenosis. Lancet. 2003;361(9352):107-16. Epub 2003/01/18.
48. Abbott AL. Medical (nonsurgical) intervention alone is now best for prevention of stroke associated with asymptomatic severe carotid stenosis: results of a systematic review and analysis. Stroke. 2009;40(10):e573-83. Epub 2009/08/22.
49. Fell G, Phillips DJ, Chikos PM, Harley JD, Thiele BL, Strandness DE, Jr. Ultrasonic duplex scanning for disease of the carotid artery. Circulation. 1981;64(6):1191-5. Epub 1981/12/01.
50. Kirsch JD, Wagner LR, James EM, Charboneau JW, Nichols DA, Meyer FB, et al. Carotid artery occlusion: positive predictive value of duplex sonography compared with arteriography. Journal of vascular surgery : official publication, the Society for Vascular Surgery [and] International Society for Cardiovascular Surgery, North American Chapter. 1994;19(4):642-9. Epub 1994/04/01.

51. Clevert DA, Sommer WH, Zengel P, Helck A, Reiser M. Imaging of carotid arterial diseases with contrast-enhanced ultrasound (CEUS). European journal of radiology. 2011;80(1):68-76. Epub 2011/03/01.
52. van den Oord SC, ten Kate GL, Akkus Z, Renaud G, Sijbrands EJ, ten Cate FJ, et al. Assessment of subclinical atherosclerosis using contrast-enhanced ultrasound. European heart journal cardiovascular Imaging. 2013;14(1):56-61. Epub 2012/05/31.
53. Mantese VA, Timaran CH, Chiu D, Begg RJ, Brott TG. The Carotid Revascularization Endarterectomy versus Stenting Trial (CREST): stenting versus carotid endarterectomy for carotid disease. Stroke. 2010;41(10 Suppl):S31-4. Epub 2010/10/13.
54. Virmani R, Burke AP, Farb A, Kolodgie FD. Pathology of the vulnerable plaque. J Am Coll Cardiol. 2006;47(8 Suppl):C13-8. Epub 2006/04/25.
55. Mofidi R, Crotty TB, McCarthy P, Sheehan SJ, Mehigan D, Keaveny TV. Association between plaque instability, angiogenesis and symptomatic carotid occlusive disease. The British journal of surgery. 2001;88(7):945-50. Epub 2001/07/10.
56. McCarthy MJ, Loftus IM, Thompson MM, Jones L, London NJ, Bell PR, et al. Angiogenesis and the atherosclerotic carotid plaque: an association between symptomatology and plaque morphology. Journal of vascular surgery : official publication, the Society for Vascular Surgery [and] International Society for Cardiovascular Surgery, North American Chapter. 1999;30(2):261-8. Epub 1999/08/07.
57. Doyle B, Caplice N. Plaque neovascularization and antiangiogenic therapy for atherosclerosis. J Am Coll Cardiol. 2007;49(21):2073-80. Epub 2007/05/29.
58. Vicenzini E, Giannoni MF, Puccinelli F, Ricciardi MC, Altieri M, Di Piero V, et al. Detection of carotid adventitial vasa vasorum and plaque vascularization with ultrasound cadence contrast pulse sequencing technique and echo-contrast agent. Stroke. 2007;38(10):2841-3. Epub 2007/09/01.
59. Huang PT, Huang FG, Zou CP, Sun HY, Tian XQ, Yang Y, et al. Contrast-enhanced sonographic characteristics of neovascularization in carotid atherosclerotic plaques. Journal of clinical ultrasound : JCU. 2008;36(6):346-51. Epub 2008/02/21.
60. Staub D, Partovi S, Schinkel AF, Coll B, Uthoff H, Aschwanden M, et al. Correlation of Carotid Artery Atherosclerotic Lesion Echogenicity and Severity at Standard US with Intraplaque Neovascularization Detected at Contrast-enhanced US. Radiology. 2010. Epub 2010/10/26.
61. Staub D, Patel MB, Tibrewala A, Ludden D, Johnson M, Espinosa P, et al. Vasa vasorum and plaque neovascularization on contrast-enhanced carotid ultrasound imaging correlates with cardiovascular disease and past cardiovascular events. Stroke. 2010;41(1):41-7. Epub 2009/11/17.
62. Hoogi A, Adam D, Hoffman A, Kerner H, Reisner S, Gaitini D. Carotid plaque vulnerability: quantification of neovascularization on contrast-enhanced ultrasound with histopathologic correlation. AJR American journal of roentgenology. 2011;196(2):431-6. Epub 2011/01/25.
63. Huang PT, Chen CC, Aronow WS, Wang XT, Nair CK, Xue NY, et al. Assessment of neovascularization within carotid plaques in patients with ischemic stroke. World J Cardiol. 2010;2(4):89-97. Epub 2010/12/17.
64. Owen DR, Shalhoub J, Miller S, Gauthier T, Doryforou O, Davies AH, et al. Inflammation within carotid atherosclerotic plaque: assessment with late-phase contrast-enhanced US. Radiology. 2010;255(2):638-44. Epub 2010/04/24.
65. Shalhoub J, Monaco C, Owen DR, Gauthier T, Thapar A, Leen EL, et al. Late-phase contrast-enhanced ultrasound reflects biological features of instability in human carotid atherosclerosis. Stroke. 2011;42(12):3634-6. Epub 2011/10/01.
66. Thapar A, Shalhoub J, Averkiou M, Mannaris C, Davies AH, Leen EL. Dose-Dependent Artifact in the Far Wall of the Carotid Artery at Dynamic Contrast-enhanced US. Radiology. 2011. Epub 2011/12/14.
67. Fowkes FJ, Price JF, Fowkes FG. Incidence of diagnosed deep vein thrombosis in the general population: systematic review. European journal of vascular and endovascular surgery : the official journal of the European Society for Vascular Surgery. 2003;25(1):1-5. Epub 2003/01/15.

68. NICE. Venous thromboembolism: reducing the risk. National Institute for Health and Clincal Exellence. 2010;CG92.
69. Kahn SR, Partsch H, Vedantham S, Prandoni P, Kearon C. Definition of post-thrombotic syndrome of the leg for use in clinical investigations: a recommendation for standardization. Journal of thrombosis and haemostasis : JTH. 2009;7(5):879-83. Epub 2009/01/30.
70. Kahn SR. The post-thrombotic syndrome: progress and pitfalls. British journal of haematology. 2006;134(4):357-65. Epub 2006/07/11.
71. Kahn SR, Shbaklo H, Lamping DL, Holcroft CA, Shrier I, Miron MJ, et al. Determinants of health-related quality of life during the 2 years following deep vein thrombosis. Journal of thrombosis and haemostasis : JTH. 2008;6(7):1105-12. Epub 2008/05/10.
72. Watson LI, Armon MP. Thrombolysis for acute deep vein thrombosis. Cochrane Database Syst Rev. 2004(4):CD002783. Epub 2004/10/21.
73. Hirsh J, Guyatt G, Albers GW, Harrington R, Schunemann HJ. Executive summary: American College of Chest Physicians Evidence-Based Clinical Practice Guidelines (8th Edition). Chest. 2008;133(6 Suppl):71S-109S. Epub 2008/07/24.
74. Prandoni P, Lensing AW, Prins MH, Frulla M, Marchiori A, Bernardi E, et al. Below-knee elastic compression stockings to prevent the post-thrombotic syndrome: a randomized, controlled trial. Annals of internal medicine. 2004;141(4):249-56. Epub 2004/08/18.
75. Brandjes DP, Buller HR, Heijboer H, Huisman MV, de Rijk M, Jagt H, et al. Randomised trial of effect of compression stockings in patients with symptomatic proximal-vein thrombosis. Lancet. 1997;349(9054):759-62. Epub 1997/03/15.
76. Kahn SR, Elman E, Rodger MA, Wells PS. Use of elastic compression stockings after deep venous thrombosis: a comparison of practices and perceptions of thrombosis physicians and patients. Journal of thrombosis and haemostasis : JTH. 2003;1(3):500-6. Epub 2003/07/23.
77. Augustinos P, Ouriel K. Invasive approaches to treatment of venous thromboembolism. Circulation. 2004;110(9 Suppl 1):I27-34. Epub 2004/09/02.
78. Casey ET, Murad MH, Zumaeta-Garcia M, Elamin MB, Shi Q, Erwin PJ, et al. Treatment of acute iliofemoral deep vein thrombosis. Journal of vascular surgery : official publication, the Society for Vascular Surgery [and] International Society for Cardiovascular Surgery, North American Chapter. 2012;55(5):1463-73. Epub 2012/03/24.
79. Chinsakchai K, Ten Duis K, Moll FL, de Borst GJ. Trends in management of phlegmasia cerulea dolens. Vascular and endovascular surgery. 2011;45(1):5-14. Epub 2011/01/05.
80. Meissner MH. Rationale and indications for aggressive early thrombus removal. Phlebology. 2012;27 Suppl 1:78-84. Epub 2012/02/15.
81. Enden T, Haig Y, Klow NE, Slagsvold CE, Sandvik L, Ghanima W, et al. Long-term outcome after additional catheter-directed thrombolysis versus standard treatment for acute iliofemoral deep vein thrombosis (the CaVenT study): a randomised controlled trial. Lancet. 2012;379(9810):31-8. Epub 2011/12/17.
82. Kasirajan K, Gray B, Ouriel K. Percutaneous AngioJet thrombectomy in the management of extensive deep venous thrombosis. J Vasc Interv Radiol. 2001;12(2):179-85. Epub 2001/03/27.
83. Martinez Trabal JL, Comerota AJ, LaPorte FB, Kazanjian S, DiSalle R, Sepanski DM. The quantitative benefit of isolated, segmental, pharmacomechanical thrombolysis (ISPMT) for iliofemoral venous thrombosis. Journal of vascular surgery : official publication, the Society for Vascular Surgery [and] International Society for Cardiovascular Surgery, North American Chapter. 2008;48(6):1532-7. Epub 2008/09/23.
84. Bush RL, Lin PH, Bates JT, Mureebe L, Zhou W, Lumsden AB. Pharmacomechanical thrombectomy for treatment of symptomatic lower extremity deep venous thrombosis: safety and feasibility study. Journal of vascular surgery : official publication, the Society for Vascular Surgery [and] International Society for Cardiovascular Surgery, North American Chapter. 2004;40(5):965-70. Epub 2004/11/24.

85. Lin PH, Zhou W, Dardik A, Mussa F, Kougias P, Hedayati N, et al. Catheter-direct thrombolysis versus pharmacomechanical thrombectomy for treatment of symptomatic lower extremity deep venous thrombosis. American journal of surgery. 2006;192(6):782-8. Epub 2006/12/13.
86. O'Sullivan GJ, Lohan DG, Gough N, Cronin CG, Kee ST. Pharmacomechanical thrombectomy of acute deep vein thrombosis with the Trellis-8 isolated thrombolysis catheter. J Vasc Interv Radiol. 2007;18(6):715-24. Epub 2007/06/01.
87. Francis CW, Blinc A, Lee S, Cox C. Ultrasound accelerates transport of recombinant tissue plasminogen activator into clots. Ultrasound Med Biol. 1995;21(3):419-24. Epub 1995/01/01.
88. Grommes J, Strijkers R, Greiner A, Mahnken AH, Wittens CH. Safety and feasibility of ultrasound-accelerated catheter-directed thrombolysis in deep vein thrombosis. European journal of vascular and endovascular surgery : the official journal of the European Society for Vascular Surgery. 2011;41(4):526-32. Epub 2011/01/25.
89. Comerota AJ. The ATTRACT trial: rationale for early intervention for iliofemoral DVT. Perspectives in vascular surgery and endovascular therapy. 2009;21(4):221-4; quiz 4-5. Epub 2010/01/06.
90. Malgor RD, Gasparis AP. Pharmaco-mechanical thrombectomy for early thrombus removal. Phlebology. 2012;27 Suppl 1:155-62. Epub 2012/02/15.
91. Wells PS, Anderson DR, Rodger M, Forgie M, Kearon C, Dreyer J, et al. Evaluation of D-dimer in the diagnosis of suspected deep-vein thrombosis. The New England journal of medicine. 2003;349(13):1227-35. Epub 2003/09/26.
92. Wells PS, Anderson DR, Bormanis J, Guy F, Mitchell M, Gray L, et al. Value of assessment of pretest probability of deep-vein thrombosis in clinical management. Lancet. 1997;350(9094):1795-8. Epub 1998/01/15.
93. Wells PS, Hirsh J, Anderson DR, Lensing AW, Foster G, Kearon C, et al. Accuracy of clinical assessment of deep-vein thrombosis. Lancet. 1995;345(8961):1326-30. Epub 1995/05/27.
94. Venous Thromboembolic Diseases: The Management of Venous Thromboembolic Diseases and the Role of Thrombophilia Testing. London2012.
95. Cronan JJ, Leen V. Recurrent deep venous thrombosis: limitations of US. Radiology. 1989;170(3 Pt 1):739-42. Epub 1989/03/01.
96. Merli G. Diagnostic assessment of deep vein thrombosis and pulmonary embolism. The American journal of medicine. 2005;118 Suppl 8A:3S-12S. Epub 2005/08/30.
97. Kurklinsky AK, Kalsi H, Wysokinski WE, Mauck KF, Bhagra A, Havyer RD, et al. Fibrin d-dimer concentration, deep vein thrombosis symptom duration, and venous thrombus volume. Angiology. 2011;62(3):253-6. Epub 2010/09/14.
98. Chong LY, Fenu E, Stansby G, Hodgkinson S. Management of venous thromboembolic diseases and the role of thrombophilia testing: summary of NICE guidance. BMJ. 2012;344:e3979. Epub 2012/06/29.
99. Kearon C, Akl EA, Comerota AJ, Prandoni P, Bounameaux H, Goldhaber SZ, et al. Antithrombotic therapy for VTE disease: Antithrombotic Therapy and Prevention of Thrombosis, 9th ed: American College of Chest Physicians Evidence-Based Clinical Practice Guidelines. Chest. 2012;141(2 Suppl):e419S-94S. Epub 2012/02/15.
100. Bauersachs R, Berkowitz SD, Brenner B, Buller HR, Decousus H, Gallus AS, et al. Oral rivaroxaban for symptomatic venous thromboembolism. The New England journal of medicine. 2010;363(26):2499-510. Epub 2010/12/07.
101. Meissner MH, Gloviczki P, Comerota AJ, Dalsing MC, Eklof BG, Gillespie DL, et al. Early thrombus removal strategies for acute deep venous thrombosis: clinical practice guidelines of the Society for Vascular Surgery and the American Venous Forum. Journal of vascular surgery : official publication, the Society for Vascular Surgery [and] International Society for Cardiovascular Surgery, North American Chapter. 2012;55(5):1449-62. Epub 2012/04/04.
102. Baekgaard N, Foegh P, Wittens CH, Arnoldussen C. Thrombus age is ideally measured by history or MRV prior to thrombus removal. Phlebology. 2015;30(1 Suppl):20-6. Epub 2015/03/03.

103. Moher D, Liberati A, Tetzlaff J, Altman DG. Preferred reporting items for systematic reviews and meta-analyses: the PRISMA statement. BMJ. 2009;339:b2535. Epub 2009/07/23.
104. Whiting PF, Rutjes AW, Westwood ME, Mallett S, Deeks JJ, Reitsma JB, et al. QUADAS-2: a revised tool for the quality assessment of diagnostic accuracy studies. Annals of internal medicine. 2011;155(8):529-36. Epub 2011/10/19.
105. Diaz JA, Obi AT, Myers DD, Jr., Wrobleski SK, Henke PK, Mackman N, et al. Critical review of mouse models of venous thrombosis. Arterioscler Thromb Vasc Biol. 2012;32(3):556-62. Epub 2012/02/22.
106. Myers DD, Jr. Nonhuman primate models of thrombosis. Thromb Res. 2012;129 Suppl 2:S65-9. Epub 2012/03/14.
107. Dharmarajah B, Sounderajah V, Rowland S, Leen E, Davies A. Aging techniques for deep vein thrombosis: a systematic review. Phlebology. 2014. Epub 2014/03/29.
108. Parsons RE, Sigel B, Feleppa EJ, Golub RM, Kodama I, Loiacono LA, et al. Age determination of experimental venous thrombi by ultrasonic tissue characterization. Journal of vascular surgery : official publication, the Society for Vascular Surgery [and] International Society for Cardiovascular Surgery, North American Chapter. 1993;17(3):470-8. Epub 1993/03/01.
109. Fowlkes JB, Strieter RM, Downing LJ, Brown SL, Saluja A, Salles-Cunha S, et al. Ultrasound echogenicity in experimental venous thrombosis. Ultrasound Med Biol. 1998;24(8):1175-82. Epub 1998/12/02.
110. Kakkos SK, Stevens JM, Nicolaides AN, Kyriacou E, Pattichis CS, Geroulakos G, et al. Texture analysis of ultrasonic images of symptomatic carotid plaques can identify those plaques associated with ipsilateral embolic brain infarction. European journal of vascular and endovascular surgery : the official journal of the European Society for Vascular Surgery. 2007;33(4):422-9. Epub 2006/12/13.
111. Tegos TJ, Stavropoulos P, Sabetai MM, Khodabakhsh P, Sassano A, Nicolaides AN. Determinants of carotid plaque instability: echoicity versus heterogeneity. European journal of vascular and endovascular surgery : the official journal of the European Society for Vascular Surgery. 2001;22(1):22-30. Epub 2001/07/20.
112. Maria Fernanda Cassou-Birckholz CAE, Se´rgio Xavier Salles-Cunha, Ana Luiza Engelhorn, Cassiana Casagrande Zanoni, Carlos Jose´ Gosalan, Emerson Ribas, Ana Carolina Alves dos Santos Chociai, Camila Faversani Camargo. Assessment of Deep Venous Thrombosis by Grayscale Median Analysis of Ultrasound Images. Ultrasound Quarterly. 2011;27(1):1-7.
113. Emelianov SY, Chen X, O'Donnell M, Knipp B, Myers D, Wakefield TW, et al. Triplex ultrasound: elasticity imaging to age deep venous thrombosis. Ultrasound Med Biol. 2002;28(6):757-67. Epub 2002/07/13.
114. Geier B, Barbera L, Muth-Werthmann D, Siebers S, Ermert H, Philippou S, et al. Ultrasound elastography for the age determination of venous thrombi. Evaluation in an animal model of venous thrombosis. Thrombosis and haemostasis. 2005;93(2):368-74. Epub 2005/02/16.
115. Aglyamov S, Skovoroda AR, Rubin JM, O'Donnell M, Emelianov SY. Model-based reconstructive elasticity imaging of deep venous thrombosis. IEEE transactions on ultrasonics, ferroelectrics, and frequency control. 2004;51(5):521-31. Epub 2004/06/26.
116. Xie H, Kim K, Aglyamov SR, Emelianov SY, Chen X, O'Donnell M, et al. Staging deep venous thrombosis using ultrasound elasticity imaging: animal model. Ultrasound Med Biol. 2004;30(10):1385-96. Epub 2004/12/08.
117. Xie H, Kim K, Aglyamov SR, Emelianov SY, O'Donnell M, Weitzel WF, et al. Correspondence of ultrasound elasticity imaging to direct mechanical measurement in aging DVT in rats. Ultrasound Med Biol. 2005;31(10):1351-9. Epub 2005/10/15.
118. Rubin JM, Aglyamov SR, Wakefield TW, O'Donnell M, Emelianov SY. Clinical application of sonographic elasticity imaging for aging of deep venous thrombosis: preliminary findings. J Ultrasound Med. 2003;22(5):443-8. Epub 2003/05/20.

119. Rubin JM, Xie H, Kim K, Weitzel WF, Emelianov SY, Aglyamov SR, et al. Sonographic elasticity imaging of acute and chronic deep venous thrombosis in humans. J Ultrasound Med. 2006;25(9):1179-86. Epub 2006/08/25.
120. Itoh A, Ueno E, Tohno E, Kamma H, Takahashi H, Shiina T, et al. Breast disease: clinical application of US elastography for diagnosis. Radiology. 2006;239(2):341-50. Epub 2006/02/18.
121. Cochlin DL, Ganatra RH, Griffiths DF. Elastography in the detection of prostatic cancer. Clinical radiology. 2002;57(11):1014-20. Epub 2002/11/01.
122. Weitzel WF, Kim K, Rubin JM, Wiggins RC, Xie H, Chen X, et al. Feasibility of applying ultrasound strain imaging to detect renal transplant chronic allograft nephropathy. Kidney international. 2004;65(2):733-6. Epub 2004/01/14.
123. Fraquelli M, Rigamonti C, Casazza G, Conte D, Donato MF, Ronchi G, et al. Reproducibility of transient elastography in the evaluation of liver fibrosis in patients with chronic liver disease. Gut. 2007;56(7):968-73. Epub 2007/01/27.
124. Cosgrove D, Piscaglia F, Bamber J, Bojunga J, Correas JM, Gilja OH, et al. EFSUMB guidelines and recommendations on the clinical use of ultrasound elastography. Part 2: Clinical applications. Ultraschall Med. 2013;34(3):238-53. Epub 2013/04/23.
125. Gennisson JL, Deffieux T, Fink M, Tanter M. Ultrasound elastography: principles and techniques. Diagnostic and interventional imaging. 2013;94(5):487-95. Epub 2013/04/27.
126. Bamber J, Cosgrove D, Dietrich CF, Fromageau J, Bojunga J, Calliada F, et al. EFSUMB guidelines and recommendations on the clinical use of ultrasound elastography. Part 1: Basic principles and technology. Ultraschall Med. 2013;34(2):169-84. Epub 2013/04/06.
127. Orbell JH, Smith A, Burnand KG, Waltham M. Imaging of deep vein thrombosis. The British journal of surgery. 2008;95(2):137-46. Epub 2008/01/16.
128. Froehlich JB, Prince MR, Greenfield LJ, Downing LJ, Shah NL, Wakefield TW. "Bull's-eye" sign on gadolinium-enhanced magnetic resonance venography determines thrombus presence and age: a preliminary study. Journal of vascular surgery : official publication, the Society for Vascular Surgery [and] International Society for Cardiovascular Surgery, North American Chapter. 1997;26(5):809-16. Epub 1997/12/31.
129. Arnoldussen C, Strijkers R, Lambregts D, Lahaye M, de Graaf R, Wittens C. Feasibility of identifying deep vein thrombosis characteristics with contrast enhanced MR-Venography. Phlebology. 2014;29(1 suppl):119-24. Epub 2014/05/21.
130. Marckmann P, Skov L, Rossen K, Dupont A, Damholt MB, Heaf JG, et al. Nephrogenic systemic fibrosis: suspected causative role of gadodiamide used for contrast-enhanced magnetic resonance imaging. Journal of the American Society of Nephrology : JASN. 2006;17(9):2359-62. Epub 2006/08/04.
131. Moody AR. Magnetic resonance direct thrombus imaging. Journal of thrombosis and haemostasis : JTH. 2003;1(7):1403-9. Epub 2003/07/23.
132. Gomori JM, Grossman RI, Goldberg HI, Zimmerman RA, Bilaniuk LT. Intracranial hematomas: imaging by high-field MR. Radiology. 1985;157(1):87-93. Epub 1985/10/01.
133. Jansen CH, Perera D, Makowski MR, Wiethoff AJ, Phinikaridou A, Razavi RM, et al. Detection of intracoronary thrombus by magnetic resonance imaging in patients with acute myocardial infarction. Circulation. 2011;124(4):416-24. Epub 2011/07/13.
134. Corti R, Osende JI, Fayad ZA, Fallon JT, Fuster V, Mizsei G, et al. In vivo noninvasive detection and age definition of arterial thrombus by MRI. J Am Coll Cardiol. 2002;39(8):1366-73. Epub 2002/04/17.
135. Moody AR, Pollock JG, O'Connor AR, Bagnall M. Lower-limb deep venous thrombosis: direct MR imaging of the thrombus. Radiology. 1998;209(2):349-55. Epub 1998/11/10.
136. Westerbeek RE, Van Rooden CJ, Tan M, Van Gils AP, Kok S, De Bats MJ, et al. Magnetic resonance direct thrombus imaging of the evolution of acute deep vein thrombosis of the leg. Journal of thrombosis and haemostasis : JTH. 2008;6(7):1087-92. Epub 2008/04/25.

137. Phinikaridou A, Andia ME, Saha P, Modarai B, Smith A, Botnar RM. In vivo magnetization transfer and diffusion-weighted magnetic resonance imaging detects thrombus composition in a mouse model of deep vein thrombosis. Circulation Cardiovascular imaging. 2013;6(3):433-40. Epub 2013/04/09.
138. Saha P, Andia ME, Modarai B, Blume U, Humphries J, Patel AS, et al. Magnetic resonance T1 relaxation time of venous thrombus is determined by iron processing and predicts susceptibility to lysis. Circulation. 2013;128(7):729-36. Epub 2013/07/04.
139. Andia ME, Saha P, Jenkins J, Modarai B, Wiethoff AJ, Phinikaridou A, et al. Fibrin-targeted magnetic resonance imaging allows in vivo quantification of thrombus fibrin content and identifies thrombi amenable for thrombolysis. Arterioscler Thromb Vasc Biol. 2014;34(6):1193-8. Epub 2014/04/12.
140. Bates SM, Lister-James J, Julian JA, Taillefer R, Moyer BR, Ginsberg JS. Imaging characteristics of a novel technetium Tc 99m-labeled platelet glycoprotein IIb/IIIa receptor antagonist in patients With acute deep vein thrombosis or a history of deep vein thrombosis. Archives of internal medicine. 2003;163(4):452-6. Epub 2003/02/18.
141. Brighton T, Janssen J, Butler SP. Aging of acute deep vein thrombosis measured by radiolabeled 99mTc-rt-PA. Journal of nuclear medicine : official publication, Society of Nuclear Medicine. 2007;48(6):873-8. Epub 2007/05/17.
142. Karpiouk AB, Aglyamov SR, Mallidi S, Shah J, Scott WG, Rubin JM, et al. Combined ultrasound and photoacoustic imaging to detect and stage deep vein thrombosis: phantom and ex vivo studies. Journal of biomedical optics. 2008;13(5):054061. Epub 2008/11/22.
143. Karpiouk AB, Aglyamov SR, Mallidi S, Scott WG, Rubin JM, Emelianov SY. Combined ultrasonic and photoacoustic imaging to age deep vein thrombosis: Preliminary studies. Ultrason. 2005:403-6.
144. Tachibana K. Enhancement of fibrinolysis with ultrasound energy. J Vasc Interv Radiol. 1992;3(2):299-303. Epub 1992/05/01.
145. Francis CW, Onundarson PT, Carstensen EL, Blinc A, Meltzer RS, Schwarz K, et al. Enhancement of fibrinolysis in vitro by ultrasound. J Clin Invest. 1992;90(5):2063-8. Epub 1992/11/01.
146. Kawata H, Naya N, Takemoto Y, Uemura S, Nakajima T, Horii M, et al. Ultrasound accelerates thrombolysis of acutely induced platelet-rich thrombi similar to those in acute myocardial infarction. Circ J. 2007;71(10):1643-8. Epub 2007/09/27.
147. Maxwell AD, Owens G, Gurm HS, Ives K, Myers DD, Jr., Xu Z. Noninvasive treatment of deep venous thrombosis using pulsed ultrasound cavitation therapy (histotripsy) in a porcine model. J Vasc Interv Radiol. 2011;22(3):369-77. Epub 2011/01/05.
148. Nilsson AM, Odselius R, Roijer A, Olsson SB. Pro- and antifibrinolytic effects of ultrasound on streptokinase-induced thrombolysis. Ultrasound Med Biol. 1995;21(6):833-40. Epub 1995/01/01.
149. Maxwell L, Collecutt T, Gledhill M, Sharma S, Edgar S, Gavin JB. The augmentation of leucocyte adhesion to endothelium by therapeutic ultrasound. Ultrasound Med Biol. 1994;20(4):383-90. Epub 1994/01/01.
150. Riggs PN, Francis CW, Bartos SR, Penney DP. Ultrasound enhancement of rabbit femoral artery thrombolysis. Cardiovasc Surg. 1997;5(2):201-7. Epub 1997/04/01.
151. Rha JH, Saver JL. The impact of recanalization on ischemic stroke outcome: a meta-analysis. Stroke. 2007;38(3):967-73. Epub 2007/02/03.
152. Donnan GA, Fisher M, Macleod M, Davis SM. Stroke. Lancet. 2008;371(9624):1612-23. Epub 2008/05/13.
153. Pfaffenberger S, Devcic-Kuhar B, Kollmann C, Kastl SP, Kaun C, Speidl WS, et al. Can a commercial diagnostic ultrasound device accelerate thrombolysis? An in vitro skull model. Stroke. 2005;36(1):124-8. Epub 2004/12/14.
154. Alexandrov AV, Molina CA, Grotta JC, Garami Z, Ford SR, Alvarez-Sabin J, et al. Ultrasound-enhanced systemic thrombolysis for acute ischemic stroke. The New England journal of medicine. 2004;351(21):2170-8. Epub 2004/11/19.

155. Daffertshofer M, Gass A, Ringleb P, Sitzer M, Sliwka U, Els T, et al. Transcranial low-frequency ultrasound-mediated thrombolysis in brain ischemia: increased risk of hemorrhage with combined ultrasound and tissue plasminogen activator: results of a phase II clinical trial. Stroke. 2005;36(7):1441-6. Epub 2005/06/11.
156. Meairs S, Alonso A, Hennerici MG. Progress in sonothrombolysis for the treatment of stroke. Stroke. 2012;43(6):1706-10. Epub 2012/04/27.
157. The Interventional Management of Stroke (IMS) II Study. Stroke. 2007;38(7):2127-35. Epub 2007/05/26.
158. Broderick JP, Palesch YY, Demchuk AM, Yeatts SD, Khatri P, Hill MD, et al. Endovascular therapy after intravenous t-PA versus t-PA alone for stroke. The New England journal of medicine. 2013;368(10):893-903. Epub 2013/02/09.
159. Kennedy RJ, Kenney HH, Dunfee BL. Thrombus resolution and hemodynamic recovery using ultrasound-accelerated thrombolysis in acute pulmonary embolism. J Vasc Interv Radiol. 2013;24(6):841-8. Epub 2013/04/23.
160. Schrijver A, Vos J, Hoksbergen AW, Fioole B, Fritschy W, Hulsebos R, et al. Ultrasound-accelerated thrombolysis for lower extremity ischemia: multicenter experience and literature review. The Journal of cardiovascular surgery. 2011;52(4):467-76. Epub 2011/07/28.
161. Owens CA. Ultrasound-Enhanced Thrombolysis: EKOS EndoWave Infusion Catheter System. Seminars in interventional radiology. 2008;25(1):37-41. Epub 2008/03/01.
162. Tachibana K, Tachibana S. Albumin microbubble echo-contrast material as an enhancer for ultrasound accelerated thrombolysis. Circulation. 1995;92(5):1148-50. Epub 1995/09/01.
163. Mizushige K, Kondo I, Ohmori K, Hirao K, Matsuo H. Enhancement of ultrasound-accelerated thrombolysis by echo contrast agents: dependence on microbubble structure. Ultrasound Med Biol. 1999;25(9):1431-7. Epub 2000/01/08.
164. Nishioka T, Luo H, Fishbein MC, Cercek B, Forrester JS, Kim CJ, et al. Dissolution of thrombotic arterial occlusion by high intensity, low frequency ultrasound and dodecafluoropentane emulsion: an in vitro and in vivo study. J Am Coll Cardiol. 1997;30(2):561-8. Epub 1997/08/01.
165. Birnbaum Y, Luo H, Nagai T, Fishbein MC, Peterson TM, Li S, et al. Noninvasive in vivo clot dissolution without a thrombolytic drug: recanalization of thrombosed iliofemoral arteries by transcutaneous ultrasound combined with intravenous infusion of microbubbles. Circulation. 1998;97(2):130-4. Epub 1998/01/28.
166. Wu Y, Unger EC, McCreery TP, Sweitzer RH, Shen D, Wu G, et al. Binding and lysing of blood clots using MRX-408. Invest Radiol. 1998;33(12):880-5. Epub 1998/12/16.
167. Culp WC, Porter TR, McCowan TC, Roberson PK, James CA, Matchett WJ, et al. Microbubble-augmented ultrasound declotting of thrombosed arteriovenous dialysis grafts in dogs. J Vasc Interv Radiol. 2003;14(3):343-7. Epub 2003/03/13.
168. Tsutsui JM, Xie F, Johanning J, Lof J, Cory B, He A, et al. Treatment of deeply located acute intravascular thrombi with therapeutic ultrasound guided by diagnostic ultrasound and intravenous microbubbles. J Ultrasound Med. 2006;25(9):1161-8. Epub 2006/08/25.
169. Xie F, Lof J, Everbach C, He A, Bennett RM, Matsunaga T, et al. Treatment of acute intravascular thrombi with diagnostic ultrasound and intravenous microbubbles. JACC Cardiovasc Imaging. 2009;2(4):511-8. Epub 2009/07/08.
170. Chuang YH, Cheng PW, Chen SC, Ruan JL, Li PC. Effects of ultrasound-induced inertial cavitation on enzymatic thrombolysis. Ultrason Imaging. 2010;32(2):81-90. Epub 2010/08/07.
171. Roessler FC, Ohlrich M, Marxsen JH, Stellmacher F, Sprenger A, Dempfle CE, et al. The platelet-rich plasma clot: a standardized in-vitro clot formation protocol for investigations of sonothrombolysis under physiological flows. Blood Coagul Fibrinolysis. 2011;22(5):407-15. Epub 2011/04/27.
172. Holscher T, Raman R, Ernstrom K, Parrish J, Le DT, Lyden PD, et al. In vitro sonothrombolysis with duplex ultrasound: first results using a simplified model. Cerebrovasc Dis. 2009;28(4):365-70. Epub 2009/07/31.

173. Petit B, Gaud E, Colevret D, Arditi M, Yan F, Tranquart F, et al. In Vitro Sonothrombolysis of Human Blood Clots with BR38 Microbubbles. Ultrasound Med Biol. 2012;38(7):1222-33. Epub 2012/05/01.
174. Kutty S, Xie F, Gao S, Drvol LK, Lof J, Fletcher SE, et al. Sonothrombolysis of intra-catheter aged venous thrombi using microbubble enhancement and guided three-dimensional ultrasound pulses. J Am Soc Echocardiogr. 2010;23(9):1001-6. Epub 2010/08/11.
175. Kutty S, Wu J, Hammel JM, Xie F, Gao S, Drvol LK, et al. Microbubble mediated thrombus dissolution with diagnostic ultrasound for the treatment of chronic venous thrombi. PloS one. 2012;7(12):e51453. Epub 2012/12/20.
176. Porter TR, Xie F. Ultrasound, microbubbles, and thrombolysis. Progress in cardiovascular diseases. 2001;44(2):101-10. Epub 2001/09/25.
177. Prokop AF, Soltani A, Roy RA. Cavitational mechanisms in ultrasound-accelerated fibrinolysis. Ultrasound Med Biol. 2007;33(6):924-33. Epub 2007/04/17.
178. Furie B, Furie BC. Mechanisms of thrombus formation. The New England journal of medicine. 2008;359(9):938-49. Epub 2008/08/30.
179. Sobieszczyk P, Fishbein MC, Goldhaber SZ. Acute pulmonary embolism: don't ignore the platelet. Circulation. 2002;106(14):1748-9. Epub 2002/10/03.
180. Van Kruchten R, Cosemans JM, Heemskerk JW. Measurement of whole blood thrombus formation using parallel-plate flow chambers - a practical guide. Platelets. 2012;23(3):229-42. Epub 2012/04/17.
181. Xie F, Tsutsui JM, Lof J, Unger EC, Johanning J, Culp WC, et al. Effectiveness of lipid microbubbles and ultrasound in declotting thrombosis. Ultrasound Med Biol. 2005;31(7):979-85. Epub 2005/06/24.
182. Ricci S, Dinia L, Del Sette M, Anzola P, Mazzoli T, Cenciarelli S, et al. Sonothrombolysis for acute ischaemic stroke. Cochrane Database Syst Rev. 2012;6:CD008348. Epub 2012/06/15.
183. Molina CA, Barreto AD, Tsivgoulis G, Sierzenski P, Malkoff MD, Rubiera M, et al. Transcranial ultrasound in clinical sonothrombolysis (TUCSON) trial. Annals of neurology. 2009;66(1):28-38. Epub 2009/08/12.
184. ClinicalTrials.gov. Microvascular Reperfusion Utilizing Sonothrombolysis in Acute Myocardial Infarction (MRUSMI TRIAL). 2014 [updated 19 June 2014]; NCT02170103:[Available from: http://clinicaltrials.gov/show/NCT02170103.
185. Zwaginga JJ, Sakariassen KS, Nash G, King MR, Heemskerk JW, Frojmovic M, et al. Flow-based assays for global assessment of hemostasis. Part 2: current methods and considerations for the future. Journal of thrombosis and haemostasis : JTH. 2006;4(12):2716-7. Epub 2006/08/30.
186. Zwaginga JJ, Nash G, King MR, Heemskerk JW, Frojmovic M, Hoylaerts MF, et al. Flow-based assays for global assessment of hemostasis. Part 1: Biorheologic considerations. Journal of thrombosis and haemostasis : JTH. 2006;4(11):2486-7. Epub 2006/08/30.
187. Michelson AD. Methods for the measurement of platelet function. The American journal of cardiology. 2009;103(3 Suppl):20A-6A. Epub 2009/02/14.
188. Roest M, Reininger A, Zwaginga JJ, King MR, Heemskerk JW. Flow chamber-based assays to measure thrombus formation in vitro: requirements for standardization. Journal of thrombosis and haemostasis : JTH. 2011;9(11):2322-4. Epub 2012/09/06.
189. Jackson SP, Mistry N, Yuan Y. Platelets and the injured vessel wall-- "rolling into action": focus on glycoprotein Ib/V/IX and the platelet cytoskeleton. Trends Cardiovasc Med. 2000;10(5):192-7. Epub 2001/04/03.
190. Sakariassen KS, Hanson SR, Cadroy Y. Methods and models to evaluate shear-dependent and surface reactivity-dependent antithrombotic efficacy. Thromb Res. 2001;104(3):149-74. Epub 2001/10/24.
191. Cosemans JM, Kuijpers MJ, Lecut C, Loubele ST, Heeneman S, Jandrot-Perrus M, et al. Contribution of platelet glycoprotein VI to the thrombogenic effect of collagens in fibrous atherosclerotic lesions. Atherosclerosis. 2005;181(1):19-27. Epub 2005/06/09.

192. Wu YP, de Groot PG, Sixma JJ. Shear-stress-induced detachment of blood platelets from various surfaces. Arterioscler Thromb Vasc Biol. 1997;17(11):3202-7. Epub 1997/12/31.
193. Auger JM, Kuijpers MJ, Senis YA, Watson SP, Heemskerk JW. Adhesion of human and mouse platelets to collagen under shear: a unifying model. FASEB J. 2005;19(7):825-7. Epub 2005/03/11.
194. Munnix IC, Cosemans JM, Auger JM, Heemskerk JW. Platelet response heterogeneity in thrombus formation. Thrombosis and haemostasis. 2009;102(6):1149-56. Epub 2009/12/08.
195. Kuijpers MJ, Nieuwenhuys CM, Feijge MA, Kloots W, Giesen PL, Jerling JC, et al. Regulation of tissue factor-induced coagulation and platelet aggregation in flowing whole blood. Thrombosis and haemostasis. 2005;93(1):97-105. Epub 2005/01/05.
196. Endenburg SC, Hantgan RR, Lindeboom-Blokzijl L, Lankhof H, Jerome WG, Lewis JC, et al. On the role of von Willebrand factor in promoting platelet adhesion to fibrin in flowing blood. Blood. 1995;86(11):4158-65. Epub 1995/12/01.
197. Cosemans JM, Iserbyt BF, Deckmyn H, Heemskerk JW. Multiple ways to switch platelet integrins on and off. Journal of thrombosis and haemostasis : JTH. 2008;6(8):1253-61. Epub 2008/06/03.
198. Heemskerk JW, Bevers EM, Lindhout T. Platelet activation and blood coagulation. Thrombosis and haemostasis. 2002;88(2):186-93. Epub 2002/08/28.
199. Haig Y, Enden T, Grotta O, Klow NE, Slagsvold CE, Ghanima W, et al. Post-thrombotic syndrome after catheter-directed thrombolysis for deep vein thrombosis (CaVenT): 5-year follow-up results of an open-label, randomised controlled trial. The Lancet Haematology. 2016;3(2):e64-71. Epub 2016/02/09.
200. Maxwell MJ, Westein E, Nesbitt WS, Giuliano S, Dopheide SM, Jackson SP. Identification of a 2-stage platelet aggregation process mediating shear-dependent thrombus formation. Blood. 2007;109(2):566-76. Epub 2006/09/23.
201. Mizuno T, Sugimoto M, Matsui H, Hamada M, Shida Y, Yoshioka A. Visual evaluation of blood coagulation during mural thrombogenesis under high shear blood flow. Thromb Res. 2008;121(6):855-64. Epub 2007/09/29.
202. Jones KL, Hughan SC, Dopheide SM, Farndale RW, Jackson SP, Jackson DE. Platelet endothelial cell adhesion molecule-1 is a negative regulator of platelet-collagen interactions. Blood. 2001;98(5):1456-63. Epub 2001/08/25.
203. Ono A, Westein E, Hsiao S, Nesbitt WS, Hamilton JR, Schoenwaelder SM, et al. Identification of a fibrin-independent platelet contractile mechanism regulating primary hemostasis and thrombus growth. Blood. 2008;112(1):90-9. Epub 2008/03/04.
204. Pugh N, Simpson AM, Smethurst PA, de Groot PG, Raynal N, Farndale RW. Synergism between platelet collagen receptors defined using receptor-specific collagen-mimetic peptide substrata in flowing blood. Blood. 2010;115(24):5069-79. Epub 2010/03/31.
205. Lecut C, Schoolmeester A, Kuijpers MJ, Broers JL, van Zandvoort MA, Vanhoorelbeke K, et al. Principal role of glycoprotein VI in alpha2beta1 and alphaIIbbeta3 activation during collagen-induced thrombus formation. Arterioscler Thromb Vasc Biol. 2004;24(9):1727-33. Epub 2004/07/03.
206. Lampaskis M, Averkiou M. Investigation of the relationship of nonlinear backscattered ultrasound intensity with microbubble concentration at low MI. Ultrasound Med Biol. 2010;36(2):306-12. Epub 2010/01/05.
207. Jimenez N, Krouwer VJ, Post JA. A new, rapid and reproducible method to obtain high quality endothelium in vitro. Cytotechnology. 2013;65(1):1-14. Epub 2012/05/11.
208. Li M, Hotaling NA, Ku DN, Forest CR. Microfluidic thrombosis under multiple shear rates and antiplatelet therapy doses. PloS one. 2014;9(1):e82493. Epub 2014/01/10.
209. Pugh N, Jarvis GE, Koch A, Sakariassen KS, Davis B, Farndale RW. The impact of factor Xa inhibition on axial dependent arterial thrombus formation triggered by a tissue factor rich surface. Journal of thrombosis and thrombolysis. 2012;33(1):6-15. Epub 2011/11/29.
210. Jackson SP. The growing complexity of platelet aggregation. Blood. 2007;109(12):5087-95. Epub 2007/02/22.

211. Maxwell MJ, Dopheide SM, Turner SJ, Jackson SP. Shear induces a unique series of morphological changes in translocating platelets: effects of morphology on translocation dynamics. Arterioscler Thromb Vasc Biol. 2006;26(3):663-9. Epub 2005/12/31.
212. Roessler FC, Ohlrich M, Marxsen JH, Schmieger M, Weber PK, Stellmacher F, et al. Introduction of a new model for time-continuous and non-contact investigations of in-vitro thrombolysis under physiological flow conditions. BMC Neurol. 2011;11:58. Epub 2011/05/28.
213. Karthikesalingam A, Young EL, Hinchliffe RJ, Loftus IM, Thompson MM, Holt PJ. A systematic review of percutaneous mechanical thrombectomy in the treatment of deep venous thrombosis. European journal of vascular and endovascular surgery : the official journal of the European Society for Vascular Surgery. 2011;41(4):554-65. Epub 2011/02/04.
214. Organisation WH. Cerebrovascular disorders: a clinical and research classification. Geneva. 1978.
215. Tyrrell P, Swain S, Rudd A. Diagnosis and initial management of transient ischaemic attack. Clin Med (Lond). 2010;10(2):164-7. Epub 2010/05/05.
216. S Mendis PP, Norrving B. Global atlas on cardiovascular disease prevention and control. World Health Organization; Geneva. 2011.
217. Saka O, McGuire A, Wolfe C. Cost of stroke in the United Kingdom. Age and ageing. 2009;38(1):27-32. Epub 2009/01/15.
218. National Clinical Guideline for Stroke. Royal College of Physicians. 2012 [cited 4th Ed.]; Available from: www.rcplondon.ac.uk/resources/stroke-guidelines.
219. van Swieten JC, Koudstaal PJ, Visser MC, Schouten HJ, van Gijn J. Interobserver agreement for the assessment of handicap in stroke patients. Stroke. 1988;19(5):604-7. Epub 1988/05/01.
220. Stroke NIoNDa. NIH Stroke Scale. 2011; Available from: https://www.ninds.nih.gov/sites/default/files/NIH_Stroke_Scale_Booklet.pdf.
221. Johnston SC, Rothwell PM, Nguyen-Huynh MN, Giles MF, Elkins JS, Bernstein AL, et al. Validation and refinement of scores to predict very early stroke risk after transient ischaemic attack. Lancet. 2007;369(9558):283-92. Epub 2007/01/30.
222. Wolfe CD, Rudd AG, Howard R, Coshall C, Stewart J, Lawrence E, et al. Incidence and case fatality rates of stroke subtypes in a multiethnic population: the South London Stroke Register. Journal of neurology, neurosurgery, and psychiatry. 2002;72(2):211-6. Epub 2002/01/18.
223. Hajat C, Heuschmann PU, Coshall C, Padayachee S, Chambers J, Rudd AG, et al. Incidence of aetiological subtypes of stroke in a multi-ethnic population based study: the South London Stroke Register. Journal of neurology, neurosurgery, and psychiatry. 2011;82(5):527-33. Epub 2010/10/27.
224. Fairhead JF, Rothwell PM. The need for urgency in identification and treatment of symptomatic carotid stenosis is already established. Cerebrovasc Dis. 2005;19(6):355-8. Epub 2005/04/20.
225. Thapar A, Jenkins IH, Mehta A, Davies AH. Diagnosis and management of carotid atherosclerosis. BMJ. 2013;346:f1485. Epub 2013/03/20.
226. de Weerd M, Greving JP, Hedblad B, Lorenz MW, Mathiesen EB, O'Leary DH, et al. Prevalence of asymptomatic carotid artery stenosis in the general population: an individual participant data meta-analysis. Stroke. 2010;41(6):1294-7. Epub 2010/05/01.
227. Kakkos SK, Sabetai M, Tegos T, Stevens J, Thomas D, Griffin M, et al. Silent embolic infarcts on computed tomography brain scans and risk of ipsilateral hemispheric events in patients with asymptomatic internal carotid artery stenosis. Journal of vascular surgery : official publication, the Society for Vascular Surgery [and] International Society for Cardiovascular Surgery, North American Chapter. 2009;49(4):902-9. Epub 2009/02/19.
228. Dawkins AA, Evans AL, Wattam J, Romanowski CA, Connolly DJ, Hodgson TJ, et al. Complications of cerebral angiography: a prospective analysis of 2,924 consecutive procedures. Neuroradiology. 2007;49(9):753-9. Epub 2007/06/28.
229. Oates CP, Naylor AR, Hartshorne T, Charles SM, Fail T, Humphries K, et al. Joint recommendations for reporting carotid ultrasound investigations in the United Kingdom. European

journal of vascular and endovascular surgery : the official journal of the European Society for Vascular Surgery. 2009;37(3):251-61. Epub 2008/12/03.
230. Chappell FM, Wardlaw JM, Young GR, Gillard JH, Roditi GH, Yip B, et al. Carotid artery stenosis: accuracy of noninvasive tests--individual patient data meta-analysis. Radiology. 2009;251(2):493-502. Epub 2009/03/12.
231. Jahromi AS, Cina CS, Liu Y, Clase CM. Sensitivity and specificity of color duplex ultrasound measurement in the estimation of internal carotid artery stenosis: a systematic review and meta-analysis. Journal of vascular surgery : official publication, the Society for Vascular Surgery [and] International Society for Cardiovascular Surgery, North American Chapter. 2005;41(6):962-72. Epub 2005/06/10.
232. Thapar A, Shalhoub J, Dharmarajah B, Davies AH. Should we stop testing for asymptomatic carotid atherosclerosis? Journal of neurointerventional surgery. 2013;5(2):94-6. Epub 2012/09/07.
233. Fine-Edelstein JS, Wolf PA, O'Leary DH, Poehlman H, Belanger AJ, Kase CS, et al. Precursors of extracranial carotid atherosclerosis in the Framingham Study. Neurology. 1994;44(6):1046-50. Epub 1994/06/01.
234. Halliday A, Harrison M, Hayter E, Kong X, Mansfield A, Marro J, et al. 10-year stroke prevention after successful carotid endarterectomy for asymptomatic stenosis (ACST-1): a multicentre randomised trial. Lancet. 2010;376(9746):1074-84. Epub 2010/09/28.
235. Payne DA, Jones CI, Hayes PD, Thompson MM, London NJ, Bell PR, et al. Beneficial effects of clopidogrel combined with aspirin in reducing cerebral emboli in patients undergoing carotid endarterectomy. Circulation. 2004;109(12):1476-81. Epub 2004/03/10.
236. Collaborative meta-analysis of randomised trials of antiplatelet therapy for prevention of death, myocardial infarction, and stroke in high risk patients. BMJ. 2002;324(7329):71-86. Epub 2002/01/12.
237. Spence JD, Coates V, Li H, Tamayo A, Munoz C, Hackam DG, et al. Effects of intensive medical therapy on microemboli and cardiovascular risk in asymptomatic carotid stenosis. Archives of neurology. 2010;67(2):180-6. Epub 2009/12/17.
238. Kadoglou NP, Sailer N, Moumtzouoglou A, Kapelouzou A, Gerasimidis T, Liapis CD. Aggressive lipid-lowering is more effective than moderate lipid-lowering treatment in carotid plaque stabilization. Journal of vascular surgery : official publication, the Society for Vascular Surgery [and] International Society for Cardiovascular Surgery, North American Chapter. 2010;51(1):114-21. Epub 2009/10/20.
239. Yang D, Iyer S, Gardener H, Della-Morte D, Crisby M, Dong C, et al. Cigarette Smoking and Carotid Plaque Echodensity in the Northern Manhattan Study. Cerebrovasc Dis. 2015;40(3-4):136-43. Epub 2015/08/01.
240. Munster AB, Thapar A, Davies AH. History of Carotid Stroke. Stroke. 2016;47(4):e66-9. Epub 2016/01/23.
241. Rerkasem K, Rothwell PM. Patch angioplasty versus primary closure for carotid endarterectomy. Cochrane Database Syst Rev. 2009(4):CD000160. Epub 2009/10/13.
242. Gough MJ, Bodenham A, Horrocks M, Colam B, Lewis SC, Rothwell PM, et al. GALA: an international multicentre randomised trial comparing general anaesthesia versus local anaesthesia for carotid surgery. Trials. 2008;9:28. Epub 2008/05/23.
243. National Vascular Registry 2013 Report on Surgical Outcomes Consultant-level statistics. Vascular Services Quality Improvement Programme. June 2013; Available from: http://www.vsqip.org.uk/wp/wp-content/uploads/2013/07/NVR-2013-Report-on-Surgical-Outcomes-Consultant-Level-Statistics.pdf.
244. Favre JP, Nourissat A, Duprey A, Nourissat G, Albertini JN, Becquemin JP. Endovascular treatment for carotid artery stenosis after neck irradiation. Journal of vascular surgery : official publication, the Society for Vascular Surgery [and] International Society for Cardiovascular Surgery, North American Chapter. 2008;48(4):852-8. Epub 2008/08/30.
245. Kasivisvanathan V, Thapar A, Davies KJ, Dharmarajah B, Shalhoub J, Davies AH. Periprocedural outcomes after surgical revascularization and stenting for postradiotherapy carotid stenosis. Journal of vascular surgery : official publication, the Society for Vascular Surgery [and]

International Society for Cardiovascular Surgery, North American Chapter. 2012;56(4):1143-52 e2. Epub 2012/07/24.
246. McPhee JT, Schanzer A, Messina LM, Eslami MH. Carotid artery stenting has increased rates of postprocedure stroke, death, and resource utilization than does carotid endarterectomy in the United States, 2005. Journal of vascular surgery : official publication, the Society for Vascular Surgery [and] International Society for Cardiovascular Surgery, North American Chapter. 2008;48(6):1442-50, 50 e1. Epub 2008/10/03.
247. Kerber CW, Cromwell LD, Loehden OL. Catheter dilatation of proximal carotid stenosis during distal bifurcation endarterectomy. AJNR American journal of neuroradiology. 1980;1(4):348-9. Epub 1980/07/01.
248. Vogel TR, Dombrovskiy VY, Haser PB, Scheirer JC, Graham AM. Outcomes of carotid artery stenting and endarterectomy in the United States. Journal of vascular surgery : official publication, the Society for Vascular Surgery [and] International Society for Cardiovascular Surgery, North American Chapter. 2009;49(2):325-30; discussion 30. Epub 2008/12/09.
249. Bonati LH, Lyrer P, Ederle J, Featherstone R, Brown MM. Percutaneous transluminal balloon angioplasty and stenting for carotid artery stenosis. Cochrane Database Syst Rev. 2012;9:CD000515. Epub 2012/09/14.
250. Brott TG, Howard G, Roubin GS. Long-Term Results of Stenting Versus Endarterectomy for Carotid-Artery Stenosis. Journal of vascular surgery : official publication, the Society for Vascular Surgery [and] International Society for Cardiovascular Surgery, North American Chapter. 2016;64(2):535-6. Epub 2016/10/21.
251. Provision of Services for Patients with Vascular Disease. The Vascular Society of Great Britain and Ireland. 2012; Available from: http://www.vascularsociety.org.uk/vascular/wp-content/uploads/2012/11/Provision-of-Services-for-Patients-with-Vascular-Disease.pdf.
252. Bonati LH, Lyrer P, Ederle J, Featherstone R, Brown MM. Percutaneous transluminal balloon angioplasty and stenting for carotid artery stenosis. Cochrane Database Syst Rev. 2012(9):CD000515. Epub 2012/09/14.
253. Rudarakanchana N, Dialynas M, Halliday A. Asymptomatic Carotid Surgery Trial-2 (ACST-2): rationale for a randomised clinical trial comparing carotid endarterectomy with carotid artery stenting in patients with asymptomatic carotid artery stenosis. European journal of vascular and endovascular surgery : the official journal of the European Society for Vascular Surgery. 2009;38(2):239-42. Epub 2009/06/23.
254. Berkhemer OA, Fransen PS, Beumer D, van den Berg LA, Lingsma HF, Yoo AJ, et al. A randomized trial of intraarterial treatment for acute ischemic stroke. The New England journal of medicine. 2015;372(1):11-20. Epub 2014/12/18.
255. Goyal M, Demchuk AM, Menon BK, Eesa M, Rempel JL, Thornton J, et al. Randomized assessment of rapid endovascular treatment of ischemic stroke. The New England journal of medicine. 2015;372(11):1019-30. Epub 2015/02/12.
256. Behme D, Mpotsaris A, Zeyen P, Psychogios MN, Kowoll A, Maurer CJ, et al. Emergency Stenting of the Extracranial Internal Carotid Artery in Combination with Anterior Circulation Thrombectomy in Acute Ischemic Stroke: A Retrospective Multicenter Study. AJNR American journal of neuroradiology. 2015;36(12):2340-5. Epub 2015/08/22.
257. Rothwell PM, Eliasziw M, Gutnikov SA, Warlow CP, Barnett HJ. Endarterectomy for symptomatic carotid stenosis in relation to clinical subgroups and timing of surgery. Lancet. 2004;363(9413):915-24. Epub 2004/03/27.
258. The 2nd European Carotid Surgery Trial (ECST-2) Protocol. 2013 [updated 1 May 2013]; 2.00:[Available from: http://www.ion.ucl.ac.uk/cavatas_icss/ECST2/download.htm.
259. Salem MK, Sayers RD, Bown MJ, West K, Moore D, Robinson TG, et al. Features of unstable carotid plaque during and after the hyperacute period following TIA/stroke. European journal of vascular and endovascular surgery : the official journal of the European Society for Vascular Surgery. 2013;45(2):114-20. Epub 2012/12/29.

260. Rothwell PM, Warlow CP. Timing of TIAs preceding stroke: time window for prevention is very short. Neurology. 2005;64(5):817-20. Epub 2005/03/09.
261. Naylor AR, AbuRahma AF. Debate: Whether carotid endarterectomy is safer than stenting in the hyperacute period after onset of symptoms. Journal of vascular surgery : official publication, the Society for Vascular Surgery [and] International Society for Cardiovascular Surgery, North American Chapter. 2015;61(6):1642-51. Epub 2015/05/26.
262. Mandavia R, Qureshi MI, Dharmarajah B, Head K, Davies AH. Safety of carotid intervention following thrombolysis in acute ischaemic stroke. European journal of vascular and endovascular surgery : the official journal of the European Society for Vascular Surgery. 2014;48(5):505-12. Epub 2014/09/14.
263. Endarterectomy for asymptomatic carotid artery stenosis. Executive Committee for the Asymptomatic Carotid Atherosclerosis Study. JAMA. 1995;273(18):1421-8. Epub 1995/05/10.
264. Halliday A, Mansfield A, Marro J, Peto C, Peto R, Potter J, et al. Prevention of disabling and fatal strokes by successful carotid endarterectomy in patients without recent neurological symptoms: randomised controlled trial. Lancet. 2004;363(9420):1491-502. Epub 2004/05/12.
265. Naylor AR. Time to rethink management strategies in asymptomatic carotid artery disease. Nature reviews Cardiology. 2011;9(2):116-24. Epub 2011/10/13.
266. Thapar A, Garcia Mochon L, Epstein D, Shalhoub J, Davies AH. Modelling the cost-effectiveness of carotid endarterectomy for asymptomatic stenosis. The British journal of surgery. 2013;100(2):231-9. Epub 2012/11/28.
267. Munster AB, Franchini AJ, Qureshi MI, Thapar A, Davies AH. Temporal trends in safety of carotid endarterectomy in asymptomatic patients: systematic review. Neurology. 2015;85(4):365-72. Epub 2015/06/28.
268. Kotseva K, Wood D, De Bacquer D, De Backer G, Ryden L, Jennings C, et al. EUROASPIRE IV: A European Society of Cardiology survey on the lifestyle, risk factor and therapeutic management of coronary patients from 24 European countries. European journal of preventive cardiology. 2016;23(6):636-48. Epub 2015/02/18.
269. Rothwell PM, Warlow CP. Prediction of benefit from carotid endarterectomy in individual patients: a risk-modelling study. European Carotid Surgery Trialists' Collaborative Group. Lancet. 1999;353(9170):2105-10. Epub 1999/06/26.
270. Rothwell PM, Mehta Z, Howard SC, Gutnikov SA, Warlow CP. Treating individuals 3: from subgroups to individuals: general principles and the example of carotid endarterectomy. Lancet. 2005;365(9455):256-65. Epub 2005/01/18.
271. Fox KA, Dabbous OH, Goldberg RJ, Pieper KS, Eagle KA, Van de Werf F, et al. Prediction of risk of death and myocardial infarction in the six months after presentation with acute coronary syndrome: prospective multinational observational study (GRACE). BMJ. 2006;333(7578):1091. Epub 2006/10/13.
272. Schnabel RB, Sullivan LM, Levy D, Pencina MJ, Massaro JM, D'Agostino RB, Sr., et al. Development of a risk score for atrial fibrillation (Framingham Heart Study): a community-based cohort study. Lancet. 2009;373(9665):739-45. Epub 2009/03/03.
273. Topakian R, King A, Kwon SU, Schaafsma A, Shipley M, Markus HS. Ultrasonic plaque echolucency and emboli signals predict stroke in asymptomatic carotid stenosis. Neurology. 2011;77(8):751-8. Epub 2011/08/19.
274. Setacci C, Chisci E, Setacci F, Iacoponi F, de Donato G, Rossi A. Siena carotid artery stenting score: a risk modelling study for individual patients. Stroke. 2010;41(6):1259-65. Epub 2010/05/01.
275. Nicolaides AN, Kakkos SK, Kyriacou E, Griffin M, Sabetai M, Thomas DJ, et al. Asymptomatic internal carotid artery stenosis and cerebrovascular risk stratification. Journal of vascular surgery : official publication, the Society for Vascular Surgery [and] International Society for Cardiovascular Surgery, North American Chapter. 2010;52(6):1486-96 e1-5. Epub 2010/12/15.
276. Sila CA, Higashida RT, Clagett GP. Clinical decisions. Management of carotid stenosis. The New England journal of medicine. 2008;358(15):1617-21. Epub 2008/04/12.

277. Klein A, Solomon CG, Hamel MB. Clinical decisions. Management of carotid stenosis--polling results. The New England journal of medicine. 2008;358(20):e23. Epub 2008/05/16.
278. Brott TG, Hobson RW, 2nd, Howard G, Roubin GS, Clark WM, Brooks W, et al. Stenting versus endarterectomy for treatment of carotid-artery stenosis. The New England journal of medicine. 2010;363(1):11-23. Epub 2010/05/28.
279. Jensen MP. Questionnaire validation: a brief guide for readers of the research literature. The Clinical journal of pain. 2003;19(6):345-52. Epub 2003/11/06.
280. Spence JD. Is there a role for revascularisation in asymptomatic carotid stenosis? No. BMJ. 2010;341:c4900. Epub 2010/09/17.
281. Roffi M. Is there a role for revascularisation in asymptomatic carotid stenosis? Yes. BMJ. 2010;341:c4898. Epub 2010/09/17.
282. Schneider PA, Naylor AR. Transatlantic debate. Asymptomatic carotid artery stenosis--medical therapy alone versus medical therapy plus carotid endarterectomy or stenting. European journal of vascular and endovascular surgery : the official journal of the European Society for Vascular Surgery. 2010;40(2):274-81. Epub 2010/07/27.
283. Sitzer M, Muller W, Rademacher J, Siebler M, Hort W, Kniemeyer HW, et al. Color-flow Doppler-assisted duplex imaging fails to detect ulceration in high-grade internal carotid artery stenosis. Journal of vascular surgery : official publication, the Society for Vascular Surgery [and] International Society for Cardiovascular Surgery, North American Chapter. 1996;23(3):461-5. Epub 1996/03/01.
284. Rathenborg LK, Jensen LP, Baekgaard N, Schroeder TV. Carotid endarterectomy after intravenous thrombolysis for acute cerebral ischaemic attack: is it safe? European journal of vascular and endovascular surgery : the official journal of the European Society for Vascular Surgery. 2013;45(6):573-7. Epub 2013/04/16.
285. Jayasooriya GS, Shalhoub J, Thapar A, Davies AH. Patient preference survey in the management of asymptomatic carotid stenosis. Journal of vascular surgery : official publication, the Society for Vascular Surgery [and] International Society for Cardiovascular Surgery, North American Chapter. 2011;53(6):1466-72. Epub 2011/04/12.
286. Stary HC. Natural history and histological classification of atherosclerotic lesions: an update. Arterioscler Thromb Vasc Biol. 2000;20(5):1177-8. Epub 2000/05/16.
287. Fisher M, Paganini-Hill A, Martin A, Cosgrove M, Toole JF, Barnett HJ, et al. Carotid plaque pathology: thrombosis, ulceration, and stroke pathogenesis. Stroke. 2005;36(2):253-7. Epub 2005/01/18.
288. Eliasziw M, Streifler JY, Fox AJ, Hachinski VC, Ferguson GG, Barnett HJ. Significance of plaque ulceration in symptomatic patients with high-grade carotid stenosis. North American Symptomatic Carotid Endarterectomy Trial. Stroke. 1994;25(2):304-8. Epub 1994/02/01.
289. Chambers BR, Donnan GA. Carotid endarterectomy for asymptomatic carotid stenosis. Cochrane Database Syst Rev. 2005(4):CD001923. Epub 2005/10/20.
290. Shalhoub J, Owen DR, Gauthier T, Monaco C, Leen EL, Davies AH. The use of contrast enhanced ultrasound in carotid arterial disease. European journal of vascular and endovascular surgery : the official journal of the European Society for Vascular Surgery. 2010;39(4):381-7. Epub 2010/01/12.
291. Ricotta JJ, Aburahma A, Ascher E, Eskandari M, Faries P, Lal BK. Updated Society for Vascular Surgery guidelines for management of extracranial carotid disease: executive summary. J Vasc Surg. 2011;54(3):832-6. Epub 2011/09/06.
292. Ten Kate GL, van Dijk AC, van den Oord SC, Hussain B, Verhagen HJ, Sijbrands EJ, et al. Usefulness of Contrast-Enhanced Ultrasound for Detection of Carotid Plaque Ulceration in Patients With Symptomatic Carotid Atherosclerosis. The American journal of cardiology. 2013. Epub 2013/04/17.
293. Madani A, Beletsky V, Tamayo A, Munoz C, Spence JD. High-risk asymptomatic carotid stenosis: ulceration on 3D ultrasound vs TCD microemboli. Neurology. 2011;77(8):744-50. Epub 2011/08/19.
294. Spence JD, Tamayo A, Lownie SP, Ng WP, Ferguson GG. Absence of microemboli on transcranial Doppler identifies low-risk patients with asymptomatic carotid stenosis. Stroke. 2005;36(11):2373-8. Epub 2005/10/15.

295. Thapar A, Shalhoub J, Averkiou M, Mannaris C, Davies AH, Leen EL. Dose-dependent artifact in the far wall of the carotid artery at dynamic contrast-enhanced US. Radiology. 2012;262(2):672-9. Epub 2011/12/14.
296. Ricotta JJ, Aburahma A, Ascher E, Eskandari M, Faries P, Lal BK. Updated Society for Vascular Surgery guidelines for management of extracranial carotid disease. Journal of vascular surgery : official publication, the Society for Vascular Surgery [and] International Society for Cardiovascular Surgery, North American Chapter. 2011;54(3):e1-31. Epub 2011/09/06.
297. Dunmore BJ, McCarthy MJ, Naylor AR, Brindle NP. Carotid plaque instability and ischemic symptoms are linked to immaturity of microvessels within plaques. Journal of vascular surgery : official publication, the Society for Vascular Surgery [and] International Society for Cardiovascular Surgery, North American Chapter. 2007;45(1):155-9. Epub 2007/01/11.
298. Russell DA, Abbott CR, Gough MJ. Vascular endothelial growth factor is associated with histological instability of carotid plaques. The British journal of surgery. 2008;95(5):576-81. Epub 2008/03/18.
299. Xiong L, Deng YB, Zhu Y, Liu YN, Bi XJ. Correlation of carotid plaque neovascularization detected by using contrast-enhanced US with clinical symptoms. Radiology. 2009;251(2):583-9. Epub 2009/03/24.
300. Moreno PR, Purushothaman KR, Fuster V, Echeverri D, Truszczynska H, Sharma SK, et al. Plaque neovascularization is increased in ruptured atherosclerotic lesions of human aorta: implications for plaque vulnerability. Circulation. 2004;110(14):2032-8. Epub 2004/09/29.
301. Akkus Z, Hoogi A, Renaud G, van den Oord SC, Ten Kate GL, Schinkel AF, et al. New quantification methods for carotid intra-plaque neovascularization using contrast-enhanced ultrasound. Ultrasound Med Biol. 2014;40(1):25-36. Epub 2013/10/29.
302. Christofides D, Leen E, Averkiou M. Automatic respiratory gating for contrast ultrasound evaluation of liver lesions. IEEE transactions on ultrasonics, ferroelectrics, and frequency control. 2014;61(1):25-32. Epub 2014/01/10.
303. Shah F, Balan P, Weinberg M, Reddy V, Neems R, Feinstein M, et al. Contrast-enhanced ultrasound imaging of atherosclerotic carotid plaque neovascularization: a new surrogate marker of atherosclerosis? Vasc Med. 2007;12(4):291-7. Epub 2007/12/01.
304. Dietrich CF, Averkiou MA, Correas JM, Lassau N, Leen E, Piscaglia F. An EFSUMB introduction into Dynamic Contrast-Enhanced Ultrasound (DCE-US) for quantification of tumour perfusion. Ultraschall Med. 2012;33(4):344-51. Epub 2012/07/31.
305. Gauthier TP, Muhammad A, Wasan HS, Abel PD, Leen EL. Reproducibility of quantitative assessment of altered hepatic hemodynamics with dynamic contrast-enhanced ultrasound. J Ultrasound Med. 2012;31(9):1413-20. Epub 2012/08/28.
306. Jansen A, Mischi M, Bracke F, van Dantzig JM, Peels K, Lamfers E, et al. Novel ultrasound contrast agent dilution method for the assessment of ventricular ejection fraction. European journal of echocardiography : the journal of the Working Group on Echocardiography of the European Society of Cardiology. 2008;9(4):489-93. Epub 2007/10/02.
307. Coli S, Magnoni M, Sangiorgi G, Marrocco-Trischitta MM, Melisurgo G, Mauriello A, et al. Contrast-enhanced ultrasound imaging of intraplaque neovascularization in carotid arteries: correlation with histology and plaque echogenicity. J Am Coll Cardiol. 2008;52(3):223-30. Epub 2008/07/12.
308. Marquardt L, Geraghty OC, Mehta Z, Rothwell PM. Low risk of ipsilateral stroke in patients with asymptomatic carotid stenosis on best medical treatment: a prospective, population-based study. Stroke. 2010;41(1):e11-7. Epub 2009/11/21.
309. Cheung WK, Gujral DM, Shah BN, Chahal NS, Bhattacharyya S, Cosgrove DO, et al. Attenuation Correction and Normalisation for Quantification of Contrast Enhancement in Ultrasound Images of Carotid Arteries. Ultrasound Med Biol. 2015;41(7):1876-83. Epub 2015/04/07.
310. Vedantham S, editor. ATTRACT TRIAL - medical treatment versus intervention (pharmocomechanical thrombolysis). Charing Cross Vascular and Endovascular International Symposium; 2017; London: BIBA Medical.